ISSN (Print) : 2277-7261
ISSN (on-line) : 2278-3857

PRATIBHA

INTERNATIONAL JOURNAL OF SCIENCE, SPIRITUALITY, BUSINESS & TECHNOLOGY (IJSSBT)

Vol. 8, No. 2, January 2022

www.ijssbt.org

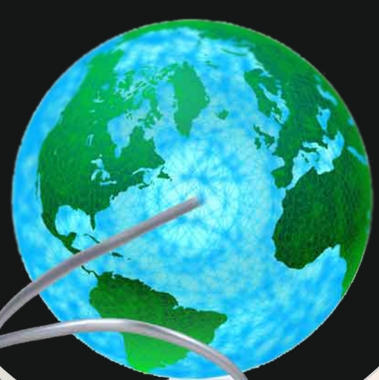

SHRAM SADHANA BOMBAY TRUST'S

COLLEGE OF ENGINEERING & TECHNOLOGY, BAMBHORI, JALGAON (INDIA)

PRATIBHA

INTERNATIONAL JOURNAL OF SCIENCE, SPIRITUALITY, BUSINESS & TECHNOLOGY (IJSSBT)

Vol. 8, No. 2, January 2022

ISSN (Print) : 2277-7261
ISSN (on-line) : 2278-3857

www.ijssbt.org

SHRAM SADHANA BOMBAY TRUST
COLLEGE OF ENGINEERING AND TECHNOLOGY
श्रम साधना
ESTD. 1983
BAMBHORI, JALGAON
IJSSBT

Smt Pratibha Devisingh Patil
Former President of India

Our inspiration
to impart Quality Education for
societal development

PRATIBHA

INTERNATIONAL JOURNAL OF SCIENCE, SPIRITUALITY, BUSINESS & TECHNOLOGY

Vol. 8, No. 2, January 2022 | ISSN (Print) : 2277-7261 | ISSN (On-line) : 2278-3857

PRATIBHA: INTERNATIONAL JOURNAL OF SCIENCE, SPIRITUALITY, BUSINESS AND TECHNOLOGY (IJSSBT)

Pratibha: International Journal of Science, Spirituality, Business and Technology (IJSSBT) is a research journal published by Shram Sadhana Bombay Trust's, COLLEGE of ENGINEERING & TECHNOLOGY, Bambhori, Jalgaon, MAHARASHTRA STATE, INDIA. Founder Chairperson of the college is Honourable Sau. Pratibha Devisingh Patil, the former President of India.

Shram Sadhana Bombay Trust runs the COLLEGE of ENGINEERING & TECHNOLOGY at Bambhori, Jalgaon, which is the one of the important industrial town & district headquarters of Maharashtra state. SSBT COET campus is lush green spread over 25 acres area and located on the bank of River Girna. The campus is well equipped with important amenities such as classrooms, drawing halls, laboratories, seminar halls, library, computer center, workshop, hostels, canteens, indoor as well as outdoor sports facilities etc.

The College was accredited by National Board of Accreditation, New Delhi for three times:

- Four Programmes (Civil, Bio-Technology, Chemical and Electronics & Tele-communications Engineering) were provisionally accredited for two years with effect from 01/07/2014 Vide Letter F. No. 28-235/2010-NBA, dated October 01, 2014.
- Seven Programmes (Civil, Chemical, Computer, Electrical, Electronics and Telecommunication, Information Technology and Mechanical,) were accredited for five years with effect from 19/07/2008 vide letter F. No. NBA/ACCR-414/2004, dated July 18, 2008.
- Four Programmes (Civil, Chemical, Computer, and Mechanical) were accredited for three years with effect from -18/02/2005 vide letter no. NBA/ACCR-414/2005.

Under Graduate (UG) courses permanently affiliated to K.B.C. North Maharashtra University are: Bio-Technology, Civil Engineering, Chemical Engineering, Computer Engineering, Electronics and Telecommunication Engineering, Electrical Engineering, Mechanical Engineering, Information Technology.

The College also offers Post Graduate (PG) courses: Master of Business Administration (MBA) & Master of Computer Applications (MCA). The College also offers Ph.D. programmes in: Bio-Technology, Chemical Engineering, Civil Engineering, Computer Engineering, Electronics & Tele-Communications, Electrical Engineering and Mechanical Engineering.

The International Journal of Science, Spirituality, Business and Technology (IJSSBT) is an excellent, intellectual, peer reviewed journal that takes scholarly approach in creating, developing, integrating, sharing and applying knowledge about all the fields of study in Engineering, Spirituality, Management and Science for the benefit of humanity and the profession.

The audience includes researchers, managers, engineers, curriculum designers administrators as well as developers.

EDITOR(s)-IN-CHIEF

Prof. Dr. G.K. PATNAIK
M.E., Ph.D. (Computer Science Engineering)
Principal,
S.S.B.T.'s College of Engineering and Technology, Bambhori, Jalgaon
Mobile No. +919422790559
Phone No. (0257) 2258393, Fax No. (0257) 2258392
Email id: girishpat2001@yahoo.com

Prof. Dr. SANJAY P. SHEKHAWAT
Ph.D. (Mechanical Engineering)
Professor,
Department of Mechanical Engineering,
S.S.B.T.'s College of Engineering and Technology, Bambhori, Jalgaon
Mobile No. +91 9423621653
Phone No. (0257) 2258393, Fax No. (0257) 2258392
Email id: spshekhawat@rediffmail.com

Web Address : **www.ijssbt.org/com**

Journal Indexing

COSMOS IMPACT FACTOR

PUBLICATION COMMITTEE

Prof. Dr. SANJAY P. SHEKHAWAT
Professor
Department of Mechanical Engineering

Mr. SUHAS M. SHEMBEKAR
Assistant Professor
Department of Electrical Engineering

RESEARCH REVIEW COMMITTEE

S.N.	Name of Reviewer	Subject
1	Dr. G.K.Patnaik, Principal	Computer Science Engineering
2	Dr. S.B. Pawar, Vice-Principal	Civil Engineering
3	Dr. S.P.Shekhawat	Mechanical Engineering
4	Dr. M. Husain	Civil Engineering
5	Dr. S.R. Suralkar	Electronics & Telecommunication Engineering
6	Dr. P. J. Shah	Electrical Engineering
7	Dr. I.D. Patil	Bio-Technology
8	Dr. V.R. Diware	Chemical Engineering
9	Dr. K.S. Patil	Applied Science
10	Dr. V. S. Rana	Management
11	Dr. K.P.Adhiya	Computer Science Engineering
12	Dr. M.P. Deshmukh	Electronics & Telecommunication Engineering
13	Dr. P.G. Damle	Mechanical Engineering
14	Dr. M.B.Ahirrao	Management
15	Dr. M.E.Patil	Computer Science Engineering
16	Dr. Archana K. Bhavsar	Computer Science Engineering
17	Dr. Saroj B. Patil	Management
18	Dr. Sunita S. Patil	Mathematics
19	Dr. P.A. Shirule	Civil Engineering
20	Dr. V.M.Deshmukh	Electronics & Telecommunication Engineering
21	Dr. R.A. Modiyani	Management
22	Dr. U. S. Bhadade	Electronics & Telecommunication Engineering
23	Dr. P. V. Thakare	Electrical Engineering
24	Dr. S.D. Suryawanshi	Mechanical Engineering
25	Dr. S.V. Bansod	Mechanical Engineering
26	Dr. Madhuri Bhavsar	Computer Science Engineering
27	Dr. A. M. Vaidya	Mechanical Engineering
28	Dr. V.H. Patil	Mechanical Engineering
29	Dr. S.V. Bansod	Mechanical Engineering
30	Dr. R.B. Barjibhe	Mechanical Engineering
31	Dr. H.A Salunkhe	Management
33	Dr. R.N. Khairnar	Account

INTERNATIONAL JOURNAL OF SCIENCE, SPIRITUALITY, BUSINESS AND TECHNOLOGY
(IJSSBT)
Special Issue: International Conference on Global Trends in Science, Technology, Humanities, Commerce & Management 2022
(ICGTSTHCM 2022)

Table of Contents

Volume 8, No.2, January 2022

PRATIBHA: INTERNATIONAL JOURNAL OF SCIENCE, SPIRITUALITY, BUSINESS AND TECHNOLOGY (IJSSBT)
Special Issue: International Conference on Global Trends in Science, Technology, Humanities, Commerce & Management 2022 (ICGTSTHCM 2022)
Vol. 8, No. 2, January 2022,ISSN (Print) 2277-7261

A REVIEW ON EXTRACTION OF ESSENTIAL OILS BY HYDRODISTILLATION

Vijay Sangore[1], Dr. Pratima Gajbhiye[2]*

[1]SSBT's COET, Jalgaon,[2]Lovely Professional University, Punjab
[1*]sanvijay2912@gmail.com [2]pratima.24280@lpu.co.in

Abstract

Essential oils are basically plant extracts. They're made by steaming or pressing various parts of a plant (flowers, bark, leaves or fruit) to capture the compounds that produce fragrance. Essential oil finds extensive applications in variety of consumer goods apart from medicinal and antibacterial activity. Though various methods available to obtain essential oils from plant extract, hydrodistillation is widely accepted method of extraction. Hydro-distillation uses water (steam) as an extraction solvent to recover volatile and polar components of plant materials. As the hydrodistillation method of extraction of essential oils is easy to execute and operate, it can provide the sustainable solution for improving socio-economic structure of underprivileged farmers.

Keywords: Essential oils, Extraction, Hydrodistillation **Introduction:**

Essential oils obtained from plants found extensive applications in variety of consumer products including cosmetics, perfumes, soaps & detergent industries, in production of pharmaceuticals, confectionary [1] products, alcoholic beverages, toiletry consumer products and many more consumer oriented valuable products. These essential oils are minor products as compared to conventional agricultural production, but still they cannot be ignored as they found widespread range of usages in commercially important consumer products, in spite of their presence in lower amounts. One cannot imagine making of soft drinks, deserts, body lotions without them. Essential oil therapy, which is also known as aromatherapy [2] improves health of body and mind, involves the use of medicinally important plant extracts. Traditional techniques adopted for the recovery of essential oil are known from ancient times.

Essential oils are generally extracted by distillation process, often by using steam. Solvent extraction, absolute oil extraction, resin tapping, wax embedding, and cold pressing are the techniques available and used for oil extractions.

Water distillation, steam distillation, combination of water and steam distillation are the commonly accepted and used methods of oil extraction on commercial basis. Hydro distillation is one of them, which involve use of water or steam. This technique is used for the extraction of essential oils and compounds from plant materials, since long times.

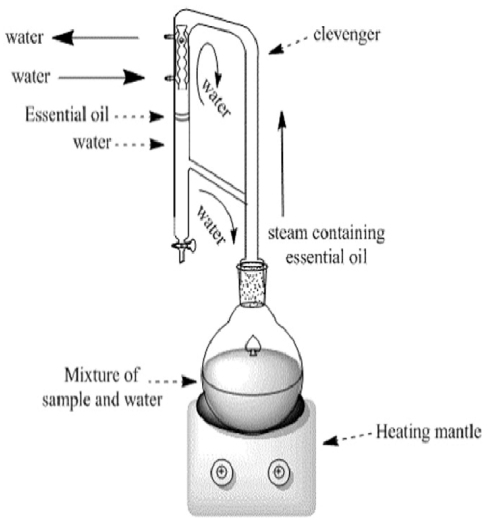

Schematic set-up for hydrodistillation

A plant matrix when it is used in hydrodistillation, water and steam plays a vital role to free the bioactive compounds from it. From drying of essential oils and other bio-active compounds sodium sulfate in anhydrous form is used. Temperature plays an important part in hydrodistillation and it is established to perform hydrodistillation operation well above the boiling point of water. But this high temperature also has the disadvantages of losing important volatile components and other valuable temperature sensitive bio-active compounds.

Industrial set-up for hydrodistillation

In actual practice for extraction of essential oil from plant materials, plant material is placed along with water which is present in sufficient quantity in a vessel or tank. These contains of the vessel are allowed to boil by heating medium. Sometimes steam is also injected to facilitate extraction. The combination of steam and boiling water, volatile essential oil separates out from the plant bodies. These volatile components alternatively taken away by water vapor and collected in receiving flask after condensation. Clevenger apparatus [4] is a set-up available to carry out hydrodistillation.

The technique gas chromatography coupled to mass spectrometry (GC-MS)[3] are used for the analysis of volatile and semi-volatile compounds found in plant materials during extraction by hydrodistillation. Along with that chemical composition, physical properties and yield percentage of essential oils are the parameters investigated during characterization.

Discussion:

Essential oils can be extracted by variety of methods, but hydrodistillation dominates rests by providing easy applicability, yield and quality of oils extracted. Numerous researches are going in different parts of the world to extract oils from local variety of plants. Essential oils are extracted from various parts of plants such as stem, flowers, leaves, fruits, roots.

Nur Nasulhah Kasim &etl. studied potential activity of Cinnamon essential oil as a natural insecticides and ants repellent[5] and found that solvent extraction shows an effective method on cinnamon essential oil extraction with positive insecticidal and repellent activity on ants.

Yu-Chang Su etl studied essential oil compositions and antimicrobial activities of various parts of Litsea cubeba[6] and found that essential oils present a potentially good choice as antibacterial agents.

Ahlem Haj Ammar &etl. carried research on optimization of operating conditions[7] of Tunisian myrtle (Myrtus communis L.) essential oil extraction by a hydrodistillation process and found that experimental design methodology could efficiently be applied to characterize the analytical parameters affecting the hydrodistillation process.

Rui Wang, Ruijiang Wang and BaoYang carried out investigations on extraction of essential oils from cinnamon leaves[8] and identification of volatile compound compositions and trans-Cinnamaldehyde was detected to exist in all the species tested as an important volatile component.

Ana Cristina, Atti-Santos &etl. carried extraction of essential oils from lime[9] (Citrus latifolia Tanaka) by hydrodistillation and supercritical carbon dioxide for various parameters and proposed optimum conditional parameters for oil extraction.

Mohammad H.Eikania &etl. carried out research on subcritical water extraction[10] of essential oils from coriander seeds (Coriandrum sativum L.) and studied extraction efficiencies by subcritical water extraction, hydrodistillation and Soxhlet extraction.

Various technologies are adopted by numerous research groups to obtain essential oils from plant extracts. Amongst these steam and boiling water combination through hydrodistillation is found to be most suitable as far as yield, qualitative and quantitative parameters are considered. This relatively simple and easy to operate technique, hydrodistillation can provide a sustainable solution for extracting oils from parts of the plants. This technique can be easily understood, installed, executed and operated by even uneducated population which is living in rural ares of developing countries like India. If such types of small essential oil extraction plants are installed by government agencies or by non profit organizations in rural areas and if they are handed over to the under privileged people, definitely it will boost their confidence for improving their socio-economic status. At the same time it will also reduce their dependency and really the dream of Atmanirbhar Bharat will come into existence.

Conclusion:

Agriculture sector is increasingly dominated by large scale industrial production, the production of essential oils from plant extracts is still conquered by small farmer communities and as such makes an important contribution in earning, and livelihoods of relatively poor rural populations in economically emerging countries especially of Asia region. Impact of change in export/import policies for agricultural based commodities, falling prices of agricultural commodities, decreasing profitability of agricultural crops, dependency on monsoon, maintenance of ecological balance are the problems faced by agricultural sector.

A economical extraction of essential oils can provide the viable solution to the the problems which are faced by low income agricultural groups and small farmers. As the hydrodistillation method of extraction of essential oils is easy to execute and operate, it can provide the sustainable solution for improving socio-economic structure of underprivileged farmers.

References:

[1] Sharmeen Jugreet, Shanoo Suroowan,R.R.Kannan,Rengasamy, M.Fawzi, Mahomoodally ,Elsevier, Trends in Food Science & Technology, Volume 101, July 2020, Pages 89-105
[2] Debra Rose Wilson, Ph.D., MSN, R.N., IBCLC, AHN-BC, CHT Yvette Brazier on March 20, 2017
[3] Sandra, P, and Bicchi, C. Capillary gas chromatography in essential oil analysis. Germany: N. p., 1987. Web.
[4] Bouchra Louaste, Imane Nechad, Taha Elkamli, Abdelhak Bouia, Mustapha Taleb, Mahdi Chaouch, and Noureddine Eloutassi , The Scientific World Journal, vol. 2019, Article ID 3659432, 6 pages, 2019. https://doi.org/10.1155/2019/3659432
[5] Nur Nasulhah Kasim etl., Potential of Cinnamon essential oil as a natural insecticides and ants repellent, International Journal of Scientific and Research Publications, Volume 4, Issue 7, July 2014 1 ISSN 2250-3153
[6] Yu-Chang Su, Chen-Lung Ho, Essential Oil Compositions and Antimicrobial Activities of Various Parts of Litsea cubeba from Taiwan'Sage journa https://doi.org/10.1177/1934578X1601100425
[7] AH Ammar, F Zagrouba Optimization of operating conditions of Tunisian myrtle (Myrtus communis L.) essential oil extraction by a hydrodistillation process using a 24 complete factorial.,Wiley online library, https://doi.org/10.1002/ffj.2011
[8] Rui Wang, Ruijiang Wang, Bao Yang, Extraction of essential oils from five cinnamon leaves and identification of their volatile compound compositions, Elsevier, Innovative Food Science & Emerging Technologies, Volume 10, Issue 2, April 2009, Pages 289-292
[9] Ana Cristin, Atti-Santos, Marcelo Rossato, Luciana Atti Serafini, Eduardo Cassel, Patrick Moyna Extraction of essential oils from lime (Citrus latifolia Tanaka) by hydrodistillation and supercritical carbon dioxide, Engineering and Technology, Braz. arch. biol. technol. 48 (1) Jan 2005 https://doi.org/10.1590/S1516-89132005000100020
[10] Mohammad H., Eikania, Fereshteh Golmohammada, Soosan Rowshanzamirb Subcritical water extraction of essential oils from coriander seeds (Coriandrum sativum L.), Elsevier, Journal of Food Engineering, Volume 80, Issue 2, May 2007, Pages 735-740

PRATIBHA: INTERNATIONAL JOURNAL OF SCIENCE, SPIRITUALITY, BUSINESS AND TECHNOLOGY (IJSSBT)
Special Issue: International Conference on Global Trends in Science, Technology, Humanities, Commerce & Management 2022 (ICGTSTHCM 2022)
Vol. 8, No. 2, January 2022,ISSN (Print) 2277-7261

A Review on performance simulation of heat pipe based Li-ion battery thermal management system

Mr. Satish Patil
Research Scholar, Mechanical Department SSBT's College of Engineering, Jalgaon
Srpatil247@gmail.com
Dr. Prajitsen Damle
Associate Professor, Mechanical Department SSBT's College of Engineering, Jalgaon
Pgdamle2@gmail.com

ABSTRACT
It is essential to maintain desired temperature range to obtain an optimum performance of battery. Battery thermal management system reduces the surface temperature. Literature review suggests the use of hybrid cooling system along with heat pipe based cooling. Battery pack containing five cells are tested for three different cooling systems; natural convection, cold plate and heat pipe with extended fins. The comparative analysis shows results for various discharge rates of battery i.e. 4C, 6C and 8C. With reference to the simulated results it seems that temperature at the centre of each battery is higher compare to the other region. The shows that heat pipe effectively reduce battery temperature within desired limit for various discharge rates.

I. INTRODUCTION

Every country in the world wants to gain a title of developed country rather than developing or undeveloped country. While developed countries aiming for more betterment in different sectors. This race is bounded with one common point i.e. Energy. So, there is direct relation between energy utilization and development of country. In the fulfillment of this objective from last few decades different energy resources are mugged up like fossils fuels, oils, nuclear etc. This leads to global issue of environmental pollution. Different types of emissions caused climatic changes which are hazardous for us and mother earth as well. Transport section is the biggest contributor around 24% for direct carbon dioxide emission to the environment after fuel combustion [1].

On the other side we are still short with energy availability for our development. To resolve this issue of energy shortage and global pollution a sustainable solution is required. Sustainable development will take care of environmental, economical development as well. Concept of electric vehicles (EVs) strongest alternative for the internal combustion engines, which may reduce the air pollution up to certain extent. Li-ion batteries gaining popularity due their numerous advantages like zero emission, recyclability, good power density in the electronic appliances and EVs.

Although Li-ion batteries are having positive attribute, it has few limitations during high current applications and overheating problem due to excessive heat generation [2]. The Li-ion batteries perform better for the temperature range 15 ^{0}C to 40 ^{0}C [3]. Operation of batteries below and above to the given limits may lead to the serious issue like explosion or short circuit. Therefore it is essential to provide optimize thermal management system for given temperature range.

Henceforth many of the researcher working extensively on developing optimized battery thermal management system. Researchers categorized these systems in to two basic types i.e. active and passive cooling [6]. The active cooling preferred the use of air and liquid to fulfill the target, while passive cooling utilizes phase change materials (PCM), heat pipe and nano materials. Each of these methods has their own limitations and advantages. While choosing a BTMS few factors needs to be keep in mind like volumetric constraints, cost of installations and efficiency of system.

Air and liquid cooling comes under the external cooling category. Many researchers worked on natural and forced cooling and reported their work. In comparison with natural cooling, the forced cooling serves better results [4]. The air cooling consistently increasing day by day by optimizing few parameters like; cell arrangement, air flow rate and flow path etc. [5, 6, 7]. Though air cooling is easy and simple to implement, its use is limited due to low heat carrying capacity with increased battery pack.

The passive cooling can satisfy requirement of battery thermal management along with active cooling system. On the other hand, liquid cooling is a successful method for thermal management of high-power battery packs. The limitations of individual

systems can be overcome by optimize battery thermal management system (BTMS); which may provide solution to overcome restrictions of individual methods. The BTMS promotes the use of two or more cooling systems to improve the performance of system. This work tries to highlight use of heat pipe based hybrid cooling systems. In this heat pipe can be comprise with other systems like air cooling, cold plate, PCM etc. Heat pipe assisted cooling compared individually with natural cooling, cold plate and heat pipe with extended fins. This innovative idea can be betterly optimize and much work is already going to design and optimize BTMS for EVs.

II. LITERATURE SURVEY

Li-ion batteries are main power source of energy for automotive industry in the future due to its numerous advantages. Hence to ensure maximum effective utilization of power source is of prime importance. Previous studies identified that, battery performance is much more affected by battery operating temperature. The efficient working temperature range for the battery is 25 ^{0}C to 40 ^{0}C [4, 5]. If the battery temperature increased beyond this limit, its performance decreasing considerably.

So, battery thermal management is an integrated component for battery pack design. Zhang *et al*. [17] enlisted basic functions of BTMS, which are: maintain the desired temperature range for battery efficient operation, dissipate excessive heat and preheat the battery when required. The BTMS are categorized in to three parts: air, liquid and phase change material. Though air cooling method have significant advantage of simple design and light weight, it has comes up with challenge of increased volume of battery pack and low thermal conductivity. To prevail over this liquid cooling system comes with solution of high thermal conductivity. Liquid cooling proves an efficient technique in comparison with air cooling. Irrespective of this, it has some drawbacks like complex structure design, high pumping power and leakage risk.
With reference to above highlighted points a concept of hybrid BTMS is introduced in which two categories of BTMS are united together to accomplish superior results. Wei and Agelin-Chaab [15] collective air cooling and liquid cooling BTMS. The authors conducted an experimental study utilizing a arrangement of evaporative phase change, convective, and conductive cooling effects. The hybrid BTMS displayed a 56% and 20% improvement in temperature uniformity and battery cooling, respectively. Saw *et al*. [35] also investigated hybrid battery pack with mist cooling. The results of the study accomplished that 3% mist and 5 g/s mass flow rate is essential to maintain the cell's surface temperature to less than 40 ^{0}C. Hybrid BTMS are displaying promising results and more follow a line of investigation is required in this area.

So, heat pipe based battery thermal management could be alternative near future. Various authors worked on heat pipe based cooling systems. The summery of that literature mentioned in table1.1.

Reference	**Method**	**Remark**	**Scope for future work**
Q.L. Yue *et. al* [9]	Micro heat pipe, air convection and spray water	Significant reduction in maximum temperature	1.8% power loss for water circulation, High discharge rate
Yunhua Gan *et. al* [10]	Heat pipe along with Aluminium sleeves	Significant reduction in maximum temperature	High temperature at centre of battery pack Shape of heat pipe and Sleeve material
Hamidreza Behi *et. al* [11]	Heat pipe copper sheet (HPCS)	Temperature uniformity improved by 73.4%	High temperature at centre of battery pack Heat pipe fluid
Hamidreza Behi *et. al* [12]	Sandwiched heat pipe cooling system (SHCS) and air cooling	Maximum temperature reduced by 33.4%	Battery pack module should be tested Optimize of the SHCS in different boundary conditions and wet cooling

			option to increase the efficiency of the cooling system.
Yuan Li *et. al* [13]	Heat pipe and cold plate	Temperature uniformity improved by 6.94%	Should be high tested for discharge rate Coolant flow can be improved
Mohamed H. A. Elnaggar *et. al* [14]	Finned L Shape heat pipe	Thermal resistance reduced	Integration of heat pipe with liquid cooled systems required
Jianqin Wang *et. al* [15]	Optimization of heat pipe geometry	Best performance at 4 mm thickness and 60 mm height	CFD simulations can be done for battery pack module
Hussein Mbulu *et. al* [16]	L and I shape heat pipe testing under high power input	Maximum Temperature is in desirable range	Evaporator design can be improved, higher thermal conductivity cooling liquid.
Z. Liang *et. al* [17]	Flat heat pipe with cell to cell variation	Maximum Temperature and temp. difference limits to 50 ^{0}C and 5 ^{0}C	Insufficient cooling capacity for high tolerance cells
Kai Chen *et. al* [23]	Heat pipe with PCM material	Maximum Temperature difference reduced to 30%	Effective PCM material thickness is required
Rui Zhao *et. al* [24]	Heat pipe with wet cooling	Maximum Temperature is in desirable range	High discharge rate

Table 1.1 Summery of heat pipe literature.

III. METHODOLOGY

Electrochemical reactions exhibit large amount of heat during high discharge rates. Movement of electrons during charging and discharging results in heat generation. The electrochemical reactions represented below:

At positive electrode: $LiFePO_4 \underset{\text{Discharging}}{\overset{\text{Charging}}{\rightleftharpoons}} Li_{1-x}FePO_4 + xLi^+ + xe^-$ … (1)

At negative electrode: $xLi+ xe- + 6C \underset{\text{Discharging}}{\overset{\text{Charging}}{\rightleftharpoons}} LixC6$ … (2)

Simplified transient heat transfer model for prismatic battery is considered neglecting the heat transfer due to radiation and convection inside the battery. Basically this work comprises testing experimental set for three different battery packs: 1) Natural Convection, 2) Cold Plate, 3) Heat pipe with extended fins. For natural convection battery pack the batteries are equally spaced and air gap of 3 mm is maintained.

In case of cold plate, batteries are separated by cold plate of given size [1].

For the third case, heat pipe is used along with extended fins. The experiments were conducted for different discharge rates like 4C, 6C, 8C and rise in maximum temperature to analyze the cooling performance of battery in comparison with each system. The experimental results validated with simulation on STAR CCM+. Free convection boundary convection was imposed [1]. Five battery cells in series connected to each other to form battery module pack. The specifications of battery cell listed in table 4.1. The aim of experimental set up was to record the thermal effects and modify battery thermal management. The battery packs are sandwiched by flat heat pipes from both sides as shown in figure 4.1.

PRATIBHA: INTERNATIONAL JOURNAL OF SCIENCE, SPIRITUALITY, BUSINESS AND TECHNOLOGY (IJSSBT)
Special Issue: International Conference on Global Trends in Science, Technology, Humanities, Commerce & Management 2022 (ICGTSTHCM 2022)
Vol. 8, No. 2, January 2022,ISSN (Print) 2277-7261

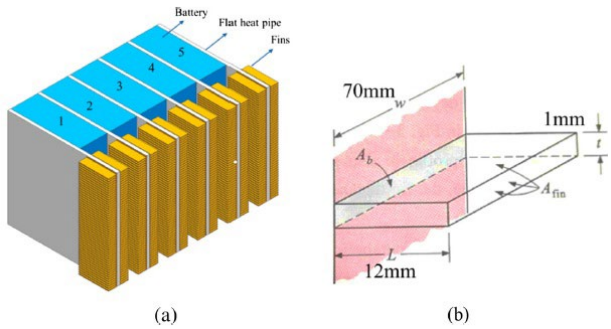

Figure 4.1: Battery packs with heat pipe and extended fins [1].

Parameter	Value	Parameter	Value
Battery	LiFePO4	Height	100 mm
Shape	Prismatic	Normal Capacity	8.5 Ah
Length	70 mm	Charging voltage (V)	3.65
Width	27 mm		

Table 4.1: Battery specification [1].

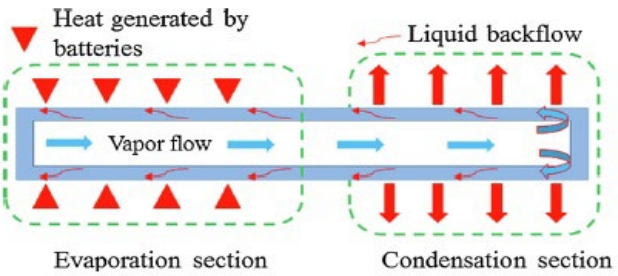

Figure 4.2: Heat transfer in heat pipe [4]

Evaporation section of flat heat pipe is in contact with battery surface, from where heat is carried away to the condensation section. The condensation section of heat pipe comprised with arrangement of additional fins to dissipate as much as possible heat form system as shown in figure 4.2.

The specification of heat pipe and fins are tabulated below in table 4.2.

Parameter	Heat pipe	Fins
Length	70 mm	70 mm
Width	12 mm	12 mm
Thickness	3 mm	1 mm
Material	Aluminum	Aluminum
Working fluid	Water or ethanol	Air

Table 4.2: Specifications of heat pipe and Fins [1].

IV. SUMMARY

A. Thermal behavior at 2C dischege rate

The data shows that the temperature during the charge process was much lower than that during the discharge process. Therefore, only the surface temperature during discharging is discussed in this section. Fig. 5.1 shows the temperature variations with time at a 2C discharge rate. The temperature difference at the symmetry point did not exceed 0.2 ^{0}C, and the temperature uniformity on the front and back of the battery was good. Hence, only the temperatures at five locations on one surface were collected and analyzed in the subsequent experiments.

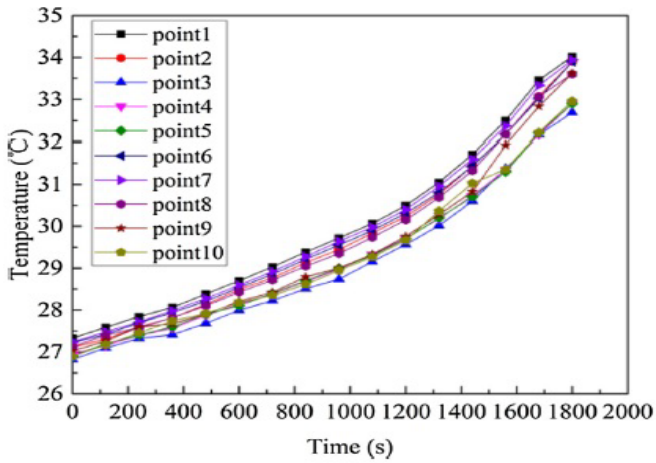

Figure 5.1: Temperature distribution in battery pack [1]

The maximum temperature, the temperature difference between different batteries in the module was also of major concern. The thermocouples records that the temperature for discharging process much higher as compare to charging process.

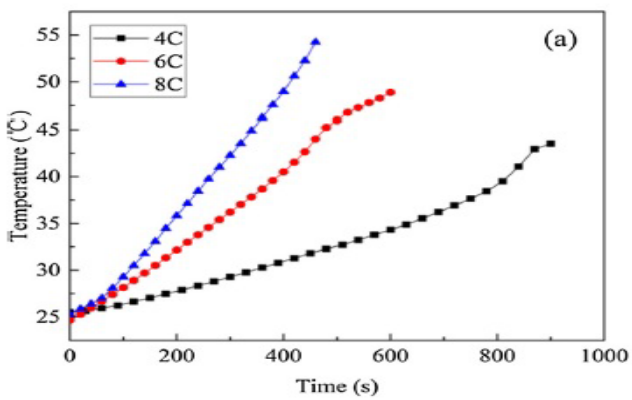

Figure 5.2: Temperature variation for different discharge rates [1]

The maximum temperature and temperature differences across the pack level are significant factors that may influence the long-term performance of a battery system. Fig. 5.2 shows the maximum temperature and temperature difference distribution of the battery module at different discharge rates (4C, 6C, and 8C). When the battery module was discharging at 6C, the surface maximum temperature reached 48.9 ^{0}C

at the end of the discharge process. The maximum temperature was up to 54.3 ^{0}C for a discharge rate of 8C, which greatly exceeded the safe temperature range. Therefore, the battery thermal management system for a high discharge rate of the battery is particularly important.

B. Simulation of heat pipe with extended fins

Figure 5.3 shows the temperature distribution contour of the flat heat pipe cooling system at a 4C discharge rate. The internal temperature field and the center section (x=35 mm) temperature distribution contours are shown in figure 5.3. The surface temperature of the battery pack far from the fins was higher, and the highest temperature appeared in the middle of the battery pack, which was about 30.5 ^{0}C, while the average temperature of the fins was 27.7 ^{0}C. This was mainly because the heat transfer rate of the battery pack near the side of the flat heat pipe was faster, and the heat could be dissipated quickly. The lowest temperature of the battery pack was 27.2 ^{0}C, and the maximum temperature was 30.5 ^{0}C at a 4C discharge rate, which was lower than the upper limit of the safe working temperature.

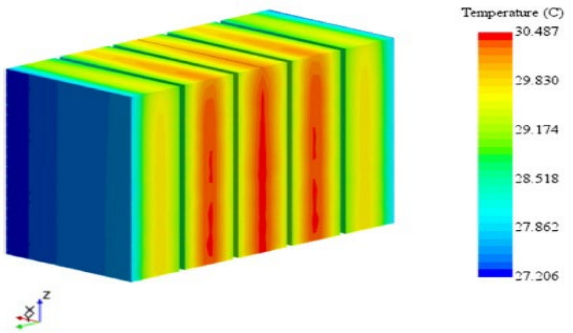

Figure 5.3: Battery pack temperature distribution countor [1]

Moreover, the maximum temperature difference between the battery packs was only 3.3 ^{0}C, which meets the requirement of the maximum temperature difference within battery packs.

C. Comparison at different discharge rates

To highlight the advantages of the flat heat pipe cooling system, we set up two other battery packs for comparison to analyze the temperature variations under different discharge rates (4C, 6C, and 8C). In one pack, natural convection occurred, and every cell of the pack had a 3mm air gap. The other pack used aluminum plate cooling, where the flat heat pipes were replaced with aluminum plates of the same size and configuration. Figure 5.4 shows the maximum temperature variations of the battery pack under the three thermal management modes. In figure 5.4, at the beginning of the discharge, there was little difference between the three modes. Over time, the temperatures of the batteries increased. The maximum temperature was 42.4 ^{0}C under natural convection.

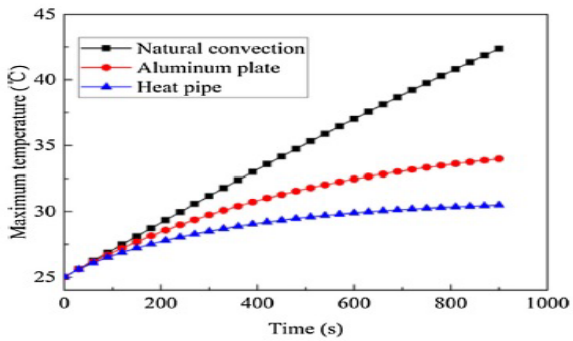

Figure 5.4: Battery surface temperature curves for 4C [1]

For the aluminum plate cooling and flat heat pipe cooling, the maximum temperatures were 34.0 and 30.5 ^{0}C, respectively. Compared with natural convection and aluminum plate cooling, the maximum surface temperature of the flat heat pipe was less by 28.1% and 10.3%, respectively. Thus, the heat dissipation due to the flat heat pipes was significant. As shown in Fig. 5.5, the discharge time was 600 s. Under natural convection, the temperature exceeded 40 ^{0}C at 380 s, and the temperature reached 49 ^{0}C by the end of the discharge, corresponding to a temperature rise rate of 0.04 ^{0}C /s. The maximum temperature did not exceed 35 ^{0}C under heat pipe cooling. The final temperature rises for the natural convection and aluminum plate cooling were 24.2 ^{0}C and 15.0 ^{0}C, respectively.

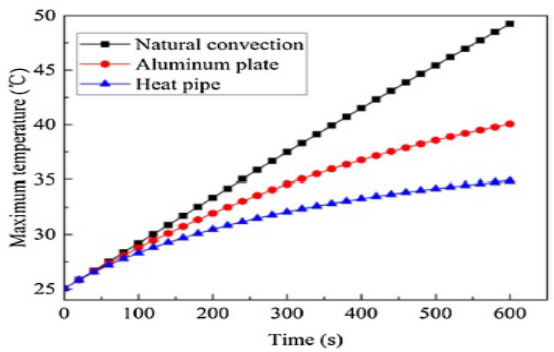

Figure 5.5 Battery surface temperature curves for 6C [1]

The maximum temperature for the heat pipe cooling was 29.2% and 12.9% less than the surface temperatures for the natural convection and aluminum plate cooling, respectively. When the discharge rate increased to 8C, the temperature of natural convection increased sharply to about 53 ^{0}C, as shown in fig. 4.6, which exceeds the design requirements.

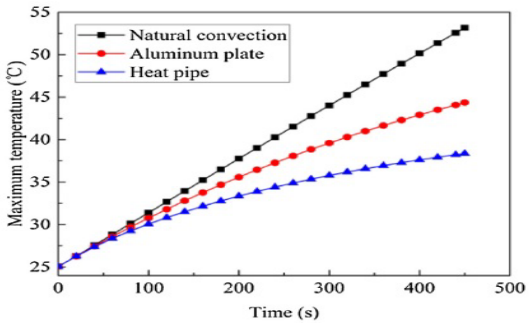

Figure 5.6 Battery surface temperature curves for 8C [1]

When the flat heat pipes were added to the battery thermal management system, the maximum temperature was no more than 38 ^{0}C. Although the aluminum plate cooling mode was better than the natural convection, the maximum temperature still increased to 44 ^{0}C, which is 6 ^{0}C higher than that of the flat heat pipe cooling mode. During the 8C rate discharge, the temperature rise rate of the flat heat pipe was 0.03 ^{0}C /s. Compared with natural convection and aluminum plate cooling, the temperature rise rate was reduced by 52.7% and 31.1%, respectively.

V. Conclusion

Battery thermal management system is an essential component to utilize battery energy efficiently. The temperature of battery during charging and discharging is major concern; especially for battery pack at high discharge rates. The heat pipe is an effective solution as compare to air cooling. But the performance of battery at high discharge is still challenge. Flat heat pipe achieves good results as compare to circular heat pipe; due to maximum surface contact area. The volumetric constrains will be the major challenge for such hybrid systems.

During this study three different systems i.e. natural convection, cold plate and heat pipe with extended fins are compared. A pack of five prismatic battery packs optimized for discharge rates 4C, 6C and 8C. Uniform temperature distribution is observed at the front and back of batteries as compare to centre of battery. The hybrid cooling with heat pipe shows better results even for high discharge rates with maximum temperature around 40 ^{0}C. It proves that heat pipe based cooling systems perform better than any other systems if comprised with other systems. The performance of such systems can be improved, if systems are optimize for geometry of heat pipe, volumetric constrains, high discharge rates and large battery pack module etc.

VI. REFERENCES

1. A. Tomaszewska, Z. Chu, X. Feng, (2019) “Lithium-ion battery fast charging: A review” E Transportation 1: 100011
2.. Hamidreza Behia, Danial Karimi (2020) “A new concept of thermal management system in Li-ion battery using air cooling and heat pipe for electric vehicles” Applied Thermal Engineering 174:115280.
3. S. Arora, (2018) “Selection of thermal management system for modular battery packs of electric vehicles: A review of existing and emerging technologies” J. Power Sources
400: 621–640.
4. Fan LW, Khodadadi JM, Pesaran A A, (2013) “A parametric study on thermal management of an air-cooled lithium-ion battery module for plug-in hybrid electric vehicles” J Power Sources; 238:301–12.
5. He F, Li Xs, Ma L. (2014) “Combined experimental and numerical study of thermal management of battery module consisting of multiple Li-ion cells” Inte. J Heat Mass Transfer; 72:622–9.
6. Park S, Jung D H. (2013) “Battery cell arrangement and heat transfer fluid effects on the parasitic power consumption and the cell temperature distribution in a hybrid electric vehicle” J Power Sources 2013; 227:191–8.
7. Wei Jiang, Jiateng Zhao, Zhonghao Rao, (2021) “Heat transfer performance enhancement of liquid cold plate based on mini V-shaped rib for battery thermal management” Applied Thermal Engineering 189: 116729.
8.. Q.L. Yue, C.X. He (2021) “A hybrid battery thermal management system for electric vehicles under dynamic working conditions” Inte. Journal of Heat and Mass Transfer 164: 120528.
9.. Yunhua Gan, Linfeng He (2020) “A numerical study on the performance of a thermal management system for a battery pack with cylindrical cells based on heat pipes” Applied Thermal Engineering 168:116927.
10.. Hamidreza Behi *et. al* (2020) “A new concept of thermal management system in Li-ion battery using air cooling and heat pipe for electric vehicles” Applied Thermal Engineering 174:115280.
11 Yuan Li, Hao Guo (2021) “Investigation on liquid cold plate thermal management system with heat pipes for LiFePO4 battery pack in electric vehicles” Applied Thermal Engineering 185:116382.
12. Q. Wang, B. *et. al* (2014) “Experimental investigation on EV battery cooling and heating by heat pipes” Appl. Therm. Eng. 88: 54–60.
13.. Park H. (2013) “A design of air flow configuration for cooling lithium ion battery in hybrid electric vehicles”. J Power Sources, 239:30–6.
14. Mohamed H. A. *et. al* (2013) “Experimental and Numerical Studies of Finned L-Shape Heat Pipe for Notebook-PC Cooling” IEEE Transactions on Components, Packaging and Manufacturing Technology, Volume: 3, Issue: 6.
15. Jianqin Wang *et. al* (2019) “Sensitivity analysis of factors influencing a heat pipe-based thermal management system for a battery module with cylindrical cells” Applied Thermal Engineering Volume 151, Pages 475-485.
16. Z. Liang a , R. Wang (2021) “Systematic evaluation of a flat-heat-pipe-based thermal management: Cell-to-cell variations and battery ageing” Applied Thermal Engineering
Volume 192: 116934.
17. He F, Wang HT, Ma L. (2015) “Experimental demonstration of active thermal control of a battery module consisting of multiple Li-ion cells” Int J Heat Mass Transfer 91:630–9.
18. Fan H, Lin M. (2015) “Thermal management of batteries employing active temperature control and

reciprocating cooling flow" Int J Heat Mass Transfer 83:164–72.

19. Tong W, Somasundaram K *et. al* (2016) Thermo-electrochemical model for forced convection air cooling of a lithium-ion battery module Applied Thermal Engineering, 99:672–82.
20. Smart MC, Ratna kumar BV et al. (2003) "Improved low-temperature performance of lithium-ion cells with quaternary carbonate- based electrolytes" J Power Sources, 119–121:349–58.
21. Ouyang MG *et. al* (2020) "Low temperature aging mechanism identification and lithium deposition in a large format lithium iron phosphate battery for different charge profiles" J Power Sources, 286:309–20.
22. Kai Chen, Junsheng Hou *et. al* (2021) "Design of battery thermal management system based on phase change material and heat pipe" Applied Thermal Engineering, 188:116665.
23. Yu Kh, Yang X, Cheng YZ, Li CH. (2014) "Thermal analysis and two-directional air flow thermal management for lithium-ion battery pack" J Power Sources; 270:193–200.
24. Zhuqian Zhang, Ke Wei (2020) "Experimental and numerical study of a passive thermal management system using flat heat pipes for lithium-ion batteries" Applied Thermal Engineering 166: 114660.

PRATIBHA: INTERNATIONAL JOURNAL OF SCIENCE, SPIRITUALITY, BUSINESS AND TECHNOLOGY (IJSSBT)
Special Issue: International Conference on Global Trends in Science, Technology, Humanities, Commerce & Management 2022 (ICGTSTHCM 2022)
Vol. 8, No. 2, January 2022,ISSN (Print) 2277-7261

A STUDY ON WOMAN EDUCATION : A Pilot Study

Dr. Saroj Patil. Asst. Prof (MBA)

SSBT's College of Engineering and Technology, Jalgaon.

Email: sarojpatil74@rediff.com

ABSTRACT

Education is an important mechanism for improving woman's social and economic status, which cause health problems. Female education must be helps for the improvement and growth of the society. This paper presents what we know now about the education of woman throughout their lives and across the different regions of the world. Everyone must get an opportunity to be educated. The right to free and compulsory primary education, without discrimination and of good quality, has been reaffirmed in all major international human rights conventions. Many of these same instruments encourage, but do not guarantee, post-primary education. These rights have been further elaborated to address issues like quality and equity, moving forward the issue of what the right to education means, and exploring how it can be achieved.

KEYWORDS: woman, right education.

1. INTRODUCTION

Woman are an integral part of every economy. For development and cordial growth of a nation would be possible only when woman are equality treated in progress with men. Empowerment of woman is must for economic growth. Woman development, economic development is of all most important in order to achieve a tenable development of society

Woman, the word sounds so powerful. Since eternity, woman have played a role more important than men and that is no exaggeration. The world would not have been the same lovely adorable and livable place without wonderful contribution so selflessly made by woman. It has been said that, you teach a female and you build up a nation and truth can't be closer than that. Woman have always carried the burden of being a wife, mother, sister all on their own and we need not to explain how magnificently they have carried this position.

In India the literacy rate of woman is much lower than men because boys receive more schooling than girls.. So stark is the gender inequality in India that it is one of the 43 countries in the world where male education percentage are at least 15 percent greater than female percentage. Educational deprivation is intimately associated with poverty.

However, modest improvement is gradually coming up in educational level of woman. After independence of India many changes are made to improve the education towards woman. Many laws have also been passed. Many programmers in the areas of education, health and employment have been initiated for development of woman, rural as well as urban. It is observed that education percentage are going up and fertility rates are down enough . Technical Institutions for woman and distinct emphasis on health, nutrition and family welfare programmers' etc. are some such initiatives.

Woman education in India has a key role in the development of country . Educating woman uplifts her life and also her family too. A girl child would provide good better future guidelines for her education. An educated woman is independent and can make her own decision firmly and confidently does not depends on others for everything,

Women have very less educated ratio then men. Very less girls are educated and send to schools and colleges. The Indian government has launched many schemes for female literacy . The aim is to bring down female illiteracy ratio upto some extent.

Education of women plays an important role to upgrade living standards. Growth in women literacy ratio upgrades the life quality,

OBJECTIVE OF THE STUDY:

1. To study the woman education issues in general
2. To study the family support to encourage the woman for higher education
3. To study the financial help for woman in their education

Education Equality

Higher involvement of women in literacy action the gender gap in education level is decreased. The world has gained growth equality in co- education very less countries have completed target at all level of literacy.

Women Education In India

Women education is very important for the country to fully develop society. It is like an effective medicine to cure a patient completely. Educated women are the weapon who fight for positive impact on the Indian society through their contribution at home and professional fields. Education changes world view improves their chances of employment facilities their participation in several studies indicate that educated women progess in each fields. Total enrolment in higher education has been estimated to be 37.4 million with 19.2 millon males and 18.2 million females. Females constitute 48.6 percent of the total enrolment .

The major schemes

The Balika Samriddhi Yojana: Lauched in 2021 . Is a scholarship program that gives **financial assistance to poor girls** and their families. The main goal is to improve girls' social status, raise and increase enrolment particularly for females in school.

CBSE Udaan Scheme: : : Lauched in 2021 . This program is one of the most important government girl child schemes in India that aims to increase the number of girls enrolled in prestigious **engineering and technical colleges** across India. Free course materials/ online resources for female students in 11th and 12th grades, such as video study materials. On weekends, virtual contact classes for female students in 11th and 12th grades are held

National Scheme of Incentives to Girls for secondary Education: : Lauched in 2021 The aim of the scheme is to encourage girls to continue secondary education.A pan-India scheme is administered by the Department of School Education and Literacy, Human Resource Development Ministry, Government of India.The scheme is primarily designed to assist girls from India's lower socioeconomic levels in completing their secondary education. Under the initiative, a meritorious girl will **receive Rs. 3000** as a fixed deposit, which she will be able to withdraw with interest once she reaches the age of 18 and has passed her 10th-grade exam.

Skills Training in Higher Education

The National Education Policy 2020 envisages that the school curricula and pedagogy will aim for holistic development of learners by equipping them with key 21st century skills and reduction in curricular content to enhance essential learning and critical thinking. The policy emphasizes integration between vocational and academic streams in all schools and higher education institutions in a phased manner. As per policy vocational education will start in school from the 6th grade and will include internship.

HYPOTHESIS OF THE STUDY:

H0: Education of woman is not allowed in Joint family structure as compared to nuclear family.
H1: Education of woman is allowed in Joint family structure as compared to nuclear family.

METHODOLOGY OF STUDY

The research design for the study is fact finding in nature. The response of the respondent were through visiting personally and discussing with them. By the survey of 200 woman were selected as a sample size from Jalgaon city. After searching the literate woman and their higher qualification after survey the researcher found a lot of woman were lack of higher education.

TESTING OF HYPOTHESIS

H_0 = Higher education of girls is not preferred in nuclear family structure as compared to Joint family structure.
H_1= Higher education of girls is preferred in nuclear family structure as compared to Joint family structure

Chi-square Calculator

	Secondary Education	**Higher Education**	***Marginal Row Totals***
Joint Family	30 (39) [2.08]	48 (39) [2.08]	78
Nuclear Family	70 (61) [1.33]	52 (61) [1.33]	122
Marginal Column Totals	**100**	**100**	**200 (Grand Total)**

Result:
The Chi-square statistic is 6.8096. The P value is 0.009067. The result is significant at $p < 0.05$. Hypothesis is observe at 5% level of significance and degree of freedom is 1.

INTERPRETAION
Chi-square statistic is 6.09 that is more than table value of Chi-Square Distribution Table (3.84). That

means result is significant at $P < 0.05$. Hence null hypothesis is rejected. And H1 is Accepted.

FINDINGS

It was observed that 50% of girls are studied higher education in rural areas as compare to other qualification. We found that only 78% woman's family provides financially support to their girls for higher education.

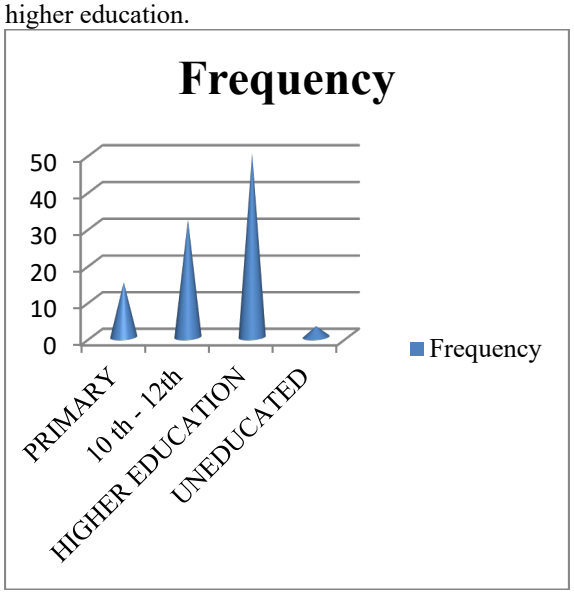

According to graph the education of girl child in respondent family mostly are higher educated i.e. 50%, 32% of girls are 10^{th}- 12^{th}, 15% of girls in primary education & 3% of girls are uneducated respectively. We found that 50% of girls are higher education in rural areas as compare to other qualification.

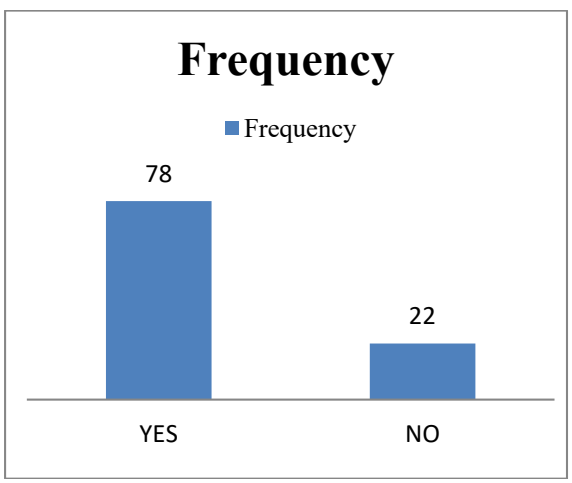

As per graph 78% woman answered YES to provide the financial support to girls in primary & higher secondary education and 22% woman answered NO for their education. We found that a rural areas woman to financial supports of girl's education is only i.e.78%.

CONCLUSION

"Education cannot wait for anyone" . The chances of women in various areas of the Indian economy have been increased by permitting and opportunity for girl rights to education. The study conclude that the women are finding difficulties by both internal and external problems.

Due to the actual imbalance against woman, compounded by hold up shortage, the development of woman's education in India has been a hard journey. Despite the efforts made by the Indian government over the past decades, the large gap between male and female education rates in India persists

This report examined woman's education and the factors that contribute to woman's dignity and well-being. The findings indicate that although against have been stated that woman are educated, problems still exist and woman continue to face challenges that carry higher education risk. All about the woman, those with lower economic and education are often at large risk.

Encourage the educational attainment, providing safe homes, schools and neighborhoods, and teaching healthy behavior, improve their status in society. Increase opportunities for woman. By increasing access to training and education and improving quality and access to child care, we can increase the number of opportunities available to woman. By changing woman's status in society.

REFERENCES / BOOKS

- Women and Men in India - 2011 13th Issue Central Statistics Office , Ministry of Statistics and Programme Implementation
- ICMR and ICSSR , *Health For All: An Alternate Strategy*, Published by Indian Institute of Education, 1981.
- Intemational Institute of Population Science (2000) National Family
- Health Survey 1998-99 (NFHS-2) I.I.P.S, Mumbai.

Website:

- www.shodhganga.com
- Wikipedia.com
- www.socscistatistics.com
- (http://www.who.int/healthinfo/survey/en/, accessed 18 June 2009).

PRATIBHA: INTERNATIONAL JOURNAL OF SCIENCE, SPIRITUALITY, BUSINESS AND TECHNOLOGY (IJSSBT)
Special Issue: International Conference on Global Trends in Science, Technology, Humanities, Commerce & Management 2022 (ICGTSTHCM 2022)
Vol. 8, No. 2, January 2022,ISSN (Print) 2277-7261

An Experimental Study on Performance of Titania Blended Rubbercrete

Sonali B. Patil[1], J.N.Kale[2],J.R.Mali[3],Dr.M.Husain[4]

[1]Civil Engineering Department,SSBT's College of Engineering & Technology, Bambhori, Jalgaon, MS, India.

[2]Civil Engineering Department,SSBT's College of Engineering & Technology, Bambhori, Jalgaon, MS, India.

[3] Civil Engineering Department ,SSBT's College of Engineering & Technology, Bambhori, Jalgaon, MS, India.

[4] Civil Engineering Department ,SSBT's College of Engineering & Technology, Bambhori, Jalgaon, MS, India.

borsesp14@gmail.com, jyntkale7@gmail.com,jyotimali23.71@gmail.com, ermujahidhusain@gmail.com

ABSTRACT

The waste tyres are creating several environmental hazards. At the same time natural aggregates required for concrete are depleting. Their over exploitation has created lot of environmental hazards. The use of rubber in concrete will solve both the problems with a single stroke. Apart from this, titania is being used in concrete now a days with an objective of air purification. The present work has proposed to use both the concepts together, that is to use titania in rubbercreteThe waste tyre rubber used as partial replacement of coarse aggregate to produce rubbercrete. The replacement is in the range of 0%, 10%, 25%, 33% and 50% by volume of coarse aggregate.Also titania is added 1%, 2% and 3% of weight of cement respectively. Thus the various proportions of titania based rubberized concrete cubes are casted and The testing is done after curing and atmospheric exposure of concrete for 28 days, 6 months, 1 year and two years. The present experimentation has shown that as the titania blended rubbercrete ages, it looses its structural strength.

Keywords: Rubbercrete, endurance, compressive strength, titania, long term performance

INTRODUCTION

Concrete is revolutionary construction material compared to steel and stone. It is a very recent material. It is just a century ago the use of concrete in constructions and buildings has started. But a great deal of very wide and effective research has been done for enhancing the properties of concrete. One of the technique has been incorporating supplementary cementing materials such as pozzolans and nanoparticles. These materials are having a wide range of types as well as applications. Titania and scrap rubber have been used in concrete for different objectives. The use of rubber reduces stress on natural aggregates. It also gives some beneficial properties like reducing density of concrete etc., thereby making it suitable for specific non structural applications. At the same time it also degrades the strength of concrete and makes it unfit for structural applications.

The titania has advantages in concrete that it enhances the structural strength of concrete as it is good filler owing to its fine size. It does not create any hindrance in the hydration process of the cement. It also serves as a self cleaning material for the concrete. It purifies the air which comes in contact with its surface by a well known phenomenon called as photo-catalysis. When rubbercrete is used in actual site conditions, the rubber is likely to degrade owing to the action of Sun, rains, freezing and thawing etc. Hence it is highly desirable to assess the performance of rubbercrete under real site conditions.

Experimental Procedure

The titania based rubberized concrete is prepared with different proportions of rubber and titania. Replacement of coarse natural aggregates in plain cement concrete is done with rubber particles of equivalent size under proportions 10%, 25%, 33%, 50%. In each case titania is added 1%, 2% and 3% of weight of cement respectively. Thus the various proportions of titania based rubberized concrete cubes are casted and The testing is done after curing and atmospheric exposure of concrete for 28 days, 6 months, 1 year and two years

Results & Discussion: Testing Coarse aggregates

The various characteristics of coarse aggregate as determined in the laboratories are presented in table.

Table 1: Tests on Gravel (Coarse aggregate)

Parameter	Specific	Fineness	Water absorption	Impact	Crushing

	Gravity	Modulus		Value	Strength
Value	2.80	7.13	0.53%	10.4 %	9.30 %

Testing Fine aggregates (Sand)

The various characteristics of natural Fine aggregate (Sand) as determined in the laboratories are presented in table.

Table 2: Tests on Sand (Fine aggregate)

Parameter	Fineness Modulus	Water absorption	Specific Gravity
Value	2.63	0.73%	2.62

* IS 2386 (part – 3) – 1963 has recommended the water absorption to be between 0.5 to 2%. Thus the water absorption of aggregates used is within permissible limit.

Testing of Ordinary Portland cement:

The most important ingredient of concrete is cement. Its properties are summarized in table

Table 3: Tests on Ordinary Portland Cement

Parameter	**Standard Consistency**	**Soundness**	**Fineness**	**Initial Setting Time**	**Final Setting Time**	**Compressive Strength After 28 days curing**
Value	32 %	3 mm	3.43 %	55minute	550 minute	53.25N/mm^2

Initial setting time for 53 grade OPC should be > 30 minutes as per IS 12269. Similarly the FST should be < 600 minutes Thus the cement used duly meets the requirements. Soundness should be < 10 mm. The cement satisfies this criterion also. Fineness up to 10% is permissible. This requirement is also satisfied.

* **Replacement of coarse Aggregate:**

The effect of replacement of coarse aggregates on long term performance (endurance) has been assessed in the present work. The natural coarse aggregates of concrete are replaced by equivalent size scrape tyres rubber particles. The replacement is done in proportions 0%, 10%, 25%, 33%, 50%. In each case titania is added 1%, 2% and 3% respectively. Thus the various proportions of titania based rubbercrete is prepared.

Table shows Compressive Strength of titania blended rubbercrete with replacement of coarse aggregate

Table 4: Compressive Strength of titania blended rubbercrete with replacement of coarse aggregate (28 days)

	28 days Compressive Strength		
Scrap Tyre Rubber proportion (%)	1% titania	2% titania	3% titania
0	38.15	38.15	38.15
10	38.2	33.4	30.1
25	26.7	24.8	21.1
33	23.3	21.6	19.7
50	18.2	16.3	14.6

Table 5: Compressive Strength of titania blended rubbercrete with replacement of coarse aggregate (6 Month)

	6 Month Compressive Strength		
Scrap Tyre Rubber proportion (%)	1% titania	2% titania	3% titania
0	38.15	38.15	38.15
10	37.2	32.4	29.2
25	27	23.9	20.5
33	23.8	22	19.2
50	19.9	15.8	13.7

Table 6: Compressive Strength of titania blended rubbercrete with replacement of coarse aggregate (12 Month)

	12 Month Compressive Strength		
Scrap Tyre Rubber proportion (%)	1% titania	2% titania	3% titania
0	38.15	38.15	38.15
10	33.2	29.4	26.7
25	20.7	18.4	16.5
33	19.5	17.5	15.2
50	16.1	15	13.4

Table 7: Compressive Strength of titania blended rubbercrete with replacement of coarse aggregate (18 Month)

	18 Month Compressive Strength		
Scrap Tyre Rubber proportion (%)	1% titania	2% titania	3% titania
0	38.15	38.15	38.15
10	31.5	27.9	25.2
25	18.2	17.6	15.8
33	17.4	16.3	14.5
50	15.2	13.9	12.2

Table 8: Compressive Strength of titania blended rubbercrete with replacement of coarse aggregate (24 Month)

	24 Month Compressive Strength		
Scrap Tyre Rubber proportion (%)	1% titania	2% titania	3% titania
0	38.15	38.15	38.15
10	30.2	26.5	24.3
25	17.6	15.7	13.2
33	15.7	14.1	13
50	14.1	12.5	11.5

Conclusion: Use of titania to enhance the structural performance of concrete is a well stablished concept. However the present work is to assess the performance of amalgamation of the both, that is the titania blended rubbercrete. It is seen that the titania blended rubbercrete also behaves in the same manner as the plain concrete with regard to the addition of titania.

The titania up to 1% is optimum for enhancing the structural strength of concrete. Higher proportion of titania can reduces the structural strength.The present experimentation has shown that as the titania blended rubbercrete ages, it looses its structural strength

Acknowledgement

We take this opportunity to express our deepest sense and gratitude and sincere thanks to those who have helped us in completing this task.We express our sincere thanks to Head of Civil engineering department DR. M. Husain. Who has given us excellent guidance continuous encouragement for the completion of this work. His kind assistance and constant inspiration will always help us in our future also.

References

1) Abhijeet Shukla, Rao Faraz Waris, Mohd Arhab, and Syed Sajid Husain (2018) A Review on Pollution Eating and Self Cleaning Properties of Cementitious Materials, *International Journal of Innovative Research in Science, Engineering and Technology* .
2) Adriana Zaleska (2008) "A Review Article on Doped-TiO_2," *Recent Patents on Engineering*, 2, 157 – 164.
3) Ali Nazari, Shadi Riahi, Shirin Riahi, Seyedeh Fatemeh Shamekhi and A. Khademno (2010) Improvement the mechanical properties of the cementitious composite by using TiO_2 nanoparticles, *Journal of American Science*, 6(4), 98 – 102.
4) Baoguo Ma, Hainan Li, Junpeng Mei, Xiangguo Li, and Fangjie Chen (2015) Effects of Nano-TiO_2 on the Toughness and Durability of Cement-Based Material, Advances in Materials Science and Engineering, 2015, Hindawi Publishing Corporation.
5) Guerrini G L (2010) "Photocatalytic cement based materials-Situations, challenges and perspectives" *World Cement*, 28.
6) Jay Sorathiya , Siddharth Shah and Smit Kacha (2017) Effect on Addition of Nano "Titanium Dioxide" (TiO_2) on Compressive Strength of Cementitious Concrete, *Kalpa Publications in Civil Engineering*, 1, 219 – 225.
7) Jitendra Patil, Umesh Pendharkar (2016) Study of Effect of Nanomaterials as Cement Replacement on Physical Properties of Concrete, *International Research Journal of Engineering and Technology*, 03 (1), 300 – 309.
8) Laurent Barcelo, Matthieu Horgnies, Isabelle Dubois-Brugger, Julie Buffenbarger and Ellis Gartner, (2014) "Smog—eating

concrete": A New Technology for BetterCities, 9th International Concrete Sustainability Conference (NRMCA) a: Boston (USA).

9) Srivastave A., Bansal A. Kumar J. (2013) "Production of self-cleaning cement using modified titanium dioxide," International Journal of Innovative Research in Science, Engineering and Technology, 2 (7), 2688 – 2693.

PRATIBHA: INTERNATIONAL JOURNAL OF SCIENCE, SPIRITUALITY, BUSINESS AND TECHNOLOGY (IJSSBT)
Special Issue: International Conference on Global Trends in Science, Technology, Humanities, Commerce & Management 2022 (ICGTSTHCM 2022)
Vol. 8, No. 2, January 2022,ISSN (Print) 2277-7261

Assessment of Water Quality Index for River Tapi at Shirpur - Chopda Region

Pramod Sambhaji Patil[1], Dr. Pawar Sudhakar Bhika[2], Dr. Mujahid Husain[3], Dr. Pravin Ashok Shirule[4]

[1] Asst. Professor, Department of Civil Engineering,

SES's R C Patel Institute of Technology, Shirpur, Maharashtra, India

[2,4] Associate Professor, Department of Civil Engineering, SSBT's COET, Bambhori, Jalgaon, Maharashtra, India

[3] Professor, Department of Civil Engineering, SSBT's COET, Bambhori, Jalgaon, Maharashtra, India
[1] pramodpatil97@gmail.com

ABSTRACT

Tapi is a major river in North Maharashtra that is primarily used for drinking water irrigation and industrial purposes. It flows through three major states, with Gujarat having the largest catchment area. In the middle of its session, there is an established relationship between one associated plant and the Tapi River, which is polluted by agricultural, domestic, and industrial waste. It has several small and medium sized cities located along the river's main stem and tributaries. Because of this, the river takes in a lot of organic waste from upstream. The amount of harmful industrial discharge is very lesser, but agricultural discharge is most commonly collected from it's own catchment area; such activities are most common in the river's final 45 km stretch (Chopda to Shirpur) The primary objective of this research is to investigate the pollutant range at each intake point and the causes of Tapi Water contamination. Samples were collected from 9 multiple places, each 5 kilometres apart. Both steady and flowing test conditions were run for pH, turbidity, DO, COD, BOD, chloride, fluoride, coliform, and heavy metals. These boundaries were chosen dependent on drinking water quality norms for the country.

Keywords: Water quality, industrial discharge, agricultural, pH, TDS, Pollution, Tapi.

I. Introduction

Agriculture, industry, and many other fields have seen tremendous growth during the modern era of civilization, followed by global warming, other environmental challenges, and fresh water contamination. "Pollutant" is a term used to describe organic waste, inorganic waste, as well as pesticides and other chemicals used to kill or control pests. There are herbicides (weeds), insect sprays (creepy crawlies), fungicides (parasites), (nematodes), and rodenticides (vertebrate toxins) utilized in agribusiness. In the waste stream of industries, it includes pesticides, pharmaceuticals, chemical, agrochemical, paper & pulp, soap & detergent. All of the above-mentioned pollutants are more likely to degrade water quality. Our globe is rapidly globalising, and both emerging and developed countries are becoming increasingly concerned about water scarcity. The search for additional water sources or even the reuse of wastewater treatment plant effluents are examples of possible water resource exploitation. (10). The problem of drug deposits in the environment is becoming more well recognised these days. They're used in human and veterinary medicine, as well as in animal farming. (11). Most drugs undergo metabolic changes as they enter target living animals, reducing their pharmacological development and assisting with release. (12). A wide range of human activities, such as the introduction of poisonous compounds, metals, and metalloids, as well as the revamping of usual cycles like harmful waste, can wreak havoc on water quality. (13, 14, 15, 16)

Industrial pollutants will not treated with the help of conventional method (1, 2). Also they are deposited at the bottom of river bank which reduces the water carrying capacity of river but fortunately river bed erosiondue to clay mining disturbed the bank of river (3-5) the Water quality as a global issue Now we consider Tapi its mythological name tapti is called tapi a word coming from ancient language Sanskrit tapti which means daughter of Surya and sister of Shani, Bhadra, Yamuna, Yama. The Tapti River is a waterway in focal India between the Godavari and Narmada streams which streams westwards prior to depleting into the Arabian Sea. The waterway extends for 724 kilometers. Its starting point is close to Multai Reserve woods in MP.As it courses through Maharashtra and Khandesh in the western

PRATIBHA: INTERNATIONAL JOURNAL OF SCIENCE, SPIRITUALITY, BUSINESS AND TECHNOLOGY (IJSSBT)
Special Issue: International Conference on Global Trends in Science, Technology, Humanities, Commerce & Management 2022 (ICGTSTHCM 2022)
Vol. 8, No. 2, January 2022,ISSN (Print) 2277-7261

piece of the express, the waterway enters Maharashtra. Bowl size 65,145Sq.Km..Average Discharge 489 m3/s (17,300 (347,000 cubic feet each second), Minimum Discharge 2 m3/s (71 (347,000 cubic feet each second), Maximum Discharge 9830 m3/sec. (347,000 cubic feet each second) (6).

Tapi river coordinate in chopada and shirpur region Latitude: 21° 20' 53.56" N andLongitude: 74° 52' 49.26" E.According to the Code of Practice for Using Plant Protection Products, pesticides are defined as substances, preparations, or organisms that are formulated or applied to control pests. A major global issue is environmental pollution. Agriculture has become a prominent contributor to water pollution in enumerations of sources. While countries try to address maltreatments of their water assets, it is important to decide the reasons for water quality corruption and to measure contamination commitments from numerous sourcesTapi river coordinate in chopada & shirpur region Latitude: 21° 20' 53.56" N and Longitude: 74° 52' 49.26" E. According to the Code of Practice for Using Plant Protection Products, pesticides are defined as substances, preparations, or organisms that are formulated or applied to control pests. A major global issue is environmental pollution. Agriculture has become a prominent contributor to water pollution in enumerations of sources. While countries try to address maltreatments of their water assets, it is important to decide the reasons for water quality corruption and to measure contamination commitments from numerous sources.

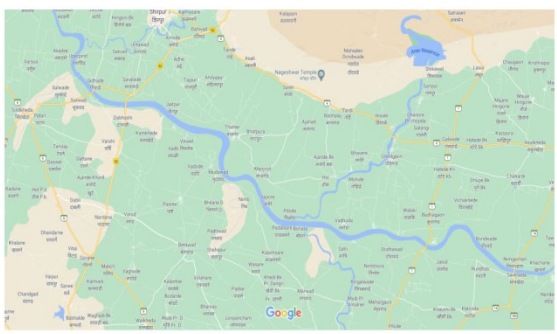

Fig. 1Google map showing Tapi river (9)

Within the calendar year, Tapi River is drier than other rivers except for rain, which increases pollution significantly. Water quality assessment of Tapi River is carried out from 9 points that are spread out equally over a 45 km trench within the chopda of shirpur city, spread out at a distance of 5 km each. Among the pollutants are primarily domestic wastes, industrial wastes from thermal power plants, and agricultural waste. The quality of water is dependent on the geological environment, its recovery and usage as per human need as well as human activities such as domestic, industrial, commercial, mining, agricultural etc.(7).

During the dry season (stream discharge* 18 m3/s) from January to March, the river has a low flow rate and during the wet season (stream discharge >18 m3/s) from April to December it has a high flow rate. (8)

II. Objectives

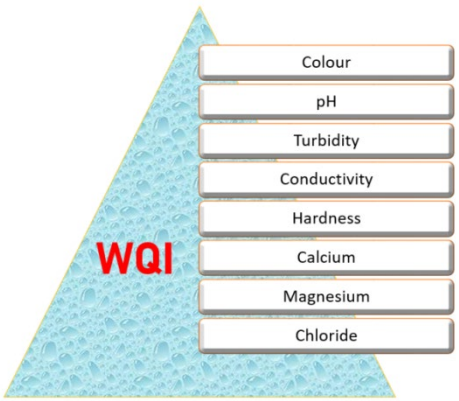

Fig. 2 Parameters that affect the study.

The various reasons why water is impure.Assessment of water quality indexing in the Tapi River between Chopada and Shirpur in three ways.

I) Assessment of water quality indexing in the Tapi River between Chopada and Shirpur in three ways. Physical characteristics of water in a particular region.

A) Test, odour, temperature, etc.

II) Chemical characteristics of water in a particular region.

A) pH, Acidity, Alkalinity, Hardness, etc.

III) Biological characteristics of water in a particular region.

1. COD, BOD, phosphate, nitrate, sulphate, chloride, fluoride, coliform, and heavy metals are all contaminants.
2. To suggest applicability of water for various applications without treatment and after partial treatment.
3. To identify the sources of water pollution.
4. To predict the future sources of water pollution.
5. To suggest the remedies at a specific change to enhance the WQI.

All sample collected are then investigated by following tests

III. Approach methodology

The present work aims to workout the WQI at different stretches(are mentioned in table), identify the sources of present water pollution, predict the future likely sources and propose mitigation measures, with techno – economic details, to eliminate the pollution.

SN	Sample Stations	Source of pollutants	Sample station Map/ location	Elevation (msl)
1	Nimgavan (Chopada)	Sullage and sewage waste, Tharmal Power Plant of Deepnagar.	21°17'08"N75°13'12"E	120m
2	Budhgaon	Sugar mill and Textile Mill.	21°03'40"N75°50'02"E	185m
3	Vadhoda	Agriculture waste	21°11'02"N75°03'28"E	159m
4	Padalsare [Three Rivers Junction point (Tapi , Bori, Aner)]	Domestic and Industrial waste from Amalner, Agriculture waste,	21°11'20"N75°00'07"E	144m
5	Mudavad Kapileshwar (Two river junction point Tapi and Panzara)	Seepage waste from plastic Dye industries waste, Domestic waste from Dhule, Songir	21°13'23"N74°56'08"E	156m

Table 1 Source of pollutants

Different technological Methods to eliminate the pollutants- waste water treatment plant (effluent)

A. Future Scope- The total trench of 45 km encompasses industrial, residential, recreational & commercial zone which are, growing day by day hence responsible to increase the load of pollutants in to the river. This Review work provides the different sources of pollutant at the same time future capacity of treatment plant to treat the waste.

B. Material & Method- Water test accumulated from tapi stream which are 5 km from each other with unprecedented importance are given to Dissolved oxygen, Fecal coliform, pH, 5-days regular oxygen premium, nitrates, phosphates, temperature deviations, turbidity (in NTU) and complete solids. Satring point of test assortment is at Nimgaon, which is acxactly upstream of sulwade torrent (45 KM apert structure one another), henceforth it comprises of 9 diffrenet point of test assortment.

All sample collected are then investigated by following tests

1. This is the preliminary observation based test, which gives first-hand information of dissolved solids.

2. These test noting but provide the hydrogen ion concentration in different water sample. Which also responcible to deside acidic & basic nature of water.

3. Acidity these test gives an information of industrial effluent discharge, which are commonly utilises the different acid for treatments, manufacturing, cleaning etc. in their day to day process.(industries are like pesticides, pharmaceutical industries, chemical industries etc.

4. Alkalinity these test gives an information of basic salt in an industry effluent from different industries. Like Agro chemical , automobile. Detergent & soap industries etc.

5. Total dissolved solids these test provides an idesa related to TDS present in water. These test gives information range of molecular attaraction of difeerent location (soil liquification noting but responcible for the increase of viscosity of water)

6. It shows total amount of oxygen required for degration of organic and inorganic componants.

It shows presence of Ecoli bacteria.

Volumetric or volatile organic compound it implicates formation of new fumes.

It is measured in percentage of COD(TOC = 2.5*COD)

In that strategy for enlightening examination of seven unmistakable anions (Fluoride, Chloride, Bromide, Nitrite, Nitrate, Phosphate, and Sulfate) This exploration works principally centers around discover the various boundaries of water test gathered from 9 unique focuses. Major moto is to discover the convergence of contaminations, its variety from one highlight another and its cures.

C. Result & Discussion:

1. The review of literature above indicates that water samples are collected and analyzed in all three seasons since water levels in rivers change from season to season, which in turn affects the percentage of pollutants present in the water.

2. Tests so gathered from various 9 focuses shows the distinctive toxin scope of water test from specific focuses.

IV. Conclusion

From above survey paper it is inferred that, the water quality detoriate inside the range or channel of each 5 km which incorporates various kinds of contamination like agrarian, mechanical, instructive, sporting waste and so on these toxin are dealt with ostensible treatment strategy at each source. It is likewise seen that the progression of waterway shifts season astute which influence the amount of poisons.

References

[1] APHA (American General Wellbeing Affiliation). Standard Techniques for the Assessment of Water and Wastewater, twentieth ed. Washington, D.C, Water Climate Organization (1998).

[2] Central Environmental Authority. Proposed Ambient Water quality Standards for Inland Water Sri Lanka, Colombo, Sri Lanka : Environment Action 1 Project (Funded by ADB) (2001).

[3] DANIDA Maha Oya Basin; Detailed Basin Assessment. Danish International Development Agency, Danish Hydraulic Institute, Lanka Hydraulic Institute Ltd, Sir William Halcrow and Partners Ltd. (1999).

[4] DANIDA Western River Basins Sector Project, TA 3030 - SRI: Phase 1 report, Executive summary. Danish International Development Agency, Danish Hydraulic Institute, Lanka Hydraulic Institute Ltd, Sir William Halcrow and Partners Ltd. (1999).

[5] Sri Lanka, National Water Supply and Drainage board Sector planning report Kegalle District, 41, (1998).

[6] "Tapti Basin Station: Kathore". UNH/GRDC. Retrieved 1 October 2013.
[7] Wagh G.S, Sayyed M.R.G, Sayadi M. H (2014), Evaluating groundwater pollution using statistical analysis of hydrochemical data: A case study from southeastern part of Pune metropolitan city (India), International Journal of Geomatics and Geosciences, 4(3), 456-476.
[8] India, National Water Supply and Drainage board Sector planning report-Dhule District.
[9] https://www.google.com/maps/@21.2288464,74.9996791,12z MAPS
[10] J. Smit, J. Nasr, Urban agriculture for sustainable cities: using wastes and idle land and water bodies as resources, Environ. Urban. 4 (2) (1992) 141–152.
[11] C.G. Daughton, T.A. Ternes, Pharmaceuticals and personal care products in the environment: agents of subtle change?, Environ Health Perspect. 107 (1999) 907–938.
[12] V.L. Cunningham, Special characteristics of pharmaceuticals related to environmental fate, in: K. Kümmerer (Ed.), Pharmaceuticals in the Environment: Sources, Fate, Effects and Risks, Springer-Verlag, Germany, 2004, pp. 13–23.
[13] Gomshei MM, Allen DM (2000) Potential application of oxygen-18 and deuterium in mining efuent and acid rock drainage studies. Environ Geol 39:767–773.
[14] Zhu C, Anderson G (2002) Environmental applications of geochemical modelling. Cambridge University Press, Cambridge.
[15] "Edraki M, Golding SD, Baublys KA, Lawrence MG (2005) Hydrochemistry, mineralogy, and sulphur isotope geochemistry of acid mine drainage at the Mt. Morgan mine environment, Queensland, Australia. Appl Geochem 20:789–805".
[16] "Ribeiro L, Kretschmer N, Nascimento J, Buxo A, Rotting TS, Soto G, Soto M, Oyarzun J, Maturana H, Oyarzun R (2014) Water quality assessment of the mining-impacted Elqui River Basin, Chile. Mine Water Environment33:165–176"

PRATIBHA: INTERNATIONAL JOURNAL OF SCIENCE, SPIRITUALITY, BUSINESS AND TECHNOLOGY (IJSSBT)
Special Issue: International Conference on Global Trends in Science, Technology, Humanities, Commerce & Management 2022 (ICGTSTHCM 2022)
Vol. 8, No. 2, January 2022,ISSN (Print) 2277-7261

Collection of Floating Material by Bandlog Litter Trap

Pawan R. Wani[1] , Pratik R. Sisodiya[2] , Vrushali A. Mahadik[3] , F.I.Chavan[4]
[1,2,3,4]Assistant Professor, Department of Civil Engineering, Shram Sadhana Bombay Trust's college of Engineering and Technology, Bambhori, Jalgaon, Maharashtra, India.
1pawanrwani@gmail.com , 2Pratiksisodiya2@gmail.com,
3mahadikvrushali02@gmail.com, 4farooqamaravati@gmail.com

Abstract
The water pollution trouble, water covers over 70% of the Earth's surface. It's miles a very essential resource for humans and the surroundings. Water pollution influences drinking water, rivers, lakes, oceans and agriculture all around the global. In lots of growing international locations, it also includes a main purpose of demise, of humans with the aid of consuming polluted water resources and it's have an effect on aquatic lifestyles too. The current design guidelines of this paper provides various information with regard to the definition of gross pollutants and litter traps therefore the scope of this paper will make a bridge between these knowledge gaps and will address the issues: identification of the various types of devices currently available, with performance achievements, benefits and limitations outlined carry out a literature review of design factors, methodologies low glide and excessive go with the flow bypass structures for diverse gadgets litter booms are floatation systems with suspended curtains that may be used to comprise floating trash. Litter booms have a five to seven-year lifespan earlier than they are deteriorated by way of ultraviolet light, or are torn by captured debris. The prime objective is to develop a suitable mechanism for garbage trap on river.

Keywords: Litter trap, Bandlog, litterboom

I Introduction

The most litter booms are mounted with the boom attached to factors on the alternative side of the channel with enough slack to permit the boom to shape a semicircle. Booms are positioned downstream of one or extra outfalls, preferably in slow transferring commercial pollutants has been and remains a primary aspect causing the degradation of the environment around us, affecting the water we use, the air we breathe and the soil we live on. But of those, the pollution of water is arguably the maximum serious hazard to current human welfare. Water is polluted not best through industries but also by families. Each industries and family wastewater include chemicals and organic rely that impose excessive demands on the oxygen found in water. Polluted water consequently contains low tiers of dissolved oxygen as a end result of the heavy biological oxygen demand (BOD) and chemical oxygen demand (COD) positioned by means of commercial and family waste materials discharged into water bodies and water systems, both above and below the earth's surface. In addition to low levels of dissolved oxygen in water, industrial wastes (effluents) also contain chemicals and metals that are directly harmful to human health and the ecosystem. The supply of water through river valley projects and ground water extraction thus has repercussions for the health and safety of people. Apart from health effects, which indirectly affect human productivity, polluted water also affects land productivity.

II Literature Review

B. Franz [1] - In lots of growing countries, multiple population boom, city enlargement in flood under iable regions, growing intake , inadequate strong waste series and environmental control guide lines lead to dumping of strong waste into canals and rivers and onto its banks, which correspond to the 'floating muddle'. In Brazil, this happens in particular in metropolitan areas, like in the megacity of Rio de Janeiro, placed within the southeast of the USA. The nation Environmental Institute, in an try to restriction the improvement of floating clutter in the coastal zones, established limitations across the mouth of contributory rivers, classified 'eco-obstacles'. In this situation take a look at he check out the technology and effect of floating litter on canal and rivers.

NellArmitage[2]-
A large amount of city muddle is locating its ma nner into the drainage structures to grow to be an eyesore and a capability fitness threat. despite the fact that a good deal effort has been expended on the improvement oftrapping devices, most ofthe traps currently mounted are extremely useless att rappingandstoring urban litter. therehasbeen thus a urgent want fora bodily version observe into the layout of litter traps. such a observe changed into completed in the hydraulic laboratories at thecolleges of Cape city and Stellen bosch. It inreality showed why most designsfail,and cert ainly recognized theusageof declined screens asa n method thatholds great promiseforthe future.T hefindings broadly concur with the effects of a similar model look at that was these days achieved in Australia.

Mohd Nashruddin Mohd Shah [3]-
The river became increasingly contaminated over the years and within the wake of fast development within the town. The motive of this paper is to invent and provide a trash collector for mini hydro this is easily detachable in order that the trashes accrued may be without problems disposed of layout of the trash trap need to be like minded with current movement structures.Trash lure ought to save you any trash and particles from passing through the mini hydro. Fieldwork turned into done at the flow river to research the encompassing and circulate shape.The statistics amassed had been mass of trash amassed with diverter and with out diverter a complete of 10.0 kg of trashes had been accrued. The performance of the trash lure became calculated through the share of the common mass of diverted trashes by using the overall mass of trapped trashes. The targeted efficiency for this trash entice undertaking is 70% based totally on the data accumulated, the performance of this trash entice is 84%. The focused efficiency became achieved and layout improvement of this trash trap might be discussed at the recommendation. In conclusion, the trash lure had been validated as a capability solution for the mini hydro system trouble, diverts and forestalls maximum of the trashes from getting into the mini hydro and blocked the turbine from rotating.

Gary R. Hopkins [4]-
Water and water problems have always stirred human feelings as we are all related to water. whether it's miles a flowing river or the oceans into which it flows, easy and trash-loose water is vital to our lives. It turned into Jacques Cousteau who once proclaimed that "water and air, the two maximum vital fluids, on which all lifestyles relies upon, The fantastic Pacific garbage Patch become brou ght to the arena's attention by way of Captain Charles Moore in 1997, after he observed large islands of floating plastic waste even as returning to southern California from Hawaii. through the years, Captain Moore, together with the Algalita Marine research foundation and limitless differe nt clinical groups,have determined thereare prese ntly 5 gyres or patches of anthropogenic marine particles in the world's oceans: one in the Indian Ocean.

III Need of Study
After the case we find that the floating material and any material such as dead animal, laves are collected effectively, about two tone material are collected weekly. The plastic bottles and recyclable material are separated. Our waterways, rivers, creeks and lakes are an important environmental resource and keeping them clean and healthy is a vital task, especially when they lead to our bays and oceans. That where Bandalong and our range of Litter Traps and Boom Systems provide the ideal solution for controlling and removing litter from our waterways.

IV Objective of Study
a. The prime objective is to developed a suitable mechanism for garbage trap on river.
b. To find out the most effective way to help or create a more stable environment.
c. Increase the capacity of residents and stockholders to improve care it and promote their local environment.
d. Reclaim vacant and neglected lands for conservation, recreation, and economic development.

V Methodology
a. Search the lake as water Resourse.
b. Lake is having different types of litter traps.
c. Prepare model of collection of floating material.
d. Installation this model on site.
e. Collect the litter in water by using bandlog litter trap.
f. Discussion.
g. Conclusion

Fig. 1 Litter trap in river

VI Result and Discussion

The primary purpose of this study was to examine and determine the effectiveness of the bandlog litter traps**.** Earlier research suggests that there are benefits of working on the study of bandlog litter traps so that the solid waste can be collected more in more proper ways and the water pollution due to solid waste can be control.

Our results revealed the significance of the economical method of collection of floating material, in addition with it different strategies to make it more and more effective and as we all know we want to get rid of litter and especially plastic which is one the main causes of pollution in every aspect.

This method is about trapping a litter that has landed in stream of river, heavier floating debris may have a draft of 20 cm. considering the upper part of water therefore is sufficient in determining a method of capturing floating litters, the litter traps can be designed in different shapes and sizes and there capacities may varies with their shapes and sizes.

VII Conclusion

They are designed to capture only the floatable portion of gross solids loading, which might be a very low fraction of the total loading. Smaller mesh sizes could impede capacity of the storm drain system if not designed properly. Nets which break away could reintroduce trash into the water body if not designed properly. Booms are relatively expensive and all debris is directed via collection booms through a patented one way flap or gate to capture floating litter.

After the study of this project we observed that,

- Estimation cost is to less of this model
- Anyone can be purchase or made easily.
- Design is too simple than other methods.
- Can be transported easily anywhere.

It is very economical over all the other methods adopted

VIII Acknowledgement

We take this opportunity to express our deepest sense and gratitude and sincere thanks to those who have helped us in completing this task.
We express our sincere thanks to Head of Civil engineering department DR. M. Husain. Who has given us excellent guidance continuous encouragement for the completion of this work. His kind assistance and constant inspiration will always help us in our future also.

References

[1] B. Franz & M. A. V. Freitas “Generation and impact of floating litter on urban canals and rivers: Rio de janeiro megacity case study ” WIT Transaction on Ecology and The Environment, Vol 167, ISSN 1743-3541.

[2] Nell Armitage and albert Rooseboom “The removal of urban litter from stormwater conduits and streams” ISSN 0378-4738, Water SA Vol. 26 No. 2 April 2000. UNEP. Marine Litter, an analytical overview. Nairobi, Kenya, 2005.U.S. Environmental Protection Agency. Assessing and Monit projects oring Floatable Debris. USEPA: Washington, 2002.

[3] Mohd Nasuruddin mohd shah, faridamin ahemad, “Design and development of trash trap of stream for mini hydro projects”.

[4] Gary R. Hopkins Storm Water Systems, Cleveland, Georgia Journey to Capture Marine Debris—Before It Reaches the ocean.

PRATIBHA: INTERNATIONAL JOURNAL OF SCIENCE, SPIRITUALITY, BUSINESS AND TECHNOLOGY (IJSSBT)
Special Issue: International Conference on Global Trends in Science, Technology, Humanities, Commerce & Management 2022 (ICGTSTHCM 2022)
Vol. 8, No. 2, January 2022,ISSN (Print) 2277-7261

Comparison of oil zappers from fungi and bacteria used for bioremediation of oil contaminated soil

Shital S. Agrawal[1], Sarika S. Pawar[2], Jayant P. Parpalliwar[3] and Swapnil S.Khillare[4]

Assitant Professor, SSBT's COET, Jalgaon[1], Assitant Professor, SSBT's COET, Jalgaon[2]

Assitant Professor, SSBT's COET, Jalgaon[3], Assitant Professor, SSBT's COET, Jalgaon[4]

[1]Shital744agrawal@gmail.com, [2]sarika_p17@rediffmail.com

ABSTRACT:

The global processes like exploration, extraction, refining, transporting and marketing petroleum products are major part of petroleum industry. Raw materials from petroleum industries have many applications. They are also used as raw materials for many chemical products. But this petroleum industry is mostly responsible for soil pollution. Waste generated in oil industries though various processes also causes soil pollution. Here we are using a new more effective and cheap technology for the treatment of crude oil present as pollutants in soil. This technology involves the use of strains of bacteria and fungi having capacity of digesting crude oil. Bioremediation is the use of microbes to treat polluted soil and water by total degradation or removal of the toxic substances. Here we are using oil zapper technology for bioremediation. It is nothing but microbial combination developed for the bioremediation of oil contaminated soil. The technology is very effective mainly in case of petroleum hydrocarbon contamination. Oil zappers are added in contaminated soil and results are recorded after every 10 days. The TPH content was analyzed using Muffle furnace. Finally the samples were analyzed using HPLC. And from the results obtained we conclude that fungal oil zipper is more effective than bacterial oil zipper.

Keywords: bioremediation, oil zappers, Microorganism.

1. INTRODUCTION

Bioremediation is a bioprocess in which microbes detoxify pollutants in the soil and other environments. For effective bioremediation, microbes must attack the contaminants by enzyme action. Bioremediation needs feasible environmental parameters to permit microbial growth and degradation more rapidly.

Factors affecting bioremediation

1. Existence of a microbial population capable of degrading the contaminants;
2. The availability of impurities to the microbial population;
3. The environment factors (type of soil, temperature and pH, availability of oxygen or other e^- acceptors and nutrients).

1.1 Significance of oil zapper

TERI has developed OILZAPPER – a crude oil and oily sludge degrading bacteria deriving from various bacterial cultures existing in the natural environment for bioremediation[1]. Oil zapper degrades every layers of crude waxy element, aromatic component, and tar. Oil zapper can work in temperatures ranging from 8-40 degrees Celsius. Oil zapper technology is 40 times cheaper than the traditional method. [1]

2. MATERIALAND METHODOLOGY

Material: Microorganisms:

Different strains of Bacteria and Fungi are use for preparation of oil zapper, a combination of organisms using for the bioremediation method.

Media:- Nutrient agar, Potato dextrose agar, MGYP, Czapek-dox broth, Corn cob powder, nutrient broth. [1]

Chemicals:- Silicone oil, Hexane, Acetone, Concentrated nitric acid, Ethanol, distilled water.

Materials:- Whatman filter paper, Vials for collection of oil, Soxhlet extractor unit

Methodology

1. Sample collected from oil refineries.

2. The microbial cultures were prepared from strains. Neutral solution Nutrient medium, were used to prepare bacterial strains *Acinetobater calcoacetius*, *Pseudomonas aeruginosa* and *Pseudomonas desmolyticum* slants. Fungal strains *Aspergillus flavus*, *Aspergillus niger*, *Aspergillus orchraceous*, *Phanerochaete chrysosporium* prepared on Potato Dextrose Agar at pH 5.6 and yeast strain *Candida catenulate* were prepared on Malt Glucose Yeast

PRATIBHA: INTERNATIONAL JOURNAL OF SCIENCE, SPIRITUALITY, BUSINESS AND TECHNOLOGY (IJSSBT)
Special Issue: International Conference on Global Trends in Science, Technology, Humanities, Commerce & Management 2022 (ICGTSTHCM 2022)
Vol. 8, No. 2, January 2022,ISSN (Print) 2277-7261

Peptone media at pH 6.4. [1]

Fig. 1.Culture tubes

Fig. 2.Testing fertility of soil.

3.Oil contaminated soil is usually infertile, when high content of oil is present. We tested the fertility of soil by plantation. As a result, those plants were died.

4. Extraction of TPH from soil sample by Soxhlet extraction unit was carried out. Acetone was used for extraction. 50gm of sample was taken in thimble for extraction. One day required for this extraction process. After that separated oil was collected in Dionex vials for testing.

5. Oil zapper was developed by assemble of three bacterial species those can biodegrade aliphatic, aromatic, nitrogen, sulphur, oxygen containing compounds and asphaltene fractions of crude oil/oily sludge as well as a combination of four fungi species[1] and a yeast which have oil degrading capacity. Oil zapper is produced in a bioreactor under optimal conditions. [1]

The growth conditions for the oil zapper were as follows:

T: 32°C **V**: 500 ml, **Rotation speed**: 250 rpm , **pH** 7.0 ,**time required for growth**: 12 hours.

6. In tray various sections were formed in which the soil samples were distributed.

7. Oil zapper was applied according to the types of soil sample used and also on the basis of the type of microorganisms used in oil zapper and regular nutrients were supplied for the growth of microbes. After the application of oil zapper, the soil sample was analyzed at regular interval of 10 days.

8. Samples were heated at 80^0C to calculate moisture content. Total petroleum hydrocarbon was extracted from the soil samples by using extractor unit. A solvent was evaporated in a fume hood by a gentle nitrogen stream. The residue was taken in crucibles and heated at 600°C in a Muffle furnace for 5-6 hours. After cooling, the amount of ash was quantified. [1]

9. High Performance Liquid Chromatography was used for analysis of total petroleum hydrocarbons.

3. OBSERVATION

Initial reading: 1gm of oil contaminated soil sample contains 0.95gm TPH and 0.05gm Ash.

A) After Bacterial oil zapper treatment:

Oil zapper was applied on 100gm oil contaminated soil sample.

Concentration (ml)	Sample wt.(gm)	After muffle sample wt. (gm)				TPH content			
		10TH day	20th day	30th day	40th day	10th day	20th day	30th day	40th day
50	1	0.05	0.12	0.28	0.38	0.95	0.88	0.72	0.62
100	1	0.07	0.14	0.30	0.41	0.93	0.86	0.70	0.59
150	1	0.09	0.15	0.37	0.50	0.91	0.85	0.63	0.50
200	1	0.10	0.18	0.41	0.55	0.90	0.82	0.59	0.45

B) After fungal oil zapper application

4. RESULT AND DISCUSSION:

Applied oil zapper on this oil contaminated soil differentiating with various concentrations of doses of oil zapper and took readings after each 10 days

Concentration (ml)	Sample wt.(gm)	After muffle sample wt. (gm)				TPH content			
		10 TH day	20 th day	30th day	40th day	10 th day	20 th day	30 th day	40 th day
50	1	0.05	0.12	0.34	0.46	0.95	0.88	0.60	0.54
100	1	0.07	0.17	0.38	0.51	0.93	0.86	0.58	0.49
150	1	0.11	0.18	0.41	0.54	0.89	0.82	0.51	0.46
200	1	0.13	0.20	0.43	0.60	0.87	0.80	0.48	0.40

interval. The periodic result is as below:

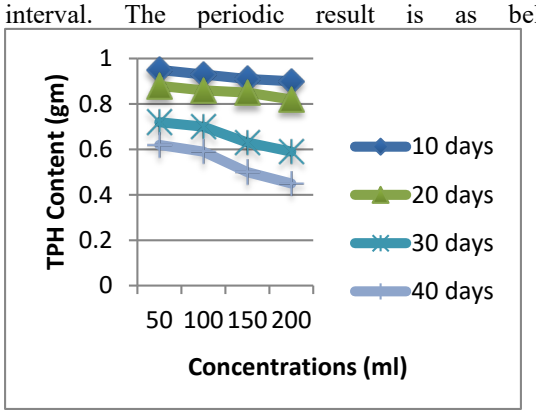

Graph A: - Effect of oil zapper from Bacteria This graph gives bioremediation of TPH through oil zapper from bacteria.

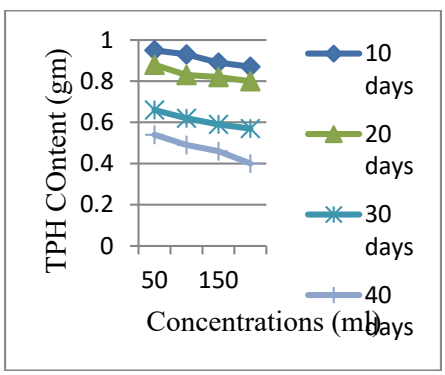

Graph B: Effect of oil zapper from fungus

This shows the biodegradation of TPH using oil zapper from fungus. TPH content in the sample treated by 200 mili liters of oil zapper from fungus was 0.40grams. This shows oil zapper from fungus is more effective than oil zapper from bacteria, but large biomass remain present in soil after treatment.

HPLC RESULTS

the sample analysis report: this is the HPLC graph for sample treated with fungal broth

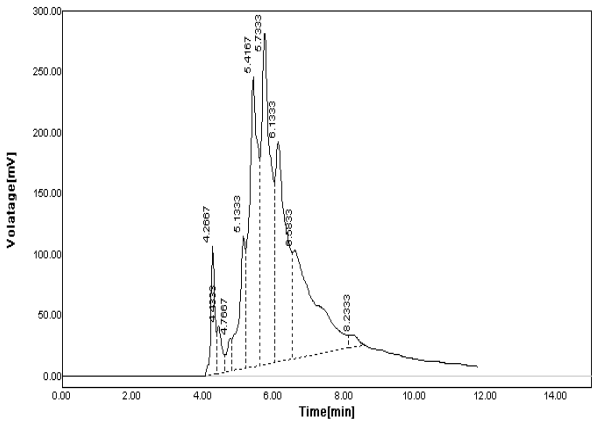

5. CONCLUSION

On the basis of result and observation we conclude that oil zapper from fungus degrades the TPHs more rapidly as compared to oil zapper from bacteria. Use fungal oil zapper to obtain quicker results and control toxicity by intoxicants. One of its advantage is its convenience and efficiency make it an attractive option for future.

6. REFERENCES

1. Gaurav D. Khodape, Dr. V.R.Diware, Jayant P.Parpalliwar ,Restoration of oil contaminated soil by Bioremediation for Environmental Protection, , Pratibha: International Journal Of Science, Spirituality, Business And Technology (Ijssbt), Vol. 7, No. 1, September 2019 ISSN (Print) 2277-7261.
2. Admon, S., Green, M., Avnimelech, Y., 2001. Biodegradation kinetics of hydrocarbons in soil during land treatment of oily sludge. Bioremed. J. 5, 193–209.
3. Alef, K., 1995. Estimation of microbial activities: dehydrogenase activity. In: Alef, K., Nannipieri, P. (Eds.), Methods in Applied Soil Microbiology and Biochemistry.
4. Atlas, R.M., Bartha, R., 1998. Microbial Ecology: Fundamentals and Applications. Benjamin/Cummings Publishing, Menlo Park, CA. Barathi, S., Vasudevan, N., 2001. Utilization of petroleum hydrocarbons by Pseudomonas fluorescence isolated from a petroleumcontaminated soil. Environ Int. 26, 413–416.

5. Bento, F.M., Camargo, F.A.O., Okeke, B.C., Frankenberger Jr., W.T., in press. Diversity of biosurfactant producing microorganisms isolated from soils contaminated with diesel oil.Microbiol. Res. Braddock, J.F.
6. Catterall, P.H., 1999. A simple method for enumerating gasoline and diesel-degrading microorganisms. Bioremed. J. 3, 81–84. Capelli, S.M., Busalmen, J.P., Sanchez, S.R., 2001. Hydrocarbon bioremediation of a mineral-base contaminated waste from crude oil extraction by indigenous bacteria. Int. Biodet. Biod. 47, 233–238.
7. Devinny, J., Chang, S.H., 2000. Bioaugmentation for soil bioremediation. In: Wise, D.L. Trantolo, D.J. (Eds.), Bioremediation of Contaminated Soils. Marcel Dekker, New York, pp. 465–488.
8. Frankenberger Jr., W.T., 1992. The need for a laboratory feasibility study in bioremediation of petroleum hydrocarbons. In: Calabrese, E.J., Kostecki, P.T. (Eds.),
9. Hydrocarbon contaminated soils and groundwater. Lewis, Boca Raton, FL, pp. 237–293.
10. Frankenberger Jr., W.T., Emerson, K.D., Turner, D.W., 1989. In situ bioremediation of an underground diesel fuel spill: a case history. Environ. Manage. 13, 325–332.
11. Richard, J.Y., Vogel, T.M., 1999. Characterization of a soil bacterial consortium capable of degrading diesel fuel. Int. Biodet. Biod. 44, 93–100.

PRATIBHA: INTERNATIONAL JOURNAL OF SCIENCE, SPIRITUALITY, BUSINESS AND TECHNOLOGY (IJSSBT)
Special Issue: International Conference on Global Trends in Science, Technology, Humanities, Commerce & Management 2022 (ICGTSTHCM 2022)
Vol. 8, No. 2, January 2022,ISSN (Print) 2277-7261

Design and development of Hydraulically operated loading machine for fatigue testing of plates.

Dnyandeep H Baviskar, Prashant N Ulhe
(Lecturer VCDET, Virar, Asst. Prof. Ssbt coet Jalgaon)
dnyandeep.baviskar@gmail.com, ulheprashant@gmail.com

Abstract

Large numbers of manufacturers are manufacturing fatigue testing machines such Zwick, Milwaukee, Shimadzu to test different components under different loads. But is difficult every time to reach a manufacturer to purchase machine for a single trial. So, it was thought to develop a machine which can satisfy the needs of students to test material under fatigue loading.

Problem definition To design and develop a hydraulically operated loading machine for fatigue of plates Need The machine is thus capable of simulating a real world loading of components. The machine was designed for low load conditions, so it can be moved if it is required without much difficulty Limitations of existing machines These machines are costlier due to customization of results they offer and also due to different sensors attached. If it desired to do fatigue testing of small number components such as aluminium or steel plates of thickness 1 mm to 4 mm, it is advisable to purchase machine as it will be costlier Improvement Present machine is designed for low load conditions so ideally suited for testing of small plates up to a dimensions 300 mm X 150 mm X 5 mm. The machine is designed to take a load up to 15 kN and in occasional case can take up to 20 – 25 kN although it has been tested to withstand a static load of 50 kN as shown by finite element analysis done using Solidworks Simulation Express.

Introduction

Engineering structures are in general exposed to cyclic loads which may cause development of micro sized crack. If these micro sized are not taken care on time may propagate can cause catastrophic failure. Under fatigue loads material do not show any early signs of failure. So it was necessary to develop a machine which can be used to test components under fatigue. Fatigue testing allows to simulate a actual loading of components, thereby allowing to select different material for desired application with required dimensions Most structural members and machine components are subjected to multi axial stress – strain conditions and due to geometrical configurations, discontinuities and/or temperature fluctuations. In such cases principal stresses may be non proportional and principal directions can often change throughout the component's load cycle of life. Finite endurance limits, calculated using the predicted service life, are therefore used in the design of components and structures subject to condition of multi axial loading.

Objective

1) To study loading patterns in different types of static fatigue load testing machines
2) To define parameters of design for making a setup under different loading patterns.
3) To prepare model of setup using solid modeling software based on designed parameters.

- **Design Methodology**

- Selection of cylinder in the current project was done by choosing standard parts from manufacturers catalogue for 15 kN load as follows

  Piston diameter =38.1 mm Rod diameter = 15.38 mm

  - **Efficiency of cylinder**

    Efficiency of cylinder was selected by referring standard table from literature referred. Selected minimum efficiency of 80% for normal cylinder of 20 mm to 50 mm diameter range.

- **Piston dimensions**

  Considered equal velocities for extending and retracting of piston for easy installation and rigidity. L/D ratio was calculated which was found to be 15.74 where, L being length of piston and D being diameter. L/D ratio was lesser than permissible value of 20.

- **Selection of reservoir**

  Assumed velocity of flow to be 75 lpm and total distance travelled in 1 cycle to be 0.5m. Reservoir capacity found to 102 lit. considering additional oil requirement to compensate for leakage and reserve capacity.

- **Supporting bar**

  Supporting bar was designed considering material C25Mn75, diameter of supporting bar from calculations found as 16.67 mm. under buckling diameter was found to be 36.85 mm. so chosen as 40 mm.

- **Screw**

  It was designed for a load of 10 kN considering equal distribution of load of 20 kN on cylinder. Diameter d = 25 mm, pitch = 5 mm, coefficient of friction taken as $\mu = 0.2$.

  Direct stress, $\sigma = 31.83$ N/mm^2, Shear stress, $\tau = 36.67$ N/mm^2, maximum shear stress = 39.69 N/mm^2. Bearing pressure on threads taken as 5.6 N/mm^2.

RESULTS AND DISCUSSIONS

Frequency of cyclic load is taken as 15 Hz and tested for 135,000 cycles. Similarly, setup is designed for static loading under 15 kN load.
CAD model of assembly is prepared in Solid Works 2017 version. Static Finite Element analysis in Solid Works Simulation Express under a load 15 kN shows that model of machine is safe.

Major components list along with materials and dimensions

sr. no	Name of Component	Material	Dimensions
1	Piston diameter	Stainless steel	38.1 mm
2	Rod diameter	Stainless steel	15.88 mm
3	Supporting bar	C25Mn75	36.85 mm
4	Oil reservoir		Reservoir capacity: 102.6 lit.
5	Crosshead		600 X 300 X 50 mm

- **Simulation results**

Load of 15 kN is applied on the base of hydraulic cylinder.

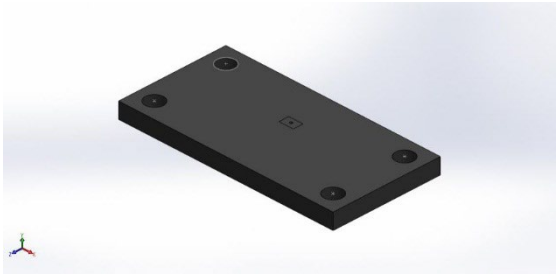

- **Fig.1 Location of applied load on crosshead of assembly**

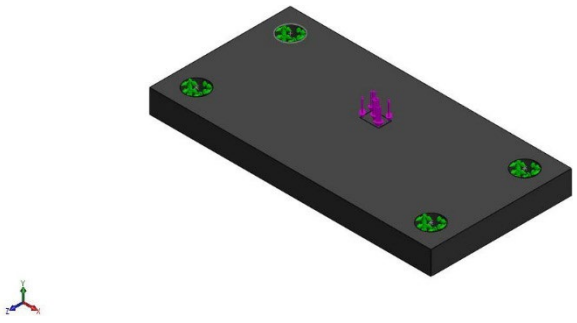

Fig. 2 Load distribution of applied load for calculation of stresses

Study name	Static
Analysis type	Static
Mesh type	Solid Mesh
Thermal Effect:	On
Thermal option	Include temperature loads
Zero strain temperature	298 Kelvin
Include fluid pressure effects from SOLIDWORKS Flow Simulation	Off
Solver type	FFEPlus
Inplane Effect:	Off
Soft Spring:	Off
Inertial Relief:	Off
Incompatible bonding options	Automatic
Large displacement	Off
Compute free body forces	On
Friction	Off
Use Adaptive Method:	Off

Units

Unit system:	SI (MKS)
Length/Displacement	mm
Temperature	Kelvin
Angular velocity	Rad/sec
Pressure/Stress	N/mm^2 (MPa)

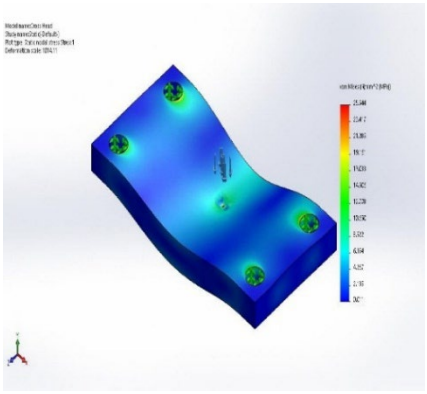

Fig. 3 Cross Head: Static-Stress-Stress1

Name	Type	Min	Max
Strain 1	ESTRN: Equivalent Strain	1.805e-007 Element: 29746	2.574e-004 Element: 10037

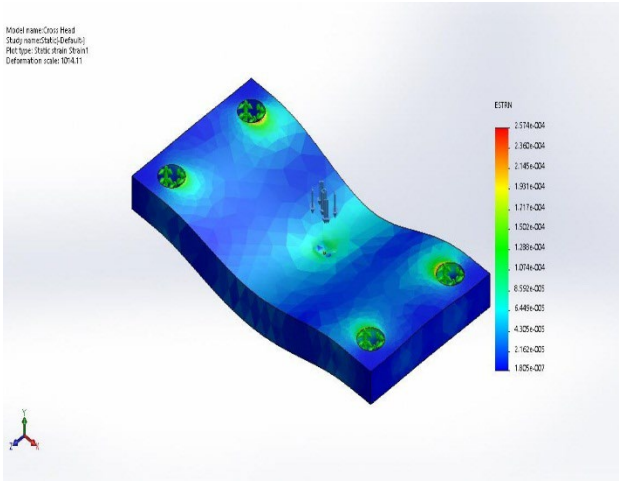

Fig .4 Cross Head: Static-Strain-Strain1

As per the FEA analysis it was observed that von mises stresses induced are well below permissible stresses. So, the design of model is safe, when load was applied as per the selected method.

- **Boundary conditions**
  Boundary conditions are considered as supporting bars are fixed with reference to the crosshead. The material of the crosshead is chosen as plain carbon steel considering its superiority under tensile loads. The simulation results show that stresses generated in the crosshead are well below allowable stress values

SETUP OF A FATIGUE LOADING MACHINE

The setup consists of a fatigue loading machine of capacity 15 kN under dynamic loading and 10 kN under static loading for crack detection in an aluminium plate.

DESIGN PARAMETERS OF HYDRAULIC CYLINDER:

The designed parameters considered are:

Base : T – slot,

Axial Servo hydraulic dynamic two column load frame

1) Selection of cylinder
2) Efficiency of cylinder
3) Determination of piston rod diameter and length
4) Design of piston rod
5) Design of supporting bar

DESIGN PARAMETERS OF SCREW FOR 10 KN LOAD

The designed parameters considered are:

1) Tangential force required at the circumference of the screw
2) Stresses in screw
3) Bearing pressure on threads

4.3 DESIGN PARAMETERS OF SCREW VISE

1) Load on screw thread
2) Stresses in lead screw
3) Number of thread in engagement

DESIGN CALCULATION

DESIGN OF HYDRAULIC CYLINDER

From the manufacturers catalogue of Shimadzu, it is observed that for low load conditions capacity of the machine is to 50 kN. taking the capacity of hydraulic cylinder in the designed model as follows:

Capacity: 5 kN to 15 kN

Base: T – slot

SELECTION OF CYLINDER

Load on hydraulic cylinder = 15 kN

For the hydraulic cylinder selecting piston diameter and rod diameter from Milwaukee cylinder design engineering guide for the given load conditions

Selecting, piston diameter = 38.1 mm

Rod diameter = 15.88 mm

$$Pressure = \frac{Force}{Area} \qquad (3.12)$$

$$Pressure = \frac{15000}{\frac{\pi}{4}(38.1X10^{-3})^2}$$

$$Pressure = 131.56834\ N/mm^2$$

5.1.2 EFFICIENCY OF CYLINDER

$$\eta_{cyl.} = 1 - \frac{\epsilon Fr}{Fs} \qquad (3.13)$$

Where, ϵFr = total frictional force, kN

Fs = static force= 12 kN

Expected efficiency of various hydraulic cylinders is

1) for normal cylinder = 0.94 to 0.98

2) for telescopic cylinder = 0.88 to 0.9

Selection of efficiency on basis of diameter of piston

Diameter of piston	Efficiency of cylin
20 to 50	80 -85
50 to 120	85 – 90
Above 120	90 - 95

Selecting minimum efficiency = 80 %

$$0.80 = 1 - \frac{\epsilon Fr}{12}$$

$$12\ X\ 0.80 = 12 - \epsilon Fr$$

$$9.6 = 12 - \epsilon Fr$$

$$\epsilon Fr = 2.4\ kN$$

DETERMINATION OF PISTON ROD DIAMETER AND LENGTH

This setup designed with equal velocities for extending and retracting of piston,

$$d = 0.2\ D\ to\ 0.3\ D$$

For easy installation & rigidity

$$\frac{L}{D} \leq 20 \quad (3.14)$$

Piston rod diameter = 0.2 D to 0.3 D

Piston rod diameter = 15.88 mm

Assuiming lenth of piston rod = 250 mm

Checking,

$$\frac{L}{D} \leq 20$$

$$\frac{0.25}{0.01588} \leq 20$$

$$15.74 \leq 20$$

Hence Design is safe.

SELECTION OF COMPONENTS

considering flow velocities

consider 75 rpm (75 rev/min)

So, total flow velocity = total distance in 1 cycle = 0.5 m

Velocity are constant for extending and retracting = 0.5 m/s

$$Q = Area\ X\ velocity$$

$$Q = \frac{\pi}{4}\ X\ (0.0381)^2\ X\ 0.5$$

$$Q = 5.7005\ X\ 10^{-4}\ m^3/s$$

$$Q = 34.2\ lpm$$

From literature it is observed that it is desirable to take 3 times the discharge value of oil to have sufficient quantity of oil to flow in the system for generating desired pressure.

So, oil reservoir is taking 3 times the discharge required = 3 X 34.2 = 102.61 lit.

DESIGN OF PISTON ROD

From literature it is found that piston is subject to tensile loads as well as compressive loads, so selective a material which will give reliable results in both tensile loading and compressive loading,

Material = stainless steel

E = 210 GPa = 210 X 10^9 N/mm^2

selecting if is short column or long column

$\frac{L}{D} < 10$ ….Short column

$\frac{L}{D} > 10$ ……Long column

In our case,

L = 0.25 m , d = 0.0381 mm

$$\frac{0.25}{0.0381} = 6.5616 < 10$$

so, short column.

According to Eulers formula,

$$W_{cr} = \frac{\pi^2 EI}{l^2}$$

Where W_{cr} = 2.5 X 10X10^3

$$W_{cr} = \frac{\pi^2 X\ 2\ X\ 10^5 X \frac{\pi}{64} X d^4}{700^2}$$

d = 15.85 mm say 16 mm

DESIGN OF SCREW FOR 10 KN LOAD

Considering the equal distribution of two supporting columns load of 20 kN is divided on each as 10 kN

p = pitch of screw

d = mean diameter of screw

α = helix angle

P = Effort applied

W = Load to be lifted

μ = Coefficient of friction between screw and nut = tan ϕ

ϕ = Friction angle

tan α = p/πd

Torque required to overcome friction between screw and nut,

$$T1 = p\ X \frac{d}{2} = W \tan(\alpha + \emptyset)$$

(5.1)

Taking design parameters for design of screw as,

Load = 10 kN, d = 25 mm, pitch = 5 mm, μ = tan ϕ = 0.2.

Torque required to rotate the screw

Mean diameter of screw,

$$d = do - p/2 = 25 - 5/2 = 22.5 \text{ mm}$$

$$\tan\alpha = \left(\frac{pitch}{\pi d}\right) = \frac{5}{\pi X 22.5} = 0.0707$$

(5.2)

Tangential force required at the circumference of screw,

$$P = W \tan(\alpha + \emptyset) = W \left(\frac{\tan\alpha + \tan\emptyset}{1 - \tan\alpha \tan\emptyset}\right)$$

(5.3)

$$P = 10\ X\ 10^3 \left(\frac{0.0707 + 0.2}{1 - 0.0707\ X 0.2}\right)$$

P = 2745.826 N

Mean radius of screw collar

$$R = \frac{R_1 + R_2}{2} = \frac{25 + 10}{2} = 17.5\ mm$$

Torque required rotating screw

$$T = P\ X\ \frac{d}{2} + \mu_1\ WR$$

$$= 2745\ X\ 22.5$$

$$+ 0.15\ X\ 10^3 X\ 17.5$$

T = 57.1312 X 10^3 Nmm

T = 57.1312 Nm

PRATIBHA: INTERNATIONAL JOURNAL OF SCIENCE, SPIRITUALITY, BUSINESS AND TECHNOLOGY (IJSSBT)
Special Issue: International Conference on Global Trends in Science, Technology, Humanities, Commerce & Management 2022 (ICGTSTHCM 2022)
Vol. 8, No. 2, January 2022,ISSN (Print) 2277-7261

STRESSES IN SCREW

$d_c = d_o - p = 25 - 5 = 20$ mm

Cross – section area of screw,

$$A = \frac{\pi}{4} X {d_c}^2 = \frac{\pi}{4} X 20^2 = 314.2\ mm^2$$

Direct stress,

$$\sigma_c = \frac{W}{A_c} = \frac{10\ X\ 10^3}{314.2} = 31.83\ N/mm^2$$

Shear stress,

$$\tau = \frac{16\ T}{\pi\ X\ {d_c}^3} = \frac{16\ X\ 57131.2}{\pi\ X\ 20^3} = 36.37\ N/mm^2$$

Maximum shear stress in screw,

$$\tau_{max} = \frac{1}{2}\sqrt{({\sigma_c}^2 + 4\ \tau^2}$$
$$= \frac{1}{2}\sqrt{31.83^2 + 4\ X\ 36.37^2}$$
$$= 39.699\ N/mm^2$$

NUMBER OF THREADS OF NUT IN ENGAGEMENT WITH SCREW

n = number of threads of nut in engagement with screw

t = thickness of threads = $\frac{p}{2} = \frac{5}{2} = 2.5\ mm$

Bearing pressure on threads, p_b

Assuming constant bearing pressure on nut = 5.8 N/mm^2

$$5.8 = \frac{W}{\pi\ X\ d\ X\ t\ X\ n} = \frac{10\ X\ 10^3}{\pi\ X\ 22.5\ X\ 2.5\ X\ n} = \frac{56.6}{n} \quad (5.4)$$

$$n = \frac{56.6}{5.8} = 9.76 \approx 10$$

5.3 DESIGN OF VISE SCREW

From literature it sis found that material SAE 3140 gives satisfactory results for the given load conditions

Material of vise screw SAE 3140

Assuming,

W = Load applied at the end of lever = 300 N, F.O.S. = 2, S_{yt} = 350 N/mm^2

By Rankine formula,

Yield stress in tension is calculated as,

$$S_{yt} = \frac{F_{cr}}{A}\left[1 + \frac{1}{\alpha_n}\left(\frac{l}{k}\right)^2\right] \quad (5.5)$$

F_{cr} = W X F.O.S. = 300 X 2 = 600 N

Radius of gyration,

$k = d_c/4$

$$350 = \frac{600}{\frac{\pi}{4}{d_c}^2}\left[1 + \left(\frac{300}{\frac{d_c}{4}}\right)^2 X \frac{1}{0.25\ X\ 10.03\ X10^3}\right]$$

Core diameter of screw, $d_c = 6.04\ mm$

Nominal diameter of screw,

$d_o = d_c / 0.84 = 7.19$ mm ≈ 8 mm

Screw Terms

Mean diameter, $d_m = d_o - p/2 = 24 - 5/2 = 21.5$ mm

Lead = 2 X p = 2 X 5 = 10 mm

$$\alpha = \tan^{-1}\left(\frac{Lead}{\pi\ X\ d_m}\right) = \tan^{-1}\left(\frac{10}{\pi\ X\ 21.5}\right)$$

$\alpha = 8.42^o$

Friction angle,

$$\varphi = \tan^{-1}\left(\frac{\mu}{\sin\beta}\right) = \tan^{-1}\left(\frac{0.12}{\sin 90}\right)$$

$\phi = 6.84^o$

5.3.1 LOAD ON SCREW THREAD

$$T = \frac{Wd_m}{2}\tan(\alpha + \varphi)$$

$$T = \frac{W\ X\ 21.5}{2}\tan(8.42 + 6.84)$$

T = 2.93 W Nmm (5.6)

Torque due to applied force by lever,

Assuming Length of lever = 200 mm

T = 300 X 200

T = 60000 Nmm (5.7)

Substituting value of eq. 5.2 in eq 5.1,

$$W = \frac{60000}{2.93}$$

W = 20477.81 N

POWER REQUIRED

To engage load, Torque required is given by,

$$T_1 = \frac{Wd_m}{2}\tan(\alpha + \varphi) \quad (5.8)$$

$$T_1 = \frac{20477.81\ X\ 21.5}{2}\tan(8.42 + 6.84)$$

T_1 = 60057 Nmm

T_1 = 60.057 Nm

Torque required to disengage load

$$T_2 = \frac{W\mu_c}{2} \quad (5.9)$$

$$T_2 = \frac{20477.81\ X\ 19.01X0.12}{2}$$

T_2 = 23356 Nmm = 23.356 Nm

Total torque,

$T = T_1 + T_2$

T = 60.057 + 23.356

T = 83.413 Nm

Power required to drive screw,

N = 20 rpm, assume for human being

$$P = \frac{2\pi NT}{60}$$

$$P = \frac{2\ X\ \pi X20X\ 83.413}{60}$$

P = 174.69 W

STRESSES IN LEAD SCREW

d_c = 19.01 mm

d_o = 24 mm

Compressive stresses in screw,

PRATIBHA: INTERNATIONAL JOURNAL OF SCIENCE, SPIRITUALITY, BUSINESS AND TECHNOLOGY (IJSSBT)
Special Issue: International Conference on Global Trends in Science, Technology, Humanities, Commerce & Management 2022 (ICGTSTHCM 2022)
Vol. 8, No. 2, January 2022,ISSN (Print) 2277-7261

$$\sigma_c = \frac{W\ X\ 4}{\pi\ X\ {d_c}^2}$$

$$\sigma_c = \frac{300\ X\ 4}{\pi\ X\ 19.01^2}$$

σ_c = 1.056 N/mm^2

shear stress in screw,

$$\tau = \frac{16\ T}{\pi {d_c}^3}$$

$$\tau = \frac{16\ X\ 67478}{\pi\ X\ 19.01^3}$$

τ = 50.02 N/mm^2

Principal stresses developed in screw,

$$\sigma_{max} = \frac{1}{2}\left[\sigma_c + \sqrt{{\sigma_c}^2 + 4\tau^2}\right]$$

$$\sigma_{max} = \frac{1}{2}\left[1.056^2 + \sqrt{1.056^2 + 4\ X\ 50.02^2}\right]$$

σ_{max} = 50.55 N/mm^2

$$\tau_{max} = \frac{1}{2}\sqrt{{\sigma_c}^2 + 4\ \tau^2}$$

$$\tau_{max} = \frac{1}{2}\sqrt{1.056^2 + 4\ X\ 50.02^2}$$

τ_{max} = 50.02 N/mm^2

NUMBER OF THREADS IN ENGAGEMENT

$$p_b = \frac{W}{\frac{\pi}{4}({d_o}^2 - {d_c}^2)n} \quad (5.10)$$

Take, p_b = 15 N/mm^2, safe bearing stress

$$15 = \frac{4\ X\ 20477.81}{(24^2 - 19.01^2)n}$$

n = 25.44

n = 25.44 X 3 = 76 mm

CONCLUSION

Conclusion from literature review

Engineering structures are in general exposed to cyclic or stochastic mechanical loading. Exhibiting incipient cracks, particularly light-weight shell and plate structures suffer from fatigue crack growth, limiting the life time of the structure and supplying the risk of a fatal failure. Due to the uncertainty of loading boundary conditions and the geometrical complexity of many engineering structures, numerical predictions of fatigue crack growth rates and residual strength are not reliable. Most experimental monitoring techniques, nowadays, are based on the principle of wave scattering at the free surfaces of cracks. Many of them are working well, supplying information about the position of cracks. One disadvantage is, that those methods do not yield any information on the loading of the crack tip. On the other hand, there are techniques to measure the stress intensity factors e.g. applying a strain gauge in front of the crack tip. However, this method does not allow for crack growth. The goal of our work is the development of a monitoring concept supplying both the information on the actual crack position and the stress intensity factors [1].

Most structural members and machine components are subjected to multi-axial stress – strain conditions due to geometrical configuration, discontiniues and or temperature fluctuations.Author shows that principal stresses may be nonproportional and the principal directions can often change throughout the component's load cycle of life. Finite endurance

limits, calculated using the predicted service life, are therefore used in the designof components and structures subject to conditions of multiaxial loading. In order to improve accuracy of fatigue criteria, reliable experimental methods must be selected. Paper highlights existoig multiaxial fatigue loading systems and outlines the requirements of the experimental methods needed to obtain reliable fatigue results under laod configurations and for different specimens. The importance of using loading methods which ensure that all possible $\varepsilon_2/\varepsilon_1$ ratios (where ε_2, ε_1 are principal strains) which reference to local multiaxial stress – strain states and stress – strain gardients [2].

Long-span spatial structures are widely used in stadiums, theaters, exhibition centers, airport terminals, and many other large scale structures. Any one of these structures can simultaneously house a large number of occupants. As a result, guaranteeing the integrity of these structures is of great importance. Structural health monitoring (SHM) systems should be established for important buildings. For important buildings undergoing construction, a long-term health monitoring system should also be set up to monitor the health condition of the buildings during the construction and service stages. It is essential to monitor structural conditions and detect damage in real-time for future construction projects. For structural health monitoring projects, one of the core approaches used is damage identification.

The damage identification of a reticulated shell is a challenging task, facing various difficulties, such as the large number of degrees of freedom (DOFs), the phenomenon of modal localization and transition, and low modeling accuracy. Based on structural vibration responses, the damage identification of a reticulated shell was studied. At first, the auto-regressive (AR) time series model was established based on the acceleration responses of the reticulated shell. According to the changes in the coefficients of the AR model between the damaged conditions and the undamaged condition, the damage of the reticulated shell can be detected. In addition, the damage sensitive factors were determined based on the coefficients of the AR model. With the damage sensitive factors as the inputs and the damage positions as the outputs, back-propagation neural networks (BPNNs) were then established and were trained using the Levenberg–Marquardt algorithm (L–M algorithm) The locations of the damages can be predicted by the back-propagation neural networks. At last, according to the experimental scheme of single-point excitation and multi-point responses, the impact experiments on a K6 shell model with a scale of 1/10 were conducted. The experimental results verified the efficiency of the proposed damage identification method based on the AR time series model and back-propagation neural networks. The proposed damage identification method can ensure the safety of the practical engineering to some extent [3].

Santosh Chauhan et al. [7] developed a rotating bending fatigue testing as a part of laboratory development project. Specimen of mild steel attached to the shaft of high carbon alloy steel EN8 was selected to rotate the specimen and it was under action of bending from dead weights hanged to overhang bearings. Theoretical values of equivalent stress development vs. number of cycles to failure were compared for different diameter specimens such as 6 kg and 7 kg with 15 kg dead weights attached to the overhang bearing. Experimental values were compared with the theoretical values found to be good agreement. Machine could be used to generate bending stress– number of cycles data. Martin et al. [8] fabricated a setup for fatigue testing machine, which was mounted on table and it was designed for low load application for specimen of stainless steel grade. Results were plotted for stress vs. number of cycles. Endurance limit was calculated experimentally for the specimen selected which was found to be 176.83 Mpa compared actual endurance limit of 220 Mpa. Error was 19.62% in experimental and actual values of endurance limit.

Cracks in structures takes place due to certain reasons such as mechanical defects, faults from the manufacturing process. Because of the occurrence of cracks in the structures may lead to change the whole behaviour of the element and consequently decreases

its safety. Also the presence of crack indicates fatigue problem. So the detection or identification of cracks in the structures is a relevant issue. According to Rytter there are four different levels of damage detection in a structure can be attained, they are

• Level 1: detection of the existence of damage
• Level 2:level 1 + damage location
• Level 3: level 2 + damage quantification
• Level 4: level 3 + prediction of the remaining service life [10].

References

[1] Ramdane Boukellif, Andreas Ricoeur, "Monitoring fatigue cracks and stress intensity factors based on local strains", PAMM · Proc. Appl. Math. Mech. 12, 141 – 142 (2012).

[2] J. Ziebs, J. Meersmam, H. J. Kiihn, S. Ledworuski, "Experimental techniques for testing materials under multiaxial loading", ESIS, Mechanical Engineering Publication, London. pp. 173-193.

[3] Jiang Xu, Jiajia Hao, Hingnan Lim Minzhang Luo, Wen Guo, Weijie Li, "Experimental damage identification of model reticulated shell", MDPI, Applied science, April 2017.

[4] Farnaz Raeisi, Aftab Mufti, Douglas J. Thomson, "Crack detection in steel girders of bridges using a broken wire electronic binary sensor., Journal of Civil and structural health monitoring, March 2017.

[5] M. S. Cao, G. G. Sha, Y. F. Gao, W. Ostachowicz, "Structural damage identification using damping: a compendium of uses and features", Smart materials and structures, 26 (2017) 043001 (14 pp).

[6] Gbasouzor Austine Ikechukwu, Okeke Ogochukwu Clementina, Chima Lazarus Onyebuchi, " Design and characterization of a fatigue testing machine", Proceedings of the World Congress on Engineering and Computer Science 2013 Vol I, WCECS 2013, 23-25 October, 2013, San Francisco, USA.

[7] Santosh J. Chauhan, Aarti Misal, Akanksha Jadhav, Rahul Jadhav, Abhir Bhalavi, Rohit Jagdale, "Design and fabrication of rotating bending fatigue testing machine – A laboratory development project", International Research Journal of Engineering and Technology (IRJET), Volume: 03, Issue: 04, Apr-2016.

[8] Martin K Vincent, Vipin Varghese V., Suneeth Sukumaran, "Fabrication and analysis of fatigue testing machine", The International Journal Of Engineering And Science (IJES), Volume 5, Issue 7, pages 15-19, 2016.

[9] Ioannis Pitropakis, Helge Pfeiffer, Thomas Gesang, Stein Janssens and Martine Wevers, "Crack Detection in Aluminium 2024-T3 Plates and in an Airbus A320 Slat-Track using Electrical Crack Gauges"

[10] D. R. Parhi, Manoj Kumar Muni and Chinmaya Sahu, "Diagnosis of cracks in structures using fea analysis", IJAAIES, Vol. 4, No. 1, 2012.

[11] Harshal Vispute, Akshay Kamane, Vardhan Patil, Suraj Shaha, Santosh Katkar,"Design of mechanical test setup to find the endurance limit of coil/compression spring using modified slider – crank mechanism", International Journal of Scientific & Technology Research, volume 4, issue 10, october 2015

[12] Mr. Shrikant M. Chougule, Prof. D. B. Waghmare, "Design and manufacturing of components of modified bench vise on rapid prototype machine", International Journal of Application or Innovation in Engineering & Management (IJAIEM), Volume 4, Issue 7, July 2015.

[13] Akshay Kamane, Harshal Vispute, Vardhan Patil, Suraj Shaha, Santosh Katkar, "Design of hydraulic test setup to find the endurance limit of coil/compression springs using limit swaitches", International Journal of Engineering Trends and Technology (IJETT) – Volume 27 Number 4 - September 2015.

[14] Jarkko Tikka, Risto Hedman, Aslak Siljander, "Strain gauge capabilities in crack detection", 4th International Workshop on Structural Health Monitoring, Stanford, CA 15-17 September 2003.

[15] M. Fitzka, H. Mayer, "Variable amplitude testing of 2024 – T351 aluminium alloy using ultrasonic and servo – hydraulic fatigue testing equipment", 3rd International conference on material and component performance under variable amplitude loading, procedia Engineering 101 (2015), 169 – 176.

[16] Jatin Patel, Prof. Mitesh Mungla, "Crack detection of pipe using static deflection method", International Journal of

Engineering Research & Technology (IJERT), Vol. 3 Issue 1, January – 2014.

[17] Hong-Ming Chen, Guo-Wei Yang, Chong-Cyuan Liao, "Precision Force Control for an Electro-Hydraulic Press Machine", Smart *Science* Vol. 2, No. 3, pp. 132-138(2014).

[18] Ehsan Jalayeri, Ahmed Imam, Zeljko Tomas, Nariman Sepehri, "A throttle – less single – rod hydraulic cylinder positioning system: Design and experimental evaluation", Advances In Mechanical engineering, Vol. 7(5), 1-14, 2015

PRATIBHA: INTERNATIONAL JOURNAL OF SCIENCE, SPIRITUALITY, BUSINESS AND TECHNOLOGY (IJSSBT)
Special Issue: International Conference on Global Trends in Science, Technology, Humanities, Commerce & Management 2022 (ICGTSTHCM 2022)
Vol. 8, No. 2, January 2022,ISSN (Print) 2277-7261

Designing of Membrane Bio-reactor for Sewage Treatment Plant

Sakshi Baniya[*1], *Dr. N. Y. Ghare*[2]

[*1]Assistant Professor, SSBT's COET, Jalgaon

[2]Assistant Professor, SSBT's COET, Jalgaon
[*1]sakshibaniya07@gmail.com,[2] nyghare@gmail.com

Abstract

Membrane bio reactor is one of an effective technology for municipal waste water treatment, industrial waste water treatment and reprocess of waste water in large buildings. Submerged anaerobic membrane bio- reactor (AnMBR) is grouping of biological activated sludge process and membrane filtration. It is a success technology due to its altered recompenses over conventional membrane bio-reactors, AnMBR suggested many advantages with excellent effluent quality, steady operation performance, reduction of surplus sludge production, reuse of effluent, reduction of risk substances and with important removal of contaminants, AnMBR is simple, consistent and cost-effective process. The foremost drawback inhibiting extensive application of AnMBRs is membrane fouling which particularly ensuing in excellent increase maintenance and operating cost, reduces membrane performance and lifespan. The design methodology of AnMBR was established on the basis of simulation and experimental results from plant helping industrial scale hollow fibre membranes. The finest porosity range for MBR is 55-60%. Industrial scales hollow fibre membranes.

Keywords: Membrane bioreactor, Sewage Treatment Plant, Activated sludge

A design methodology was developed on the basis of simulation, knowledge and operation experience gained from an AnMBR plant supporting industrial-scale hollow-fibre membranes that fed with wastewater from pre-treatment of municipal WWTP (Waste Water Treatment Plant).[1]
The MBR technology revolutionized the wastewater treatment.[3]

1) Lack of access to safe water has several effects including:

A. Access to safe water nearby to home will save amounts of time that can be devoted to productive activities and education, which place the origin for economic growth.
B. Lack of access to water decreases the quantity of food available in both crops and depreciates the quality.
C. Lack of access to water increase gender discrimination and reducing the opportunities of girls and women for education, literacy and income producing activities.
D. Lack of access to water can have an consequence on environmental and climate variation because of landscape erosion and damage of habitat like desertification and declines bio-diversity.

I. MATERIAL AND METHODOLOGY

Material:

Raw sewage water from Municipal Corporation, PTFE membrane, bioreactor.

Methodology

A. Collected raw water as inlet to reactor, which is heated at many temperature ranges.
B. Filled it to reactor or aeration tank upto the membrane entirely deeped.
C. Stopwatch was started.
D. Calculated the time required to permit water through the membrane walls.
E. Samples were collected.
F. Checked out the water characteristics of outlet or treated water.

Fig.1 Membrane Element

PRATIBHA: INTERNATIONAL JOURNAL OF SCIENCE, SPIRITUALITY, BUSINESS AND TECHNOLOGY (IJSSBT)
Special Issue: International Conference on Global Trends in Science, Technology, Humanities, Commerce & Management 2022 (ICGTSTHCM 2022)
Vol. 8, No. 2, January 2022,ISSN (Print) 2277-7261

Fig 2 : Experimental arrangement

II. OBSERVATION

From the specified data of several water features of inlet and outlet which will help to calculate % of exclusion at respectively stage of sewage water treatment.

Characteristics	Raw sewage (inlet)	ppm	%removal
pH	6.6-7.2	7	2.78
Total Dissolved Solid	600-650	50-100	84.6
Chemical Oxygen Demand	400-450	-	99.99
Biological Oxygen Demand	250-300	-	99.99
Hardness	175-200	20-50	75
NH4-N	20-30	<1	96.6
Chlorides	150-180	10-20	88.8
Silica	10-15	<1	93.3
Oil & grease	20-30	-	100
Sulphates	40-60	10-15	75

Table No. 1: Treated water characteristics

III. RESULT AND DISCUSSION:

From Fig.3 it is concluded that, as temperature increases the conductivity of inlet also increases means that viscosity of sewage water decreases with respect to temperature, but in case of outlet there is no main change in the conductivity.

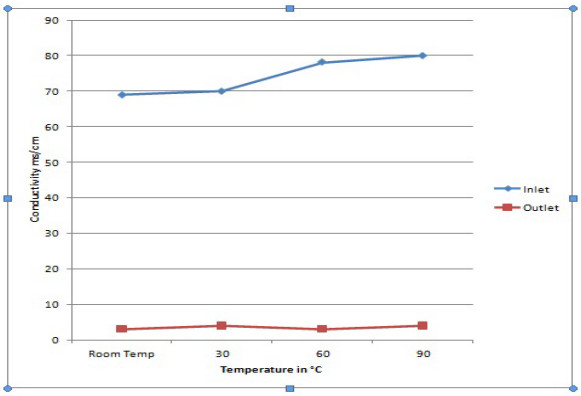

Fig 3: Temperature vs Conductivity

From the Fig 4 it is concluded that, at inlet TDS of the raw water is high as compare to the outlet data, as the temperature increases TDS also increases, if this raw water treated in the membrane bio-reactor we acquire water with very low TDS in range of (10-20).

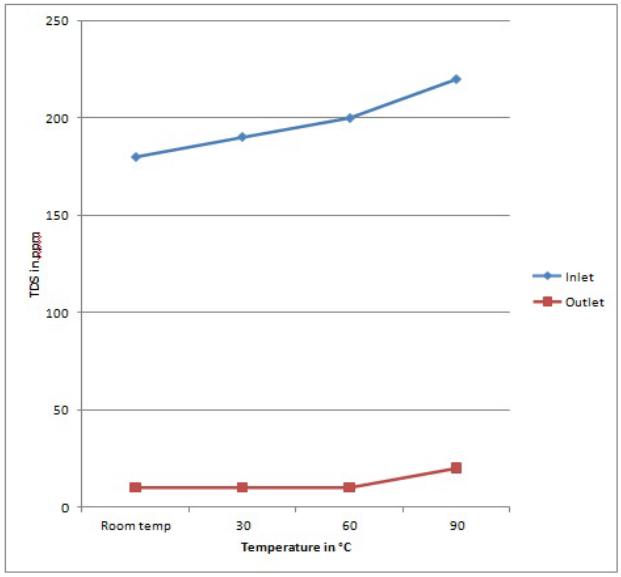

Fig 4: Temperature vs TDS

IV. CONCLUSION

A. AnMBR is the complete virus removal process.
B. Membrane bioreactors (MBRs) has produce to be serious competitors to other procedures on the part of quality of water cleaning. This is the fresh and perspective technology; however it is still

slightly expensive, although not so complex to control it.

C. The treatment performance of the MBR is improved than in conventional activated sludge processes. A high conversion of ammonium to nitrate and constant COD removal efficiency was achieved, irrespective of influent fluctuation.

D. As comparing and examining performance of external and internal MBR the effective choice for the waste water treatment is AnMBR or internal/submerged MBR with the Polytetra fluroethylene (PTFE) membrane material.

V. REFERENCES

1. Ferrer, J.; Pretel, R.; Durán Pinzón, F.; Giménez, J.; Robles Martínez, Á.; Ruano García, MV.; Serralta Sevilla, J.... (2015). Design methodology for submerged anaerobic membrane bioreactors (AnMBR): A case study. Separation and Purification Technology. 141:378-386. doi:10.1016/j.seppur.2014.12.018
2. Chaize, Huyard (1991), Membrane bioreactors on domestic was the water treatment sludge production and modeling approach. Water Science and Technology 231591 – 1600.I.S.Chang,
3. Naghizadeh .A,. Mahvi (B) A. H. Mesdaghinia. A. R. Alimohammadi. M. (2011). Application of MBR Technology in Municipal Wastewater Treatment.36.pp.3-10.
4. Clech, Jefferson128 (2002), Judd, Membrane fouling in membrane bioreactors for waste water treatment, J. Environ. Eng. 1018 – 102 Germain, Stephenson (2005),
5. Biomass characteristics, aeration and oxygen transfer in membrane bioreactors: Their interrelations explained by a review of aerobic biological processes, Environmental Science and Bio/Technology, 4:223 – 233
6. Judd S (2006) The MBR Book. Elsevier, Oxford, UK 5. Chang IS, Lee CH(1998) Desalin 120:221
7. Choi J G, Bae TH, Kim J H, Tak TM, Randall A A (2002) J Membr Sci 203:103.
8. Metcalf and Eddy, “Wastewater Engineering”, Mc Graw Hill, Fourth Edition,Pg.492,2003
9. Metcalf and Eddy, “Wastewater Engineering”, Mc Graw Hill, Fourth Edition,Pg.548,2003
10. Eleventh International Water Technology Conference, IWTC11 2007 Sharm El-Sheikh, Egypt
11. Ahansazan.B, Afrashteh.H, Ahansazan.N, and Ahansazan.Z. 2014.” Activated Sludge Process Overview”. International Journal of Environmental Science and Development, 5, (1),pp.81-85

PRATIBHA: INTERNATIONAL JOURNAL OF SCIENCE, SPIRITUALITY, BUSINESS AND TECHNOLOGY (IJSSBT)
Special Issue: International Conference on Global Trends in Science, Technology, Humanities, Commerce & Management 2022 (ICGTSTHCM 2022)
Vol. 8, No. 2, January 2022,ISSN (Print) 2277-7261

Effect of Impact Location on FRF in Terms of Relative Displacement for Composite Material by FEA

[1]Nilesh S. Navagale, [2]Rahul B. Barjibhe
[1]Research Scholar, K.B.C.N.M.U. Jalgaon (M.S.)
[2] Prof. S.S.G.B.C.O.E.T., Z.T.C. Bhusawal. (M.S.)
[1,2] Mechanical Engineering Department, S.S.G.B.C.O.E.T., Z.T.C. Bhusawal,
E-mail:[1]nsnavagale_2008@rediffmail.com,[2]rahulbarjibhe@yahoo.com

Abstract

The vibration characteristics of mechanical structures or constituents are easy to understand by modal analysis. The modal analysis is used to alter the vibration response. The excitation and responses restrained on a composite specimen or structure. For discover the main mutable in a difficult condition the F. E. Analysis is an influential statistical method. In this research work, the influence of the impact position on the subsequent Frequency Response Function (FRF) in terms of relative displacement is deliberated [7]. To perform this analysis, Aluminum (Al 6061T6) and Butyl Rubber are used as the main material and Viscoelastic Damping Material (VDM) correspondingly to make the complex material sample. This sample contains a butyl rubber plate that is inserted among two AL6061T6 plates. The sizes of the sample are 350mm in length (with at one side 50mm constrained) and a breadth of 50 mm. The thickness of the sample is different and it is 4.8mm, 5mm, and 5.5 mm. This wideness of sample is dependent on the thickness of VDM which is Butyl Rubber. The chief purpose of this research work here is to analyze the result of impact position towards the natural modal frequency and Frequency Response Function. This study and analysis are particularly in terms of displacement magnitude for composite structure/specimen. The software used here in this analysis is Abacus.

Keywords: VDM, Natural Frequency, Impact Location, Composite Material, Abacus.

I. INTRODUCTION

Normally, the displacement, velocity, or acceleration response of a structure/specimen is measured by Frequency Response Function (FRF) analysis. To discover the displacement usually the acceleration signal is divided by an aspect which is relational to the square of the frequency. The measuring device is normally used to compute this. Commonly for measuring small frequencies viz. less rotations per minute, displacement is utilized whereas acceleration is utilized for determining great frequencies such as bearing frequencies. Acceleration is the rate of alteration of velocity which is the next derivative of displacement. The result on the comparative level displacement of the chief 6 natural frequencies for the dissimilar impact positions is analyzed in this effort.

A. Frequency Response Measurement

The frequency response dimensions depend on a few major factors. Some of this contain the form of sample which is verified and the level of consequences preferred. Another features are the backing fixture and the excitation appliance which also affect the volume of hardware desired to accomplish the trial. It is to deliberate the fix Turing appliance essential to get the preferred constraints such as boundary circumstances which is the head stage to locale a sample/test plate for determining the frequency reaction. As it marks the overall structural characteristics, particularly for subsequent analyses it is called the chief step in the process. Logically, boundary circumstances could be identified in a totally free or totally constrained condition. Also the constrained condition indicates that the motion i.e. displacement or rotation is set to zero. However, in actual practice or reality, most of the structures show some degree of flexibility at the grounded contacts.

II. FINITE ELEMENT MODAL ANALYSIS

The Finite Element Modal Analysis, in this research work, is carried out by using the real boundary conditions. This analysis supports to the discovery of Natural frequency, Mode shapes, and Frequency Response Functions (FRFs). Consequently, three specimens of composite plate or specimen are prepared whose material properties and specimen proportions are shown in the following table.

PRATIBHA: INTERNATIONAL JOURNAL OF SCIENCE, SPIRITUALITY, BUSINESS AND TECHNOLOGY (IJSSBT)
Special Issue: International Conference on Global Trends in Science, Technology, Humanities, Commerce & Management 2022 (ICGTSTHCM 2022)
Vol. 8, No. 2, January 2022,ISSN (Print) 2277-7261

Table-1 Material Properties

Properties	Materials	
	Al 6061 T6	Butyl Rubber (VDM)
Density	2.7 g/cm^3	1.35 g/cm^3
Young's Modulus	68.9 GPa	0.0015GPa
Poisson's Ratio	0.33	0.4

Table-2 Sample Description

Sample	Composites	Thickness (mm)		
		Al	B.R.	Al
1	Al –BR- Al	2	0.8	2
2	Al –BR- Al	2	1	2
3	Al –BR- Al	2	1.5	2

This analysis includes a CAD model of the control sample using CAD software/tools such as CATIA V56R (2016). This model is used to generate geometry and assemblies. In meshing the neutral format of CAD geometry is introduced in Pre-processor such as Hypermesh. For discretizing or for meshing, the geometries and relate material and boundary circumstances, Hypermesh v-12 is used. The meshed model is submitted to the solver to discover the natural frequencies and mode shapes of the test sample by use of ABAQUS. Here ABAQUS 6.13-1 type is recycled to group the level and track the investigation to gain natural frequencies and FRFs in constrained conditions

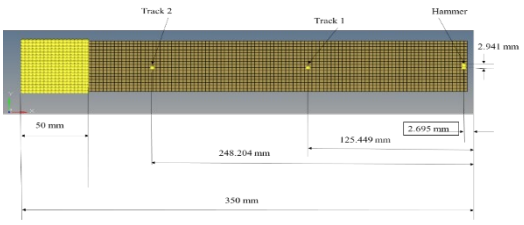

Figure 1. Position of Impact Location

III. RESULT AND DISCUSSION

A. Frequency Response Functions of Relative Displacement

The relative displacements for each frequency are recorded at all 3 points viz. hammer, first track and second track and are as shown in the following tables.

Table 3 Displacement at Hammer, First Track and Second Track (Sample 1)

Relative Displacement				
Sr. No.	Freq. No.	Hammer	First Track	Second Track
1	0	0	0	0
2	1	57.4092	24.5459	2.6288
3	2	57.4169	24.5495	2.62922
4	3	57.4263	24.554	2.62974
5	4	57.4381	24.5595	2.63039
6	5	57.4535	24.5668	2.63123
7	6	57.4742	24.5765	2.63237
8	7	57.5036	24.5904	2.63399
9	8	57.5489	24.6118	2.63649
10	9	57.6303	24.6502	2.64097
11	10	57.8453	24.7516	2.65282
12	11	64.5873	27.9328	3.02451
13	12	71.5536	31.2218	3.4091
14	13	79.7566	35.0966	3.86246
15	14	90.4356	40.143	4.45322
16	15	105.228	47.136	5.27225
17	16	127.198	57.5262	6.48972
18	17	163.16	74.5384	8.48387
19	18	231.739	106.989	12.2889
20	19	398.863	186.083	21.5653
21	**20**	**2.62885**	**1.47956**	**0.438123**
22	21	536.135	256.499	30.3535

Table 4 Displacement at Hammer, First Track and Second Track (Sample 2)

Relative Displacement				
Sr. No.	Freq. No.	Hammer	First Track	Second Track
1	0	0	0	0
2	1	58.3986	25.0155	2.71564
3	2	58.4067	25.0192	2.71609
4	3	58.4166	25.0239	2.71664
5	4	58.429	25.0298	2.71734
6	5	58.4452	25.0374	2.71824
7	6	58.4669	25.0477	2.71946
8	7	58.4977	25.0622	2.72118
9	8	58.5452	25.0847	2.72384
10	9	58.6302	25.1248	2.7286
11	10	58.8543	25.2307	2.74115
12	11	65.8057	28.5159	3.13082
13	12	72.9571	31.8976	3.53225
14	13	81.3668	35.8764	4.00483
15	14	92.3069	41.0544	4.62019
16	15	107.453	48.2261	5.4729
17	16	129.941	58.8776	6.73993
18	17	166.733	76.3104	8.81443
19	18	236.85	109.541	12.7701
20	19	407.316	190.344	22.3908
21	**20**	**2.67014**	**1.50209**	**0.456902**
22	21	545.447	261.357	31.4026

Table 5 Displacement at Hammer, First Track and Second Track (Sample 3)

Relative Displacement

Sr. No.	Freq. No.	Hammer	First Track	Second Track
1	0	0	0	0
2	1	58.9796	25.2737	2.7434
3	2	58.9882	25.2778	2.74388
4	3	58.9987	25.2827	2.74447
5	4	59.012	25.289	2.74521
6	5	59.0291	25.2971	2.74617
7	6	59.0522	25.308	2.74746
8	7	59.0848	25.3234	2.74929
9	8	59.1349	25.3471	2.7521
10	9	59.2244	25.3893	2.75711
11	10	59.4594	25.5004	2.77028
12	11	66.6302	28.8892	3.17237
13	12	73.9569	32.3538	3.58378
14	13	82.5552	36.4217	4.06712
15	14	93.7276	41.7098	4.69577
16	15	109.184	49.0281	5.56621
17	16	132.117	59.8904	6.85875
18	17	169.614	77.657	8.97364
19	18	240.999	111.487	13.002
20	19	413.891	193.438	22.7624
21	**20**	**2.68779**	**1.51085**	**0.461965**
22	21	550.848	263.928	31.7225
23	22	372.934	179.593	21.6774

B. Frequency Response Functions (FRF's) Plots of Relative Displacement

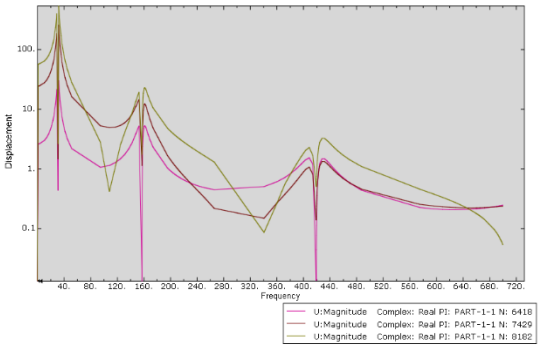

Sample 1

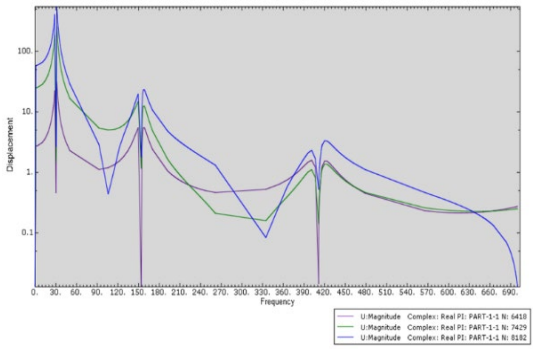

Sample 2

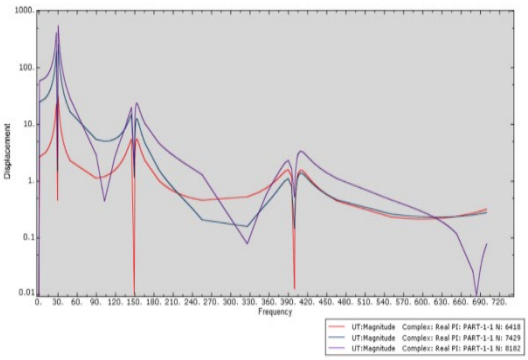

Sample 3

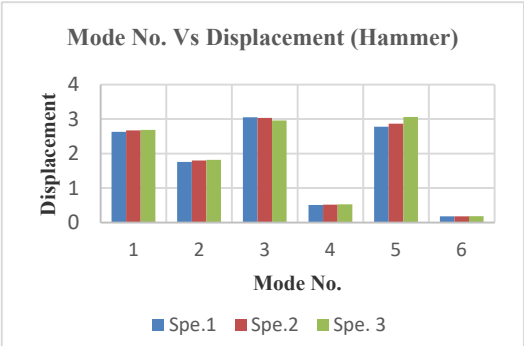

Graph 1 Relative Displacement at Hammer, First Track and Second Track

Table 6 Relative Displacement of Composite Samples (Hammer Position)

Mode No.	Hammer Position		
	Sam.1	Sam.2	Sam.3
1	2.62885	2.67014	2.68779
2	1.75902	1.79832	1.81948
3	3.05322	3.03455	2.9616
4	0.507641	0.51735	0.525924
5	2.77916	2.86649	3.06231
6	**0.181141**	**0.181084**	**0.183766**

Table 7 Relative Displacement of Composite Samples (First Track)

Mode No.	First Track		
	Sam.1	Sam.1	Sam.1
1	1.47956	1.47956	1.47956
2	1.1389	1.1389	1.1389
3	0.8591	0.8591	0.8591
4	0.139675	0.139675	0.139675

5	1.12353	1.12353	1.12353
6	**0.224491**	**0.224491**	**0.224491**

Table 8 Relative Displacement of Composite Samples (Second Track)

Mode No.	Second Track		
	Sam.1	**Sam.1**	**Sam.1**
1	0.438123	0.438123	0.438123
2	0.013314	0.013314	0.013314
3	0.697034	0.697034	0.697034
4	0.013484	0.013484	0.013484
5	1.21617	1.21617	1.21617
6	**0.215469**	**0.215469**	**0.215469**

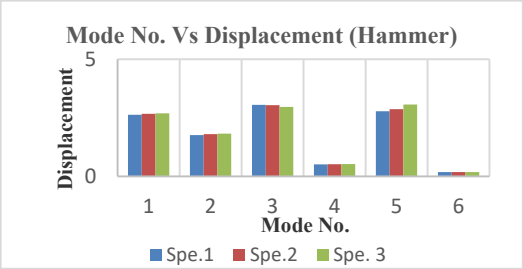

Graph 2 Hammer Disp.

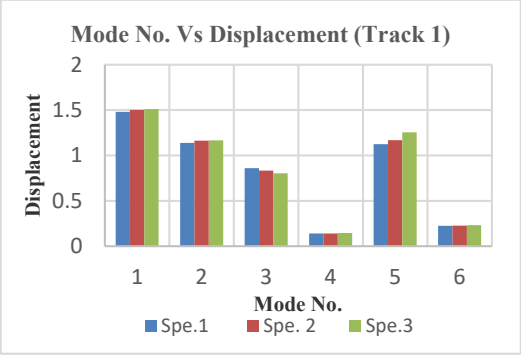

Graph 3 First Track Disp.

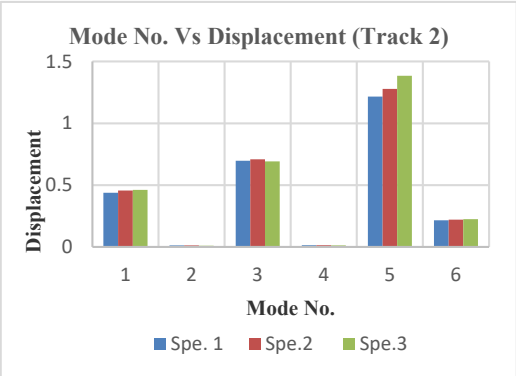

Graph 4 Second Track Disp.

The above relative displacements at hammer, first track and second track for each mode are characterized graphically in the above graphs.
Later the F.E. analysis for F.R.F., the proportional data for the readings of relative displacement for every specimen no. 1, 2, and 3. These readings are at the position of the impact hammer. Here the 3 positions of impact are reflected which are at hammer point, at first track and at second track. Also the relative displacement is intended at every location.

IV. CONCLUSION

From the table of displacement, it is evaluated that the displacement magnitude which is relative displacement magnitude is supreme at the first point i.e. Hammer point which is very close to the exciting edge of the sample from its right hand side. For the second point which is the first track the relative displacement goes on reducing as associated to the first point which is Hammer position. Also for the third point which is second track, the relative displacement is lower than the other two positions. After words, it can be evaluated that,
Relative Displacement (T.P. 2) < Relative Displacement (T.P.1) < Relative Displacement (H. P.).
Also relative displacement at Hammer, Track 1and Track 2 point get reducing from sample 1 to sample 3 excluding at mode 6 at which it is somewhat accumulative. The FRF is nearly similar irrespective of the hammer position. All this analysis is also characterized graphically by scheming the graphs as indicated overhead. Also by relating samples 1,2 and sample 3, it may be recommended that composite sample 2 (with VDM of width 1mm) have an improved FRF for relative displacement as compared to other

composite samples. Also it may be the greatest appropriate substitute composite material.

REFERENCES

[1] A.S.Adkine, V.S.Kathavate, G.P.Overikar, S.N.Doijode,"Static Behaviour of Engine Mounting Bracket,"Int. Advanced Research Journal in Science, Engineering and Technology, ISSN: 2393-8021Vol. 2, Issue 4, April 2015 pp-68-73.

[2] S. K. Panda • B. N. Singh, "Nonlinear free vibration analysis of thermally post-buckled composite spherical shell panel," Int Journal Mech Mater Des (2010) 6:175–188, DOI10.1007/s10999-010-9127-1 pp. 175-188.

[3] Pavan B. Chaudhari, Dr.D. R. Panchagade, "Comparison of Magnesium, Aluminium and Cast Iron to obtain Optimum Frequency for Engine Bracket using Finite Element Analysis", International Journal of Engineering Research and Applications (IJERA) ISSN: 2248-9622 Vol. 2, Issue 5, September- October 2012, pp.1016-1020.

[4] Avinash Kadam, et all, "Finite Element Analysis of Damping Performance of VEM Materials Using CLD Technique", Inter. Journal of Engg. Research and Applications, ISSN: 2248-9622, Vol. 4, Issue 7, July 2014, pp. 150-153.

[5] Puneet Sharma, Ashish Gupta, et. all. "Dynamic Modelling and Validation of Continuous Beam with Free-Free Boundary Conditions", International Advanced Research Journal in Science, Engineering, and Technology (IARJSET), ISSN (online):2393-8021, ISSN (print):2394-1588, volume 4, Special Issue 3, Feb. 2017, pp.47-53.

[6] Victor Zavodinsky, Yuri Kabaldin "Investigation of Aluminium Based Composites Durability", International Journal of Composite Materials 2017,4 (4) DOI: 10.5923/J.C Materials.20170704.03, pp.127-129.

[7] Gourav Gupta, Ankur Kumar, et all, "Application and Future of Composite Materials:- A Review", International Journal of Innovative Research in Science, Engineering and Technology (IJIRSET), ISSN(Online): 2319-8753, ISSN(Print): 2347-6710, vol. 5, Issue 5, May 2016, pp.6907-6911.

[8] Ahmed Maher, Fawkia Ramadan, Mohamed Ferra, "Modeling of vibration damping in composite structures", Composite Structures 46 (1999) pp-163-170.

PRATIBHA: INTERNATIONAL JOURNAL OF SCIENCE, SPIRITUALITY, BUSINESS AND TECHNOLOGY (IJSSBT)
Special Issue: International Conference on Global Trends in Science, Technology, Humanities, Commerce & Management 2022 (ICGTSTHCM 2022)
Vol. 8, No. 2, January 2022,ISSN (Print) 2277-7261

Effect of Waste Tyre Rubber on Strength Characteristics of Concrete

Sonali B. Patil[1],Dr. Mujahid Husain[2]

[1]Research Scholar,Civil Engineering Department,SSBT's College of Engineering & Technology, Bambhori, Jalgaon, MS, India.
borsesp14@gmail.com
[2]Professor& Head ,Civil Engineering Department ,SSBT's College of Engineering & Technology, Bambhori, Jalgaon, MS, India.
ermujahidhusain@gmail.com

Abstract

The use of rubber in concrete is increasing due to both the reasons, the scarcity of natural aggregates and environmental reasons. The rubber makes the concrete light in weight and economical. In the present work waste tyre rubber is used as partial replacement of fine aggregate to produce rubbercrete. The replacement is in the range of 0, 10, 25, 33 and 55,66,75% by volume of fine aggregate. The uniform cubes are casted and tested for compressive strength for duration of 28 days, and exposed to the natural environmental conditions for 6 months, 1 year and 2 years. This work has done a pioneer attempt to assess the long term performance of rubbercrete It has been found that in the course of two years, when the rubbercrete is exposed to the natural environmental conditions, it looses the strength very marginally.

Keywords: *Rubbercrete, endurance, compressive strength of rubbercrete, , long term performance*

INTRODUCTION

One of the most important sectors for the economic growth of a country is considered to be the construction sector. This sector also plays a significant role in providing housing facility for the continually growing population. The rapid growth of construction sector, consequently requires considerably large amount of construction materials to be produced for consumption e.g. rock materials and sand also called as coarse and fine aggregates. The most important material in the construction industry is concrete. Rock materials and sand are depended upon the mining and quarry industry as a main source of raw construction material There should be guarantee for the adequate and regular availability of raw materials to the construction sector to continue their production and thus to sustain the economic development. The natural aggregates are non-renewable sources. The aggressive consumption will reduce them if no control measures are imposed (Hamid, et al., 2006). Proper planning and use of alternatives are essential and to avoid shortage . Therefore, There are so many alternative ways suggested. Recycling the aggregates obtained from demolished structures is one of the ways. Use of manufactured materials is another. Now a days, use of scrap tyre rubber is also considered to be a way as it is used in concrete successfully.

Experimental Procedure

Materials and Methods

Materials - Cement, sand, gravel, water and crumb rubber

are used for the work.

Cement: 53 grade Ordinary Portland cement is used

Sand: ordinary river sand has been used.

Gravel: Natural gavel characterized in accordance with Indian Standards Code 383 [8] is used.

Crumb rubber- it is waste obtained from tyre remoulding section of a factory

Concrete mix design: concrete mix design is done. The objective of present work is to study the strength characteristics of concretes with varying proportions of crumb rubber. Hence a nominal concrete mix of proportion 1: 1.5: 3 with water cement ratio 0.5 is prepared. Concrete mix is prepared as per Indian Standards Code 456 (2000)

rubbercrete is prepared with crumb tyre rubber with partial replacement of fine aggregate in various proportion as 0%,10%,20%,30%,40%,50%,66%& 75%..The compressive strength is determined after curing of 28 days and atmospheric exposure for 6 month,12 month,18 month & 24 month

Results & Discussion

Test on Coarse aggregates

The various characteristics of coarse aggregate as determined in the laboratories are presented in table.

Table 1: Tests on Gravel (Coarse aggregate)

Parameter	Specific Gravity	Fineness Modulus	Water absorption	Impact Value	Crushing Strength
Value	2.80	7.13	0.53%	10.4 %	9.30%

Test on Fine aggregates (Sand)

The various characteristics of natural Fine aggregate (Sand) as determined in the laboratories are presented in table.

Table 2: Tests on Sand (Fine aggregate)

Parameter	Fineness Modulus	Water absorption	Specific Gravity
Value	2.65	0.63%	2.66

IS 2386 (part – 3) – 1963 has recommended the water absorption to be between 0.5 to 2%. Thus the water absorption of aggregates used is within permissible limit.

Test on Ordinary Portland cement:

The most important ingredient of concrete is cement. Its properties are summarized in table.

Table 3: Tests on Ordinary Portland Cement

Parameter	Value
Standard Consistency	32%
Soundness	3 mm
Fineness	3.43%
Initial Setting Time	55 minute
Final Setting Time	550 minute
Compressive Strength (28 days)	53.25 N/mm^2

Initial setting time for 53 grade OPC should be >30 minutes as per IS12269. Similarly the FST should be <600 minutes Thus the cement used

duly meets the requirements. Soundness should be <10 mm. The cement satisfies this criteration also. Fineness up to 10% is permissible. This requirement is also satisfied.

Replacement of Fine Aggregate:

The effect of replacement of fine aggregates on long term performance (endurance) has been assessed in the present work.

* The natural fine aggregates of concrete are replaced by equivalent size scrape tyres rubber particles. The replacement is done in proportions 0%, 10%, 25%, 33%, 50%, 66% and 75%. Table shows the compressive strength of various blends of rubbercrete.

Table 4: Compressive Strength of Concrete with Replacement of Fine Aggregate

Crumb Rubber proportion	Average compressive Strength 28 day (N/mm^2)	Average compressive Strength, 6 month (N/mm^2)	Average compressive Strength, 12 month (N/mm^2)	Average compressive Strength, 18 month (N/mm^2)	Average compressive Strength, 24 month (N/mm^2)
0%	38.15	38.3	39.60	37.6	37.31
10%	34.31	34	31.05	30.35	30.18
25%	24.78	24.62	22.85	21.80	20.78
33%	21.96	21.69	19.86	19.57	19.49
50%	15.73	18.15	16.52	15.95	15.52
66%	14.71	13.91	12.13	11.66	11.39
75%	10.00	9.02	7.70	7.02	6.87

CONCLUSIONS

The use of rubber in concrete is getting popularity owing to both the reasons, the scarcity of natural aggregates and environmental concerns. The rubber makes the concrete light in weight and economical. At the same time it makes the concrete weak in compression and other structural properties. Researchers have already established that rubber in very small proportion (<10%) can be used in structural concrete. But it can always be used for non structural members like partition walls.

It has been found that in the course of two years, when the rubbercrete is exposed to the natural environmental conditions, it looses the strength very marginally. The loss of strength is within 5% only.

Hence it can be concluded that rubber can be effectively used in concrete with non structural applications

Acknowledgement

I take this opportunity to express my deepest sense and gratitude and sincere thanks to those who have helped us in completing this task. I express my sincere thanks to Head of Civil Engineering department Dr.. M. Husain who has given me excellent guidance, continuous encouragement for the completion of this work. His kind assistance and constant inspiration will always help me in future also.

References

1. Ashraf M Ghaly and James D Cahill IV (2005) Correlation of strength, rubber content, and water to cement ratio in rubberized concrete, *Canadian Journal of Civil Engineering*, 32, 6.
2. Chen Bing, and Liu Ning (2014) Experimental Research on Properties of Fresh and Hardened

Rubberized Concrete, Journal of Masters in Civil Engineering, 26 (8).

3. H. E. M. Sallam, A. S. Sherbini, M. H. Seleem and M. M. Balaha (2008) Impact Resistance of Rubberized Concrete, *Engineering Research Journal*, 31 (3), 265 – 271.
4. Hernandez-Olivares F, Barluenga G (2004) Fire Performance of recycled rubber-filled highstrength concrete. Cement and Concrete Research 34 (10): 109–117.
5. M. A. Aiello and F. Leuzzi (2010) Waste tyre rubberized concrete: Properties at fresh and hardened state, Waste Management, 30 (8 – 9), 1696 – 1704.
6. Parveen , Sachin Dass , Ankit Sharma (2013) Rubberized Concrete: Needs of Good Environment (Overview), International Journal of Emerging Technology and Advanced Engineering, 3 (3), 192 – 196.
7. Rafat Siddique and Tarun R. Naik (2004) Properties of concrete containing scrap-tire rubber – an overview, Waste Management, 24 (6) 6, 563 – 5
8. Zaher K. Khatib and Fouad M. Bayomy (1999) Rubberized Portland Cement Concrete, Journal of Materials in Civil Engineering

PRATIBHA: INTERNATIONAL JOURNAL OF SCIENCE, SPIRITUALITY, BUSINESS AND TECHNOLOGY (IJSSBT)
Special Issue: International Conference on Global Trends in Science, Technology, Humanities, Commerce & Management 2022 (ICGTSTHCM 2022)
Vol. 8, No. 2, January 2022,ISSN (Print) 2277-7261

Effects of additives on Biodiesel combustion characteristics and pollutant formation

Kiran Dinkar Chaudhari[*], *Dr. Nilesh P. Salunke*[2] *and Dr. Vijay R. Diware*[3]

[1] Asst. Professor, SES's R C Patel Institute of Technology, Shirpur, Maharashtra, India

[2] Principal, SVKM's Institute of Technology, Dhule, Maharashtra, India

[3] Associate Professor, SSBT's College of Engineering & Technology, Bambhori, Jalgaon, Maharashtra, India

[1] kiran.chaudhari@rcpit.ac.in, [2] nilesh.salunke@svkm.ac.in, [3] vrdiware65@rediffmail.com

Abstract

Despite the pandemic setback, rising demand for fossil fuels and global CO2 emissions have prompted researchers to investigate renewable energy sources such as biodiesel and biofuels. The use of neat biodiesel or biodiesel blends in compression ignition engines still faces a few challenges, such as high viscosity, low energy density, lower BSFC, and emissions such as NOx and unburnt HC. The purpose of this paper is to highlight the effects of additive use on CI engine performance characteristics and pollutant formation.

Keywords: CI Engine, biodiesel, combustion characteristics, emission.

I. Introduction

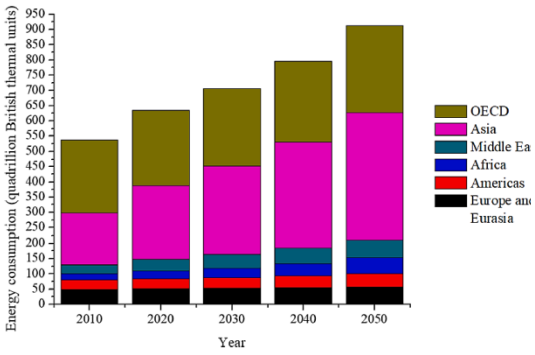

Fig. No. 1 The regional energy consumption across the world

The demand for energy has risen dramatically in recent years as a result of the rapid increase in human population. According to data from the US Energy Information Administration (EIA), as shown in Figure 1, global energy consumption is expected to increase by nearly 50% between 2018 and 2050 [1]. Asia's strong economic growth, particularly in China and India, is expected to drive energy demand to the highest level in comparison to other regions. This is a major concern because the world's supply of fossil fuels is dwindling by the day. Furthermore, global carbon dioxide (CO2) emissions are rapidly increasing as energy consumption rises. As a result, many researchers are concerned about the search for renewable fuels that can replace traditional fossil fuels, not only to address fossil fuel depletion but also to reduce environmental pollution [2]. Due to environmentally friendly properties such as non-toxicity and eco-friendliness, biodiesel and ethanol have been discovered to be a great source of energy to replace conventional fuels in recent decades.

However, biodiesel has higher viscosity, density, and volatility properties than conventional diesel, which are unfavorable in combustion systems due to poor atomization performance and incomplete combustion. Ethanol, on the other hand, has a low volumetric energy density, requiring more fuel to achieve the same power output [3]. As a result, one strategy for improving the performance of biofuels is to partially replace liquid biofuels with fuel additives.

II. Biodiesel as a promising alternative

In recent years, biodiesel has emerged as one of the most effective substitutes for petroleum diesel fuel. Biodiesel can be used either in its pure form (B100) or in combination with petroleum diesel. B20 and B5 are the most common biodiesel blends used in vehicle fuel (20 percent and 5 percent of biodiesel in the biodiesel-diesel blends respectively) [4]. Biodiesel is made up of mono-alkyl esters of long-chain fatty acids (FAs) that are non-toxic and biodegradable. Figure 2 depicts

how biodiesel is made from various natural resources such as animal fats, vegetable oils, and waste cooking oil. Fatty acid methyl ester is another name for biodiesel (FAME).
The process of producing biodiesel is known as transesterification. Transesterification is a reversible reaction in which alcohol (methanol or ethanol) is added to neat oil in the presence of a catalyst under mild conditions to produce methyl ester, biodiesel, and glycerin. In the biodiesel transesterification process, catalysts such as sodium hydroxide (NaOH) and potassium hydroxide (KOH) are commonly used. First-generation biofuels are derived from edible sources such as vegetable oils derived from corn, canola, coconut, sunflower, and rapeseed.

First-generation, second-generation and third-generation biofuels

	First-generation biofuels	Second-generation biofuels	Third-generatio biofuels
Type	Edible oil	Non-edible oil	–
Feedstock	Palm Coconut Sunflower Corn Canola Peanut Grape	Jatropha Mahua Castor Pongamia Neem Rubber seed Jojoba	Biomass pyroly oil Fish oil Waste cooking Dunaliella salin algae Spirulina algae Chlorella vulga algae
Advantages	• Simple conversion process to biofuels	• No conflict with the food usage	• Reduce sewa treatment co • Land usage is minimal
Disadvantages	• Competition with food production • Deforestation and scarce high quality cropland	• More complicated process on the conversion of the biofuels	• Large scale biofuel production through microalgae c not be implemented

Fig. No. 2 Sources of biodiesel fuel

The supply of edible oils with the food industry is competed with by first-generation biofuels. As a result, in recent years, the focus on biodiesel production has shifted to non-edible sources. Non-edible oils derived from mahua, pongamia, and jatropha plants are used to produce second-generation biofuel. Third-generation biofuels are primarily composed of raw materials such as microalgae, used cooking oil, and plant waste biomass. Microalgae are a primary source of third-generation biofuels. These algal species can survive in harsh conditions, lowering the cost of cultivation in our environment [5] [6] [7].

III. Effect of the additives on combustion performance of biodiesel

A. Combustion characteristics

Flame temperature: Flame temperature affects both combustion and pollutant formation. A higher flame temperature usually indicates a complete combustion process, which results in more energy in the engine. Lowering the flame temperature proves effective in reducing pollutant formation, particularly NOx. [8] As the Di-Butyl Ester DBE blending ratio increased from 10% to 40%, the flame temperature increased due to a decrease in soot loadings, indicating a complete combustion process. This was due to the fact that DBE increased the oxygen content of the biodiesel, which aided in the oxidation reaction of the fuel chemical species [9].
The temperature of the droplet flame is calculated using the twin-color pyrometry method by analyzing the thermal imaging of the flame. By adding ferrous picrate to the biodiesel fuel droplet raises the flame temperature compared to neat biodiesel, and that increasing the ferrous picrate dosing ratio raises the flame temperature even more [10]. The ferrous picrate improved the burning rate of the fuel vapour due to an increase in iron ions in the combustion region. It reduced radiation heat loss due to low soot formation in the combustion process.

Heat release rate: The amount of heat energy released by a fuel species when burned is referred to as heat release. The combustion parameter obtained by applying the first law of thermodynamics is the heat release rate (HRR). The heat release is proportional to the energy and calorific value of the fuel blends. Fuel blends with a high calorific value will have a high HRR, which means that a smaller amount of fuel is required to keep the engine speed stable at different loads.

B. Ignition characteristics

The key ignition characteristics are ignition delay, ID, ignition probability, and ignition temperature. Various studies have been conducted to investigate the effect of additives on liquid biofuels in engines. The measurement of ID is in time and crank angle interval from the start of injection to the start of combustion. In general, the shorter the ID, the higher is the quality of the fuel [11].

According to the literature, the addition of additives to biodiesel reduced the ID. For example, the addition of 0.1 m/v percent graphite oxide nanoparticles reduced the ID of the biodiesel droplet by approximately 11.5 percent when compared to neat biodiesel. The high thermal conductivity of graphite oxide increased

the evaporation rate, causing particles to diffuse away from the droplet. The lower ignition temperature of graphite oxide, which is around 180 C, compared to biodiesel, promoted earlier ignition at the combustible region as a result of greater surface exposure to the surrounding air.
The addition of acetylene black increased the ignition delay of the soybean-based biodiesel droplet by up to 10.2 percent when compared to the neat biodiesel case when 3 percent acetylene black was added [12]. The addition of multi walled Carbon Nano tubes, MWCNTs or Al2O3 nanoparticles improves the ignition probability of the blended Kusum biodiesel droplet. Using the same hot plate temperature, MWCNTs were found to be more effective than Al2O3 in terms of increasing ignition probability, with approximately 1.84 percent greater by adding 30 ppm of the nanoparticle to each blended fuel. This result was attributed to the nanoparticle' doping of the cetane index.

C. Pollutant formation and emissions

Particulate matter (PM) and soot: Particulate matter is a mixture of solid-phase particles and liquid droplets in the air. Some PMs are large and dark enough to be seen as soot or smoke with the naked eye. Soot is a broad term for impure solid carbon particles produced by a variety of polycyclic aromatic hydrocarbons (PAHs) resulting from the incomplete combustion of hydrocarbon fuels. These pollutants cause severe pollution of the environment. They are a serious threat to human health. The formation of PM and soot is primarily influenced by the ID and oxygen content of the combustion region. Several additives have been found to reduce soot during biodiesel combustion.
The experimental results showed that increasing the mole fraction of DBE in biodiesel surrogate reduced soot formation non-linearly, with the reduction of soot loading significantly accelerated when the DBE mole fraction exceeded 30% [13]. The addition of low carbon number alcohols, such as methanol and ethanol, could reduce the carbon supply to soot formation because these oxygenates were mostly decomposed into CO, inhibiting the formation of C2-C4 intermediates, which would eventually contribute to the subsequent PAH and soot growth process.

Oxides of nitrogen (NOx): Nitrogen oxides, NOx is made up of two major species: nitric oxide (NO) and nitrogen dioxide (NO2). Several factors could contribute to NOx formation, including local temperature (thermal NOx), the residence time of the fuel–air mixture at high temperatures, and the local concentration of oxygen. It was discovered that the high oxygen content in biofuels could increase the flame temperature and HRR when compared to neat fossil fuels due to the increased oxygen concentration in the fuel, which promoted the complete combustion process. These factors were found to be advantageous because combustion efficiency could be improved; however, the drawback would be an increase in NOx emissions. As a result, it is critical to include several additives in the biofuel blend to reduce NOx formation.

With the addition of Fe(CO)5, the peak NO emission is reduced. The catalyst resulted in the presence of additional thermal mass in the form of iron oxide (Fe2O3) particles, which reduced the peak flame temperature and, as a result, thermal NO formation [14]. It is investigated NOx reduces in palm biodiesel by using rapid mixing of biodiesel-water–air technique. Increasing the water blending ratio reduced NOx emissions even more.

Carbon monoxide (CO) and carbon dioxide (CO2): Carbon monoxide is a poisonous byproduct of incomplete combustion of carbon compounds. The toxicity of CO is higher than that of CO2, raising public concern due to the negative effects on the human body. Carbon monoxide emissions are primarily determined by the combustion region's Equivalence ratio and the cetane number of the fuel blends. The fuel-rich mixtures result in incomplete combustion and an increase in CO concentration in the exhaust. The CO emission from the ethanol-palm biodiesel spray combustion can be measured using a gas chromatograph [15]. The CO emission in the exhaust gas was found to decrease monotonically with increasing ethanol content in biodiesel blends under stoichiometric conditions.

Hydrocarbons (HCs): Hydrocarbons are carbon and hydrogen compounds. Incomplete combustion of diesel and gasoline results in HC emissions, which pose serious health and safety risks. Long ID, low air–fuel ratio, and low combustion temperature are the primary causes of HCs emissions. Longer ID, for example, would result in some fuel being diffused out without completing the combustion process, which are also known as unburned hydrocarbon emissions (UHCs).

It was discovered experimentally that increasing the fuel mass flow rate to achieve the same energy output as neat biodiesel could reduce NOx emissions from the ethanol-biodiesel diffusion flame. The disadvantage is that it increased the level of CO and HCs in the exhaust compared to the neat biodiesel. They explained that the higher fuel mass flow rate caused poor atomization, reducing the fuel blends' combustion efficiency.
Water addition in palm biodiesel spray flame increased HCs emission at lower concentrations and decreased HCs concentration at higher concentrations. The cause was related to the fuel–air mixing ratio and, as a result, combustion efficiency [16].

IV. Conclusion and future scope

From the above discussion it can be concluded that

1 Most of the additives raise the flame stabilization limit and the laminar flame speed, making them compatible as the biofuels additives.
2 The enhanced combustion efficiency due to use of fuel additives generally leads to a reduction of pollutant formations such as PM, soot, NOx, CO, CO2 and HCs.
3 Due to the increasing conflicts of the edible oils, the additives studies should also be performed using the second-generation and third-generation biofuels.

Following are some relevant issues and challenges for the future investigation directions.

1 To overcome the difficulty in introducing the nanoparticles to the liquid fuels while ensuring uniform dispersion and minimal chances of particle agglomerations.
2 Recent research is focused on the effect of additives on the first-generation biofuels. The additives studies should also be performed using the second-generation and third-generation biofuels.

References

[1] US Energy Information Administration, “International Energy Outlook 2019 with projections to 2050”, 2019. Available: https://www.eia.gov/outlooks/ieo/pdf/ieo2019.pdf.
[2] Chen L, Hu X, Wang J, Yu Y. “Impacts of alternative fuels on morphological and nano-structural characteristics of soot emissions from an aviation piston engine”. Environ Sci Technol (2019);53(8):4667–74.
[3] Dahman Y, Syed K, Begum S, Roy P, Mohtasebi B. “Biofuels: their characteristics and analysis”. In: Verma D, Fortunati E, Jain S, Zhange X, editors. Biomass, biopolymer-based materials, and bioenergy. Cambridge: Woodhead Publishing; 2019. p. 277–325.
[4] Singh DP, Dwevedi A. “Production of clean energy by green ways” In: Dwevedi A, editor. Solutions to Environmental Problems Involving Nanotechnology and Enzyme Technology, Academic Press; 2019, p. 49–90.
[5] Singh D, Sharma D, Soni SL, Inda CS, Sharma S, Sharma PK, et al. “A comprehensive review of physicochemical properties, production process, performance and emissions characteristics of 2nd generation biodiesel feedstock: Jatropha curcas” Fuel 2021; 285:119110.
[6] Leong W-H, Lim J-W, Lam M-K, Uemura Y, Ho Y-C. “Third generation biofuels: a nutritional perspective in enhancing microbial lipid production” Renew Sust Energ Rev 2018;91:950–61.
[7] Atabani AE, El-Sheekh MM, Kumar G, Shobana S. “Edible and nonedible biodiesel feedstocks: microalgae and future of biodiesel”. In: Rasul MG, AK Agrawal, Sharma SC, editors. Clean energy for sustainable development. Academic Press; 2017. p. 507–56.
[8] Khalid A, Sies MF, Manshoor B, Latip L, Amirnordin SH. “Investigation of mixture formation and flame development in emulsified biodiesel burner combustion”. Proc 2014 int conf ind eng oper manage; 2014.
[9] Zhu M, Setyawan HY, Zhang Z, Zhang D. “Effect of n-butanol addition on the burning rate and soot characteristics during combustion of single droplets of diesel–biodiesel blends”. Fuel 2020;265:117020.
[10] Zhu M, Ma Y, Zhang D. “Effect of a homogeneous combustion catalyst on combustion characteristics of single droplets of diesel and biodiesel”. ProcCombust Inst 2013;34(1):1537–44.
[11] Jiang Z, Gan Y, Ju Y, Liang J, Zhou Y. “Experimental study on the electrospray and combustion characteristics of biodiesel-ethanol blends in a meso-scale combustor”. Energy 2019; 179:843–9.
[12] Singh G, Esmaeilpour M, Ratner A. “The effect of acetylene black on droplet combustion and flame regime of petrodiesel and soy biodiesel”. Fuel 2019;246: 108–16.
[13] Gao Z, Zhu L, Zou X, Liu C, Tian B, Huang Z. “Soot reduction effects of dibutyl ether (DBE) addition to a biodiesel surrogate in laminar coflow diffusion flames”. Proc Combust Inst 2019;37(1):1265–72.
[14] Yan F, Xu L, Wang Y, Park S, Sarathy SM, Chung SH. “On the opposing effects of methanol and ethanol addition on PAH and soot formation in ethylene counterflow diffusion flames”. Combust Flame 2019;202:228–42.
[15] Gautam R, Kumar N. “Effect of ethanol addition on the properties of Jatropha ethyl ester”. Energy Sources Part A Recover Util Environ Eff 2016; 38:3464–9.
[16] Abdul Karim ZA, Yahaya Khan M, Aziz AAR. “Evolution of microexplosion phenomenon in parent-child droplets of water in bio diesel emulsions enhanced by different surfactant dosages and HLB values”. J Energy Resour Technol 2019; 141(10):102204

PRATIBHA: INTERNATIONAL JOURNAL OF SCIENCE, SPIRITUALITY, BUSINESS AND TECHNOLOGY (IJSSBT)
Special Issue: International Conference on Global Trends in Science, Technology, Humanities, Commerce & Management 2022 (ICGTSTHCM 2022)
Vol. 8, No. 2, January 2022,ISSN (Print) 2277-7261

Extraction of sugarcane wax from filter cake

Sanjay L.Bhagat[1], Sandeep A.Thakur[2], Pranav Pathak[3]

[1]P.V.P.Institute of Technology, Budhgaon,Sangli
[2]SSBT's College of Engineering and Technology, Bambhori, Jalgaon
[3]School of Bioengineering Sciences & Research, MIT-ADT University, Pune
Email: [1]callbsanjay@yahoo.com, [2]satsan17@rediffmail.com, [3]pranav.pathak@mituniversity.edu.in

Abstract

Waxes have important specific properties for food and cosmetic uses, and for cleaning and polishing applications. The knowledge of the characteristics of waxes is essential for their application. Wax recovered from sugarcane (Saccharum officinarum) filter cake, a by-product of the sugar and alcohol industry, represents a potential alternative to carnauba, beeswax, and synthetic waxes, considering the enormous resources of raw material in sugarcane growing countries. Crude wax solvent extraction and fractionation were studied in this paper. Filter cake extracted with Benzene yields 6 to 7 % crude sugarcane wax. Purified sugarcane waxes presented analytical indexes similar to those of commercial bee and carnauba waxes.

Keywords: *Sugarcane wax, Extraction, Press mud, Benzene*

Introduction-

Sugar cane (Saccharum officinarum L.) is one of the industrially important crops mainly grown in Brazil and India. India has just over 500 sugar mills, with nine states (Uttar Pradesh, Bihar, Punjab and Haryana in the northern region; Maharashtra & Gujarat in the western region and Andhra Pradesh, Tamil Nadu and Karnataka in the southern region) holding 95 % of them. Most mills are either privately owned or co-operatives

The global production in the year 2009 was reported to be 1900 million tones of which India produced 285 million tones accounting for 14.9%. In India, sugarcane supports one of the largest agro-processing industries and more than 6 million farmers are engaged in its cultivation. According to the Indian Institute of Sugarcane Research (IISR) Vision 2030 report, India is expected to increase sugar cane production to 520 million tones.

Sugar industry has many by-products like bagasse, molasses, press mud, and leaves (trash) Sugarcane bagasse is the fibrous residue of sugarcane (Saccharum officinarum) after the extraction of juice. Bagasse, as agro-based fibers, have the composition, properties and structure that make them suitable for uses such as composite, textiles, pulp and paper manufacture and animal feed, among others. In addition, bagasse biofibers can also be used to produce fuel, chemicals, enzymes and food and is one of the most relevant sugarcane by-products of the cane sugar production industry, a mixture of hard fiber, with soft and smooth parenchymatous (pith) tissue, having high hygroscopicity, soil, wax, residual sugars, etc., remaining after the cane has been crushed and extracted the juice.

Press mud from the sugar mills is a very useful source of fertilizer as well as some chemicals. The major use that has recently been developed in India is in bio composting (usually trade named as Bioearth) where it is treated with the spent wash from the distillery. The composition of press mud is given in Table 1. Its usefulness as fertilizer is based on the nutrient content of the mud and the spent wash as shown below:

Press mud – N- 1.15 to 3.0%; P- 0.60 to 3.50% and K- 0.30 to 1.80%.

Spent wash – N-2630 mg/l, P-20 mg/l and K-222 mg/l

PRATIBHA: INTERNATIONAL JOURNAL OF SCIENCE, SPIRITUALITY, BUSINESS AND TECHNOLOGY (IJSSBT)
Special Issue: International Conference on Global Trends in Science, Technology, Humanities, Commerce & Management 2022 (ICGTSTHCM 2022)
Vol. 8, No. 2, January 2022,ISSN (Print) 2277-7261

Composition of press mud:

Table No. 1: Composition of press mud

1	Crude wax	2	5-14%
3	Fiber	4	15-30%
5	Crude Protein	6	5-15%
7	Sugar	8	5-15%
9	SiO	10	4-10%
11	CaO	12	1-4%
13	PO	14	1-3%
15	MgO	16	0.5-1.5%
17	Total ash	18	9-10%

Benefits:

1. Very low power requirement.
2. Zero discharge to inland water resources and freedom from river or ground water pollution.
3. Organic fertilizer produced is rich in micronutrients and can reduce the requirement of chemical fertilizers. It also provides bacteria for nitrogen fixing, solubilisation of phosphates, humus that will keep the soil healthy and develop the self-reclamation cycle. Since bio composting is accompanied by a rise in temperature, chances are that the fertilizer is free from all pathogens, harmful bacteria, weeds and seeds. Fertilizer is free flowing, easy to handle, to pack and transport.

The bio compost contains 25-30% organic carbon, 1.2-2.0% nitrogen, 1.5-2.0% phosphorous and 2.5-3.0% potash.

The shortcoming of this operation is the limited period of operation of sugar plants. The press mud has to be stored in large open areas and large lagoons are to be set up to store the spent wash. However, the long-term effects of application of this fertilizer remain to be studied.

Sugar mills produce a range of by-products, including bagasse, filter mud and molasses. A typical sugarcane complex with a capacity of 3,000 tonnes crushed per day (TCD) can produce 345 tonnes of refined sugar, 6,000 litres of alcohol, 3 tonnes of yeast, 15 tonnes of potash fertilizer, 25 tonnes of pulp, 15 tonnes of wax, 150 tonnes of press-mud fertiliser12 and 240MWh of exportable electricity from bagasse.

Press mud like other organic materials affects the physical, chemical and biological properties of soil2. However, due to its bulky nature and wax content it causes some problems. If press mud is directly applied to soil as manure, the wax present might deteriorate the physical properties such as permeability, aeration, soil structure and composition etc. and with the passage of time the deterioration might get worsen. Therefore, extraction of wax from press mud will be helpful to enhance the quality of press mud as organic manure.

Solvent Selection:

The solvent is the key to a successful separation by liquid-liquid extraction. The several criteria are:

Distribution Coefficient

This is the ratio (at equilibrium) of the concentration of solute in the extract and raffinate phases. It gives a measure of the affinity of the solute for the two phases. A distribution coefficient other than unity implies that the solute must have different affinity in the two phases. If only one solute is involved (such as in the recovery of an impurity from an effluent stream), only the distribution coefficient need be considered, and it is desirable for this to be as large as possible.

Selectivity (Separation Factor)

If there are more than one solutes (say two solutes A and B), then consideration should be given to the selectivity of the solvent for solute A as against B. The selectivity between the 2 solutes A and B is defined as the ratio of the distribution coefficient of A to the distribution

coefficient of B. For all useful extraction operation the selectivity must exceed unity. If the selectivity is unity, no separation is possible.

Insolubility of Solvent

The solvent should have low solubility in the feed solution; otherwise the separation is not "clean". For example, if there is significant solubility of solvent in the raffinate stream, an additional separation step is required to recover the solvent.

Recoverability

It is always necessary to recover the solvent for re-use, and this must ordinarily be done by other means, e.g. distillation. If distillation is to be used, the solvent should form no azeotrope with the extracted solute and mixtures should show high relative volatility. The solvent should also be thermally-stable under the distillation temperature.

Density

A large difference in density betweenextract and raffinate phases permits high capacities in equipment. This is especially important for extraction devices utilizing gravity for phase separation.

Interfacial Tension

The larger the interfacial tension, the more readily coalescence of emulsions will occur but the more difficult the dispersion of one liquid in the other will be. The more readily coalesces the emulsions the easier phase separation will be. Low interfacial tension aids dispersion and thus improves contacting mass-transfer efficiency. Coalescence is usually of greater importance, and interfacial tension should therefore be high.

Chemical Reactivity

The solvent should be stable chemically and inert toward the other components of the system and toward the common materials of construction.

Viscosity, Vapour Pressure, Freezing Point

These should be low for ease in handling and storage, for example, a high viscosity leads to difficulties with pumping, dispersion and mass-transfer rate.

Availability and Cost

An excellent solvent may not be commercially available. Or it may represent a large initial cost for charging the system, and a heavy continuing expense for replacing inevitable operating losses.

Other Criteria

Toxicity and flammability of the solvent are important occupational health and safety considerations. Stability of the solvent (i.e. resistance to breakdown), particularly in the recovery steps, is significant, especially if the breakdown products might contaminate the products of the main separation. Corrosivity of the solvent leads to the usual problems with materials of construction. Finally, compatibility of the solvent with the mixture to be separated can have many manifestations, particularly when easily contaminated materials such as food or pharmaceuticals are being handled.

- It should be non-toxic and selective, i.e. it should dissolve only the required constituent with minimum amount of the inert materials.
- It should not cause the extract to complex or dissociate.
- It should be preservative in action.
- It should promote rapid physiologic absorption of the extract.
- It should be easily evaporated at low heat.

Fig. 1: Sugarcane wax preparation Flowchart

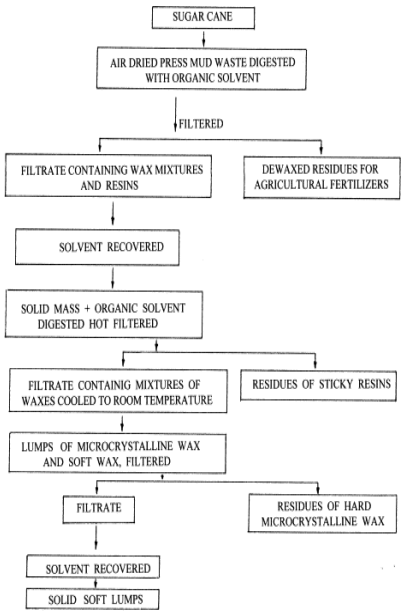

Fig. 2: Sugarcane wax preparation Unit

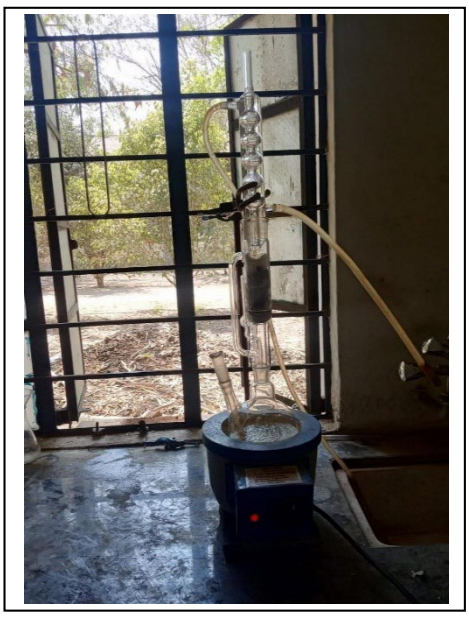

The process of the present invention is being further illustrated by the following practical examples which should not, however, be construed to limit the scope of the invention.

- Collection of press mud from sugar industry.
- Kept for drying in open atmosphere.
- Extract wax from press mud by using Benzene, Toluene as solvent in soxhlet extractor up to 6 hours. Organic solvent extraction is the most common and most economically important technique for extracting aromatics. There are different solvent used for extraction of wax but pure toluene is excellent oil solvent and has good solvent power for wax extraction as well. A crude wax extracted with benzene was used for the entire investigation. A further consideration was that benzene extraction appeared most feasible for commercial scale production.
- Collect extract from soxhlet extractor and kept it for filtration unto 3 to 4 hours.
- After filtration put the solution for distillation process.
- Collect the benzene as distillate, and wax remains at the bottom of round bottom flask.
- Collect the wax from round bottom flask.
- Add isopropyl alcohol in wax for removal of resins from wax.
- After removal of resins wax is formed

Specifications:

Table No.2: Specifications of wax

19	**Item**	**20**	**Index**
21	Acid Value	22	6~26
23	Saponification Value	24	50~150
25	Iodine Value	26	22~24
27	Melting Point	28	76~82°C
29	Color	30	Brownish black/Light yellow

Sugarcane wax, a whitish to dark yellowish coating on the surface of sugarcane, gets extracted and separated along with press mud during crushing and

processing of the cane juice. This wax portion finds applications in cosmetics, paper coating, textiles, fruit and vegetable coating, leather sizing, lubricants, adhesives, polishes, and pharmaceutical industry Thus, it can be considered as an alternative to costly carnauba wax, candelilla wax, and chitosan for edible coating applications. Sreenivas et al. found ash gourd peel a good source of wax which was used as edible coat for strawberries to enhance their shelf life. The overall crude wax has several industrial uses which include the coating of steel products for metal working and rust prevention while for uses such as polish production refinement of the crude wax into its fractions is necessary.

Applications:

The refined variety of the hard sugarcane wax having its potential use in:

1. Foodstuff industry: can be widely used as the coating and brightening agent of making gum confection, chocolate products and processing fruits;
2. Cosmetic industry: can be used for making brilliantine wax, lipstick, puff cake and eyebrow pencil.
3. Brightening agent: to be widely used for making shoe polish, glazing wax for vehicles and to make shoes;
4. Other industry: to be widely used for making electrical wire, cable, explosive packing, carbon paper and moisture-proof paper, etc.
5. Medicines,
6. In sweet meats and pastries,
7. In tinned food products,
8. In castings and recordings,
9. In carbon papers,
10. In preparation of carbonless carbon papers,
11. In electrical insulation of cables and wires,
12. in preparation of various types of paints, varnishes and polishes including shoe polishes, car polishes and floor polishes, preparation of coloured pencils, crayons, water and oil paints,
13. In cosmetics,
14. In preparation of emulsion paints for spraying.

In fact, it has its most likely entries into all the branches of industries where carnauba wax is mostly used. In bulk also it can be produced many times more than any other plant waxes combined together. The raw material, press mud is a rejected waste material of sugarcane industries that causes the unwanted problem of pollution to the surrounding supurbs of the sugar mills on accumulation. Also, the availability of the press mud is no problem at all throughout the year. While carnauba plant is a seasonal plant that produces extractable waxes only in marked period of a year

Conclusion

Press mud is a byproduct of sugar industries. Sugarcane press mud is easily available and cost effective than other sources of wax. The yield of wax found from benzene solvent was 6.% - 7 %. The color of crude wax was brownish green while the pure wax was light yellow in colour Extraction of wax from press mud was carried out with Benzene was within time of 6 hours hence it is a less time consuming process. These waste products are used as fertilizer in the agriculture field, but the presence of sugar cane wax in press mud deteriorates the physical property of soil and therefore the extraction of wax is necessary. This extracted wax has several applications in various industries which can bring products in national and international market. This study revealed presence of many classes of compound like alkane, ester, alcohol, fatty acids and so forth present in sugarcane press mud wax. The major component of wax i.e. sec-butyl isothiocyanates which has many beneficial effects can be utilised for medicinal purpose

and can be used as a flavouring agent in lipstick. Apart from medicinal semio chemical and nutritional applications, wax can be used in food preservation as an edible coating for fruits and vegetables. Thus, sugarcane wax has many compounds of biological and industrial importance.

References

1. Bhosale P. R., Chonde Sonal G. And Raut P. D.; Jan-March 2012; Studies On Extraction Of Sugarcane Wax From Press Mud Of Sugar Factories From Kolhapur District, Maharashtra Journal of Environmental Research And Development Vol. 6 No. 3A
2. J. Lois-Correa*1, A. Flores-Vela2, D. Ortega-Grimaldo3, J. Berman-Delgado4Experimental Evaluation Of Sugar Cane Bagasse Storage In Bales System
3. O Almazan, L Gonzalez and L Galvez Association De Tecnicos Azucareros De Cuba The Sugar Cane, Its By-Products And Co-Products.
4. N. Partha And V. Sivasubramanian; July-2006 ;Recovery Of Chemicals From Pressman –A Sugar Industry Waste.
5. H.H. Franken, C.E. Schwarz, J.H. Knoetze The Technical Feasibility Of Using Supercritical Fluid Extraction To Extract And Fractionate Crude Sugar Cane Wax
6. Mangesh B. Inarkar And S. S. Lele , 2012; Extraction And Characterization Of Sugarcane Peel wax.
7. R. Arul Gnanaraj April-June 2012; Applications Of Sugarcane Wax And It's Products: A Review International Journal Of Chemtech Research Coden(Usa): Ijcrgg Issn : 0974-4290 Vol.4, No.2, Pp 705-712.
8. Bhosale P.R.1, Chonde S.G.2, Nakade D.B.3 And Raut P.D.1 ; May (2012) Studies On Physico-Chemical Characteristics Of Waxed And Dewaxed Press mud And Its Effect On Water Holding Capacity Of Soil ISCA Journal of Biological Sciences Vol. 1(1), 35-41.
9. Phukan; Amal C. (Assam, IN) November 26, 2002 Process for the preparation of refined hard sugarcane wax having improved qualities from press mud, Council of Scientific & Industrial Research (CSIR) (New Delhi, IN) United States Patent 6,486,335.

PRATIBHA: INTERNATIONAL JOURNAL OF SCIENCE, SPIRITUALITY, BUSINESS AND TECHNOLOGY (IJSSBT)
Special Issue: International Conference on Global Trends in Science, Technology, Humanities, Commerce & Management 2022 (ICGTSTHCM 2022)
Vol. 8, No. 2, January 2022,ISSN (Print) 2277-7261

Fermentative Production of Actinomycin by Streptomyces Antibioticus 2123 Using Protein Rich Supplement as a Substrate

[1]Jayant P.Parpalliwar, [2]Dr. V.R. Diware, [3]Sarika S.Pawar, [4]Dr. M.Husain

1Assistant Professor, Biotechnology Engineering, 2Associate Professor & Head, Biotechnology Engineering,

3Assistant Professor, Biotechnology Engineering, Professor, Civil Engineering.

1biochannel27@gmail.com, 2vrdiware65@rediffmail.com, 3sarika_p17@rediffmail.com,

4ermujahidhusain@yahoo.com

SSBT's College of Engineering and Technology, Bambhori, Jalgaon, MS.

Abstract:

Actinomycin is a clear, yellow liquid administered intravenously and mostly used in treatment of a variety of cancers.Actinomycin producing strain is Streptomyces antibioticus 2123. Actinomycin is having ability to stop transcription of the oncogenes. Actinomycin do this by binding DNA at the transcription initiation complex and preventing elongation of RNA chain by RNA polymerase. Production of actinomycin is done by submerged fermentation process using protein rich supplement like spent grains and cereals and some vegetable sources as a substrate, under optimal condition. Fermentation period will be for 5 days at 280C at pH 6- 7. Extraction and purification of actinomycin will be done by solvent process using chloroform, ethyl acetate, methanol, etc.

Keywords: Actinomycin, submerged fermentation, protein rich supplement.

Introduction:

Actinomycin which are a class of polypeptide antitumor antibiotics isolated m soil bacteria of the genus Streptomyces. Actinomycin has been widely used in clinical practice since 1954 as an anticancer drug for treating many tumors and it is also a useful tool in biochemistry and molecular biology. There are several mechanisms of its action that are responsible for its cytotoxic and antitumor action, these being associated with DNA functionality, leading to RNA and, consequently, protein synthesis inhibition. Actinomycin interferes with the growth of cancer cells, which are eventually destroyed. Since the growth of normal cells may also be affected, other effects (side effects) will also occur. In cell biology, actinomycin is shown to have the ability to inhibit transcription. Actinomycins this by binding DNA at the transcription initiation complex and preventing elongation of RNA chain by RNApolymerase. *Streptomyces antibioticus* (*Actinomyces antibioticus*) is a bacterium discovered in 1941. It produces a large number of antibiotic compounds, including boromycin, oleandomycin, mycangimycin, actinomycin, and other

A) Materials and Methods:

For the successful fermentative production of actinomycin, Protein rich supplement included cereals such as rice, wheat, maize, corn, millet, barley, rye and pulses such as beans, peas, cowpea, dry beans like pinto beans, kidney beans, navy beans, dry peas, and peanuts, Mung bean, golden gram, greengram was collected and processed for preliminary sterilization. As Streptomyces antibioticus having ability to produce actinomycin so microbial culture with strain number namely Streptomyces antibioticus 2123 was collected from National Chemical Laboratory Pune. The culture was maintained in the laboratory by means of subculturing on agar as well as broth medium. For the analysis of substrate at quantitative line, percentage of protins and sugar were estimated using DNSA and Folin – Lowrey method. A standard curve of amount of protein against optical density at 650 nm was plotted to estimate the concentration of the test sample and a standard curve of amount of glucose against optical density at 540 nm was plotted

to estimate the concentration of the test sample.

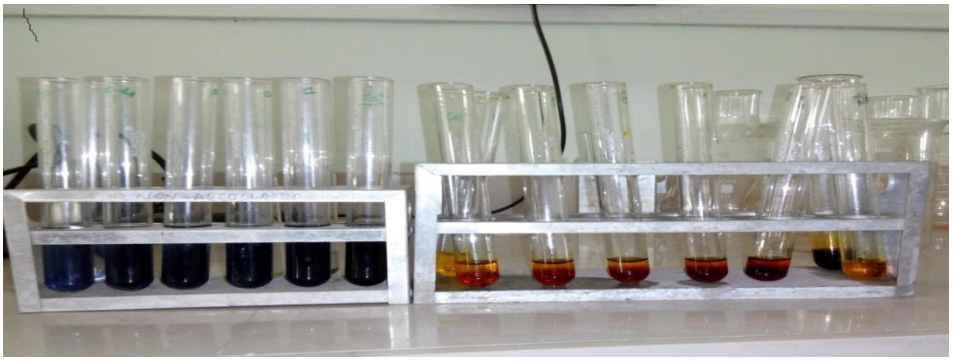

Fig. 1 Protein Estimation Fig.2 Carbohydrate Estimation

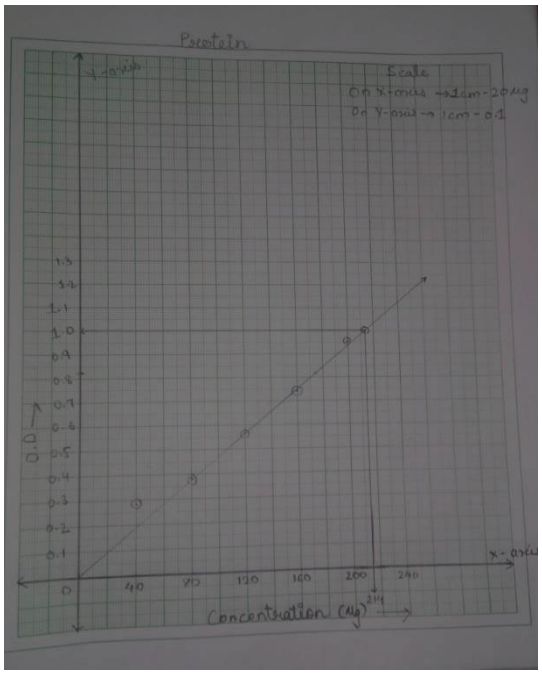

Fig. 3 Protein Estimation Graph

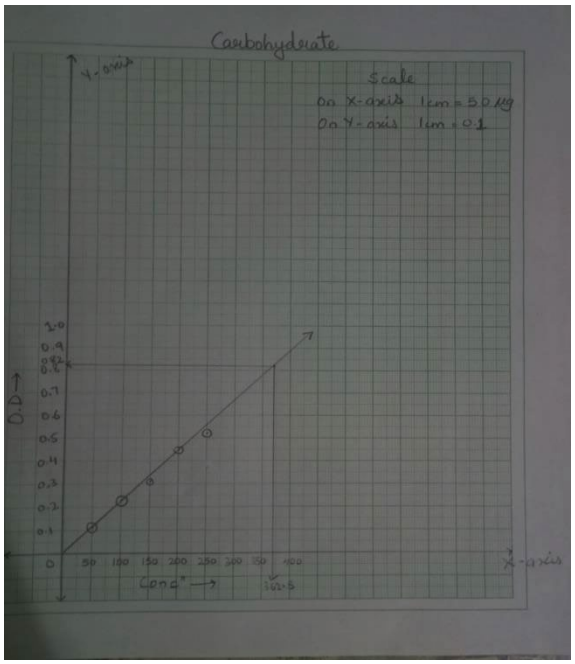

Fig.4 Carbohydrate Estimation Graph

a)Formation ofinoculums:

For the fermentative production of said antibiotics initially seed culture of Streptomyces antibioticus 2123 was prepared. For the same 500 ml of selective broth medium was prepared by following sterilization guidelines, broth was allowed to cool and loopful of mother culture of Streptomyces antibioticus 2123 was inoculated under sterilized conditions and broth was incubated for 4 days at 280C. Turbidity in the flask was observed which was the clear indication about growth of Streptomyces antibioticus 2123 in the broth. The prepared culture was used as seed culture for the production of actinomycin.

b) Fermentation media:

For the successful fermentative production of actinomycin, Protein rich supplement source were selected. After processing of raw substrate, it grinded in mixer grinder and formed the fins powder, powder were mixed in distilled water and slurry were prepared. The slurry was incubated for 2 to 3 hours in order to release macro and micronutrients outside. The suspension was filtered and filtrate was used as fermentation media. About 5 liter of media was prepared in the laboratory and introduces in lab scale fermenter with capacity of 5 liters and working volume 3.5 liters. The whole batch the again sterilized in autoclaves in order to remove the microbial load. The batch was then ready for the production of antibiotic.

c) Fermentative Production of Actinomycin by Submerged Fermentation:

In production media, bacterial culture was inoculated under sterile conditions in the lab scale fermenter. The fermentation process were carried out at 280C for 5 days with pH 7.0, Dissolved oxygen concentration,60%, and Inoculum concentration, 10%v/v from seed culture.After 5 days turbidity was obtained in solution that showed the growth ofmicrobes.The fermented broth was harvested and centrifuged at 5,000 rpm for 5 min supernatant was collected and considered it as crude extracellular extract. Chloroform or ethyl acetate was used as solvents for extraction of antimicrobial metabolites.Crude extracellular extract was taken and the solvent was added and gently mixed for 1 hr and the centrifuge was done and the supernatant was collected in petri plate and was kept todry.Crude extract was taken and methanol was added and gently mixed and was centrifuged. Supernatant was collected and transferred in petri plate and was dried in hot air oven at 50OC. result to this powderform were obtained.

Fig.5: Before Inoculation

Fig.6: After 5 days ofIncubation

B) Results:

Initially 100gms of substrate was used to prepare 200 ml of fermentation media contained:

a) 214 micro gram/ml of protein. therefore, for 200ml 42,800 micro gram/ml, i.e.42.8 mg.
b) 362.5 micro gram/ml of Glucose. therefore, for 200ml 72,500 micro gram/ml, i.e.72.5mg.
c) The obtained product in submerged fermentation is 0.1821gm/50gm of substrate, with volume 200 ml of fermentation media.
d) Total obtained product in 4 liters submerged fermentation batch was is 3.642 gm/3 kg of substrate, with volume 4000 ml of fermentation media.

C) Confirmative Test for produced Antibiotic-Actinomycin:

This test was carried out in order to check the antibacterial activity of the extracted metabolites by Agar Well Diffusion method. Zone of inhibition of 3mm were observed against the E.coli.

Fig. 7: Before Inhibition

D) Conclusion:

Actinomycin is produced using spent grain as asubstrate.Streptomyces antibioticus 2123 is actively used for the production of actinomycin by submerged fermentationprocess. Produced Actinomycin is a solid, yellow in colour.The yield of product from submerged fermentation is found 3.6gms from 4 liters of media batch. The use of spent grains as substrate for actinomycin production is the economical process for production.

E) References:

1. VineetaSingh, MahvishKhan, SaifKhan And C.K.M. Tripathi, ―OptimizationOf Actinomycin V Production By Streptomyces Triostinicus Using Artificial Neural Network And Genetic Algorithm‖, Applied Microbiology And Biotechnology 82, 2,379-385
2. ElsheikA. Elobiedet.al, ―Identification of Anticancer Actinomycin-Din a Newly Isolated Streptomyces Sp. From Sudan Soil, Journal Of Global Biosciences, ISSN 2320-1355, Vol. 3(5), PP. 858-865,2014.

3. Jirayut Euanorasetr1, 2, Arjaree Nilvongse 1,2, Srisurang Tantimavanich 3, Takuya Nihira 2,4, Yusuhiro Igarashi5 And WatanalaiPanbangred, ― Identification And Characterization of Soil-Isolated Streptomyces Sje177 Producing Actinomycin‖, Southeast Asian J Trop Med Public Health , Vol 41(5), PP. 1177-1187, September 2010.
4. C.E.Lopes And N.Pereira Jr,―Development of a Bioprocess for the Production of Actinomycin-D, Brazilian Journal of Chemical Engineering, Vol. 19(03), PP. 277 - 285, July - September2002.
5. Ahmed I. Khattab1, Eltahir H. Babiker and Humodi A. Saeed, ―Streptomyces: Isolation, Optimization Of Culture Conditions And Extraction of

Secondary Metabolites, International Current Pharmaceutical Journal, Vol.5(3), PP. 27-32, February2016.
6. Rajaa A. Hussein, ―Actinomycin- Production Assay: ASimple Bacteriological Method For Antitumor Activity Screening in Vitro, Kufa Journal for Veterinary Medical Sciences, Vol. 2(2), PP.116-126,2011.
7. Benjamin R. Clark Et.Al, ―Optimization of Fermentation Conditions For Actinomycin D Production by a Newly Isolated Streptomyces Spp. Ah 11.4, Journal of Biotechnology And Pharmaceutical Research, Vol. 4(2), PP. 29-34, February2013.
8. Maria De Fatima Vieira DeQueirozSousa, ―A Chemically Defined Medium For Production of Actinomycin D by Streptomyces Parvulus‖, Brazilian International Journal of Biology And Technology , Vol. 44(3), PP. 227 – 231, September,2001.
9. E.Katz,I'hyllisPientaAnd A.Sivak,―TheRoleofNutritionintheSynthesisof Actinomycin, Instituite of Alicrobiology, Rutgers, The State University, New Brunswick, New Jersey, PP. 236-231, November1957.
10. AbdelhalemA. HamzaEt.Al, ―Isolation and Characterisationof Actinomycin D Producing Streptomyces Spp. From Sudanese Soil, African Journal of Biotechnology, Vol. 12(19), Pp. 2624-2632, 8 May,2013.
11. VandanaPraveen Et.Al,―NutritionalRegulationof Actinomycin-DProductionbyaNew Isolate of Streptomyces Sindenensis Using Statistical Methods, Indian Journal of Experimental Biology, Vol 46, Pp. 138-144, Feb2008.

PRATIBHA: INTERNATIONAL JOURNAL OF SCIENCE, SPIRITUALITY, BUSINESS AND TECHNOLOGY (IJSSBT)
Special Issue: International Conference on Global Trends in Science, Technology, Humanities, Commerce & Management 2022 (ICGTSTHCM 2022)
Vol. 8, No. 2, January 2022,ISSN (Print) 2277-7261

GC-MS Analysis of Microwave-assisted Hexane-extract of Gooseberry Seed Oil

Minal V. Badame, Hansraj V. Patil,
*Pawan D. Meshram**
University Institute of Chemical Technology
KBC North Maharashtra University, Jalgaon
E-mail: pawan.dm@gmail.com

ABSTRACT
Microwave-assisted extraction (MAE) has been recognized as rapid, energy saving and yield efficient technique over conventional extraction methods. In present study, Emblica officinalis seeds (Gooseberry seeds) were hexane extracted under microwave irradiation. Different time levels (40-80 min) and temperature levels (60-80°C) were used in extraction methodology to optimize the seed oil extract yield. Maximum yield of oil extract, 9.2% was obtained at 70°C and 60 min of extraction time. The active compounds in oil extract were identified using GC-MS. Compounds including sitosterol (12.54%), squalene (7.22%) and tocopherol (4.32%) were among the major compounds identified in oil-extract. Oil extract was also analyzed for its physio-chemical properties.

Keywords: Gooseberry seed, microwave extraction, GC-MS analysis

1. INTRODUCTION

Natural food additives derived from herbs and spices are offering potential antimicrobial and antioxidative properties in ingredient formulations [1]. Oil extract of spices mainly contains phenolic components that possess strong antibacterial activity against food-borne pathogens [2-3]. Nevertheless, extract derivatives exhibits several biological roles, including oxidative radical reduction [4]. Indian gooseberry (*Emblica officinalis)* a deciduous plant, commonly known as Amla is native to India and sustain changing climates and variable soil conditions [5]. Indian gooseberry fruit is reported to have highest vitamin C among other natural sources. Active ingredients of Indian gooseberry extract are popular for its analgesic, anti-inflammatory and chemo protective properties [6-7]. Indian gooseberry seeds also find its use in asthma and bronchitis for its valuable antioxidant components [8]. High value low volume products of cosmetic origin has high demands for rich sources of antioxidants. Indian gooseberry can serve as a competent source among fruits category for natural antioxidants.

Numerous scientific investigations have been carried out for extraction of active ingredients from fruit source using soxhlet extraction, maceration and hydro-distillation. However, such conventional extraction methods are associated with higher process utilities (energy and time consuming) and concerns with process controlling for undamaged active components [9-10]. Therefore, novel green technique of extraction is to be developed for obtaining concentrated product; reducing process cost, extraction time and use of organic solvent consumption [11-12]. A newer energy-saving method utilizing microwaves in active component extraction from natural sources is emerged as powerful alternative to prevalent extraction methods. Microwave-assisted extraction (MAE) leads to faster processing and provides improved yield and quality of product [13].

The aim of present study was to extract the active ingredient of Indian gooseberry seeds using MAE for optimize yield. Further, hexane-extract of seeds were characterized by GC-MS for component identification and determined for its physio-chemical properties.

2. MATERIALS & METHODS

Gooseberry Seeds: Fresh fruit of Indian Gooseberry (*Phyllanthus emblica*) were purchased from local market of Jalgaon (Maharashtra). Gooseberry seeds were separated from the fruit & oven-dried at 55°C. Yield of seeds after separation was expressed as percentage of initial weight of fresh gooseberry fruits. Dried seeds were analyzed for moisture content using standard method of FSSAI-2012. Seeds were grinded coarser, stored in a airtight container and used as such in present study.

Gooseberry Seeds Extraction: Microwave assisted extraction (MAE) was carried out in a Sineo MAS-II apparatus. The microwave reactor operated in multimode equipped with twin magnetron (2 × 800 W, 2450 MHz) to deliver maximum power of 1000W. A rotating microwave diffuser ensures homogeneous microwave distribution throughout the plasma coated PTFE cavity. A shielded

thermocouple (ATC-300) in the sample container controls the set extraction temperature. MAE procedure involved hexane extraction of known weight of coarser gooseberry seeds in the ratio of 3:1(v/w) under microwave power of 300 W. Extraction temperature variations in the range 60-80 °C for 40-80 min was carried out to release the oil from seeds. The oil extract yields at different operating conditions were noted and were stored to below ambient temperature.

Analysis of Gooseberry Seeds Oil Extract: Major compounds of oil extract were determined by GC-MS (Thermo GC Trace1300 coupled to Thermo MS TSQ8000). Physio-chemical properties of the oil-extract were determined according to the standard method of FSSAI-2012.

3. RESULTS AND DISCUSSION

Gooseberry seeds yield from fresh fruit was 23.2%. Dried Gooseberry seeds were analyzed with 71.5% moisture and 14.8% non-polar extract. The experimental MAE runs were carried out under domain of varying parameters which resulted in different percentage of yield as mentioned in **Table 1**.

Table 1: Experimental runs for MAE and Gooseberry seeds oil yield

Run Order	Time (min)	Temperature (°C)	Yield (%)
1	40	65	1.78
2	60	75	2.33
3	40	80	1.42
4	60	60	2.57
5	50	60	5.60
6	60	70	9.20
7	60	65	5.43
8	80	60	5.11
9	70	75	5.21

Minimum yield, 1.42% (80°C, 40 min) and maximum yield, 9.2% (70°C, 60 min) was obtained in run number 3 and 6 respectively. The oil yield was observed to be significantly affected by extraction temperature and time. A longer extraction time in MAE usually tends to increase the extraction yield. A rapid higher yield was evident with increasing time from 40 to 60 min, however further extraction time resulted into decreased yield. Similar behavior was found by Song et al, 2011 [14], Xiao et al, 2008 [15]. Temperature has influence on extraction efficiency, which increases with increase in temperature until an optimum temperature is reached. Any further rise in temperature affected the stability of extract yield of the target compound. A similar observation was reported by Routray and Orsat, 2012 [16].

GC-MS Analysis: GC-MS chromatogram of Gooseberry seed oil obtained from experimental run 6 is shown in **Fig. 1**. The detailed analysis of oil extract was carried out using different retention time peaks of GC and MS for compound identification. The study on active principles of extract showed the presence of ten chemical compounds (**Table 2**). The major compounds with their retention time (RT) and concentrations (%) are sitosterol (12.54%), squalene (7.22%), cyclohexasiloxane dodecamethyl (6.08%) and tocopherol (4.32%).

Table 2: Chemical composition of Gooseberry seed oil analyzed by GC- MS

Compound	RT	Area (%)
2, 4 Heptadienal 1,4 Hexadiene,3ethyl	7.32	4.28
Cyclohexasiloxane, dodecamethyl	11.97	6.08
Cycloheptasiloxane, tetradecamethyl	14.18	2.97
Hexadecanoic acid, ethyl ester Pentadecanoic acid, ethyl ester	19.60	3.24
Squalene	26.74	7.22
Tocopherol	29.57	4.32
Sitosterol	34.86	12.54
Amyrin, Lupeol	36.98	1.17

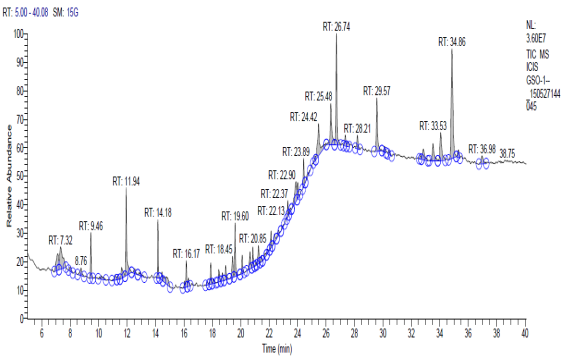

Figure 1. CG-MS spectrum of hexane extract of Gooseberry seed oil

Physio-chemical properties evaluation: The result of physio-chemical properties determined for Gooseberry seed oil in present work is shown in **Table 3**. These results are in agreement with the findings of Arora et al, 2011 [5].

Table 3: Physio-chemical characteristics of Gooseberry seed oil

Characteristics	Value
Melting point (°C)	34.0
Boiling point (°C)	191.25
Refractive index (40°C)	1.5021
Specific gravity	0.9221
Saponification Value (mg/g KOH)	207.6
Ester Value	205.2
Acid value (mg/g KOH)	2.4
Iodine Value (g I_2/100 g)	123.5

4. CONCLUSION

Microwave-assisted extraction (MAE) method was effective in obtaining valuable oil extract from Indian Gooseberry seed. MAE reduced the extraction time and allowed substantial saving of energy. Oil extract identified to have natural antioxidants like tocopherols, sterols, squalenes that are important for several pharmacological applications.

REFERENCES

[1] S. Burt, "Essential oils: Their antibacterial properties and potential applications in foods-A review", International Journal of Food Microbiology, vol. 94, no. 3, (**2004**), pp. 223–253.

[2] P. J. Delaquis, K. Stanich, S. Girard and G. Mazza, "Antimicrobial activity of individual and mixed fractions of dill, cilantro, coriander and eucalyptus essential oils", International Journal of Food Microbiology, vol. 74, no. 12, (**2002**), pp. 101–109.

[3] M. Nevas, A. R. Korhonen, M. Lindstro, P. Turkki and H. Korkeala, "Antibacterial efficiency of Finnish spice essential oils against pathogenic and spoilage Bacteria", Journal of Food Protection, vol. 67, no. 1, (**2004**), pp. 199-202.

[4] P. Mayachiew and S. Devahastin, "Antimicrobial and antioxidant activities of Indian gooseberry and galangal extracts", LWT-Food Science and Technology, vol. 41,no. 7, (2008), pp. 1153-1159.

[5] A. Arora, Indresh Kumar, R. Sen and J. Singh, "*Emblica Officinalis* (Amla): Physico-chemical and fatty acid analysis from arid zone of rajasthan", International Journal of Basic and Applied Chemical Sciences, vol. 1, no. 1, (**2011**), pp. 89-92.

[6] K.P. Sampath Kumar, D. Bhowmik, A. Dutta, A. Yadav, S. Paswan, S. Srivastava and L. Deb, "Recent trends in potential traditional indian herbs *Emblica officinalis* and its medicinal importance", Journal of Pharmacognosy and Phytochemistry , vol. 1, no. 1, (**2012**), pp. 18-28.

[7] M.T.H. Khan, I. Lampronti, D. Martello, N. Bianchi, S. Jabbar and M.S.K. Choudhuri, "Identification of pyrogallol as an antiproliferative compound present in extracts from the medicinal plant *Emblica officinalis*: Effect on in vitro cell growth of human tumor cell lines", International Journal of Oncology, vol. 21, no. 1, (**2002**), pp. 187-192.

[8] S. Madhuri, G. Pandey and K.S. Verma, "Antioxidant,immune modulatory & anticancer activities of *Emblica officinalis*: An overview", International Research Journal of Pharmacy, vol. 2, no. 8, (**2011**), pp. 38-42.

[9] A. Farhat, A.S. Fabiano-Tixier, M.E. Maataoui, J.F. Maingonnat, M. Romdhane, and F. Chemat, "Microwave steam diffusion for extraction of essential oil from orange peel: Kinetic data, extract's global yield and mechanism", Food Chemistry, vol.125, no. 1.(**2011**), pp. 255-261.

[10] H. Guolin, S. Jeffrey, Z. Kai, and H. Xiaolan, "Application of ionic liquids in the microwave assisted extraction of pectin from lemon peels", Journal of Analytical Methods in Chemistry, (**2012**), pp. 1-8. https://doi.org/10.1155/2012/302059

[11] J.P. Maran, V. Sivakumar, K. Thirugnanasambandham and R. Sridhar, "Optimization of microwave assisted extraction of pectin from orange peel", Carbohydrate polymers, vol. 97, no. 2, (**2013**), pp. 703-709.

[12] K. Hayat, S. Hussain, S. Abbas, U. Farooq, B. Ding, S. Xia, C. Jia, X. Zhang and W. Xia, "Optimized microwave assisted extraction of phenolic acids from citrus mandarin peels and evaluation of antioxidant activity in vitro", Separation and Purification Technology vol. 70, no. 1, (**2009**), pp. 63-70.

[13] J. Asghari, B. Ondruschka, and M. Mazaheritehrani, "Extraction of bioactive chemical compounds from the medicinal Asian plants by microwave irradiation", Journal of Medicinal Plants Research, vol. 5, no. 4, (**2011**), pp. 495-506.

[14] J. Song, D. Li, C. Liu and Y. Zhang, "Optimized microwave assisted extraction of total phenolics (TP) from *Ipomoea batatas* leaves and its antioxidant activity", Innovative food science & emerging technologies, vol. 12, no. 3, (**2011**), pp. 282-287.

[15] W. Xiao, L. Han, B. Shi, "Microwave assisted extraction of flavonoids from *Radix astragali*", Separation and Purification Technology, vol. 62, no. 3, (**2008**), pp. 614-618.

[16] W. Routray and V. Orsat, "Microwave assisted extraction of flavonoids: A review", Food and Bioprocess Technology, vol. 5, no. 2, (**2012**), pp. 409-424.

PRATIBHA: INTERNATIONAL JOURNAL OF SCIENCE, SPIRITUALITY, BUSINESS AND TECHNOLOGY (IJSSBT)
Special Issue: International Conference on Global Trends in Science, Technology, Humanities, Commerce & Management 2022 (ICGTSTHCM 2022)
Vol. 8, No. 2, January 2022,ISSN (Print) 2277-7261

Heat Stress in Tropical Climates Has an Effect on Poultry Birds: A Review

Kapil Saner[1], Prof. Dr. S. P. Shekhawat[2]
[1] Asst. Professor, R C Patel Institute of Technology, Shirpur, 425405, India
[2] Vice Principal, SSBT's College of Engineering & Technology, Bambhori, Jalgaon
[1] kapil_saner@yahoo.co.in, [2] spshekhawat@rediffmail.com

Abstract:

Heat stress is one of the most critical environmental challenges that global chicken growers undergo. Heat stress has a variety of negative consequences for poultry birds laying hens, including reduced growth and egg output as well as poor egg quality. Quality and safety of poultry and eggs Moreover, heat stress has a negative impact on poultry. Recently, there has been an increase in public awareness and concern about welfare. Furthermore, the negative effects of heat stress on poultry welfare have garnered considerable attention and concern recently. Heat stress's impact on poultry productivity and immunological response has been thoroughly researched. However, we know relatively little about the underlying mechanisms that cause the claimed effects, regarding poultry behaviour and welfare when exposed to extreme heat. Heat stress causes birds to death, resulting in lower productivity and a worse return on investment. Many studies have been published that have focused on intervention measures to deal with heat stress. Heat stress affects chicken behaviour, welfare, and immunity, as well as egg production, resulting in significant financial losses for the farmer. Some of the management measures used to decrease the detrimental impacts of heat stress in chicken production include ventilation, bird density, dietary manipulation, and mineral and electrolyte supplementation. For efficient poultry production and welfare, environmental variance must be controlled.

Keywords: ***Humidity, Poultry Bird, Heat Stress, Central Nervous System (CNS), Hypothalamic Pituitary Adrenal (HPA), Sympathetic Adrenal Medullar (SAM)***

I. Introduction

Poultry farming is one of the quickest expanding segments of the livestock industry in emerging countries. One of the most critical factors finding out the long-term survival of tropical animal manufacturing systems is environmental fluctuation [45] Heat stress impacts production efficiency, and poultry mortality has a dangerous influence on the profitability of the business. Heat stress reduces egg production, egg weight, and shell quality in poultry birds [46, 47, and 48]. High ambient temperatures can have an extensive effect on the performance of poultry birds. When these factors are combined with excessive humidity, the consequence can be disastrous. As a result, in order to decrease warmness stress, it is necessary to reassess chicken management and gear used in hot weather. When the temperature in a living organism exceeds the normal range (thermo-neutral zone), it disrupts normal physiological function and causes cell damage. High ambient temperature usually causes stress-related issues such productivity losses, metabolic alterations, growth depression, and inefficiency [54, 55] Heat stress now not only causes ache and demise in the birds, but it also leads to diminished or misplaced productivity, which has an unsafe impact on the company's bottom line. A bad strength stability exists between the quantity of warmth strength produced through the animal and the amount of strength moving from the animal's physique to its surroundings, ensuing in heat stress. This imbalance may want to be caused with the aid of changes in a variety of environmental elements such as (air temperature, humidity, air movement) as properly as animal traits (e.g., species, metabolism rate, and thermoregulatory mechanisms).Animal agriculture is particularly vulnerable to heat stress and other environmental factors [2–4] High ambient temperatures can have a considerable impact on commercial poultry performance. When they're mixed with high humidity, the effect can be deadly. Heat stress not only causes pain and death in the birds, but it also reduces or eliminates productivity, lowering profits. High temperatures can have a negative impact on bird performance and result in lower revenues for poultry farmers. Heat stress affects the behaviour of birds, as well as their respiratory and cardiovascular systems, immunological function, intestinal integrity, and food usage.

II. Heat Stress Symptoms

Chicks and grown hens pant to stay cool, just like dogs, and this is the first warning that they need shade and water. They open their mouths and pant while spreading their wings and crouching close to the ground when they are stressed by the heat [3].

PRATIBHA: INTERNATIONAL JOURNAL OF SCIENCE, SPIRITUALITY, BUSINESS AND TECHNOLOGY (IJSSBT)
Special Issue: International Conference on Global Trends in Science, Technology, Humanities, Commerce & Management 2022 (ICGTSTHCM 2022)
Vol. 8, No. 2, January 2022,ISSN (Print) 2277-7261

They are attempting to lose heat by altering the location of their feathers.

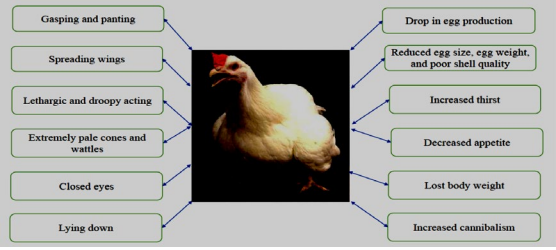

Figure 1 – Signs of Heat Stress

Heat fatigue is a problem for laying hens. An egg's main component is water. Because laying eggs necessitates a lot of fluids, it's critical to keep your hens hydrated and comfortable [59]. To avoid soft eggshells, egg layers also require a lot of calcium. Because your chickens may not eat as much while it's hot outside, calcium intake is low. 2-3 times a week, add a small bit of apple cider vinegar to their drink. This helps to balance their pH, allowing for faster calcium absorption. In the 'thermo neutral zone,' birds can lose heat at a controlled rate utilising regular activity, as shown in Diagram 1. There is no heat stress, and the body temperature is maintained at the same level. When the "upper critical temperature" is exceeded, birds must actively remove heat via panting. Panting is a natural reaction to heat and is not first seen to be a welfare issue. However, when the temperature rises, so does the pace of panting [2]. Birds may perish if heat production exceeds' maximum heat loss,' either in severity (acute heat stress) or over lengthy periods of time (chronic heat stress). The broiler's body temperature must maintain close to 410°C (1060F). The bird will perish if its body temperature rises above 40 degrees Celsius.

Heat Stress

Birds are said to be "heat stressed" when they struggle to maintain a balance between bodily heat production and loss. Chickens of all ages and breeds are susceptible to this condition. It's worth emphasising that a welfare problem is more likely to arise between the 'upper critical temperature' and 'maximum heat loss,' that is, before the bird loses heat. The stock keeper should be aware of the birds' behaviour and look for signs of distress. A basic schedule of events on a hot day when heat stress could create broiler welfare difficulties is depicted in the table at the end of the booklet.

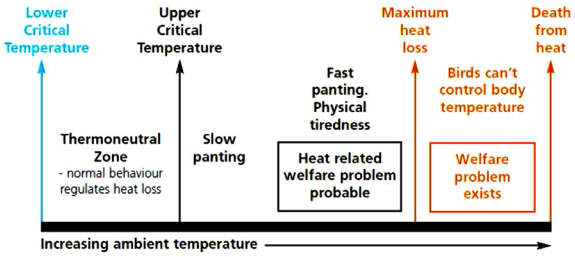

Figure 2 – Diagram of Thermo neutral Zone

III. Literature survey on Behavioural and Physiological Effects of Heat Stress

In high-temperature conditions, birds adjust their behaviour and physiological homeostasis to be seeking thermoregulation, lowering physique temperature. Heat stress affects distinct kinds of birds in comparable ways, whilst the severity and size of their responses vary. According to the findings of the lookup find out about [7] when animals are uncovered to excessive environmental temperatures, they use a range of techniques to hold thermo-regulation and homeostasis, including multiplied radiative, convective, and evaporative warmth loss thru vasodilation and perspiration [8]. These substantial physiological, neuroendocrine, and behavioural changes in chicken result in higher mortality, lower feed intake, lower ultimate body weight, lower meat and egg quality, and a higher feed conversion ratio (FCR). [56]. the characteristic signs of panting are also observed in heat-stressed birds Despite the fact that several studies have attempted to characterise the physiological mechanisms underlying the drop in egg great in heat harassed birds, no definitive knowledge exists, and quite a few achievable pathways, such as changes in reproductive hormone ranges and intestinal calcium uptake, are nonetheless being researched [11, 12]. When birds are exposed to a temperature that is higher than their thermoneutral temperature, they strive to remove the extra heat created inside the body by exhibiting distinct behavioural modifications. Finally, In general, birds react to warmth stress in a comparable way, whilst man or woman differences in response energy and duration might also be impacted via the severity and length of the heat stress episode. Heat stress is regularly experienced in combination with distinctive stressors such as restricted housing area and insufficient ventilation, as proper as social interactions and previous experiences, all of which have been validated to impact an individual's stress response. [14-17]. The thyroid hormones triiodothyronine (T3) and thyroxine (T4), as well as their balance, govern body temperature and metabolic activity. Because the thyroid is concerned

in the beginnings of puberty and reproductive function in birds, a disturbance of thyroid exercise caused by means of heat stress would be expected to harm the hens' reproductive performance, according to previous research. [13] In general, birds react to heat stress in a similar way, even as man or female variations in response energy and length might also be impacted by means of the severity and size of the heat stress episode. Heat stress is frequently experienced in combination with special stressors such as restricted housing location and insufficient ventilation, as true as social interactions and previous experiences, all of which have been tested to impact an individual's stress response [18, 19].

IV. Impact of Heat Stress on the Immune System

Various studies in poultry have looked into the impact of heat stress on the immune response in recent years. According to all research, heat stress has an immunosuppressive effect on broilers and laying hens in general, however different measures are used. Reduced relative weights of the thymus and spleen have been discovered in laying chickens subjected to heat stress [20] Chickens with weakened immune systems may be unable to respond adequately to inflammation and infection. In today's chicken housing systems, Gram-negative bacteria are a common disease [58]. It has been concluded that high environmental temperatures affect the immune response in chickens Heat stress increases susceptibility to diseases in poultry as it has an immunosuppressing effect. Heat stress has bad consequences on health recognition of birds main to changes in physiology, metabolism, hormonal and immune system. Inflection of the immune response with the aid of the central worried gadget (CNS), and is mediated through a complex network of nervous, endocrine and immune systems. , causing welfare concerns, particularly under HS. Heat-stressed hens died more quickly after receiving an Escherichia coli vaccination than hens kept in a controlled environment [57]

A. Heat Stress Effects on Poultry Production

The impact of heat stress on broiler production efficiency has been studied extensively., all of which are detrimental to their productivity, as previously stated, Heat stress inhibits gonadal steroids like progesterone, testosterone, and estradiol, which are all necessary for egg development [25] The cellular mechanism through which HS inhibits gonadotropin bioactivity is less well understood. It's most likely owing to a variety of factors impacting animals' physiological homeostasis under HS, such as feed intake reduction. [26]. Heat stress inhibits gonadal steroids like progesterone, testosterone, and estradiol, which are all necessary for egg development. [28]. Environmental stress (such as heat stress), which is likely one of the most common challenges in many production systems around the world, can decrease the productivity of laying hen flocks. Reduced feed intake is probably certainly the starting point for the majority of heat stress's detrimental effects on production, leading to poorer body weight, feed efficiency, egg output, and quality [21] The link between reduced feed intake and increased mortality could potentially be to blame for lower egg output. [31-33]. Chickens' reaction to Heat Stress is affected by multiple factors, The documented diversity in the effects of HS on chicken health could be explained by the health and production condition of the birds studied, as well as their genetic background. The variance could potentially be related to the different levels of HS intensity and duration used on the hens. Stocking density has a significant impact on both chicken productivity and physiological equilibrium. [30] When a bird is exposed to excessive levels of sun radiation, its chemical composition and meat quality deteriorate industry of broilers [52,58] Exposure of high temperature during the growing phase of broilers has been related with poor meat characteristics of broiler chicken and loss their quality. Heat stress adversely influences the efficiency of broiler manufacturing and their meat quality. High environmental temperature effect to reduced feed intake, lower physique weight, and lower feed conversion effectivity [27, 53]

B. How Does Heat Affect Food Safety?

Heat stress has been linked to poor meat quality and undesired meat attributes in broilers during their growing stage [27] The chicken and egg-producing agencies around the world have these days been involved about meals safety. In truth, meals security is turning into an extra vital section of the modern meals exceptional paradigm. The colonisation of birds by way of foodborne viruses such as Salmonella and Campylobacter, and subsequent transmission down the human meals chain, is a serious public fitness and monetary venture in fowl and egg production. The consumption and handling of undercooked chicken merchandise is, in fact, one of the most frequently implicated sources of foodborne sickness [34-37]. Many current research have established that bacteria such as Salmonella and Campylobacter can take advantage of neuroendocrine changes generated with the aid of the stress response in the host to enlarge their

proliferation and pathogenicity [41-43]. This is a significantly more sophisticated microbial system than the fowl gut microbiome. As a result, it's reasonable to think that heat stress has an effect on the bacteria populations in the intestines of chickens. This information chasm, on the other hand, needs to be investigated and appreciated deeper [20]. Oxidative stress kicks off the aberrant process of intestinal permeability. Under heat stress, increasing levels of reactive oxygen species (ROS) result in increased intestinal permeability, which facilitates in the movement of bacteria from the digestive tract. Heat stress in broilers has been associated to increased inflammation and Salmonella Enteritidis translocation [22, 23]. High ambient temperatures are anticipated to change now not solely the bacterial levels in fowl faeces, however also the period and stage of contamination in the region the place faeces are deposited, doubtlessly ensuing in increased dispersion. Heat stress did no longer end result in increased numbers or longer survival of Salmonella shed in faeces, according to a small study [44]

V. Conclusion

Heat stress is one of the most significant environmental stressors that chicken producers face around the world. Heat stress has a range of negative results on fowl birds, ranging from decreased increase and egg manufacturing to decreased fowl and egg excellent and safety. However, the hazardous effect of heat stress on poultry welfare need to be a serious issue. As this review shows, a lot of lookup has been completed on the have an impact on of warmness stress on rooster productiveness and immune response (broilers and laying hens). Heat stress has been located to have a bad have an effect on poultry birds manufacturing by means of reducing feed intake and increasing mortality. Heat stress reduces broiler and laying chook increase and egg production, resulting in low egg quality. High ambient temperatures enhance the mortality of chickens by means of suppressing immune responses.

References

1. Selye, Hans. "Forty years of stress research: principal remaining problems and misconceptions." *Canadian Medical Association Journal,* Vol.115, no. 1 (1976) pp. 53.
2. Nienaber, J. A., and G. L. Hahn. "Livestock production system management responses to thermal challenges." *International Journal of Biometeorology,* Vol. 52, no. 2 (2007) pp. 149-157.
3. Nardone, Alessandro, Bruno Ronchi, Nicola Lacetera, Maria Stella Ranieri, and Umberto Bernabucci. "Effects of climate changes on animal production and sustainability of livestock systems." *Livestock Science,* Vol. 130, no. 1-3 (2010) pp. 57-69.
4. Renaudeau, David, Anne Collin, S. Yahav, V. De Basilio, Jean-Luc Gourdine, and R. J. Collier. "Adaptation to hot climate and strategies to alleviate heat stress in livestock production." *Animal,* Vol.6, no. 5 (2012) pp. 707-728.
5. Settar, P. E. T. E. K., S. E. R. V. E. T. Yalcin, L. Turkmut, S. E. Z. E. N. Ozkan, and A. Cahanar. "Season by genotype interaction related to broiler growth rate and heat tolerance." *Poultry science,* Vol.78, no. 10 (1999) pp. 1353-1358.
6. Deeb, N., and A. Cahaner. "Genotype-by-environment interaction with broiler genotypes differing in growth rate. 3. Growth rate and water consumption of broiler progeny from weight-selected versus nonselected parents under normal and high ambient temperatures." *Poultry Science,* Vol.81, no. 3 (2002) pp. 293-301.
7. Mack, L. A., J. N. Felver-Gant, R. L. Dennis, and H. W. Cheng. "Genetic variations alter production and behavioral responses following heat stress in 2 strains of laying hens." *Poultry science,* Vol.92, no. 2 (2013) pp. 285-294.
8. Mutaf, S., N. Seber Kahraman, and M. Z. Firat. "Intermittent partial surface wetting and its effect on body-surface temperatures and egg production of white and brown domestic laying hens in Antalya (Turkey)." *British poultry science,* Vol.50, no. 1 (2009) pp. 33-38.
9. Fedde, M. R. "Relationship of structure and function of the avian respiratory system to disease susceptibility." *Poultry science,* Vol.77, no. 8 (1998) pp. 1130-1138.
10. Marder, Jacob, and Zeev Arad. "Panting and acid-base regulation in heat stressed birds." *Comparative Biochemistry and Physiology Part A: Physiolog ,* Vol.94, no. 3 (1989) pp. 395-400.
11. Elnagar, S. A., S. E. Scheideler, and M. M. Beck. "Reproductive hormones, hepatic deiodinase messenger ribonucleic acid, and vasoactive intestinal polypeptide-immunoreactive cells in hypothalamus in the heat stress-induced or chemically induced hypothyroid laying hen." *Poultry Science,* Vol.89, no. 9 (2010) pp. 2001-2009.
12. Ebeid, T. A., T. Suzuki, and T. Sugiyama. "High ambient temperature influences eggshell quality and calbindin-D28k localization of eggshell gland and all intestinal segments of laying hens." *Poultry Science,* Vol.91, no. 9 (2012) pp. 2282-2287.
13. Elnagar, S. A., S. E. Scheideler, and M. M. Beck. "Reproductive hormones, hepatic deiodinase messenger ribonucleic acid, and vasoactive intestinal polypeptide-immunoreactive cells in hypothalamus in the heat stress-induced or chemically induced hypothyroid laying hen." *Poultry Science,* Vol.89, no. 9 (2010) pp. 2001-2009.
14. Garriga, Carles, Richard R. Hunter, Concepció Amat, Joana M. Planas, Malcolm A. Mitchell, and Miquel Moretó. "Heat stress increases apical glucose transport in the chicken jejunum." *American Journal of*

Physiology-Regulatory, Integrative and Comparative Physiology, Vol.290, no. 1 (2006) pp. R195-R201.
15. Star, L., E. Decuypere, H. K. Parmentier, and B. Kemp. "Effect of single or combined climatic and hygienic stress in four layer lines: 2. Endocrine and oxidative stress responses." *Poultry Science,* Vol.87, no. 6 (2008) pp. 1031-1038.
16. Quinteiro-Filho, W. M., A. Ribeiro, V. Ferraz-de-Paula, M. L. Pinheiro, M. Sakai, L. R. M. D. Sá, A. J. P. Ferreira, and J. Palermo-Neto. "Heat stress impairs performance parameters, induces intestinal injury, and decreases macrophage activity in broiler chickens." *Poultry science,* Vol.89, no. 9 (2010) pp. 1905-1914.
17. Quinteiro-Filho, W. M., A. V. S. Gomes, M. L. Pinheiro, A. Ribeiro, V. Ferraz-de-Paula, C. S. Astolfi-Ferreira, A. J. P. Ferreira, and J. Palermo-Neto. "Heat stress impairs performance and induces intestinal inflammation in broiler chickens infected with Salmonella Enteritidis." *Avian Pathology,* Vol.41, no. 5 (2012) pp. 421-427.
18. Boissy, Alain, Gerhard Manteuffel, Margit Bak Jensen, Randi Oppermann Moe, Berry Spruijt, Linda J. Keeling, Christoph Winckler et al. "Assessment of positive emotions in animals to improve their welfare." *Physiology & behavior ,* Vol.92, no. 3 (2007) pp. 375-397.
19. Hemsworth, Paul H. "Human–animal interactions in livestock production." *Applied Animal Behaviour Science,* Vol.81, no. 3 (2003) pp. 185-198.
20. Ghazi, S. H., M. Habibian, M. M. Moeini, and A. R. Abdolmohammadi. "Effects of different levels of organic and inorganic chromium on growth performance and immunocompetence of broilers under heat stress." *Biological trace element research,* Vol.146, no. 3 (2012) pp. 309-317.
21. Deng, W., X. F. Dong, J. M. Tong, and Q. Zhang. "The probiotic Bacillus licheniformis ameliorates heat stress-induced impairment of egg production, gut morphology, and intestinal mucosal immunity in laying hens." *Poultry science,* Vol.91, no. 3 (2012) pp. 575-582.
22. Prieto, M. T., and J. L. Campo. "Effect of heat and several additives related to stress levels on fluctuating asymmetry, heterophil: lymphocyte ratio, and tonic immobility duration in White Leghorn chicks." *Poultry science,* Vol.89, no. 10 (2010) pp. 2071-2077.
23. Droge, Wulf. "Free radicals in the physiological control of cell function." *Physiological reviews,* Vol.82, no. 1 (2002) pp. 47-95.
24. Gu, X. H., Y. Hao, and X. L. Wang. "Overexpression of heat shock protein 70 and its relationship to intestine under acute heat stress in broilers: 2. Intestinal oxidative stress." *Poultry science,* Vol.91, no. 4 (2012) pp.790-799.
25. St-Pierre, N. R., B. Cobanov, and G. Schnitkey. "Economic losses from heat stress by US livestock industries." *Journal of dairy science,* Vol.86 (2003) pp. E52-E77.
26. Ajakaiye, Joachim J., Alcides Perez-Bello, and Angel Mollineda-Trujillo. "Impact of heat stress on egg quality in layer hens supplemented with l-ascorbic acid and dl-tocopherol acetate." *Veterinarski arhiv ,* Vol.81, no. 1 (2011) pp. 119-132.
27. Lu, Q., J. Wen, and H. Zhang. "Effect of chronic heat exposure on fat deposition and meat quality in two genetic types of chicken." *Poultry science,* Vol.86, no. 6 (2007) pp. 1059-1064.
28. Rozenboim, I., E. Tako, O. Gal-Garber, J. A. Proudman, and Z. Uni. "The effect of heat stress on ovarian function of laying hens." *Poultry science,* Vol.86, no. 8 (2007) pp. 1760-1765.
29. Warriss, P. D., A. Pagazaurtundua, and S. N. Brown. "Relationship between maximum daily temperature and mortality of broiler chickens during transport and lairage." *British poultry science,* Vol.46, no. 6 (2005) pp. 647-651.
30. Estevez, I. "Density allowances for broilers: where to set the limits" *Poultry Science,* Vol.86, no. 6 (2007) pp. 1265-1272.
31. Mateo, Fabián Itzá Ortiz, Leonel García Compean, and Francisco Javier Castro Aguilar. "Feed intake, cause and percentage of mortality in commercial poultry farms under the climatic conditions of the state of Yucatan, Mexico." *Veterinaria México,* Vol.37, no. 3 (2006) pp. 379-390.
32. Zhou, W. T., M. Fujita, S. Yamamoto, K. Iwasaki, R. Ikawa, H. Oyama, and H. Horikawa. "Effects of glucose in drinking water on the changes in whole blood viscosity and plasma osmolality of broiler chickens during high temperature exposure." *Poultry science,* Vol.77, no. 5 (1998) pp. 644-647.
33. Gantois, Inne, Richard Ducatelle, Frank Pasmans, Freddy Haesebrouck, Richard Gast, Tom J. Humphrey, and Filip Van Immerseel. "Mechanisms of egg contamination by Salmonella Enteritidis." *FEMS microbiology reviews,* Vol.33, no. 4 (2009) pp. 718-738.
34. Newell, Diane G., Marion Koopmans, Linda Verhoef, Erwin Duizer, Awa Aidara-Kane, Hein Sprong, Marieke Opsteegh et al. "Food-borne diseases—the challenges of 20 years ago still persist while new ones continue to emerge." *International journal of food microbiology,* Vol.139 (2010) pp. S3-S15.
35. Eisenberg, Joseph NS, James Trostle, Reed JD Sorensen, and Katherine F. Shields. "Toward a systems approach to enteric pathogen transmission: from individual independence to community interdependence." *Annual review of public health,* Vol.33 (2012) pp. 239-257.
36. Domingues, A. R., Sara Monteiro Pires, T. Halasa, and Tine Hald. "Source attribution of human salmonellosis using a meta-analysis of case-control studies of sporadic infections." *Epidemiology & Infection,* Vol.140, no. 6 (2012) pp. 959-969.
37. Rychlik, Ivan, and Paul A. Barrow. "Salmonella stress management and its relevance to behaviour during intestinal colonisation and infection." *FEMS microbiology reviews,* Vol.29, no. 5 (2005) pp. 1021-1040.
38. Humphrey, Tom. "Are happy chickens safer chickens? Poultry welfare and disease susceptibility." *British poultry science* 47, no. 4 (2006) pp. 379-391.
39. Rostagno, Marcos H. "Can stress in farm animals increase food safety risk." *Foodborne pathogens and disease,* Vol.6, no. 7 (2009) pp. 767-776.

40. Verbrugghe, Elin, Filip Boyen, Wim Gaastra, Leonie Bekhuis, Bregje Leyman, Alexander Van Parys, Freddy Haesebrouck, and Frank Pasmans. "The complex interplay between stress and bacterial infections in animals." *Veterinary microbiology,* Vol.155, no. 2-4 (2012) pp. 115-127.
41. Lyte, Mark. "Microbial endocrinology and infectious disease in the 21st century." *Trends in microbiology,* Vol.12, no. 1 (2004) pp. 14-20.
42. Freestone, Primrose PE, Sara M. Sandrini, Richard D. Haigh, and Mark Lyte. "Microbial endocrinology: how stress influences susceptibility to infection." *Trends in microbiology,* Vol.16, no. 2 (2008) pp. 55-64.
43. Wei, S., M. Morrison, and Z. Yu. "Bacterial census of poultry intestinal microbiome." *Poultry science,* Vol.92, no. 3 (2013) pp. 671-683.
44. Sinha, Ranjana, A. Ranjan, S. Lone, Abdul Rahim, Indu Devi, and Shiwani Tiwari. "The impact of climate change on livestock production and reproduction: ameliorative management." *International Journal of Livestock Research,* Vol.7, no. 6 (2017) pp. 1-8.
45. Muiruri, H. K., and P. C. Harrison. "Effect of roost temperature on performance of chickens in hot ambient environments." *Poultry Science,* Vol.70, no. 11 (1991) pp. 2253-2258.
46. Balnave, D., and S. K. Muheereza. "Improving eggshell quality at high temperatures with dietary sodium bicarbonate." *Poultry Science,* Vol.76, no. 4 (1997) pp. 588-593.
47. Whitehead, C. C. "Vitamin E can alleviate the depressed egg production of heat-stressed laying hens." *British poultry science,* Vol.39, no. S1 (1998) pp. 44-46.
48. De Rensis, Fabio, and Rex John Scaramuzzi. "Heat stress and seasonal effects on reproduction in the dairy cow—a review." *Theriogenology,* Vol.60, no. 6 (2003) pp. 1139-1151.
49. Lara, Lucas J., and Marcos H. Rostagno. "Impact of heat stress on poultry production." *Animals,* Vol.3, no. 2 (2013) pp. 356-369.
50. Ranjan, Ashish, Ranjana Sinha, Indu Devi, Abdul Rahim, and Shiwani Tiwari. "Effect of heat stress on poultry production and their managemental approaches." *International Journal of Current Microbiology and Applied Sciences,* Vol.8, no. 02 (2019) pp. 1548-1555.
51. Ebeid, T. A., T. Suzuki, and T. Sugiyama. "High ambient temperature influences eggshell quality and calbindin-D28k localization of eggshell gland and all intestinal segments of laying hens." *Poultry Science,* Vol.91, no. 9 (2012) pp. 2282-2287.
52. Sohail, M. U., M. E. Hume, J. A. Byrd, D. J. Nisbet, A. Ijaz, A. Sohail, M. Z. Shabbir, and H. Rehman. "Effect of supplementation of prebiotic mannan-oligosaccharides and probiotic mixture on growth performance of broilers subjected to chronic heat stress." *Poultry science,* Vol.91, no. 9 (2012) pp. 2235-2240.
53. Afsal, A., V. Sejian, M. Bagath, G. Krishnan, C. Devaraj, and R. Bhatta. "Heat stress and livestock adaptation: Neuro-endocrine regulation." (2018).
54. Renaudeau, David, Anne Collin, S. Yahav, V. De Basilio, Jean-Luc Gourdine, and R. J. Collier. "Adaptation to hot climate and strategies to alleviate heat stress in livestock production." *Animal,* Vol.6, no. 5 (2012) pp. 707-728.
55. Abu-Dieyeh, Z. H. M. "Effect of chronic heat stress and long-term feed restriction on broiler performance." *International Journal of Poultry Science,* Vol.5, no. 2 (2006) pp. 185-190.
56. Strong, Rebecca A. "The effects of heat stress on immunity in laying hens and dairy cattle." PhD diss., Purdue University, 2014.
57. Zucker, B-A., S. Trojan, and W. Müller. "Airborne gram-negative bacterial flora in animal houses." *Journal of Veterinary Medicine, Series B ,* Vol.47, no. 1 (2000) pp. 37-46.
58. Dai, S. F., F. Gao, X. L. Xu, W. H. Zhang, S. X. Song, and G. H. Zhou. "Effects of dietary glutamine and gamma-aminobutyric acid on meat colour, pH, composition, and water-holding characteristic in broilers under cyclic heat stress." *British Poultry Science ,* Vol.53, no. 4 (2012) pp. 471-481.
59. Boissy, Alain, Gerhard Manteuffel, Margit Bak Jensen, Randi Oppermann Moe, Berry Spruijt, Linda J. Keeling, Christoph Winckler et al. "Assessment of positive emotions in animals to improve their welfare." Physiology & behavior , Vol. 92, no. 3 (2007) pp. 375-397.

PRATIBHA: INTERNATIONAL JOURNAL OF SCIENCE, SPIRITUALITY, BUSINESS AND TECHNOLOGY (IJSSBT)
Special Issue: International Conference on Global Trends in Science, Technology, Humanities, Commerce & Management 2022 (ICGTSTHCM 2022)
Vol. 8, No. 2, January 2022,ISSN (Print) 2277-7261

Effect of Elevated Temperature On Mechanical Properties Of Fly Ash Used Concrete

Pankaj Punase [1], P. R. Asutkar [2], Dr. M. Husain [3]
[1] Assistant Professer, [2] Research Scholar, [3] Professor and Head of Civil Engineering Department
[1], [2] [3] SSBT College of Engineering and Technology, Jalgaon, MH, India.
[1] pankajpunase5@gmail.com [2]priyaasutkar1992@gmail.com,[3]ermujahidhusain@yahoo.com

Abstract:
Concrete is one the most extensively used construction material all over the world. Many scientists and researchers are in quest for developing alternate construction material that are environment friendly and contribute towards sustainable development. Huge amount of fly ash waste is generating day by day from thermal power stations which creates the disposal problem and has many environmental issues.
Also, buildings are accidently subjected to fire hazards, during fire the temperature of concrete may go high. High temperature can cause the development of cracks in concrete. These cracks like any other cracks propagate & may eventually cause loss of structural integrity and shorting of service life.
In this study fly ash is used as replacement of cement in concrete. Replacement is done up to 15 % with the increment of 5%. After curing of 28 days each concrete specimen of fly ash based concrete will be exposed to elevated temperature (30°C, 100°C, 200°, 300°C, 400°C, 500°C, 600°C, 700°C, 800°C,) by using muffle furnace. After temperature regimes compressive strength of fly ash used concrete is determined.

Key Words- Concrete, temperature, fly ash, strength etc

Introduction

fly ash is the pozzolan derive from the combustion of powdered coal during electric power generation. According to ASTM the fly ash are classified as Class N, Class C, and Class F. Class N are natural pozzolans, calcined volcanic ash etc. Class type F is fly ash nominally produced from anthracite, bituminous, and some sub- bituminous coals. C type fly ash is produced from combustion of lignite and some sub- bituminous coals. According to the report total production of Fly ash was 52.4 million tons in 1983, out of which 3.6 million tons was used in cement and concrete products [6]. extra 5.3 million tons was used as supplementary.

The components of the concrete are fine aggregates (FA), coarse aggregate (CA), cement and water. The vital environmental problems related with cement production is releasing of CO2, one of the major greenhouse gas which causes Global Warming. Keeping this ill effect of cement, various replacements include fly ash, ground granulated blast furnace slag, rice husk and silica fume is used, fly ash is the pozolaonic material cheaply available in the nearby places and therefore it is possible to prepare cheaper concrete mix..

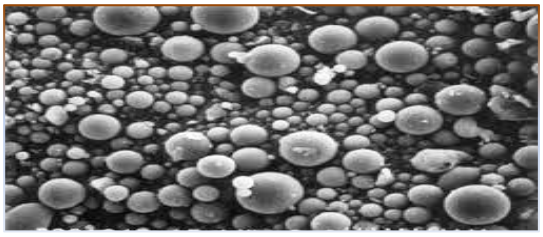

Fig. 1 Micrograph showing spherical fly ash particles

Laboratory testing of concrete is usually performed at a controlled temperature, normally constant. As the early testing was done in temperate climates, the standardized temperature chosen was generally in

the region of 180 to 210C so that much of the basic information about the properties of both fresh and hardened concrete is based on the behaviour of concrete at these temperatures. In practice however the concrete is mixed and remains in service at a variety of temperature. Indeed, the actual range of temperature has widened up considerably with much modern construction taking place in countries which have a hot climate. Also, new developments, mainly offshore, take place in very cold regions. Conventionally, researchers have used strength properties of concrete as criteria for evaluating its performance. A concrete having high strength does not necessarily imply that it will have long service-life. Thus, it is now well recognized that concrete performance should be determined in terms of both strength and durability under anticipated environmental conditions.

EFFECTS OF HIGH TEMPERATURE

Under normal conditions, most concrete structures are subjected to a range of temperature no more severe than that imposed by ambient environmental conditions. However, there are important cases where these structures may be exposed to much higher temperatures (e.g., building fires, chemical and metallurgical industrial applications in which the concrete is in close proximity to furnaces, and some nuclear power-related postulated accident conditions). Concrete's thermal properties are more complex than for most materials because not only is the concrete a composite material whose constituents have different properties, but its properties also depends on moisture and porosity. Exposure of concrete to elevated temperature affects its mechanical and physical properties.

EFFECTS ON STRENGTH OF CONCRETE

It has been found that high early temperature has negative impacts on later strength of concrete. Some researchers investigated the adverse effect on long term strength of concrete due to high initial temperature. High initial rate of hydration due to increased temperature retards the subsequent hydration and produces a non-uniform distribution of the products of hydration. Its reason is that at high initial rate of hydration, there is insufficient time available for the diffusion of the products of hydration away from the cement particle and for a uniform precipitation in the interstitial space. All this results in concentration of the products in the vicinity of the hydrating particles which causes subsequent retardation in hydration and effects strength.

4. EXPERIMENTAL WORK

Physical properties of all the material use in concrete is determine and some specifications are mention below
Cube specimens with dimensions 150*150*150 mm.
Concrete Grade: M25
Cement : Ordinary Portland Cement .
Fly Ash: obtain from deepnagar thermal power station
Coarse aggregate: Basalt aggregate (crushed stones)
Fine aggregate : Local sand
Water : 175 Liters (W/C = 0.50)
Temperatures: 30, 100, 200, 300, 400, 500 C, 600 C. 700, 800 C.
Curing age : 28 days

To determine the compressive strength of concrete after curing period specimens were kept in the oven for 4 hours to achieve a uniform temperature distribution across them. After that, specimens were allowed to cool in the oven for 20 hours, a total of 24 hours.

RESULTS AND DISCUSSION

Table: Compressive strength in N/mm2

Concrete Specimens	30	100	200	300	400	500	600	700	800
Plain concrete(M25)	34.22	34.22	33.50	33.05	31.06	29.080	27.40	18.02	12.01
Fly ash concrete(15% Fly ash)	34.22	34.22	33.01	32.90	30.95	29.02	26.45	16.9	10.89

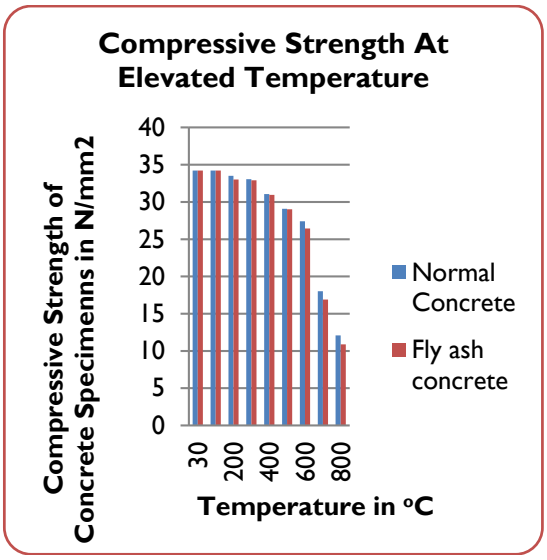

Figure 2. Compressive strength of concrete specimens

Effect of temperature on compressive strength

Figure 2, shows the comparison of compressive strength between normal and fly ash used concrete, it is observed that the strength of concrete is reduced with increase in temperature. The strength is constant up to 100°c, further increase in temperature up to 500°c there is no significant loss in compressive strength, therefore the optimum strength considered up to 500°c. At this temperature strength is reduced by 15.03 % for normal concrete and 15.19% for fly ash used concrete. Further increase in temperature case sudden drop down of strength, at 800 the strength of concrete is reduced by 64.91 % for normal concrete and 68.18 % for fly ash used concrete.

Effect of heating on the colour of concrete

Since the thermal conductivity reduces with the increase in temperature, water quenching of the heated concrete samples has not produced uniform cooling. The heat from the core of the test cylinders was unable to dissipate rapidly. Therefore, the core has sustained the elevated temperature for a longer period of time than the skin of the concrete cubes as observed from the colour differences across the section of the heated concrete specimens.

CONCLUSIONS

1. fly ash replacement up to 15% achieves optimum compressive strength
2. There was no apparent visual discoloration occurred in the concrete up to 200°C, but above 500°C effect is severe.
3. The strength is constant up to 100°c temperature, up to 500°c there is no significant loss in compressive strength, therefore the optimum strength considered up to 500°c.
4. Beyond 500°c Temperature case sudden drop down of strength is observed

REFERENCES

1. A. De Souza, A. L. Moreno JR, The effect of high temperatures on concrete compression strength, tensile strength and deformation modulus, IBRACON Structures and Materials Journal, 2010, vol. 3.
2. Dunstan, M. R. H, Development of high fly ash concrete." Proceedings Inst. Civil Engineers, (1983). 74, 495-513.

3. Joshi, R. C, Day, R. L., Langan, B. W., and Ward, M. A, Strength and durability of concrete with high proportions of fly ash and other mineral admixtures," (1987). 4, 253-270.
4. Mather, B, The partial replacement of portland cement in concrete," in Cement and Concrete, 1956, 37-73.
5. Naik, T. R. (1987). "Setting and hardening of high fly ash content concrete," Paper presented at American Coal Ash 8th International Coal Ash Utilization Symposium.
6. Osuji, and U. Ukeme, "The study of the properties of fly ash based concrete Composites with various chemical admixtures", Procedia Engineering 42 (2012) 1863 – 1872.
7. Khushal Chandra Kesharwani, Amit Kumar Biswas, Anesh Chaurasiya, Ahsan Rabbani, "Experimental Study on Use of Fly Ash in Concrete", International Research Journal of Engineering and Technology (IRJET), Volume: 04 Issue: 09 | Sep -2017.
8. P. Nath, P. Sarker, "Effect of Fly Ash on the Durability Properties of High Strength Concrete", Procedia Engineering 14 (2011) 1149–1156
9. R. Sri Ravindrarajah, R. Lopez and H. Reslan, "Effect of Elevated Temperature on the Properties of High-Strength Concrete containing Cement Supplementary Materials, 9th International Conference on Durability of Building Materials and Components, Brisbane, Australia, 17-20th March, 2002.
10. Sanita Rubene, Martins Vilnitis, Impact of low temperatures on compressive strength of concrete, International Journal of Theoretical and Applied Mechanics, Volume 2, 2017.
11. S. O. Osuji, And U. Ukeme, "Effects Of Elevated Temperature On Compressive Strength Of Concrete: A Case Study Of Grade 40 Concrete", Nigerian Journal of Technology (NIJOTECH), Vol. 34 No. 3, July 2015, pp. 472 – 477.
12. Quang X Le , Vinh TNDao, Jose LTorero, Cristian Maluk and Luke Bisby, Effects of temperature and temperature gradient on concrete performance at elevated temperatures, Advances in Structural Engineering 2018, Vol. 21(8) 1223–1233

PRATIBHA: INTERNATIONAL JOURNAL OF SCIENCE, SPIRITUALITY, BUSINESS AND TECHNOLOGY (IJSSBT)
Special Issue: International Conference on Global Trends in Science, Technology, Humanities, Commerce & Management 2022 (ICGTSTHCM 2022)
Vol. 8, No. 2, January 2022,ISSN (Print) 2277-7261

Impact of Inflation Rise on Family Expenses and Financial Management: A Study

Dr. Saroj. B. Patil
Asst. Prof. Dept. of Business Administration.
SSBT's College of Enggineering and Technology. Jalgaon.

Abstract:
Rise in inflation influences different category of people differently. From common man's point of view inflation means increase in price of goods and services on day to day bases. People with fixed income employed in either public or private sector organizations or Self-employed, working in unorganized sector are considered as victims of rising inflation, as inflation influences the consumption, expenses and investment practices of the families. This study aims to assess the relationship between inflation and individual family expenses. The findings of this study complement the economic theories and evidences that inflation also increases the cost of living, price of commodities and reduces the opportunities of getting goods jobs. This situation directly influences family income and their expenses.

Keywords: Family Income, Expenses, Rise and Inflation.

What is Inflation?

Inflation is the rate of increase in prices over a given period of time. Inflation is typically a broad measure, such as the overall increase in prices or the increase in the cost of living in a country. But it can also be more narrowly calculated—for example, for certain goods, such as food, or for services, such as school tuition. Whatever the context, inflation represents how much more expensive the relevant set of goods and/or services has become over a certain period, most commonly a year. Inflation that is too high will decrease the level of social welfare. Conversely, too low inflation reflects the economy which does not run maximally which impact on slowing economic growth, stagnant job creation, and increased poverty community. India's retail inflation rate, which is measured by the Consumer Price Index (CPI), rose to 4.48 percent in the month of October 2021, data released by the Ministry of Statistics and Programme Implementation (MoSPI) revealed on November 2021. There was a marginal increase in retail inflation in October due to an uptick in food prices, The CPI-based inflation in September 2021 was at 4.35 percent and in October 2020 it was 7.61 percent. For the fourth month in a row, CPI has been below the Reserve Bank of India's six percent margin. The Government of India had told RBI to maintain a retail inflation rate at four percent with an upper and lower margin of two percent on either side for five years.Notably, the central bank factors in CPI data while preparing its bi-monthly fiscal policy. In September, the Monetary Policy Committee (MPC) of the RBI had decided to keep the repo rate unchanged at four percent for the eighth time in a row. According to the data released by the National Statistical Office (NSO), inflation in the food basket rose to 0.85 percent in October, compared to 0.68 percent in the preceding month. The RBI had projected CPI inflation at 5.3 percent for 2021-22 -- 5.1 percent in the second quarter, 4.5 percent in third, 5.8 percent in the last quarter of the fiscal, with risks broadly balanced. The retail inflation during the April-June period of 2022-23 is projected at 5.2 percent.

India's retail price inflation rate eased to 4.35 percent in September of 2021 from 5.3 percent in August and below market forecasts of 4.5 percent. It is the lowest reading in five months, remaining within the RBI's 2-6 percent target range for the third month in a row, amid a favourable comparison with last year when prices surged 10.68 percent. Inflation slowed for food (0.68 percent vs 3.11 percent, the lowest since March of 2019), mainly due to falls in cost of vegetables (-22.47 percent). Lower increases were also seen for miscellaneous (6.38 percent vs 6.4 percent), including transport and communication (9.53 percent vs 10.24 percent); and housing (3.58 percent vs 3.9 percent). Meanwhile, inflation picked up for fuel and light (13.63 percent vs 12.95 percent) and clothing and footwear (7.16 percent vs 6.84 percent).

PRATIBHA: INTERNATIONAL JOURNAL OF SCIENCE, SPIRITUALITY, BUSINESS AND TECHNOLOGY (IJSSBT)
Special Issue: International Conference on Global Trends in Science, Technology, Humanities, Commerce & Management 2022 (ICGTSTHCM 2022)
Vol. 8, No. 2, January 2022,ISSN (Print) 2277-7261

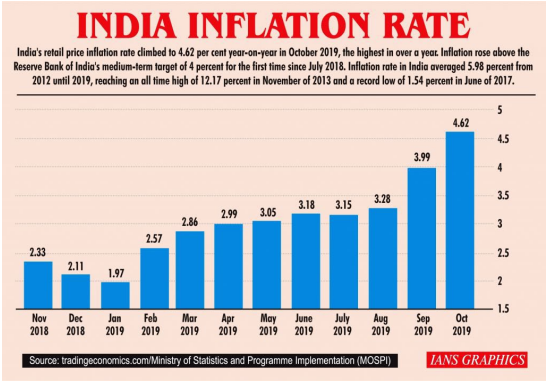

1. Evaluation of Inflation

Consumers' cost of living depends on the prices of the necessary goods and services they consume and the share of each good or service in the family budget. To evaluate the average consumer's cost of living, government agencies conduct family surveys to identify a basket of commonly purchased items and then track the cost of purchasing this basket over time. The cost of this basket at a given time expressed relative to a base year is the *consumer price index* (CPI), and the percentage change in the CPI over a certain period is *consumer price inflation*, the most widely used measure of inflation. There are other important measures of price stability.

Core consumer inflation—which excludes prices set by the government and the more volatile prices of products, such as food and energy, that are most affected by seasonal factors or temporary supply conditions—focuses on the persistent trends in inflation and is also watched closely by policymakers. The overall inflation rate for not just for consumption goods but all goods produced in an economy can be calculated by using the Gross Domestic Product (*GDP).*

Objective of the Study

1. To observe various tools which are used to measure inflation.
2. To study inflation in family expenses.
3. To classify inflation on different basis.
4. To study the relationship between inflation and individuals through the survey

Spotlight on Research Issue

Rise in inflation influences different category of various people . Management of inflation by individuals and their family is generally depends on their financial ability to face the rise in product price, income level of individuals and their ability of consumption, spending and buying power. To manage the impact of inflation various problem of families apply different techniques and that rate of inflation varies from one Indian regional state to other based on the local Government policies. For example inflation rate is high in Maharashtra (13.20 per cent), Uttar Pradesh (12.4 per cent), Tamil Nadu (7.3 per cent), Jammu and Kashmir (0.94 per cent), Puducherry (0.17 per cent) and Sikkim (0.05 per cent).

Category of Inflation

Inflation always creates negative effects not only on the economic growth and performances, but it also influences the living standards of individuals as its reduced the values of money, reduces the purchasing power of money, creates unemployment in the economy, shortage in secured job opportunities, leads to shortage of manufactured goods, increase price of the commodities and many more. Reduction in common man's spending and buying powers directly influences their consumption activities, which in turn influences business of all class of people i.e. from manufactures, wholesaler, business man retailers and the various service providers.

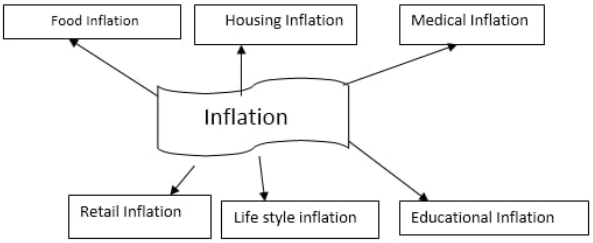

Purpose and Aim of Survey

The questionnaire was distributed among the various individual person and the anwers were collected and data was interpreted. Graphs were designed indicating the distributing the budget on various family expenses. Questions regarding the family income, expenses was asked . The justification of each question is as follows

a. Family income source was asked as it is important factor to find out the rise in inflation.
b. It also prove that the rise in the rate of petrol/diesel affects the transportation cost.
c. The survey found that the proportion of the income a family spends on house ration and other questions stated about a big extend a family will divide their budget and increase their other source of income also.
d. In future if there will be continuous rise in the price of petrol/diesel then many of

families will be shifting towards the public transport, this will lose their comfort and luxury.

e. Expenses on entertainment were surveyed and as 10% income of family were spend on entertainment like eating out, family trip, cinema, others enjoyment and fun affects a lot.
f. The final question was put on to know that whether family will reduce their expenditure if there is again rise inflation.

Needs:

1. Help us to understand how to management budget in better way
2. Need to understand the effects of supply and demand of different things as a result of increasing and decreasing in prices of certain commodities
3. Need to study about inflation in different sectors affects individuals

Methodology

Inflation is the raise of rate for goods and services which low down the purchasing capacity of people. Inflation is classified on different basis and the different types were discussed on other to gain detail knowledge of various type of inflation.

Data from different research paper were collected and used to study basic trends of inflation in various sectors of economy, the research paper were collected through various web pages.

Various methods are used to measure inflation were discussed such as WPI (Wholesale Price Index) and CPI (Consumer Price Index), rate index were also searched out.

Data regarding inflation in various division of economy was collected which include oil industry, food industry and different market places was observed. Data regarding the high price raise in petrol and diesel was obtained from local petrol station helps to understand the inflation in oil prices over a past years.

The study is of descriptive research methodology to reveal its fact and information collected through filed survey. Jalgaon district was selected as the area of the study. Families residing in district were considered as sample.

The research work adopted convenience sampling technique for the data collection with the support of well-structured close ended questioner. Survey was conducted among 100 families living in Jalgaon district and required data were collected by google forms sampling technique.

A short and detailed survey to study the effects of rising oil and food prices on the common man was obtained the survey conducted helped to find out how inflation affects the family expenses budget. The survey had several questions in which there will be suggestions box to express their views on rising of inflation at individual level.

Discussion

To assess the impact of inflation on families, a sample of 100 respondents approached, the sample populations were equally distributed men and women population living in Jalgaon city. The study observed that 23% of the sample subjects were aged between 31- 40 years, 50% of the population were married, 27% of the sample were found to be well educated i.e., graduates and employed in private sector organization . It has been observed that families participated in the survey were nuclear in their formation. The maximum families do not have any additional sources of income, i.e., they have to manage with the limited income Rs.10,000 or less (35%), Rs.10,001-Rs.20,000 (30%) and Rs.20,001-Rs.30,000 (25%).

All the families are found to be middle income family as per the NCAER (National Council for Applied Economic Research) i.e., those families income fall with Rs. 2,00,000 (Two lakhs) to Rs.10,00, 000 (Ten Lakhs) are categorised as middle income families. Out of 100 respondents surveyed, 65% of families strongly agree that rise of inflation rates results in increase of all commodity prices and it severely affects the common man living.

As reaction inflation 35% of the families have realized the due to job cut-down in the industries and various service sectors. Subsequently the respondents have realized that there is rise in inflation resulting increase in fuel cost, increase in all commodities prices (food & nonfood expenses) and they also faces problems in salary increments. Further, it has been observed that the respondents are affected by reduction in savings and they also face various problems like: increase in house rent, rise in cost of petrol , diesel , cooking fuel ,clothing, medical drugs, education and traveling expenses etc., due to inflation. In this study, the value of KMO for overall matrix was found to be excellent (0.86) and Bartlett's test of Sphericity was highly significant ($p<0.05$). Bartlett's Sphericity test was effective, as the chi-square value draws significance at five per cent level. The results thus indicated that the sample taken was appropriate to proceed with a factor analysis procedure. Factor Analysis was used to find out the family level of perception towards the rise of inflation rates.

Findings and conclusion

The findings of this study complement the economic theories and evidences that inflation also increases the cost of living, price of commodities and reduces the opportunities of getting goods jobs. Increase in education inflation. Rise is service cost This situation directly influence family income and their spending capacities.

As per the RBI (Reserve Bank of India) Report made on 1st August, 2018 inflation rates of both foods and fuel have significantly increased in the recent past. The Government of India is taking number of steps to curtail the rise in inflation like announcing MSP (Minimum Support Price) provided to the agriculturist of various food crops, revamping public welfare and financial supports offered to the public, increase in taxation policy of the Government, motivating industries to produce more, cutting down import bills of crude oil and gold and also by increasing the salary limits of public sector employees.

References

1. Aarati Krishnan (2017), Why You Don't Feel The Record-Low Inflation, The Hindu, 18thJune.
2. source: Ministry of Statistics and Programme Implementation (MOSPI)
3. http://www.rediff.com/business/report/infla-6-types-of-inflationthat-affect-our-daily-finances/20150601.html. Indian Inflation Rate (2012-18),
4. https://tradingeconomics.com/india/inflation-cpi
5. Ranjay Vardhan (2014), An Analysis of Impact of Inflation on Female Headed Households, EPRA International Journal of Economic and Business Review, Volume.No.2, Issue.No.5, ISSN: 2347 – 9671, PP: 1-5, May.
6. RBI pegs retail inflation at 4.8% for second half of FY19, Times of India, 1st August, 2018.

PRATIBHA: INTERNATIONAL JOURNAL OF SCIENCE, SPIRITUALITY, BUSINESS AND TECHNOLOGY (IJSSBT)
Special Issue: International Conference on Global Trends in Science, Technology, Humanities, Commerce & Management 2022 (ICGTSTHCM 2022)
Vol. 8, No. 2, January 2022,ISSN (Print) 2277-7261

Investigation of Zonal Thickness Variation on Thermal Storage of Salt Gradient Solar Pond

D.B. Sadaphale[1, a*], Dr. S. P. Shekhawat[2, b] and Dr. V.R. Diware[3, c]
[1, 2, 3] SSBT's College of Engineering and Technology, Bambhori, Post box no 94, Jalgaon 425 001, Maharashtra, India
[a*]devendra_sadaphale@rediffmail.com, [b] spshekhawat@rediffmail.com, [c]vrdiware65@rediffmail.com

Abstract: The use of solar energy has increased substantially as a resut of greenhouse gas emissions from the combustion of conventional fossile fules used for the various applications. Solar energy is likely to be the alternative energy source of the future and solar ponds, in particular, salinity gradient solar ponds (SGSP), facilitate simple and cost-effective thermal energy collection and storage. In the present sutudy; the influence of varying the thicknesses of the zones present in a salinity gradient solar pond on the temperatures of the upper convective zone (UCZ) and the lower convective zone (LCZ) is investigated. After critical investigation it is found that thickness variation of the zones within the pond has a countable effect on the temperature of the LCZ while it has a little bit considerable effect on the temperature of the UCZ. The optimal thicknesses of the UCZ and the nonconvective zone (NCZ) have been found to be 0.2 and 0.8 m respectively. The literature show that the type of application plays a substantial role in determining the depth of the LCZ, and that temperature of this zone varies with the rate of heat extraction. It is found out that for low-grade heat application the SGSP could be deeper with less surface area.From the present study foundation is laid for future investigation regarding the performance and financial viability of the overall depth of SGSPs

Keywords: Upper Convective Zone, Non-Convective Zone, Lower convective zone.

I. INTRODUCTION

Great efforts and Interest have been taken in reducing harmful pollution levels to create a safe and clean environment by explouring sustainable energy sources.Among all the sustainable energy sources solar energy is the ideal and clean energy source; in particular the solar pond, which absorbs and stores solar thermal energy. The most commonly used form of solar pond is the salinity gradient solar pond (SGSP), a large body of water with a depth of 2–5 m that includes a salinity gradient for absorbing and storing incident solar radiation [1–8].SGSP is a body of saline water having large lateral dimensions and three vertical zones as shown in Fig. 1. Pond's operational life-span has two phases, namely the maturation phase; and the matured phase [27]. When a pond is constructed and a gradient zone is established, its liquid content is at the ambient temperature. After absorbing solar radiation, it warms up. Initially, for a few months, the STZ temperature rises steeply. A typical SGSP consists of three zones: the upper convective zone (UCZ), the non-convective zone (NCZ) and the heat storage zone or the lower convective zone (LCZ). As the LCZ has the highest temperature and salt concentration (density), it is where solar thermal energy is stored. In the NCZ, salinity increases with the depth minimising convection in this zone and the temperature will increase uniformly by absorption of the solar radiation [9–15].

Jaefarzadeh investigated and found out that viability of solar pond is decided by considering thermal capacity, maintenance,operating and construction costs of a solar pond [26]. In most of the studies it is found that heat storage capacity can be altered by varying the thickness of the storage zone (LCZ)[16–22]. Thickness of the various zones of the SGSP has a considerable effect on its performance and stability. This issue has been discussed by several researchers in the past [23–25]. However, further investigation on the relationship between zone thickness variation and heat extraction is needed to understand the influence of zone thickness on temperatures of the LCZ. In many of the applications, rather than increasing the surface area of the pond, the depth of the LCZ could be increased, and the same performance could be achieved. This method of pond construction will reduce the surface

area and, consequently, could decrease the capital cost of the pond. However, further research is required to estimate the cost of the pond when it is deeper with less surface area.

In the present study, the influence of the thickness variation of all three zones on the performance of the SGSP in terms of the temperature achieved in the LCZ is assessed. In the study, insulated SGSP of a surface area of 1.40 m^2 and a depth of 1.14 m was built by creating different zones in it. The performance of the pond was observed for the period January 2020 to December 2020. The innovative design of the SGSP was used for the experimentation. The maximum temperature of 47^0C was recorded in the storage zone with maintaining the good stability of the interfacing zones.

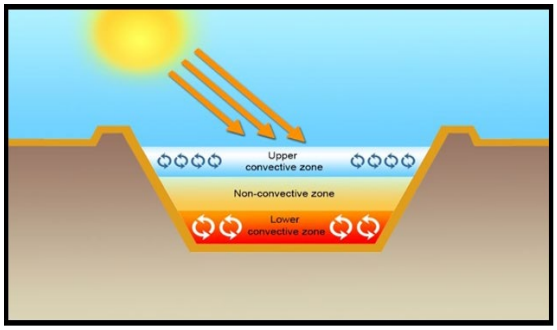

Fig. 1: Layers of Salinity Gradient Solar Pond

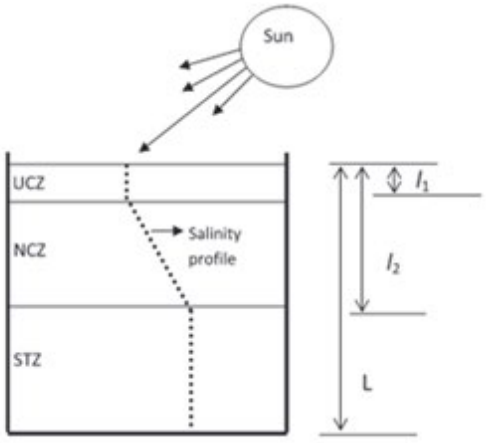

Fig. 2 : Schematic Diagram of a Salt Gradient Solar Pond Showing the Three Zone and Salinity Profile.

II. DESCRIPTION OF THE SOLAR POND

Cylindrical small-scale salt gradient solar pond was built at SSBT's College of Engineering & Technology, Bambhori, Jalgaon (Maharashtra) (21.05 N, 75.57 E, at 250 m from mean sea level) the schematic of the experimental setup is shown in Fig. 3. The pond is made of PVC material with 1mm thickness, 1.14 m height, and 1.34 m in diameter. The pond has a circular cross sectional area of 1.40 m^2 and the heights of LCZ, NCZ, and UCZ layers, respectively, 0.2 m, 0.6 m, and 0.26 m were used. refer fig 2. The NCZ layers were divided into three similar heights. The sides of the pond were initially insulated with a thickness of 1.5 cm. The internal surfaces of the ponds were painted black, which provides enough protection against corrosion and better absorption of solar radiation. Six Thermocouples (type Pt100A) $\pm(0.15^0C+0.2\%)$ were used to measure the temperature profile within the pond.[28]

Pond is equipped with a sampling tube with tap to withdraw samples from each layer to examine the salt concentrations. Each tube was located at the middle of the UCZ and LCZ layers and each NCZ sub-layer. Fresh water was introduced manually to the surface in order to compensate for the losses caused by surface evaporation. Salt chargers were employed to replace the salts or to maintain salinity of the respective zone constant in the ponds to keep the LCZ's water saturated. The cylindrical chargers (tubes) with 0.025m diameter, made of polyethylene (PE), were fixed to the wall of the ponds. Temperature sensors are fixed at the middle of each zone to measure the temperature of the respective zone. The sensors are used for LCZ, LCZ1, LCZ2, LCZ3, and upper convective zone (UCZ) and connected to a temperature indicator display. Also, for adding the salt water in the respective zone, flexible PVC pipe of diameter 0.025m is fitted inside the tank circumferentially and punctured at equal length along the circumference in order to fill the respective zone without disturbing the other layers. A cross-sectional sketch of the ponds with three zones, salt chargers, and sensors is shown in Fig. 3.

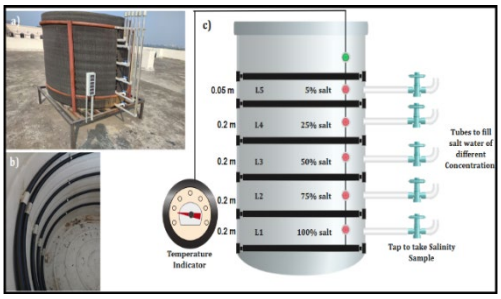

Fig. 3 : a.) Constructed Solar Pond with Salt Charger, b). Inside Tubing arrangement for Smooth Flow of Salt Solution in Respective Zone, c). Schematic Diagram Showing Different depths and Salt Concentration in each Zone.

III. RESULT AND DISCUSSION

Effect of zonal thicknesses

For this study SGSP constructed at SSBT's College of Engineering & Technology, Bambhori, Jalgaon (Maharashtra) (21.05 N, 75.57 E, at 250 m from mean sea level) Many assumptions have been made in this model; firstly, the pond is considered to comprise three zones; the UCZ, NCZ and the LCZ. Secondly, the UCZ and LCZ are well mixed, and the temperatures are uniform in these zones. Finally, the solar radiation that reaches the LCZ is entirely absorbed and stored in this zone, and there is no heat loss from the side walls of pond. [19]

i) Effect of the UCZ

Thicknesses of the NCZ and the LCZ are set to be 0.6and 0.2 m respectively while the depth of the UCZ is changed from 0.1 to 0.5 m with an interval of 0.1 m. Temperatures of the LCZ are plotted with time through out a year for these proposed thicknesses as illustrated in Fig.4

Month	1	2	3	4	5	6	7	8	9	10	11	12
Ta	23	24.2	25.3	27.8	32.8	37	39.3	38.2	36.4	29.8	20.4	19.8
0.1	23	22.8	24.7	25.6	30.8	25.3	33.4	32.2	27.6	18.8	17.5	
0.2	23	23.4	25.7	22.6	34.2	23.6	42.4	29.5		18.8	17.4	
0.3	23	22.9	25.6	26.2	33.1	23.3	32.4	24.8	28.7			
0.4	23	21.6	24.6	26.2	33.2	23.3	32.4	24.8	28.8	18.8	17.2	
0.5	23	21.4	24.6	27.1	33.2	23.3	32.4	24.8	28.4	18.8	17.1	

Table 1

The temperatures of the UCZ and the corresponding ambient temperatures in ^{0}C during a year with various thicknesses of the UCZ

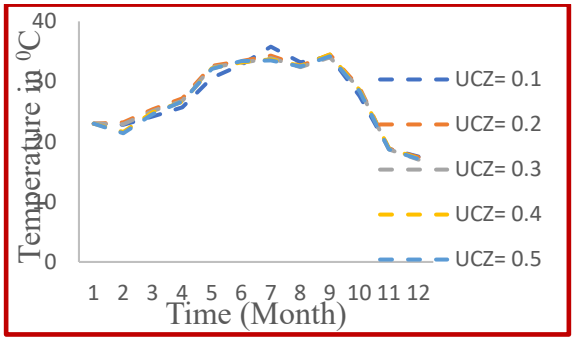

Fig.4 : The temperature profiles in the LCZ for various thicknesses of the UCZ

Fig.shows that there is decrement in LCZ temperature as the thicknessof the UCZ is increased. With 0.1 m thickness, the maximum temperature is approximately 36°C while it is 33.5^{0}C for a 0.5 m thickness. It is observed that with a further increase in the depth of the UCZ, there is a uniform decrease in the temperature of the LCZ. When the thickness is 0.2 m, the temperature in the LCZ is approximately 33°C. Additional thickness to the UCZ can decrease the probability of layers mixing

PRATIBHA: INTERNATIONAL JOURNAL OF SCIENCE, SPIRITUALITY, BUSINESS AND TECHNOLOGY (IJSSBT)
Special Issue: International Conference on Global Trends in Science, Technology, Humanities, Commerce & Management 2022 (ICGTSTHCM 2022)
Vol. 8, No. 2, January 2022,ISSN (Print) 2277-7261

due to the effect of wind, but this increase in thickness will reduce the temperature in the LCZ and is an additional cost as the evaporated fresh water would need to be replaced on a regular basis. On the other hand,the thickness can be increased in arid and windy areas to avoid disturbance of the NCZ and subsequently the LCZ which might reduce the efficiency of the pond. Jaeferzadeh emphasised that the thicknessof the UCZ should be kept as thin as possible [23]. He recommended a thickness of 0.2 m as this thickness not only should protect the NCZ below the UCZ, but also permits solar radiation to easily penetrate into the pond. Given the small effect (1.5^0C) of changing the thickness of the UCZ from 0.1 m to 0.2 m on the LCZ as well as advantages of having a deeper UCZ in terms of the stability of salinity gradient, it is concluded that 0.2 m is the optimum thickness for the UCZ.It is also observed that changing the thickness of the UCZ has an insignificant effect on its temperature. Table 1 shows temperaturesof the UCZ during a year for different thicknesses (0.1, 0.2, 0.3, 0.4 and 0.5 m) as well as the corresponding ambient temperatures.Table 1 illustrates that there is no significant change in the temperature of the UCZ with variation of its thickness throughout the year. It is also observed that the temperatures of the UCZ for all the different thicknesses are lower than the ambient temperatures during the entire 12 months of the year.

ii) Effect of the NCZ

Thickness of the NCZ is changed from 0.2 to 0.8m with an intervalof 0.1 m and simultaneously, thicknesses of the UCZ and LCZare considered to be 0.2 and 0.5 m respectively. Temperature profilesof the LCZ are plotted against time (month) as shown in Fig.5

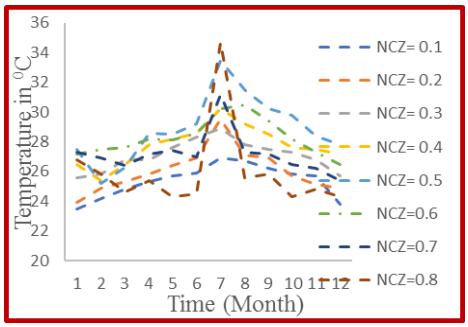

Fig.5: The temperature profiles of the LCZ for various thicknesses of the NCZ,

Fig. illustrates that with a small NCZ thickness (0.2 m), the temperature of the LCZ is, maximum temperature is around 27^0 C and minimum temperature is around 24^0 C. Changing the thickness of the NCZ from 0.1 to 0.2 m increases the temperature of the LCZ significantly. Maximum and minimum temperatures increase by approximately 3^0 C and1^0C respectively. Extending the thickness to 0.5 m adds approximately an extra 4^0 C to the maximum temperature and around 1^0 C to the minimum temperature . Further increase of the thickness to 0.8 m enhances the maximum temperature by approximately 2^0 C.. it can be observed that there is a drop in the temperatures of the LCZ during most months of the year . It is evident that any increase in the thickness of the NCZ past 0.8 m will likely be unprofitable, and it will reduce the efficiency of the pond. Therefore, the optimum thickness of the NCZ is 0.8 to 1 m. The financial implications of increasing the thickness of the NCZ from 0.8 m to 1 m must be evaluated in order to justify 1 m as the optimum. As mentioned, such increase only results in 1to 2^0 C rise in the temperature for 4–5 months of the year but leads to higher capital and operating expenditure.

These changes in temperature of the LCZ are due to the function of the NCZ as a transparent thermal insulator. Therefore, an increase in its thickness can improve the efficiency of the thermal insulation by reducing the upward heat loss from the LCZ. However, this increase in the thickness will influence the quantity of solar radiation that reaches the LCZ and will lead to a lowering of the temperature in this zone.

iii) Effect of the LCZ

In this part of the investigation, the influence of varying thethickness of the LCZ on its temperature and the UCZ temperatures is studied. Thickness of this zone (LCZ) is changed from 0.1 to 0.5 m with an interval of 0.1 m and meanwhile, the thicknesses of theUCZ and NCZ are kept at 0.2 and 0.8 m respectively. The results are illustrated in Fig.6

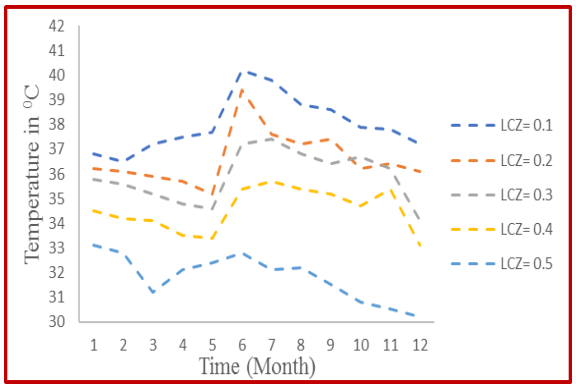

Fig.6: The temperature profiles of the LCZ for various thicknesses of the LCZ,

As shown in Fig.6 that there is a decrease in the temperature of the LCZ as it becomes deeper. The highest temperatures are obtained with 0.1 m thickness whereas the lowest temperatures are at a 0.5 m thickness. Considering the thickness of 0.1 m, its maximum temperature is about40^0 C , and the minimum temperature is around30^{0}C. This behaviour is due to the variation of volume in the LCZ. For a thickness of 0.1 m, the water volume of the LCZ is small and consequently heat accumulation in the LCZ is increased noticeably. With 0.5 m thickness the temperature in the LCZ rises slowly to reach a maximum of 33^{0}C and the minimum temperature of 30^{0}C. The previous explanation applies here again as the depth of 0.5 m results in the volume of the brine being 5 times higher than the volume with a 0.1 m thickness, and therefore the rise in the temperature will occur over a longer period of time. However, the heat capacity using a thickness of 0.5 m will be much higher which can be suitable for applications which require heat in relatively low temperatures of around 35^{0}C. Such applications will therefore benefit from increasing the depth of the LCZ rather than the surface area of the pond.

Particular industrial application coupled to a solar pond requires heat at its own particular temperature which is different to other applications. For example, power generation requires approximately 80^0 C for the turbine to operate with an organic fluid in the Rankine cycle. Hence, if the pond is implemented for power generation purposes, the depth of the LCZ cannot be higher than 2 m to provide the suitable temperature. Moreover,some domestic heating applications requires heat at about 40^o C and that means all thicknesses mentioned in the discussion can be used for this purpose. On the other hand, the capital cost and the availability of land to establish the pond are the major parameters to determine the optimum surface area and depth of the pond in terms of financial viability. Hence, the economic analysis that are required to be carried out to establish the financial viability of a solar pond will be specific to the location being considered since land prices and construction costs vary in different places. From the above discussion, it can be concluded that the depth of the LCZ must correspond to the type of application the SGSP is coupled with. However, the thickness of 0.5–0.8 m is suitable for most applications. The rationale behind this claim is that firstly, the period of warm up is around 4 months. Secondly, the maximum temperature reaches 45^o C and the minimum temperatures are 33^o C. Further increase in thickness does not enhance the minimum temperature and causes a decrease in the maximum temperature. On the other hand, a higher thickness means increasing the heat capacity of the pond, but that requires a considerable addition to the capital cost of the SGSP. In 2005, Jaefarzadeh claimed that the appropriate thickness of the LCZ depends on the design conditions and the required operating temperatures [23]. German and Muntasser pointed out that the thickness of the LCZ can be 4 m [30]. However, this value is obtained as it results in the lowest surface area.

Conclusions

In the present investigation, the optimum thickness of the three zones present in a SGSP has been examined. A model is constructed at SSBT College of Engineering, Jalgaon (M.S, India). The results show that the optimum thicknesses of the UCZ and NCZ are 0.2 and 0.8 m respectively. On the other hand, thickness of the LCZ depends mainly on the type of the application coupled with the SGSP, shape and geomerty of the pond.Thermal storage of the pond may vary with different considerations of the thickness of various zones , which required further investigation. Thickness variation of the UCZ and NCZ has a considerable impact on the LCZ temperature. Simultaneously, the thickness variation of the NCZ and the LCZ on the temperature of the

UCZ is minimal. For applications that require low-grade heat in a range of 40–50 C, there are possible cost-effective benefits to constructing a deeper pond by increasing the thickness of the LCZ rather than its surface area. However, construction costs and land prices must be assessed. Therefore, comprehensive economical studies carried out for the particular application of solar ponds are recommended to evaluate further the optimum thicknesses of the three zones in a SGSP introduced in this study.

Acknowledgements

Authors are thankful to Kavayitri Bahinabai Chaudhari North Maharashtra University, Jalgaon for providing financial support to carry out the research work under the Vice Chancellor Research Motivation Scheme.

References

[1] M. Khalilian, Assessment of the overall energy and exergy efficiencies of the salinity gradient solar pond with shading effect, Sol. Energy 158 (2017) 311– 320.

[2] J. Leblanc, A. Akbarzadeh, J. Andrews, Lu. Huanmin, P. Golding, Heat extraction methods from salinity–gradient solar ponds and introduction of a novel system of heat extraction for improved efficiency, Sol. Energy 85 (2011) 3103– 3142.

[3] A. Date, A. Akbarzadeh, Salinity gradient solar ponds, in: E. Napoleon, A. Akbarzadeh (Eds.), Energy Sciences and Engineering Applications, CRC Press, 2013, E. Book.

[4] F. Suarez, R. Urtubia, Tackling the water-energy nexus: an assessment of membrane distillation driven by salt-gradient solar ponds, Clean Technol. Environ. Policy 18 (2016) 1697–1712, https://doi.org/10.1007/s10098-016- 1210-3.

[5] Y. Yaakob, An Innovative Approach to Heat Extraction from a Salinity Gradient Solar Pond to Enhance Overall Efficiency (PhD's Thesis), RMIT University, 2013.

[6] A. Date, A. Akbarzadeh, Theoretical study of a new thermodynamic power cycle for thermal water pumping application and its prospects when coupled to a solar pond, Appl. Therm. Eng. 58 (2013) 511–521.

[7] C. Silva, D. Gonzalez, F. Suarez, An experimental and numerical study of evaporation reduction in a salt-gradient solar pond using floating discs, Sol. Energy 142 (2017) 204–214.

[8] M. Khalilian, Experimental investigation and theoretical modelling of heat transfer in circular solar ponds by lumped capacitance model, Appl. Therm. Eng. 121 (2017) 737–749.

[9] J. Srinivasan, Solar pond technology, Sadhana 18 (1) (1993 March) 39–55, Printed in India.

[10] V. Velmurugan, K. Srithar, Prospects and scopes of solar pond: a detailed review, Renew.
Sustain. Energy Rev. 12 (2008) 2253–2263.

[11] V.V.N. Kishore, V. Joshi, A practical collector efficiency equation for nonconvecting solar ponds, Sol. Energy 33 (5) (1984) 391–395.

[12] A. Abbassi Monjezi, A.N. Campbell, A comparative study of the performance of solar ponds under Middle Eastern and Mediterranean conditions with batch and continuous heat extraction, Appl. Therm. Eng. 120 (2017) 728–740.

[13] A.V. Spyridonos, A.A. Argiriou, J.K. Nickoletatos, Thermal storage efficiencies of two solar saltless water ponds, Sol. Energy 75 (2003) 207–216.

[14] A. Akbarzadeh, J. Andrews, P. Golding, Solar pond technologies: a review and future directions, in: Y. Goswami (Ed.), Advances in Solar Energy, Earthscan, London, UK, 2005, pp. 233–294.

[15] A. Abbassi Monjezi, A.N. Campbell, Regeneration of dimethyl ether as a draw solute in forward osmosis by utilising thermal energy from a solar pond, Desalination 415 (2017) 104–114.

[16] N. Bezir, D. Orhan, R. Kayali, Z. Nuri, Numerical and experimental analysis of a salt gradient solar pond performance with or without reflective covered surface, Appl. Energy 85 (2008) 1102–1112.

[17] C. Karim, Z. Slim, C. Kais, S.M. Jomaa, A. Akbarzadeh, Experimental study of the salt gradient solar pond stability, Sol. Energy 84 (2010) 24–31.

[18] F. Suarez, R. Jeffrey, A. Childress, S. Tyler, Understanding the expected performance of large-scale solar ponds from laboratory-scale observations and numerical modeling, Appl. Energy 117 (2014) 1–10.

[19] A. Alcaraz, C. Valderrama, J.L. Cortina, A. Akbarzadeh, A. Farran, Enhancing the efficiency of solar pond heat extraction by using both lateral and bottom heat exchangers, Sol. Energy 134 (2016) 82–94.

[20] S. Tundee, P. Terdtoon, S. Phrut, R. Singh, A. Akbarzadeh, Heat extraction from salinity-gradient solar ponds using heat pipe heat exchangers, Sol. Energy 84 (2010) 1706–1716.

[21] J. Andrews, A. Akbarzadeh, Enhancing the thermal efficiency of solar ponds by extracting heat from the gradient layer, Sol. Energy 78 (6) (2005) 704–716.

[22] M.R. Jaefarzadeh, A. Akbarzadeh, towards the design of low maintenance salinity gradient solar pond, Sol. Energy 73 (5) (2002) 375–384.

[23] M.R. Jaferzadeh, Thermal behaviour of a large salinity-gradient solar pond in the city of Mashhad, Iranian J. Sci. Technol. Trans. Eng. 29 (B2) (2005).

[24] Y.F. Wang, A. Akbarzadeh, A parametric study on solar ponds, Sol. Energy 30 (6) (1983) 555–562.

[25] S. Kanan, D. Jonathan, L. Gregory, A simple heat and mass transfer model for salt gradient solar ponds, Int. J. Mech. Ind. Sci. Eng. 8 (1) (2014) 27–33.
[26] M.R. Jaefarzadeh, Thermal behaviour of a small salinity-gradient solar pond with wall shading effect, Sol. Energy 77 (2004) 281–290.
[27] M. Husain, P.S. Patil, S. R. Patil and S.K. Samdarshi, Optimum size of non-convective zone for improved thermal performance of salt gradient solar pond, Solar Energy, 74(2003) 429-436
[28] Experimental Investigations on Salt Gradient Solar Pond with Additional Non-Convective Zone for Improved Thermal Performance and Stability D.B. Sadaphale .Dr. Sanjay Shekhawat, Dr. Vijay Diware Advanced Engineering Forum Volume 43 ,pp 59-71
[29] Behaviour of a salinity gradient solar pond during two years and the impact of zonal thickness variation on its performance, Asaad H. Sayer, Alireza Abbassi Monjezi, Alasdair N. Campbel Applied Thermal Engineering 130 (2018) 1191-1198
[30] M.A. Garman, M.A. Muntasser, Sizing and thermal study of salinity gradient solar ponds connecting with MED desalination unit, Desalination 222 (2008) 689–695

PRATIBHA: INTERNATIONAL JOURNAL OF SCIENCE, SPIRITUALITY, BUSINESS AND TECHNOLOGY (IJSSBT)
Special Issue: International Conference on Global Trends in Science, Technology, Humanities, Commerce & Management 2022 (ICGTSTHCM 2022)
Vol. 8, No. 2, January 2022,ISSN (Print) 2277-7261

Parametric optimization using Central Composite Design (CCD) of Synthesis of Lactic acid using tamarind de-oiled cake by Solid State Fermentation (SSF)

Miss. Payal N. Bhautik[*a], Dr. Rajendra P. Ugwekar[a], Mr. Kuldeep Singh[b]

[a]Chemical Engineering, Laxminarayan Institute of Technology, [b]Smt. Sugrata Wanjari Mahila Mahavidyalaya Wadoda, RTM University of Nagpur,

email: payalbhangh@gmail.com[*],ugwaker@gmail.com, kuldeepsingh25790@gmail.com

Abstract:

Medicines, food, and textiles all employ Solid State Fermentation (SSF). It is defined as microbial growth without a freely moving aqueous phase. The SSF microbiological method's adaptability has sparked fresh interest. As a result, SSF is a feasible method for the manufacture of microbial products such as feed. Its usage in bioprocesses including bioleaching, bio beneficiation, bioremediation, and bio pulping has several advantages. India is the world's largest producer and exporter of raw and processed spices. The food processing business is predicted to grow in India in the next years due to population growth, changing dietary trends, and rising middle- and higher-class purchasing power. Tamarind trees are commonly found in gardens, roadside plantings, and commercial plantations. India is the world's largest exporter of seed, de-oiled cake, and fruit pulp. De-oiled tamarind seed cake was used for the synthesis of lactic acid because of its content of polysaccharides, protein, fat, and minerals abound in tamarind seed cake. Tamarind seed de-oiled cake is polysaccharide-rich. The synthesis of lactic acid was studied using tamarins de-oiled by SSF and Rhizopus oryzae fungi. The influence of independent variables on the sorption process was studied using CCD. With SSF at 0.65 particle size, 35°C and pH 6.25, the maximal production of lactic acid is obtained. The culture's heterogeneity causes severe challenges with mixing, heat exchange, oxygen transfer, moisture management, pH, nutrient, and product gradients.

Keywords: Lactic acid, Solid State Fermentation (SSF), Central Composite Design (CCD), Response Surface Methodology (RSM)

Introduction:

Solid State Fermentation (SSF) is a fermentation technique used in a variety of industries, including medicines, food, and textiles, to create microbial metabolites utilising a solid substrate rather than a liquid media. It is characterised as microbial proliferation in the absence of a freely flowing aqueous phase [1]–[4]. SSF is a viable alternative to submerged fermentation for the generation of value-added products such as antibiotics, single cell protein, polyunsaturated fatty acids, enzymes, organic acids, biopesticides, biofuel, and fragrance. Grain brans, de-oiled oil seed cakes, and other similar substances are used as a support. Initially, such fermentations were dominated by fungi (as these microorganisms were considered to be very optimally active in very low water activity). Later on, numerous bacterial and yeast species were utilised to carry out such fermentations. SSF's microbiological method has garnered considerable interest in recent years because to its versatility, which has been backed up by other writers who have suggested numerous advantages over their liquid counterparts (submerged fermentation). Numerous biotechnological processes require organisms to grow on solid substrates in the absence or near lack of free water. Solid state fermentation (SSF) utilises solid and low-moisture substrates [5]–[7]. Cereal grains (rice, wheat, barley, and corn), legume seeds, wheat bran, lignocellulose materials such as straws, sawdust, or wood shavings, and a variety of plant and animal materials are the most frequently utilised solid substrates [8]. Although the majority of these compounds are polymeric polymers that are insoluble or only slightly soluble in water, the majority are inexpensive and readily available and

provide a concentrated source of nutrients for microbial growth [9].

A solid porous substrate that may or may not be biodegradable, but has a high surface area per unit volume, in the range of 103 to 106 m^2/cm^3, allowing for rapid microbial growth at the solid/gas interface [10]. Under relatively low pressure, an air mixture of oxygen and other gases and particles should flow and mix the fermenting mash. The solid/gas interface should provide an ideal environment for the rapid growth of certain moulds, yeasts, or bacteria, either pure or mixed cultures [11]–[14]. The solid matrix's mechanical qualities should be able to withstand compression or mild stirring, as required by a particular fermentation method [15]. This necessitates the use of tiny granular or fibrous particles that are resistant to breaking or adhering to one another. The solid matrix should be free of microbial inhibitors and capable of absorbing or containing accessible microbial nutrients such as carbohydrates (cellulose, starch, sugars), nitrogen sources (ammonia, urea, peptides), and mineral salts [16].

SSF has emerged as a viable technology for the production of microbial products such as feed, fuel, food, industrial chemicals, and pharmaceuticals. It is commonly used to manufacture a variety of enzymes, organic acids, and flavouring compounds, all of which must be extracted and purified before being employed in various goods [17]–[19]. Its use in bioprocesses such as bioleaching, bio beneficiation, bioremediation, and bio pulping, among others, provides a number of benefits [20]. The primary advantage of these technologies is that they generate a negligible amount of waste and liquid effluent, making them relatively benign to the environment. Solid substrate fermentation is a method of fermentation that utilises simple natural solids as the media [21], [22]. Low-tech systems consume less energy and require less capital investment. Sterilization is not required, microbiological contamination is reduced, and downstream processing is simplified. Utilizing agro-industrial residues as substrates in SSF processes adds value to these otherwise under- or non-utilized residues [23]. The items have a reasonable yield. The design of the bioreactor, the aeration process, and effluent treatment are all relatively straightforward [24]–[26]. Numerous household, industrial, and agricultural wastes can be beneficially utilised in SSF. SSF has some limits, for example, it can only be utilized with bacteria that survive low moisture content. SSF cannot be monitored precisely (e.g., O2 and CO2 levels, moisture content). Because the organisms develop slowly, product generation is constrained. Heat generation poses complications, and it is exceedingly difficult to control the development environment [27]–[32].

Tamarind trees are frequently cultivated in gardens and along roadsides, as well as in commercial plantations. India is the world's largest exporter, annually shipping hundreds of tonnes of seed, de-oiled cake, and fruit pulp. Concentrated tamarind pulp is a common ingredient in Indian and Middle Eastern cuisine. It was given the common name Aasam, which translates as 'acid,' due to their usage as acid tastes in the culinary industry. Tamarind is a key component in South Indian cuisine and a variety of processed foods around the world. Tamarind may also be used as a foundation for either raw or cooked chutneys, with its fruity acidity complementing sugar, chilli, and other flavours. Its controlled processing, backed up by cold storage, is shown to be optimal for guaranteeing price stability and rural employment. India is the world's greatest producer and exporter of a variety of spices, both raw and processed. Processed spice demand is closely related to its use in the food processing sector, which is expected to expand in India in the next years due to population expansion, rapidly changing dietary habits, and an increase in the buying power of India's middle and upper classes. Why would you trash a de-oiled tamarind seed cake: The waste's composition Tamarind seed de-oiled cake is packed with carbs, protein, oil, and minerals. The blight Tamarind seed de-oiled cake contains around 70 percent polysaccharides [33]–[40].

Material and methods

Chemicals: All the chemicals should be analytical grade used for the initial growth of microorganism are Sodium di-hydrogen phosphate di- hydrate, phosphoric acid, yeast extract, peptone, agar, D-glucose, K_2HPO_2, sodium acetate, di-ammonium citrate, $MgSO_4.7H_2O$, $MnSO_4.H_2O$, other nutrients

were supplied by Chemical Store, Laximinarayan Institute of Technology, Nagpur, Maharashtra, India.

Substrate: Tamarind seed was collected from the Tumsar, Maharashtra region, India. Initially, oil was extracted from the tamarind seed using hexane as a solvent by Soxhlet apparatus. Before go for SSF tamarind seed was grinded in various size and sterilized in autoclave at 120℃.

Organisms Used in Solid State Fermentation (SSF): SSF microorganisms can be pure cultures, mixed identifiable cultures, or wholly indigenous microbes. Certain SSF processes need the growth of organisms such as molds that ferment using extracellular enzymes generated by fermenting bacteria and require little moisture. Bacteria and yeasts, on the other hand, which require a higher moisture content for successful fermentation, can be used for SSF, although production will be reduced. Collecting microorganisms from the National Center for Industrial Microorganisms (NCIM), a part of the National Chemical Laboratory (NCL), Pune. Table 1 lists the microorganisms that produce lactic acid, along with their NCIM numbers.

Table 1: List of Microorganism

Sr. No.	NCIM No.	Organism
1	1009	Rhizopus oryzae

Solid State Fermentation (SSF)

Typically, SSF is a multistep procedure that entails the following steps: Mechanical, chemical, or biological pre-treatment of substrate raw materials to increase the availability of bound nutrients and also to minimise the size of the components, e.g., crushing straw and shredding vegetable materials to improve the physical characteristics of the process. However, the expense of pre-treatment must be evaluated against the ultimate value of the product. Hydrolysis of polymeric substrates, such as polysaccharides and proteins. Utilization of hydrolysis products (fermentation). Purification and separation of final products. SSF has a lower moisture content than LSF, which allows for a smaller reactor volume per substrate mass and facilitates product recovery [39], [41]–[44].

Characterization of Lactic Acid

The lactic acid concentration in the fermentation broth was determined using high-performance liquid chromatography (HPLC) with a UV detector using, C-18 HS reverse phase ODS column (Youcglin S.K., HPLC Column, C-18 SUPELCO 240 mm x 4 mm, 0.4 m particle size) maintained at 40°C by a column heater. Waters 2489 (UV/VIS) Detector and 515 isocratic pumps were utilised. At a flow rate of 0.8 ml min-1, the mobile phase was NaH_2PO_4 + H_3PO_4 10mM buffer system (pH 2.5). HPLC samples were produced by centrifuging them at 5000 rpm for 10 minutes in a REMI benchtop centrifuge R-4C DX (Remi, India), and then filtering the supernatant over a 0.2-m polyether sulfone (PES) membrane. Lactic acid concentrations were evaluated by comparing the area of the sample to a standard curve prepared with L (+) lactic acid stalk solutions [45], [46].

Central composite Design

A central composite design is a type of experimental design used in response surface technique that allows for the construction of a second order (quadratic) model for the response variable without the requirement for a full three-level factorial experiment. Three unique sets of experimental runs comprise the design: A factorial (perhaps fractional) design with two levels for each element evaluated; A collection of centre points, experimental runs whose factor values are the medians of the values used in the factorial part. This point is frequently reproduced in order to increase the experiment's accuracy; A set of axial points, identical to the centre points but for one factor, that will exhibit values both below and above the median of the two factorial levels, and generally both outside their range. This manner, all variables are modified [47]–[50]. In the CCD, there are 2^n factorial runs, 2n axial runs, and n_c centre run. where n is the total number of independent variables (factors), n_c denotes the total number of centre points, and N denotes the total number of experimental runs. The centre points define the experimental error and the reproducibility of the data. The axial points are chosen in such a way that

they are controlling access, and the variance of model prediction is constant at each location equidistant from the design centre. CCD was used as an optimization technique in RSM to investigate the effect of independent factors on the sorption process [47], [51]–[53]. Three process-independent factors were evaluated while determining the optimal conditions: Effect of particle size (A), pH of the media (B), Temperature of SSF system (C) and their influences on lactic acid yield were investigated. Prior to beginning the final experiment, many preliminary tests were undertaken to determine the ideal value for each variable. The effects of factors on the outcomes were modified using the quadratic following equation.

$$Y = b_0 + \sum b_i X_i + \sum b_{ij} X_i X_j + \sum b_{ii} X_i^2 \quad i \geq j \;\; i,j = 1,2,3$$

where b_0 is the constant term's coefficient, b_i is the linear term's coefficient, b_{ij} is the coefficient of two-factor interaction, and b_{ii} is the quadratic term's coefficient, respectively.

Result and discussion

RSM model development for tricomponent systems: The empirical modelling of synthesis of lactic acid using tamarind de-oiled cake by SSF and Rhizopus oryzae microorganism was created by RSM employing CCRD-based experiment design.

Table 2:Design matrix and experimental data of the yields of Lactic acid

No. Run	Parameters			Yield of Lactic Acid
	Particle Size	Temp	pH	Experimental values
1	0.65	35	6.25	81.022
2	0.3	25	8.5	79.56
3	1	45	4	59.4689
4	1	25	4	57.481
5	1	45	8.5	50.00847
6	0.65	51.8	6.25	44.00745
7	0.65	35	6.25	82.56
8	1	25	8.5	68.867
9	0.3	45	8.5	69.107
10	1.238627	35	6.25	72.44
11	0.65	35	6.25	82.31
12	0.65	35	6.25	81.3025
13	0.65	35	2.465	43.26
14	0.061373	35	6.25	95.65
15	0.3	25	4	87.0415
16	0.65	35	10.0	37.40634
17	0.3	45	4	81.3025
18	0.65	35	6.25	85.306
19	0.65	35	6.25	89.64
20	0.65	18.18	6.25	51.61

Table 2 summarises the factorial design and associated outcomes for the factors, particle size (X_A), temperature (X_B), pH (X_C). One replication was performed at the central site for CCD study in order to determine the pure error between each experiment. Thus, regression analysis was employed in Table 2 to ascertain the generation of light Lactic. The following second-order models are obtained for the lactic acid yields associated with each parameter:

Regression Equation in Uncoded Units

$$\textit{Yield of Lactic acid} = -108.2 - 76.9X_A + 7.48X_B + 32.76X_C + 23.9X_A^2 - 0.0988X_B^2 - 2.473X_C^2 - 0.024X_AX_B + 3.34X_AX_C - 0.142X_BX_C \ldots\ldots (1)$$

The regression coefficients for lactic acid yield Eq. (1) are determined using an acceptable determination coefficient R-Sq. of 0.88 as seen in Fig. 1. Additionally, the R-Sq. value indicates that this regression model well represents the

dependency of lactic acid yield on particle size (X_A), temperature (X_B), pH (X_C). As a result, the created models have a suitable degree of precision for future optimization.

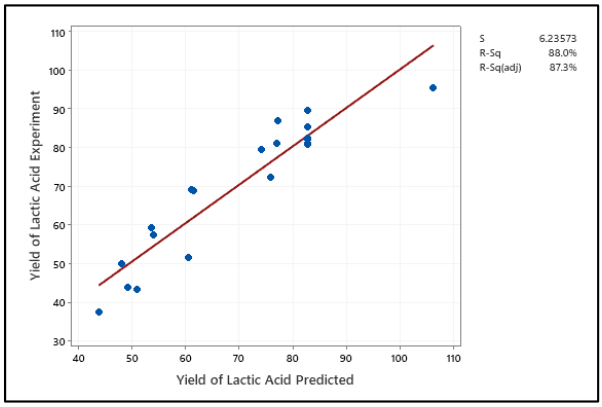

Figure 1: Yield of Lactic acid Experimental values vs Predicted values

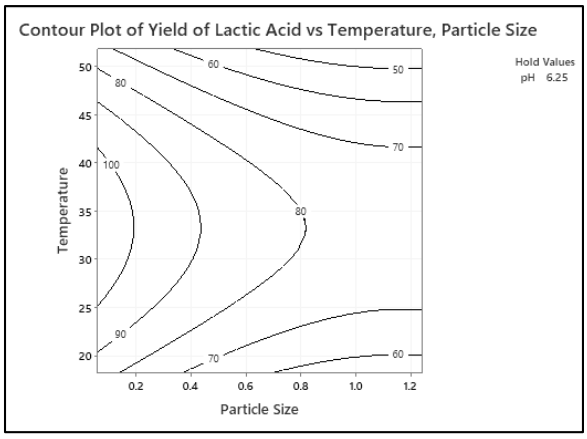

Figure 2:Contour Plots of Lactic acid vs Temperature, Particle size

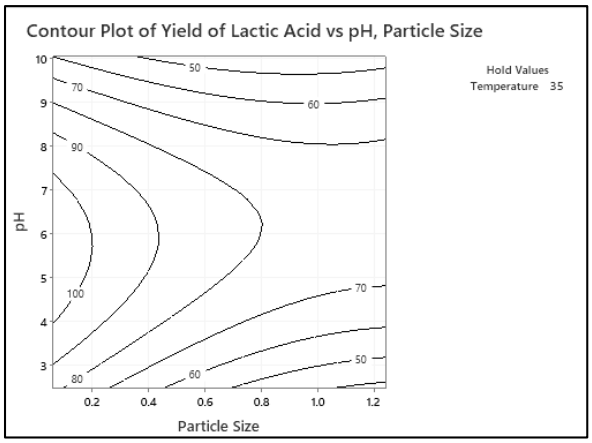

Figure 3:Contour Plots of Lactic acid vs pH, Particle size

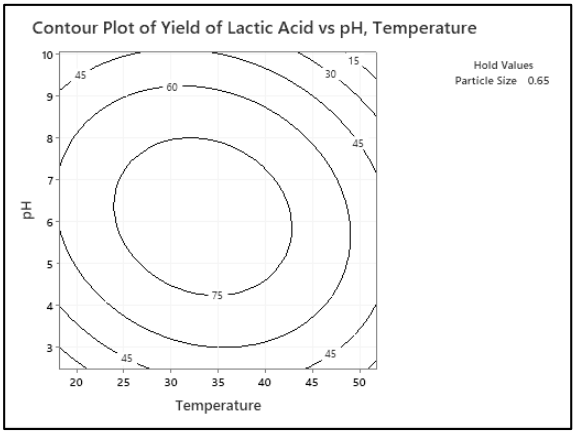

Figure 4:Contour Plots of Lactic acid vs pH, Temperature

Contour plot

Overlapping contour plots is a rather straightforward method for optimizing this effective response. Therefore, the effect of each particle size (X_A), temperature (X_B), pH (X_C) on the yields of lactic acid was discussed by contour plots. From figure 2. As increasing temperature and particle size of substrate the yield of lactic acid decreases at 6.25 pH value. According to the figure 3. As increasing particle size and pH the yield of lactic acid goes on increasing up to the 0.4 substrate particle size and 7.5 pH value. Greater values of particle size and pH value gives lower yield of lactic acid at 35℃. Similarly, from figure 4. At 0.65 particle size of substrate, as increasing temperature and pH value yield of lactic acid increases. At higher temperature and pH value more 40 ℃ and 7.5 respectively it leads to decreasing in the yield of lactic acid.

Conclusion:

Central composite coupled with the response surface methodology is used for successful modelling and optimizing of factors affecting on the yield of Lactic acid by SSF. The maximum yield of lactic acid using SSF at 0.65 particle size, 35 ℃ temperature and pH should be 6.25. However, major issues with mixing, heat exchange, oxygen transfer, moisture management, and pH, nutrient, and product

gradients develop as a result of the culture's heterogeneity. The latter property of SSF makes it difficult, tedious, and frequently incorrect to test and regulate the aforementioned parameters, hence restricting the industrial potential of this technology. As a result of these issues, the microorganisms used for SSF are more tolerant to a wide variety of growing conditions. Microorganisms with a low moisture need can be used. SSF cannot be carefully measured (e.g., oxygen and carbon dioxide levels, moisture content). Due to the sluggish development of the organisms, product generation is confined. Heat generation creates challenges, and controlling the development environment is incredibly tough.

References:

[1] R. R. Townsend, R. Yamamoto, M. Nickols, D. J. DiPette, and G. A. Nickols, "Insulin enhances pressor responses to norepinephrine in rat mesenteric vasculature," *Hypertension*, vol. 19, no. 2, pp. II-105-II–110, 1992, doi: 10.1161/01.hyp.19.2_suppl.ii105.

[2] R. Datta, S. Tsai, P. Bonsignore, S. Moon, and J. R. Frank, "Technological and economic potential of poly(lactic acid) and lactic acid derivatives," vol. 16, pp. 221–231, 1995.

[3] R. L. Evangelista and Z. L. Nikolov, "Recovery and purification of lactic acid from fermentation broth by adsorption," *Appl. Biochem. Biotechnol. - Part A Enzym. Eng. Biotechnol.*, vol. 57–58, pp. 471–480, 1996, doi: 10.1007/BF02941727.

[4] D. Garlotta, J. Z. Liu, L. P. Weng, Q. L. Zhang, H. Xu, and L. N. Ji, "A Literature Review of Poly (Lactic Acid) A Literature Review of Poly (Lactic Acid)," *Biochem. Eng. J.*, vol. 14, no. 2, pp. 63–84, 2001, doi: 10.1016/S1369-703X(02)00169-9.

[5] R. A. Sparringa, M. Kendall, A. Westby, and J. D. Owens, "Effects of temperature, pH, water activity and CO2 concentration on growth of Rhizopus oligosporus NRRL 2710," *J. Appl. Microbiol.*, vol. 92, no. 2, pp. 329–337, 2002, doi: 10.1046/j.1365-2672.2002.01534.x.

[6] J. H. Choi, S. H. Kim, and S. H. Moon, "Recovery of lactic acid from sodium lactate by ion substitution using ion-exchange membrane," *Sep. Purif. Technol.*, vol. 28, no. 1, pp. 69–79, 2002, doi: 10.1016/S1383-5866(02)00014-X.

[7] K. L. Wasewar, A. Bert M Heesink, G. F. Versteeg, and V. G. Pangarkar, "Equilibria and kinetics for reactive extraction of lactic acid using Alamine 336 in decanol," *J. Chem. Technol. Biotechnol.*, vol. 77, no. 9, pp. 1068–1075, 2002, doi: 10.1002/jctb.680.

[8] B. C. Saha and L. K. Nakamura, "Production of mannitol and lactic acid by fermentation with Lactobacillus intermedius NRRL B-3693," *Biotechnol. Bioeng.*, vol. 82, no. 7, pp. 864–871, 2003, doi: 10.1002/bit.10638.

[9] A. O. Büyükkileci and S. Harsa, "Batch production of L(+) lactic acid from whey by Lactobacillus casei (NRRL B-441)," *J. Chem. Technol. Biotechnol.*, vol. 79, no. 9, pp. 1036–1040, 2004, doi: 10.1002/jctb.1094.

[10] N. Narayanan, P. K. Roychoudhury, and A. Srivastava, "L (+) lactic acid fermentation and its product polymerization," *Electron. J. Biotechnol.*, vol. 7, no. 2, pp. 1–12, 2004, doi: 10.2225/vol7-issue2-fulltext-7.

[11] J. Ecker, T. Raab, and M. Harasek, "Nanofiltration as key technology for the separation of LA and AA," *J. Memb. Sci.*, vol. 389, pp. 389–398, 2012, doi: 10.1016/j.memsci.2011.11.004.

[12] L. Fermentations and O. C. Fermentations, "Use of Micro-organisms in Food Processing," pp. 1–20, 2012.

[13] R. Palaniraj and P. Nagarajan, "Kinetic studies in production of lactic acid from waste potato starch using Lactobacillus casei," *Int. J. ChemTech Res.*, vol. 4, no. 4, pp. 1601–1614, 2012.

[14] S. Bhattacharya, S. Bal, R. K. Mukherjee, and S. Bhattacharya, "Rheological behaviour of tamarind (Tamarindus indica) kernel powder (TKP) suspension," *J. Food Eng.*, vol. 13, no. 2, pp. 151–158, 1991, doi: 10.1016/0260-8774(91)90016-L.

[15] H. M. A. Shata, "Extraction of milk-clotting enzyme produced by solid state fermentation of Aspergillus oryzae," *Polish J. Microbiol.*, vol. 54, no. 3, pp. 241–247, 2005.

[16] M. Gündüz, "Lactic acid production by Lactobacillus casei NRRL B-441 immobilized in chitosan stabilized Ca-alginate beads," no. January, 2005, [Online]. Available: http://openaccess.iyte.edu.tr/handle/11147/3269.

[17] Y. J. Wee, J. N. Kim, and H. W. Ryu, "Biotechnological production of lactic acid and its recent applications," *Food Technol. Biotechnol.*, vol. 44, no. 2, pp. 163–172, 2006.

[18] J. Vijayakumar, R. Aravindan, and T. Viruthagiri, "Recent trends in the production, purification and application of lactic acid," *Chem. Biochem. Eng. Q.*, vol. 22, no. 2, pp. 245–264, 2008.

[19] M. I. González, S. Alvarez, F. A. Riera, and R. Álvarez, "Lactic acid recovery from whey ultrafiltrate fermentation broths and artificial solutions by nanofiltrationLactic acid recovery from whey ultrafiltrate fermentation broths and artificial solutions by nanofiltration," *Desalination*, vol. 228, no. 1–3, pp. 84–96, 2008, doi: 10.1016/j.desal.2007.08.009.

[20] S. Negi and R. Banerjee, "Optimization of extraction and purification of glucoamylase produced by Aspergillus awamori in solid-state fermentation," *Biotechnol. Bioprocess Eng.*, vol. 14, no. 1, pp. 60–66, 2009, doi: 10.1007/s12257-008-0107-3.

[21] W. Yao, J. Zhu, B. Sun, and C. Miller, "Development and optimization of a culture medium for L-lactic acid production by rhizopus oryzae using crude protein from dairy manure as a nitrogen source," *J. Environ. Sci. Heal. - Part A Toxic/Hazardous Subst. Environ. Eng.*, vol. 44, no. 12, pp. 1306–1313, 2009, doi: 10.1080/10934520903140157.

[22] M. T. Gao *et al.*, "Extractive lactic acid fermentation with tri-n-decylamine as the extractant," *Enzyme Microb. Technol.*, vol. 44, no. 5, pp. 350–354, 2009, doi: 10.1016/j.enzmictec.2008.12.001.

[23] J. H. Litchfield, "Lactic Acid, Microbially Produced," *Encycl. Microbiol.*, no. 79, pp. 362–372, 2009, doi: 10.1016/B978-012373944-5.00151-6.

[24] Z. Ali, F. M. Anjum, and T. Zahoor, "Production of lactic acid from corn cobs hydrolysate through fermentation by Lactobaccillus delbrukii," *African J. Biotechnol.*, vol. 8, no. 17, pp. 4175–4178, 2009, doi: 10.4314/ajb.v8i17.62349.

[25] O. V. Singh and S. P. Harvey, "Sustainable biotechnology: Sources of renewable energy," *Sustain. Biotechnol. Sources Renew. Energy*, no. December, pp. 1–323, 2010, doi: 10.1007/978-90-481-3295-9.

[26] B. Zhao *et al.*, "Kinetics of D-lactic acid production by sporolactobacillus sp. strain CASD using repeated batch fermentation," *Bioresour. Technol.*, vol. 101, no. 16, pp. 6499–6505, 2010, doi: 10.1016/j.biortech.2010.03.069.

[27] J. Sun, Y. Jiang, L. Zhou, and J. Gao, "Optimization and kinetic study of immobilized lipase-catalyzed synthesis of ethyl lactate," *Biocatal. Biotransformation*, vol. 28, no. 4, pp. 279–287, 2010, doi: 10.3109/10242422.2010.501893.

[28] X. Wu, S. Jiang, M. Liu, L. Pan, Z. Zheng, and S. Luo, "Production of L-lactic acid by Rhizopus oryzae using semicontinuous fermentation in bioreactor," *J. Ind. Microbiol. Biotechnol.*, vol. 38, no. 4, pp. 565–571, 2011, doi: 10.1007/s10295-010-0804-8.

[29] C. Gao, C. Ma, and P. Xu, "Biotechnological routes based on lactic acid production from biomass," *Biotechnol. Adv.*, vol. 29, no. 6, pp. 930–939, 2011, doi: 10.1016/j.biotechadv.2011.07.022.

[30] L. F. Coelho, C. J. B. De Lima, C. M. Rodovalho, M. P. Bernardo, and J. Contiero, "Lactic acid production by new lactobacillus plantarum LMISM6 grown in molasses: Optimization of medium composition," *Brazilian J. Chem. Eng.*, vol. 28, no. 1, pp. 27–36, 2011, doi: 10.1590/S0104-66322011000100004.

[31] L. Chen, "Conversion of glycerol to lactic acid under low corrosive conditions with homogeneous and heterogeneous catalysts," *Convers. glycerol to Lact. acid under low Corros. Cond. with Homog. Heterog. Catal.*, vol. 103 f., p. 103, 2011.

[32] A. Bouguettoucha, B. Balannec, and A. Amrane, "Unstructured models for lactic acid fermentation - a review," *Food Technol. Biotechnol.*, vol. 49, no. 1, pp. 3–12, 2011.

[33] P. Kelkar, Sunder; Mahanwar, "Production Of Lactic Acid From Tamarind Kernel," *Int. J. Technol. Enhanc. Emerg. Eng. Res.*, vol. 3, no. 05, pp. 25–31, 2015, [Online]. Available: http://www.ijteee.org/final-print/may2015/Production-Of-Lactic-Acid-From-Tamarind-Kernel-By-Lactobacillus-Casei.pdf.

[34] M. A. Abdel-Rahman and K. Sonomoto, "Opportunities to overcome the current limitations and challenges for efficient microbial production of optically pure lactic acid," *J. Biotechnol.*, vol. 236, pp. 176–192, 2016, doi: 10.1016/j.jbiotec.2016.08.008.

[35] C. Rodrigues, L. P. S. Vandenberghe, A. L. Woiciechowski, J. de Oliveira, L. A. J. Letti, and C. R. Soccol, "Production and Application of Lactic Acid," *Curr. Dev. Biotechnol. Bioeng. Prod. Isol. Purif. Ind. Prod.*, pp. 543–556, 2016, doi: 10.1016/B978-0-444-63662-1.00024-5.

[36] V. Juturu and J. C. Wu, "Microbial production of lactic acid: the latest development," *Crit. Rev. Biotechnol.*, vol. 36, no. 6, pp. 967–977, 2016, doi: 10.3109/07388551.2015.1066305.

[37] T. Jiang *et al.*, "Lactic acid production from pretreated hydrolysates of corn stover by a newly developed bacillus coagulans strain," *PLoS One*, vol. 11, no. 2, pp. 1–13, 2016, doi: 10.1371/journal.pone.0149101.

[38] D. R. P. Ugawekar, P. N. Bhautik, and K. Singh, "Green Plastics: Poly-lactic Acid Synthesis from Waste Tamarind Seed Powder and its Applications," *Int. J. Trend Sci. Res. Dev.*, vol. Volume-1, no. Issue-5, pp. 686–691, 2017, doi: 10.31142/ijtsrd2349.

[39] F. A. Castillo Martinez, E. M. Balciunas, J. M. Salgado, J. M. Domínguez González, A. Converti, and R. P. de S. Oliveira, "Lactic acid properties, applications and production: A review," *Trends Food Sci. Technol.*, vol. 30, no. 1, pp. 70–83, 2013, doi: 10.1016/j.tifs.2012.11.007.

[40] Payal and Bhautik, "Studies on Manufacturing Processes of Tamarind Oil, Biodegradable Plastic and Related Products From Tamarind-a Review," *Int. J. Recent Eng. Res. Dev.*, vol. 02, no. 01, pp. 75–80, 2017, [Online]. Available: www.ijrerd.com.

[41] P. Wang and F. Zhang, "Study on the Novel Strain Rhizopus Oryzae ATCC2809 ' s Growth and Fermentation," *Int. J. Sci. Eng. Res.*, vol. 1, no. 3, pp. 1–7, 2013, [Online]. Available: www.ijser.in.

[42] P. Dey and P. Pal, "Modelling and simulation of continuous L (+) lactic acid production from sugarcane juice in membrane integrated hybrid-reactor system," *Biochem. Eng. J.*, vol. 79, pp. 15–24, 2013, doi: 10.1016/j.bej.2013.06.014.

[43] M. A. Abdel-Rahman, Y. Tashiro, and K. Sonomoto, "Recent advances in lactic acid production by microbial fermentation processes," *Biotechnol. Adv.*, vol. 31, no. 6, pp. 877–902, 2013, doi: 10.1016/j.biotechadv.2013.04.002.

[44] P. T. Phan, "Kinetic Investigation In Lactic Acid Production By L. Acidophilus," *SSRN Electron. J.*, vol. 2011, pp. 1–25, 2013, doi: 10.2139/ssrn.2195809.

[45] T. Ghaffar *et al.*, "Recent trends in lactic acid biotechnology: A brief review on production to purification," *J. Radiat. Res. Appl. Sci.*, vol. 7, no. 2, pp. 222–229, 2014, doi: 10.1016/j.jrras.2014.03.002.

[46] M. A. Eiteman and S. Ramalingam, "Microbial production of lactic acid," *Biotechnol. Lett.*, vol. 37, no. 5, pp. 955–972, 2015, doi: 10.1007/s10529-015-1769-5.

[47] J. Bayuo, M. A. Abukari, and K. B. Pelig-Ba, "Optimization using central composite design (CCD) of response surface methodology (RSM) for biosorption of hexavalent chromium from aqueous media," *Appl. Water Sci.*, vol. 10, no. 6, pp. 1–12, 2020, doi: 10.1007/s13201-020-01213-3.

[48] T. A. Ntho, P. Gqogqa, and J. L. Aluha, "Oxidation of Glycerol to Lactic Acid by Gold on Acidified Alumina: A Kinetic and DFT Case Study," *Adv. Chem. Kinet.*, 2018, doi: 10.5772/intechopen.70485.

[49] B. Daengpradab and P. Rattanaphanee, "Conceptual design and scale up of lactic acid production from fermentation-derived magnesium lactate," *Chem. Eng. Trans.*, vol. 64, pp. 409–414, 2018, doi: 10.3303/CET1864069.

[50] R. Mudawaroch, S. Setiyono, L. Yusiati, and E. Suryanto, "Fermentation Kinetics of Isolate Lactic Acid Bacteria Probiotic BR 12 and BR 17 were Isolated from Broiler Chicken Meat," pp. 1–7, 2019, doi: 10.4108/eai.1-4-2019.2287183.

[51] E. Abedi and S. M. B. Hashemi, "Lactic acid production – producing microorganisms and substrates sources-state of art," *Heliyon*, vol. 6, no. 10, p. e04974, 2020, doi: 10.1016/j.heliyon.2020.e04974.

[52] M. Ziadi, S. M'Hir, A. Aydi, M. Hamdi, and A. Al Loman, "Bioreactor Scale-Up and Kinetic

Modeling of Lactic Acid and Biomass Production by Enterococcus faecalis SLT13 during Batch Culture on Hydrolyzed Cheese Whey," *J. Chem.*, vol. 2020, 2020, doi: 10.1155/2020/1236784.

[53] J. Wang *et al.*, "Parametric optimization and kinetic study of l-lactic acid production by homologous batch fermentation of Lactobacillus pentosus cells," *Biotechnol. Appl. Biochem.*, 2020, doi: 10.1002/bab.1994.

PRATIBHA: INTERNATIONAL JOURNAL OF SCIENCE, SPIRITUALITY, BUSINESS AND TECHNOLOGY (IJSSBT)
Special Issue: International Conference on Global Trends in Science, Technology, Humanities, Commerce & Management 2022 (ICGTSTHCM 2022)
Vol. 8, No. 2, January 2022,ISSN (Print) 2277-7261

Performance of Industrial Sewage Contaminated Black Cotton Soil

Akshaykumar R. Patil[1], Ganesh D.Ahire[2], Gauri A. Kale[3]
[1,2,3] Assistant Professor, Department of Civil Engineering, Shram Sadhana Bombay Trust's college of Engineering and Technology, Bambhori, Jalgaon, Maharashtra, India
[1]akshayc200patil@gmail.com , [2]gahire050@gmail.com , [3]kalegauriarvind2000@gmail.com

Abstract

Black cotton soil in industrial areas gets contaminated due to leakage of industrial sewage. This contamination of the soil adversely affects its geotechnical properties. This paper aims to study performance of contaminated soil for liquid limit plastic limit and shrinkage limit specific gravity. Test result shows decrease in specific gravity proctor density and shrinkage limit. On the other hand plastic limit, liquid limit and plasticity index were found to be increase

Keywords- Black cotton soil, Industrial sewage, specific gravity.

I Introduction

Soil infection or soil pollutants as a part of land degradation is resulting from the presence of xenobiotic (human-made) chemical substances or different alteration in the herbal soil surroundings. it's far generally due to commercial activity, agricultural chemical compounds, or incorrect disposal of waste. infection is correlated with the diploma of industrialization and intensity of chemical substance. the priority over soil contamination stems by and large from health risks, through studying the geotechnical properties of industrial sewage contaminated black cotton soil we are able to improve the weaker residences of soil that's resulting from contamination. A high liquid restriction generally suggests a excessive compressibility and a high shrinkage/swelling potential. A high-plasticity index Ip commonly effects in a low shear strength. Compaction of soil is an critical manner, because it helps it of attain sure physical houses vital for its right behaviour below loading: for example proper compaction of an earthen dam or a motorway Embankment reduces the chances of its settlement, increases the shear energy of the soil due to its increased density and reduces the permeability of the soil.

II Literature Review

As the arena call for oil products is increasing, the possibility of leakage of oil would also growth. This leakage related to many troubles to both surroundings and soil homes. There isn't always a good deal paintings at the effect of crude oil products at the geotechnical homes of soil. Lately, some researchers studied the effect of crude oil contamination on clayey and sandy soil.

Rahman Z.A.et.al (2013) [1] Studied the restored oil contaminated soil. Surfactants are frequently used as a cleansing agent for restoration of oil-infected soil. The shear energy of soil with added surfactant become tested the use of the undrained unconsolidated triaxial assessments. The presence of surfactant in soil can adjust the mechanical behaviour of the soil. The results of surfactant on silty soil had been investigated for consistency index, compaction, permeability and shear electricity. most dry densities elevated and most advantageous moisture contents decreased as contents of brought surfactant have been improved. The undrained shear power became considerably decreased. Surfactant in treated soil reduced liquid and plastic limits, permeability and shear energy. The presence of surfactant assists soil to reap most density at lower water content material.

Dr. S. S. Pusadkaret.al (2014) [2] Gave the results of have a look at on petroleum contamination of black cotton soil. The leakage of petroleum product thru vehicles plying on the street, from garage tank or via pipeline ends in the contamination of soil. The infection of those product results in modify the geotechnical residences of various soils. This paper pursuits to look at the geotechnical houses of petrol and diesel contaminant black cotton soil. Black cotton soil contributes to 70 % of important India. The observe indicates that increase in contamination ends in lower in particular gravity, swelling strain and CBR .The liquid restrict, plastic limit and shrinkage restriction discovered to be boom with growth of contaminants. The growth in shrinkage limit and decrease in

PRATIBHA: INTERNATIONAL JOURNAL OF SCIENCE, SPIRITUALITY, BUSINESS AND TECHNOLOGY (IJSSBT)
Special Issue: International Conference on Global Trends in Science, Technology, Humanities, Commerce & Management 2022 (ICGTSTHCM 2022)
Vol. 8, No. 2, January 2022,ISSN (Print) 2277-7261

swelling strain may additionally enhance swelling function of black cotton soil.

III Scope of work

We find specific gravity of industrial sewage contaminated black cotton soil and natural black cotton soil and conducted the lab test to find atterberg limits. Maximum dry density and optimum moisture content for light weight proctor test. Comparing both soils by plotting graphs and analysis of test results.

IV Objective of Study

A. Study the performance of sewage contaminated black cotton soil by comparison with same natural soil.
B. To examine changes in Geotechnical houses like atterberg limits, proctor density, precise gravity and relative grain length distribution.
C. To identify property which require stabilization.
D. To check validity of relation for Dependency of shrinkage restriction.

V Methodology

A. Collection of sample

Disturbed samples of soil were collected from industrial area v-166 MIDC Jalgaon.

B. Lab tests

The following lab test were conducted on both contaminated and natural soils as per Indian standard.

1. Specific gravity of soil
2. Light weight proctor test

a. Atterberg limits

b. Liquid limit

c. Shrinkage limit

d. Plastic limit

VI Discussion

Comparative result for contaminated and natural soil sample for mentioned tests are discussed below

Table no. 1 shows result of specific gravity of both the samples

Table 1. Specific Gravity

Mass (gm)	Natural soil	contaminated
Mass of pycnometer=M1	610	610
Pycno +soil=M2	940	920
Mass of Pycnometer, soil and water (M_3)	1690	1670
Mass of Pycnometer and water (M_4)	1495	1495
Specific gravity	2.42	2.29

Table 2. MDD and OMC

Soil type	MDD	OMC
Natural soil	15.15	29
sewage contaminated	14.6	30

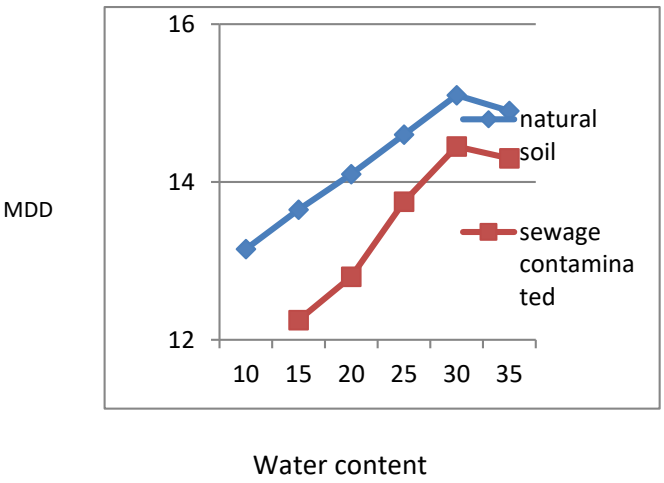

Figure 1. Compaction Curve

Figure 1 shows variation of dry density and water content of natural and uncontaminated soil

Table 3 to 6 shows variation of liquid limit, Plastic limit, Shrinkage limit, Plasticity index of natural soil and sewage contaminated soil

Table 3. liquid Limit

Type of soil	Liquid limit
Natural soil	70%
Sewage contaminated	75%

Table 4. Plastic Limit

Type of soil	Plastic limit
Natural soil	33.96
Sewage contaminated	37.67

Table 5. Plasticity Index

Type of soil	Plasticity index (WL-WP)
Natural soil	33.96
Sewage contaminated	37.67

Table 6. Shrinkage Limit

Type of soil	Shrinkage limit
Natural soil	24.84
Sewage contaminated	14.4

VII Conclusion

Industrial sewage contamination on geotechnical homes of black cotton soil has been studied. The plastic restriction, liquid restrict and plasticity index improved but not large but will increase compressibility of soil. The have a look at suggests that contamination ends in lower in precise gravity, proctor density and shrinkage limit than that of uncontaminated soils. The role of contamination is quite just like water, it will increase a threat to inter-particle slippage, consequently lessen the MDD and OMC. contamination ends in trade in relative grain size distribution which adversely have an effect on the shrinkage restriction and make soil as excessive shrinkage swelling capacity soil. therefore dependency of shrinkage restrict flawlessly valid. contaminated soils require stabilization.

References

[1] Rahman Z.A. Sahibin A. R. Lihan T. Idris.W.M.R. and Sakina M., (2013), "Effects of Surfactant on Geotechnical Characteristics of Silty Soil", Sains Malaysiana 42(7) (2013), pp. 881–891.

[2] Dr. S. S. Pusadkar, P. S. Bharambe.,(2014)," Performance of Petrol and Diesel Contaminated Black Cotton Soil", nternational Journal of Engineering Research & Technology (IJERT) IJERT ISSN: 2278-0181 www.ijert.org Vol. 3 Issue 7, July – 2014

PRATIBHA: INTERNATIONAL JOURNAL OF SCIENCE, SPIRITUALITY, BUSINESS AND TECHNOLOGY (IJSSBT)
Special Issue: International Conference on Global Trends in Science, Technology, Humanities, Commerce & Management 2022 (ICGTSTHCM 2022)
Vol. 8, No. 2, January 2022,ISSN (Print) 2277-7261

Performance Improvement of High Voltage Power Supply Using Flyback Converter with Extra High Tension

P. H. Zope, Dr. S. R. Suralkar, Vaishali B. Patil
P. H. Zope, Department of E&TC, SSBT's COET, KBC North Maharashtra University Jalgaon, India (phzope@gmail.com).
Dr. S. R. Suralkar, Department of E&TC, SSBT's COET, KBC North Maharashtra University Jalgaon, India.
RECPT's Institute of Management Research and Development, Shirpur, Jalgaon

ABSTRACT

In this study the generation of high voltage for electrospinning application is presented, the low cost design and implementation of the high voltage power supply using flyback converter with Extra High Tension(EHT) with its control circuit is discussed. The flyback converter is used as DC-DC converter of maximum wattage 100W its output is connected through control and switching circuit to the back to back connected two SCR with EHT to operate electrospinning setup. The high voltage power supply design of rating 100V to 40KV with current rating between 10mA to 100mA is obtained at the output of EHT. The result discusses the elimination of high-frequency ringing problem and the flyback converter switching between the discontinuous current mode (DCM) and continuous current mode (CCM). The complete calculation of design components and their testing of the flyback converter along with the EHT circuit are presented.

Keywords:
High voltage power supply, Electrospinning, Flyback, Extra High Tension (EHT).

INTRODUCTION

Electrospinning system is the mechanism to fabricate very fine fiber which is used in cotton, biomedical, filter, electronics devices, solar cell and medical application; it uses very high electric field to produce these fine fibers [1]. The system is composed of high voltage direct current (DC) power supply; electronics syringe pump and a rotating or stationary collector drum / plate. The high voltage source needed for electrospinning system varies depends on synthesis condition, usually from 5kV to about 30kV. In this design the high voltage DC power supply of rating 100V to 40kV with maximum output current: 20 mA is used to generate a high electric field to obtain proper synthesis condition between a droplet of the solution at the tip of a needle fitted over the electronic syringe pump and a rotating collector drum / plate.

The studies of the researchers highlight various ways to obtain the high voltage using voltage doublers, Cockcroft-Walton's Voltage Multiplier, Marx Generator, Tesla Coil and Flyback Converter [2,12].

The 32-stage voltage multiplier generate 12KV DC power supply using Cockroft-Walton technique [3], the output voltage linearly increases and reaches to this range. Some high voltage power supply generates analog square wave output which is necessary in the field of electronics and electrical engineering and applied physics, such as X-rays, electrostatic precipitators, defibrillator in a medical lab, defense shield, electron microscopes, dielectric testing, particle accelerator in nuclear physics, stunt gun [4]. The Cockcroft-Walton voltage multiplier circuit shows the ratio of output voltage to input voltage for one stage. As the number of stages increases it will generate high voltages in order of several KV. The Cockcroft-Walton voltage multiplier is isolated from the main line which results in the mitigation of switching surge voltages [5].

The research paper highlight Cockroft-Walton and Van Der Graff circuits are simplest and easiest voltage multiplier circuit is an electrical circuit that converts AC electrical power from a low voltage to a high DC voltage, typically by means of a network like voltage doubler, tripler, quadrupler and n-plexer they are constructed using capacitors and diodes [6,11] similarly the required amount of high voltage can be taken out through tapings [7-9], but they have low efficiency and they are reasonably expensive and it occupy large space. Considering these weak points, many researchers turn towards switching circuit based on MOSFET, IGBT, Power Transisitor etc, it will be best alternative in furutre industry product in the field of power electronics and control. It does not require any kind of maintenance and occupy very much less space. The next section of the paper discusses the design and implementation of high voltage power supply using flyback Converter connected with EHT using two back to back connection of SCR / MOSFET for Electrospinning System.

1. FLYBACK CONVERTER BASIC

PRATIBHA: INTERNATIONAL JOURNAL OF SCIENCE, SPIRITUALITY, BUSINESS AND TECHNOLOGY (IJSSBT)
Special Issue: International Conference on Global Trends in Science, Technology, Humanities, Commerce & Management 2022 (ICGTSTHCM 2022)
Vol. 8, No. 2, January 2022,ISSN (Print) 2277-7261

The flyback converter is a buck-boost converter with the coupled or split inductor to form a transformer, used when power requirement is lower than 100W and the isolation between input and output is required. The flyback transformer hold the energy in the coil as the current flows through the circuit it releases the energy as soon as power is removed. [10,13] discuss flyback is referred to as the on and off action of the control switch. Figure 1 shows little number of components is required to construct the flyback circuit as compared to other high voltage power supply constructed by researchers.

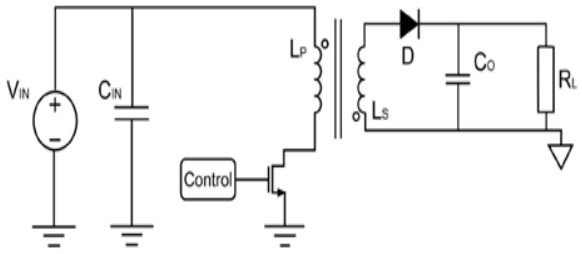

Figure 1. Flyback converter

2. FLYBACK CONVERTER DESIGN STRATEGY

In this section the flyback converter and flyback transformer design strategy is discussed. The coupled inductor shows power conversion strategy and provides isolation between the input and output. It has two operation strategies based on MOSFET's switching tON and tOFF. Figure 2.b shows during tON state, as MOSFET is turned on the drain to source current IDS flows through the primary of transformer and no voltage drop across switch, it shows linearly charging of the coupled inductor and produces a magnetic field around it. The series connected diode in the secondary of the transformer is reverse-biased, it disconnect the transformer from the output shown in Figure 2.a.

The voltage across the primary winding is same as the DC source VIN and the current Ipri is flowing through the primary winding.

$$\text{Ipri} = \frac{1}{\text{Lpri}} \int \text{VIN}\ \text{dt} \qquad \ldots\ldots 1$$

Where $Lpri$ is the primary inductor.

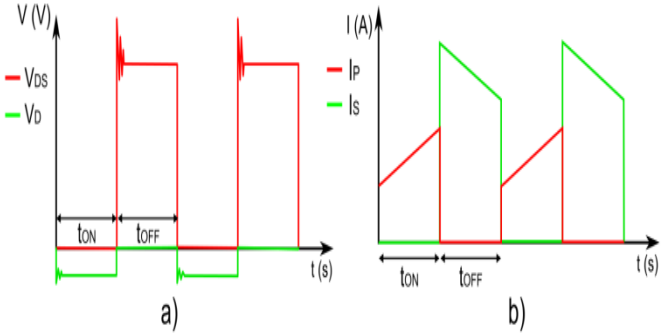

Figure 2: a) VDS across MOSFET and VD across Diode b) Current in Primary and Secondary of transformer

As the current Ipri is flows from the primary of the inductor coil, flux is induced, it results voltage $Vsec$ is induced in the secondary coil.

$$\text{Vsec} = \frac{Np}{Ns}\text{VIN} \qquad \ldots\ldots 2$$

Where Np is the primary winding turns and Ns is the secondary winding turns.

Many researchers select the duty cycle arbitrarily at 50%, but it is important to understand how to optimize this relation: maximum duty cycle, transformer turn ratio, peak current and voltage rating. In our design it is observed that if duty cycle is greater than 50%. The increase of maximum duty cycle reduces the peak current on the primary of the transformer, resulting in better copper transformer utilization on the primary and lower ripple on the input source. At the same time the increase of the maximum duty cycle increases the maximum

stress voltage between drain to source of the main switching MOSFET, and increases the peak current on the secondary side.

Assume the output voltage *V*o= 38V, Output current Io =0.416 A, ripple factor Rf =1, DC source *V*IN = 24V, efficiency η = 80% and switching frequency Fs = 100KHZ is represented by

$$V0 = \left(\frac{N1}{N2}\right)\left(\frac{D}{1-D}\right).VIN \qquad \ldots\ldots 3$$

Similarly,

$$D = \left(\frac{Vo}{Vo+VIN}\right) = \left(\frac{38}{38+24}\right) = 0.612 \qquad \ldots\ldots 4$$

Some industry designers adds diode drop of 0.3V in duty cycle equation.

To calculate the primary inductance value of coil (L) is represented by

$$Lp = \frac{\eta \times D^2 \times VIN^2}{2 \times fS \times Rf \times P} =$$

$$\frac{0.8 \times 0.612^2 \times 24^2}{2 \times 100 \times 10^3 \times 1 \times 38 \times 0.416}$$

$$= 54.58\mu H \qquad \ldots\ldots 5$$

Similarly to selection of the switching devices like power transistor, MOSFT, IGBT etc in various application the following set of calculation provided they are based on the maximum drain to source current and voltage that the switch can withstand. Consider the minimum voltage and maximum voltage range for the input voltage is 12V to 24V.

$$VDS_{MAX} = VIN_{MAX} + \frac{D \times VIN_{MIN}}{1 - D}$$

$$= 24 + \frac{0.612 \times 12}{1 - 0.612}$$

$$= 42.92V + 20\% = 51.50V \qquad \ldots\ldots 6$$

This 20% safe margin is added for safe operation of converter, the maximum current is given by

$$IP_{PK} = \frac{P_{IN}}{D \times VIN_{MIN}} + \frac{D \times VIN_{MIN}}{2 \times fS \times Lp_{MAX}}$$

$$= \frac{12 \times \frac{1}{0.8}}{0.612 \times 12} + \frac{0.612 \times 12}{2 \times 100 \times 10^3 \times 54.58 \times 10^{-6}} = 2.71A \qquad \ldots\ldots 7$$

From this calculation one can select the MOSFET of the rating approximately 80V / 3A.

Similarly during the turn off state tOFF, the drain to source voltage is reversed and gate trigger pulse is absent which result MOSFET is off and the charged coupled transformer / inductor start to demagnetize through the series connected diode. The output capacitor starts charging through the inductor and supplies power to the load.

The required turn ratio (n) calculated using,

$$n = \frac{Np}{Ns} \quad \text{or} \quad n = \frac{V_R}{V_{OUT} + V_D}\ 1 \qquad \ldots\ldots 8$$

PRATIBHA: INTERNATIONAL JOURNAL OF SCIENCE, SPIRITUALITY, BUSINESS AND TECHNOLOGY (IJSSBT)
Special Issue: International Conference on Global Trends in Science, Technology, Humanities, Commerce & Management 2022 (ICGTSTHCM 2022)
Vol. 8, No. 2, January 2022,ISSN (Print) 2277-7261

it is also represented by

$$n = \frac{VIN_{Max} \times D}{(1-D)\times(V_{OUT} + V_D)} \approx 1 \quad \ldots\ldots 9$$

Where Np is the primary turns, and Ns is the secondary number of turns, Vout signifies the output voltage, and VD tells us regarding the voltage drop across the secondary diode.

$$V_D = V_{OUT}\frac{VIN_{Max}}{n} = 38 + \frac{24}{1} = 62\ V \quad \ldots\ldots 10$$

Practically to protect the external section add 30-40% voltage as safe margin, the peak inverse voltage of the diode can carries the maximum reverse voltage is 62 + 40% = 86.8 V.

3. FLYBACK TRANSFORMER & CIRCUIT DESIGN WITH PROTOTYPE

The flyback transformer design is a complex procedure that involves several steps: determining the core size, proper selection of core material and geometry, determining the maximum peak magnetic flux density, defining the primary and secondary windings (turns number and wire gauge) as well as calculating the air-gap necessary to achieve the desired inductance. Moreover, additional considerations concerning the assembly are needed for meeting safety requirements, maximizing magnetic coupling and minimizing parasitic high frequency effects, not to mention the constraints imposed by the specific application.

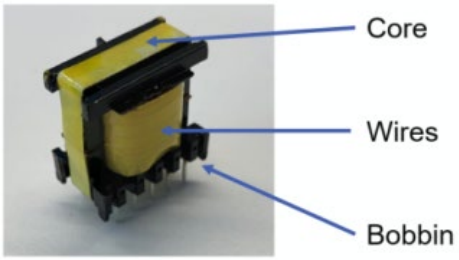

Figure 3 Flyback transformer

To find the area of the transformer (A_P) and it is the product of the winding window area (A_E) and the area of the core cross-section(A_W).

$$A_P = A_E \times A_W\ mm^2 \quad \ldots\ldots 11$$

The following area calculations are provided for a rough initial estimation of the core size in various applications.

$$A_P = \left(\frac{Lp \times IP_{max} \times IP_{RMS}}{BMAX \times 0.0085}\right)^{3/4} \times 10000 \quad \ldots\ldots 12$$

$$A_P = \left(\frac{54.58\mu H \times 2.71 \times 0.77\ A_{RMS}}{0.2 \times 0.0085}\right)^{3/4} \times 10000 \approx 168\ mm^2 \quad \ldots\ldots 13$$

The operating flux density (BMAX) is 0.2 to 0.4T.

To construct the transformer at laboratory level it is necessary to select the number of primary and secondary turns around the bobbin. The number of primary turn revolution around the bobbin is calculated as follows

$$N_P = \left(\frac{Lp \times IP_{max} \times 10^6}{BMAX \times A_E}\right) \quad \ldots\ldots 14$$

$$N_P = \left(\frac{54.58\mu H \times 2.71 \times 10^6}{0.2 \times 20.1 mm4}\right) \approx 59.40 \quad \ldots\ldots 15$$

Similarly to estimate the secondary turn number

$$Ns = \frac{Np}{n} = \frac{60}{1} = 60 \quad \ldots\ldots 16$$

The above design parameters are used to implement the flyback converter circuit prototype is shown in figure 4. The fast switching speed controls the ON and OFF action of the power transistor, IGFET or, MOSFET. The flyback converter is designed in boost mode to convert electrical energy from one voltage to a higher one. The boost converter topology is connected with switching transistor it results a direct current path between VIN and VOUT through the transformer coil and diode D.

By varying the duty cycle (D) of a boost converter, the output voltage can be controlled and with D < 1, the DC output from the boost converter is greater than input voltage VIN as a consequence of the inductors self-induced voltage.

Figure 4. Prototype Flyback converter

The high voltage output is produced using the Extra-high-tension (EHT) based power supply it is capable to deliver variable DC voltage from about 100 V to 50 kV with load current up to 500 mA. The back to back connection of SCRs is used to maintain alternating current supply input voltage at the primary of the power transformer which is capable to produce high DC voltage with lower range of load current. The SCR controlled EHT based high voltage power supply is shown in figure 5.

Figure 5. Prototype EHT and control circuit

PRATIBHA: INTERNATIONAL JOURNAL OF SCIENCE, SPIRITUALITY, BUSINESS AND TECHNOLOGY (IJSSBT)
Special Issue: International Conference on Global Trends in Science, Technology, Humanities, Commerce & Management 2022 (ICGTSTHCM 2022)
Vol. 8, No. 2, January 2022,ISSN (Print) 2277-7261

4. Result and Discussion

To validate the prototype of flyback converter based EHT with control circuit is implemented in the present study. Figure 5 show the flyback converter and EHT with control circuit. The rectified signal from the rectifier is applied as input voltage Vin=10V to flyback converter circuit operating at 150 kHz. The DC-DC flyback converter output voltage obtained between 5V and 40V it depend on the applied control signal, which are considered for adapter applications of smart phone, notebook, personal computer etc. further it is connected to EHT through control circuit to obtain extra high voltage for electrospinning application. The flyback boost converter is tested with the applied input figure 6 shows the output voltage Vout = 100V with Drain to source voltage VDS =10V.

Figure 6. Input voltage Vin, output voltage Vout, Drain to source voltage VDS

When the MOSFET is in the on state, the drain voltage is nearly equal to zero volt and the drain current is flows through the primary winding of the transformer. Due to which the magnetic field is induced and energy is stored in the primary side of the transformer. This current is rising linearly with time. On the secondary side of the transformer the series connected diode D is reversed biased due to which zero current flowing through the secondary of the transformer. In this situation the output capacitor will start discharging, it release the stored energy which causes current flows through the load I_L and Vout is present. When the gate trigger pulse turn off the MOSFET, the transformer start releasing the energy stored from the primary due to which the series connected diode conducts and the output capacitor gets charging.

Figure 7. Drain to source voltage VDS, voltage across diode VD

Initially the transformer secondary current is starts at a high peak value and start decreasing linearly. As soon as the transformer secondary current drops to zero before this instant the MOSFET is again turned on, such type of supply is called as a discontinuous current mode (DCM) supply shown in figure 8. Similarly if the transformer secondary current does not fall to zero, then such type of supply is called a continuous current mode (CCM) supply.

During turn on state of the MOSFET, the transformer holds energy which is affected by the leakage current and it is absorbed by snubber circuit, its purpose is to protect the semiconductor switch from highly inductive voltage. This type of power is dissipated only during the switching transition is

carried between the ON and OFF states.\

Figure 8. Drain to source voltage VDS, drain to source current IDS @24W and RL is 6 Ω in CCM

5. CONCLUSION

The high voltage power supply for the electronic application using flyback converter is connected through control and switching circuit to the back to back connected two SCR with EHT has been developed. The designed flyback converter, EHT 40KV and control circuit eliminates the drawback of bulky transformer, high value component and large heat sink of component. The power supply is housed inside acrylic box, it does not require routine maintenance; provide low ripple with various loads and it has provision to obtain 1000V step as well as variable output voltage.

REFERENCES

1. M. M Munir, Dian Ahmad Hapidin, and Khairurrijal, "Designing of a High Voltage Power Supply for Electrospinning Apparatus Using a High Voltage Flyback Transformer (HVFBT)", Applied Mechanics and Materials Vol. 771 (2015) pp 145-148.
2. A. SinghasatheinW. KesiS. Boonyayut A. Singhasathein, W. Kesi, S. Boonyayut, P. Suwanpingkarl, P. Poungsri, A. Pruksanubal and N.tanthanuch, "Design and Construction of 30 kV High Voltage Generator using Fly-back Converter" Applied Mechanics and Materials, Vol. 781, pp 361-365, 2014. DOI: 10.4028/www.scientific.net/AMM.781.361
3. Garba, B,"Design and construction of 12kV DC power supply", Bayero Journal of Pure and Applied Sciences, 2(2), 175-184, 2009. DOI: 10.4314/bajopas.v2i2.63808
4. Naidu, M. S. and Kamaraju, V.,"High voltage engineering" (5th ed.). New Delhi: Tata McGraw-Hill Education Pvt Ltd.
5. Dwivedi, C. K. and Daigavane, M. B, "Multi-purpose low cost DC high voltage generator (60kV output), using Cockcroft-Walton voltage multiplier circuit" International Journal of Science and Technology Education Research, 2(7), 109 -119, 2011.
6. Forouzesh, M., Siwakoti, Y. P., Gorji, S. A., Blaabjerg, F. and Lehman, B, "Step-Up DC-DC converters: A comprehensive review of voltage-boosting techniques, topologies, and applications", IEEE Transactions on Power Electronics, 2017. https://doi.org/10.1109/TPEL.2017.2652318
7. Kuffel, E., Zaengl, W. S., and Kuffel, J, "High voltage engineering fundamental. New York" 2000 https://doi.org/10.1016/b978-0-7506- 3634-6.x5000-x.
8. Mansell, A. D. and Shen., J, "Pulse converters in traction application", Power Engineering journal, 183.2002
9. Mazen, A.-S., Hussein, A., Ahdab, E. and Roshedy, R, "High voltage engineering", New York: Marcel Dekker Inc. 2000.
10. Ni, H., Wu, A.X., Zhang, X., "Transformer Selection Calculation for the design of Flyback Switching Power Supply. IOP Conference Series: Materials Science and Engineering, 544: 012054, 2018
11.https://www.monolithicpower.com/en/how-to-design-a-flyback-converter-in-seven-steps
12. Ved Parkash, Parveen Kumar, and Gaurav Sapra, Design and simulation of flyback based adjustable high voltage power supply (HVPS) for electro-spinner, International Conference on Advanced MaterialsAIP Conf. Proc. 2276, 020051-1–020051-10; https://doi.org/10.1063/5.0025800.
13. Li Chengcong, Fan Zhenfang and Luo Hui, High Voltage Transformer design based on Flyback Switching
Power Supply, Journal of Physics 1449 (2020) 012059 IOP Publishing doi:10.1088/1742-6596/1449/1/012059.
14. P. H. Zope, Dr. S. R. Suralkar "Electrospinning: Real Challenges in the production of Nanofibers and Its Application Areas", International Conference on Global Trends in Science, Technology, Humanities, Commerce & Management (ICGTSTHCM19) held at SSBT's COET Jalgaon between 28th to 30th December, 2019, ISBN 978-93-88544-95-5.
15. P. H. Zope, Dr. S. R. Suralkar, Review of Nanofiber Production Techniques, A Multidisciplinary National Conference on Managament, Engineering & Science, KCE COEIT Jalgaon, April-2019.
16. K.S. Patil, P. H Zope, U. T. Patil, P. D. Patil, R S Dubey, G R Gupta, Synthesis and thermophysical studies of polyanilines, Bulletin of Materials Science 42 (1), 24, Feb-2019.
17. P. H. Zope, K. S. Patil, Dr. S. R. Suralkar, Dr. P. R. Chaudhari, Review of Electrical conductivity properties of Conducting Polymers based electronics application, PRATIBHA: International Journal Of Science, Spirituality, Business And Technology (IJSSBT), Volume 6, No. 2, September 2018 ISSN (Print) 2277-7261.
18 P. H. Zope, Dr. S. R. Suralkar, "Infusion and Retract Rate Control of Electronic Syring Pump In Electrospinning System" International

Conference on Global Trends in Engineering and Technology (Online mode) (ICGTET), 29-30 Jan 2021

Pankaj H. Zope has received his B.E degree in Industrial Electronics in *1999* from MGM J.N.E.C Aurangabad and Master's degrees in Digital Electronics Engineering in *2007* from PRMIT Badnera, Amravati University. Subsequently he carried out his research from Jodhpur National University, Jodhpur and awarded PhD in *2013*. Presently he is working as Assistant Professor in the Post Graduate Department of Electronics and Telecommunication Engineering at SSBT C.O.E.T. Bambhori, Jalgaon. He has published more than *60* research paper of national and international repute. He is working on many project of Nano-science and Nano-Electronics and his research interests include signal processing (Digital, Image), Computer Network (MANIT, Adhoc etc),Power Electronics and Inverter, Analog Devices, Nano-Sensor, Solar Cell Fabrication and Super- Capacitors etc.

Dr. Shekhar R. Suralkar has received his B.E. degree in Electronics in 1989 from SSGMCE Shegaon and Master's degree in Control & Instrumentation in 1998 from MNREC, Allahabad. Subsequently he carried out his research from North Maharashtra University, Jalgaon and awarded Ph.D in 2015. Presently he is working as Proessor and Head of the Department Electronics and Telecommunication Engineering at SSBT C.O.E.T. Bambhori, Jalgaon. He has published more than 100 research paper of national and international repute. He is working on many projects of Image Processing, Pattern Recognition and his research interests include Pattern Recognition, signal processing (Digital, Image) etc.

PRATIBHA: INTERNATIONAL JOURNAL OF SCIENCE, SPIRITUALITY, BUSINESS AND TECHNOLOGY (IJSSBT)
Special Issue: International Conference on Global Trends in Science, Technology, Humanities, Commerce & Management 2022 (ICGTSTHCM 2022)
Vol. 8, No. 2, January 2022,ISSN (Print) 2277-7261

Photo catalytic Degradation of Azo RG19 dye using Reduced Graphene oxide and Zinc oxide (RGO/ZnO) Nanocomposites

Rajkumar Sirsam, Ravindra Puri, Deepali Bhole*
University Institute of Chemical Technology
KBC North Maharashtra University, Jalgaon
*E-mail: *rajkumarsirsam@gmail.com*

ABSTRACT

The current study is focus on the photo catalytic degradation activity of nanocomposites of RGO and ZnO (RGO/ZnO) on azo dye (dyes which contains -N=N-) RG19. The GO has been synthesized as per improved hummer's process. The nanocomposites RGO/ZnO has been synthesized by in situ reduction of GO. ZnO is considered to be a suitable because of its strong oxidizing power, non-toxicity, and being relatively inexpensive. Whereas ZnO can act as active photo catalyst while graphene as supporting & transporting material to facilitate the migration of photo generated electrons and hinders the electron-hole recombination. Furthermore, characterization of nanocomposites has been studied, surface morphology by field emission-scanning electron microscope (FE-SEM), elemental analysis by EDX, fourier transfer-infrared spectroscopy (FT-IR) & crystallinity by x-ray diffraction spectroscopy (X-RD). The dye degradation % was found out by using the UV-spectrometry test, the effect of various parameters such as catalyst loading in gm, variation in pH, and change in initial concentration of the dye in PPM on degradation has been investigated.

Keywords: Photo catalytic, Degradation, Graphene oxide, ZnO, Azo dye.

1. INTRODUCTION

Water pollution is one of major global problem. Presently many, water resources are being poised by industrial effluents. The development of fundamental and applied research in the area of environment is a need and challenge for today's generation because of environmental problems associated with organic pollutants and water contaminants [1]. Even though low concentration of these micro pollutants may cause a major health hazard due to their mutagenicity, genotoxicity and carcinogenicity [2]. A recent study reported that 70 % of industries in developing countries are discharging their effluents into water bodies without prior and necessary treatment process. Synthetic dyes are the major constituents of industrial pollutants and water contaminants [3, 4]. Dyes are used precisely in the textile industry for dying operations such as, cotton, wool, silk, and for colouring oils, fats, waxes, varnishes, and plastics. The paper, food, cosmetic, and leather industries are extensive consumers of these dyes [5] A number of technologies have been investigated for removing dye micro pollutants such as adsorption, coagulation and flocculation, membrane filtration, electrochemical treatment, bioremediation, and phytoremediation [6]. Photo catalytic oxidation process has extensively attracted considerable attention due to cost effective, clean and green technology of this process of removing toxic organic and inorganic pollutants from wastewater [7, 8].

In this study, RGO/ZnO nanomaterials have been synthesized and optical, surface morphological properties are investigated. Effectiveness of synthesized nanocomposites was studied for the degradation of RG19 dye at different operating parameters.

2. MATERIALS & CHEMICALS

Reactive Green 19 dye (sigma Aldrich), Graphite powder (SD Fine-Chem), Hydrochloric acid (35%, Merck), Sulphuric Acid (98%,Ranchem), Potassium Permanganate (SD Fine-Chem), Hydrogen peroxide (30%, Merck), Phosphoric acid (85%, Merck), Ethanol (Changshu Yangquan), Zinc acetate dehydrate (Merck), Sodium Bicarbonate (Qualigens Fine-Chem), Petroleum ether (Lobachem), Tween 20 (Merck), Hydrazine Hydrate, Liquid ammonia (Lobachem)..

2.1 Synthesis of ZnO Nanoparticles

ZnO was synthesized by the simple Co-precipitation method. Zn $(Ac)_2 \cdot 2H_2O$ was taken as the precursor for ZnO. Zn $(Ac)_2 \cdot 2H_2O$ and $NaHCO_3$ were dissolved separately in double distilled water to obtain 0.1 mol/L solutions. Zn $(Ac)_2 \cdot 2H_2O$ solution (250 ml of 0.1 mol/L) was slowly added into vigorously stirred $NaHCO_3$ (250 ml of 0.1 mol/L) and Tween 20 mixed solution. White precipitate was forms; it was filtered, repeatedly rinsed with distilled water and then washed twice with C_2H_5-OH. The precipitate was dried at 70°C for 2 hr and finally calcined at 450°C for 3 hr. Pure ZnO was prepared by the above procedure without any further modification [9, 10].

2.2 Synthesis of RGO/ZnO nanocomposites

The RGO/ZnO nanocomposites was prepared in two parts the first consists of synthesis of GO via Improved Hummer's process [11] followed by in-situ reduction process [12]. GO was added to 100 ml of distilled water as per the stoichiometry and ultrasonicated for 1 hr at ambient temperature. Zn $(Ac)_2 \cdot 2H_2O$ was added to 100 ml of ethylene glycol on stoichiometric basis and were mixed uniformly, and resulted mixture was slowly added to the GO solution. The suspension was ultrasonicated at room temperature for 1 hr. Followed by addition of hydrazine monohydrate and liquid ammonia as reducing agents. The mixture was then refluxed at 90° C for 6 hrs and cooled at room temperature. Washed several times with distilled water and ethanol and centrifuged at 4000 rpm for 5 min. Drying in hot air oven at 70° C for 2 hrs and calcination was performed at 450° C for 3 hrs in a muffle furnace. 5% and 10% w/w RGO/ZnO was prepared by above process on stoichiometric basis [12, 13].

2.3 Characterization

Functional groups of ZnO, GO and RGO/ZnO nanocomposites were recorded on FTIR spectrophotometer, Shimadzu, Tokyo, Japan. Topographical surface morphology was determined using FE-SEM, S-4800 Hitachi, Tokyo, Japan) Structural characterization was carried by X-ray diffractometer (XRD, Bruker D8 Advance, Berlin, Germany). The degradation of dye was determined by UV absorption spectra using UV-Vis spectroscopy (Agilent Technologies Cary 60 model, Japan). All the samples were run two times and analyzed at room temperature. ZnO nanoparticles and & RGO/ZnO nanocomposites i.e 250 mg at basic pH, the experiments were carried out by changing the concentration of RG19 as 50, 100, 125, 150, 180 ppm solution.

3. RESULTS AND DISCUSSION

3.1. Functional group analysis

From the Fig.1 the band located at 478 - 536 cm^{-1} is corresponding to the Zn-O stretching and a characteristic peak for the quartzite hexagonal phase of ZnO. The wide stretching at 3200 to 3600 cm^{-1} corresponds to surface bound water molecule [14, 15]. In spectra of GO (Fig. 2 a) the strong and broad absorption peaks located at 3470 and 3647 cm^{-1} assigned to the stretching vibrations of O-H, The peak at 927 cm^{-1} corresponds to C-O vibrations and is due to the epoxide groups situated at the edges of the GO sheets. In spectra of 5 % RGO/ZnO composite, the absorption peaks at 3196, 1520 and 999 cm^{-1} are attributed to the characteristic stretching vibration of O-H, C=C, and C-O respectively, which indicates the C=O group present in GO is reduced, furthermore, the absorption band at 438 cm^{-1} can be assigned to the stretching vibration of hexagonal structured Zn-O (Fig. 2 b). In FT-IR spectra of 10 % RGO/ZnO composite (Fig. 2 c), the absorption peaks at 3715, 1535 and 972 cm^{-1} are attributed to the characteristic stretching vibration of O-H, C=C, and C-O respectively, which indicates C=O group present in GO is reduced, furthermore, the absorption band at 481 cm^{-1} of 10 % RGO/ZnO can be assigned to the stretching vibration of Zn-O. [16, 17].

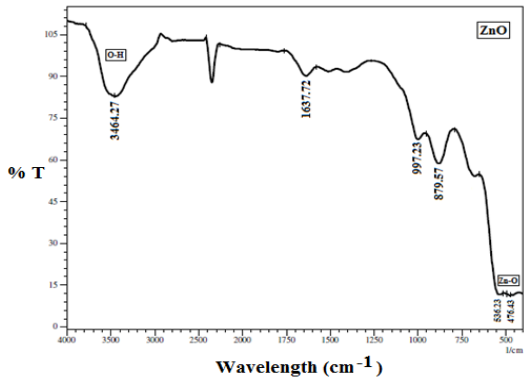

Figure 1. FT-IR Spectra of ZnO

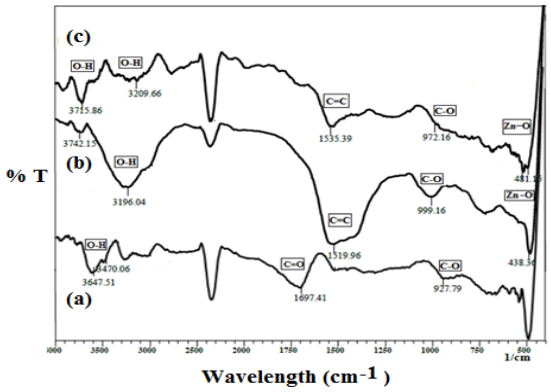

Figure 2. FT-IR spectra of (a) GO, (b) 5% RGO/ZnO, (c) 10% RGO/ZnO

3.2 Morphological structure analysis of composites

From Fig. 3 (a) in GO, sheet like structure is observed which are stacked over each other. GO has layered structure with ultrathin and homogeneous films. The films were folded or continuous at times including kinked and wrinkled areas. In RGO (Fig. 3 b) it is seen that the GO which were stacked over each other are reduced to single ultrathin sheets of carbon layer which has been exfoliated from GO by using hydrazine hydrate as a reducing agent. From Fig. 3 (c) shows ZnO nanoparticles are hexagonal cylindrical in shape, and which has less agglomeration, the average size of rods is 90 nm in length. From FE-SEM images (Fig. 3 d and e) in 5% RGO/ZnO and 10% RGO/ZnO nanocomposites, the image clearly indicates the RGO has been exfoliated to macro-porous single layered of graphene with the incorporation of hexagonal cylindrical ZnO rods synthesized by in-situ reduction process.

PRATIBHA: INTERNATIONAL JOURNAL OF SCIENCE, SPIRITUALITY, BUSINESS AND TECHNOLOGY (IJSSBT)
Special Issue: International Conference on Global Trends in Science, Technology, Humanities, Commerce & Management 2022 (ICGTSTHCM 2022)
Vol. 8, No. 2, January 2022,ISSN (Print) 2277-7261

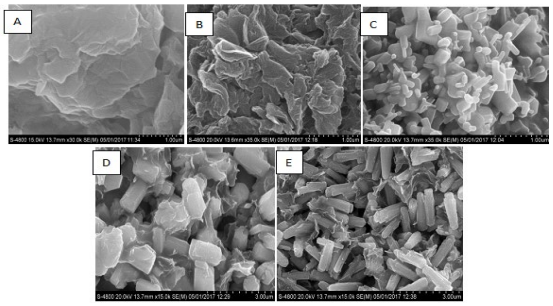

Figure 3. FE-SEM images of a) GO b) RGO c) ZnO d) 5% RGO/ZnO, e) 10% RGO/ZnO

3.3 X-Ray Diffraction Spectroscopy

The physical nature of nanocomposites with variation in percentage of RGO and ZnO were determined from the Fig. 4. The diffraction peak at 9.1° in the XRD pattern of GO (Fig. 4 a) is observed and interlayer spacing is 1.013 nm, while in RGO (Fig. 4b), 5% RGO/ZnO (Fig. 4 c) and 10% RGO/ZnO (Fig. 4d), the diffraction peak of GO is disappeared indicating that oxygen containing functional group in the GO is reduced. A broad band is obtained in RGO pattern at 24.5° and interlayer spacing is 0.365 nm [12]. GO and RGO are found amorphous in nature. The 5% RGO/ZnO, 10% RGO/ZnO and ZnO (Fig. 4e) nanoparticles showed a complex between nanosized graphene sheets along with hexagonal quartzite crystal structure of ZnO particles, which is assigned by comparing the diffraction peak position with international crystallographic data table for standard ZnO powder [18]. The intensity of ZnO diffraction peaks showing greater crystallinity of 86.2 % and sharp peaks than 5% RGO/ZnO and 10% RGO/ZnO nanocomposites their crystallinity is found as 79.4% and 82.9 %. It has been reported that crystallinity induces a larger band gape, due to the increased redox ability and this quantum size effect enhances its photo catalytic activity [19, 20]. Thus, it is expected that good crystallinity associated nanoparticles could enhance the photo catalytic activity [21].

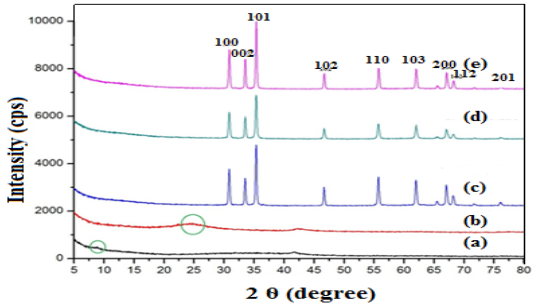

Figure 4. XRD spectra of ZnO, 10% RGO/ZnO, 5% RGO/ZnO, RGO, GO

3.4 Photo catalytic Activity

3.4.1 Effect of Variation in Initial Dye Concentration

Fig. 5 shows that when the concentration of RG19 increases the dye degradation rate is decrease. This is because; as the concentration of RG19 increases the equilibrium adsorption of RG19 on ZnO nanoparticles and RGO/ZnO nanocomposites also increases resulting in lower formation rate of hydroxyl radical, which is active species for photo catalytic degradation, hence decreasing the rate of photo catalytic degradation of RG19 dye. It is clear that 5% RGO/ZnO nanocomposite shows highest degradation percentage than reset of the catalyst. The 10% RGO/ZnO showed least degradation which might be due to dispersion of RGO in wastewater which creates barrier for the transfer of the visible light leading to less generation of hydroxyl radical formation. 5% RGO/ZnO showed the best degradation percentage because of increasing the charge mobility.

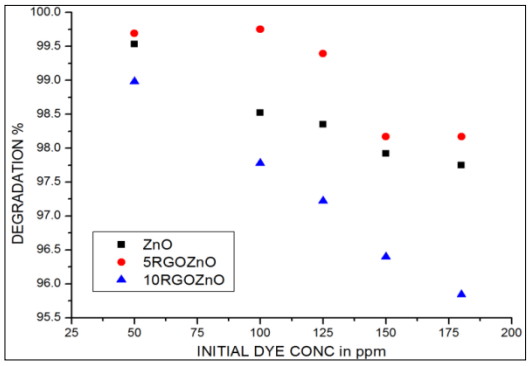

Figure 5. Degradation % Vs Variation in initial concentration of RG19

3.4.2 Effect of Catalyst Dose

Experiments were carried out with varying the photo catalyst dose from 0.5, 1, 1.5 gm/lit. With the exposure of the sunlight for the catalyst dose of 125, 250 and 375 mgs the degradation efficiency is to be found out. The result of the extent of degradation of RG19 dye with variation in catalyst dose is shown in Fig. 6. The result shows that, as the dose of photocatalyst increases the degradation rate also goes on increasing up to certain extent. The increase in degradation rate is from 0.5 to 1 gms/lit for 5% RGO/ZnO the degradation % is highest. However, for the catalyst dose of 1.5 gm/lit is 375 mgs, it is found that the degradation is decrease which could be due to over catalyst dosing creating barrier for sunlight to enter into the solution. For the 5% RGO/ZnO the optimum catalyst dose is found out to be the 1 gms/lit, which is carried further for the variation in the pH of the solution.

3.4.3 Effect of solution pH on dye removal (mg/lit)

The optimum initial concentration and optimum catalyst dose for the catalyst type the variation in the pH has been studied. The degradation rate increases from pH 5 to 10 for ZnO, 5% RGO/ZnO and 10% RGO/ZnO after 120 min. From Fig. 7 result shows that in acidic medium degradation rate becomes less as compared to the basic medium and decreased by decreasing the pH values in acidic medium. As in acidic medium, RG 19 dye has H+ ion so that hydroxyl ion produced during the photo catalysis will neutralize the H+ reduces the degradation rate. While in case of basic medium, RG 19 dye loses H+ ion so the hydroxyl ion produced in the reaction will not utilize for the neutralization and will act as an active species, also in basic medium the concentration hydroxyl ion will increase which ultimately increases the degradation rate. pH plays an important role as it is connected to the degree of ionization of the dye molecules and the surface properties of the adsorbents. So basic medium shows the better degradation of RG19 dye. Our aim is to reduce the concentration of dye; the optimized pH value for further degradation is conducted at a pH of 7.5-8. However, study at pH 10 shows higher percent than pH 7.5, but in basic pH there is a presence of sodium ions which is a pollutant.

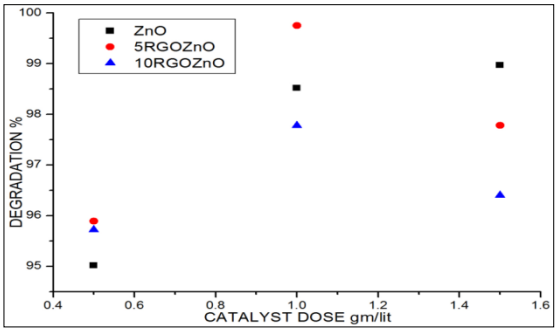

Figure 6. Degradation % Vs Variation in catalyst dose

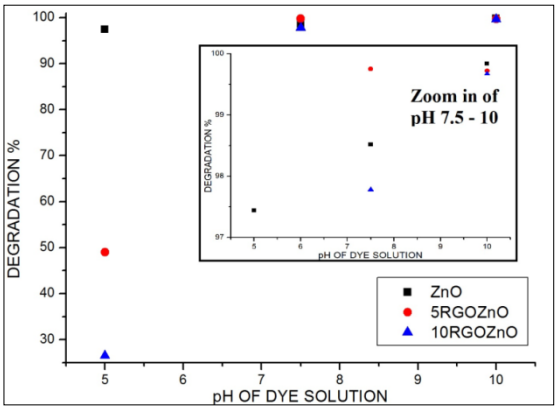

Figure 7. Degradation % Vs variations in pH of initial the dye solution

3.4.4 Consistence Test and Regeneration of Catalyst

For the confirmation regarding degradation percentage by 5% RGO/ZnO of RG19 dye with the optimized parameters are obtained by experiment. Experiments were performed for consistence and regeneration test, the results indicated that in each run the degradation % is nearly same to each other and it is consistent. The catalyst was recovered by simple filtration after performing the experimental batches, it is found that for two set of experiments, degradation efficiency of the catalyst decreases by nearly 4.71 % to 94.79%.

4. CONCLUSION

FT-IR spectra confirms that RGO/ZnO nanocomposites have been synthesized, FE-SEM image show there is complex bonding of ZnO rods and the RGO nano sheets. X-RD results indicated that the GO and RGO has amorphous nature while ZnO and RGO/ZnO composites has crystalline nature. The RGO/ZnO nanocomposites are capable of degrading the RG19 dye with maximum adsorption capability of 250 mg/gm for the 5% RGO/ZnO nanocomposites. The 10% RGO/ZnO nanocomposites shown least efficiency which might be due to poor absorption of the photons or by can be due to covering of surface by the RGO sheets. The 5% RGO/ZnO highest degradation of 99% for the catalyst loading of 1 gm/L.

REFERENCES

[1.] Ahmad M, Alrozi R., "Removal of malachite green dye from aqueous solution using rambutan peel based activated carbon: Equilibrium, kinetic and thermodynamic studies". Chem. Eng. J., **(2011),** 510 – 516

[2.] Hermann, J. M., Tahire, H., Ait-Ichou, Y., Fernández, A., Lossaletta, G., Fernández, A., "Characterization and Activity in Aqueous Medium of TiO2 and Ag-TiO2 Coating on Quartz." App. Catal. Env, **(1997).**13, 219.

[3.] Modirshahla N, Behnajady MA, Ghanbary F., "Decolorization and mineralization of C.I. Acid Yellow 23 by Fenton and photo-Fenton processes." Dyes Pigm, **(2007)** 73: 305-310.

[4.] Gupta VK, Gupta B, Rastogic A, Agarwald S, Nayaka A, "Comparative investigation on adsorption performances of mesoporous activated carbon prepared from waste rubber tire and activated carbon for a hazardous azo dye- Acid Blue", 113. J Hazard Mater **(2011)** 186:891–901

[5.] Wong YS, Ong SA, Teng TT, Nabilah Aminah L, Kumara K., "Production of bioflocculant by Staphylococcus cohnii ssp. from palm oil mill effluent (POME)." Water Air Soil Poll 223(7): **(2012)** 3775–3781

[6.] Chen Y, Li Z, Zhang Z, Psaltis D, Scherer A., "Nanoimprinted circular grating distributed feedback dye laser." Appl. Phys. Lett., **(2007)** 91: 051109.

[7.] Pruden AL, Ollis DF, "Photo-assisted heterogeneous catalysis: the degradation of trichloroethylene in water." J Catal **(1983)** 82:404–417

[8.] Rastegar, M., Shadbad, K.R., Khataee, A.R., Pourrajab, R., "Optimization of photocatalytic degradation of sulphonated diazo dye CI Reactive Green 19 using ceramic-coated TiO2 nanoparticles". Environ. Technol. 33, (2012). 995-1003.

[9.] D. K. Bhole, R. G. Puri, P. D. Meshram, R. S. Sirsam "Photocatalytic degradation of methyl orange using doped ZnO nanocatalyst" Journal of the Indian Chemical Society, (2020), 97(3): 440-445.

[10.] Selvam, N.Clament Sagaya, S. Narayanan, L.John Kennedy, and J.Judith Vijaya., "Pure and Mg-Doped Self-Assembled ZnO Nano-Particles for the Enhanced Photocatalytic Degradation of 4-Chlorophenol, a Hazardous Endocrine Disruptor." (2013).

[11.] Daniela C. Marcano, Dmitry V. Kosynkin, Jacob M. Berlin, Alexander Sinitskii, Zhengzong Sun, Alexander Slesarev, Lawrence B. Alemany, Wei Lu, James M. Tour, "Improved Synthesis of Graphene Oxide", ACS Nano 4 (2010) 4806-4814.

[12.] Kanika Anand, Onkar Singh, Ravi Chand Singh, "Different strategies for the synthesis of graphene/ZnO composite and its photocatalytic properties." Appl. Phys. A (2014) 116:1141–1148

[13.] Feng, Yan, Ningning Feng, Yuzhen Wei, and Guoying Zhang., "An in Situ Gelatine-Assisted Hydrothermal Synthesis of ZnO–reduced Graphene Oxide Composites with Enhanced Photocatalytic Performance under Ultraviolet and Visible Light." RSC Advances, **(2014),** 4(16):7933–43.

[14.] Selvam, N. Clament Sagaya, S. Narayanan, L.John Kennedy, and J.Judith Vijaya., "Pure and Mg-Doped Self-Assembled ZnO Nano-Particles for the Enhanced Photocatalytic Degradation of 4-Chlorophenol" Journal of Environmental Sciences 2013, 25(10) (**2013),** 2157–2167.

[15.] V. Online, R. Yousefi., "One-pot sol–gel synthesis of reduced graphene oxide uniformly decorated zinc oxide nanoparticles in starch environment for highly efficient photodegradation of Methylene Blue." RSC Advances: **(2015),** 1-37.

[16.] Abdolhosseinzadeh, Sina, Hamed Asgharzadeh, and Hyoung Seop Kim., "Fast and Fully-Scalable Synthesis of Reduced Graphene Oxide." Nature Publishing Group 1–7, (**2015).**

[17.] Gunti, Srikanth, Ashok Kumar, and Manoj K. Ram., "Comparative Organics Remediation Properties of Nanostructured Graphene Doped Titanium Oxide and Graphene Doped Zinc Oxide Photocatalysts." American Journal of Analytical Chemistry, **(2015),** (6):708–17.

[18.] Wang, Jinmin and Lian Gao., "Photoluminescence Properties of Nanocrystalline ZnO Ceramics Prepared by Pressureless Sintering and Spark Plasma Sintering." Journal of the American Ceramic Society (**2005),** 88(6):1637–39.

[19.] Kim, Dong Suk, Shin Jung Han, and Seung-Yeop Kwak., "Synthesis and Photocatalytic Activity of Mesoporous TiO2 with the Surface Area, Crystallite Size, and Pore Size." Journal of Colloid and Interface Science **(2007)** 316(1):85–91.

[20.] Liu, A. R., S. M. Wang, Y. R. Zhao, and Z. Zheng., "Low-Temperature Preparation of Nanocrystalline TiO2 Photocatalyst with a Very Large Specific Surface Area." Materials Chemistry and Physics, (**2006),** 99(1):131–34.

[21.] Omar, Fatin Saiha, Huang Nay Ming, Syed Muhamad Hafiz, and Lim Hong Ngee., "Microwave Synthesis of Zinc Oxide / Reduced Graphene Oxide Hybrid for Adsorption-Photocatalysis Application." (**2014).**

PRATIBHA: INTERNATIONAL JOURNAL OF SCIENCE, SPIRITUALITY, BUSINESS AND TECHNOLOGY (IJSSBT)
Special Issue: International Conference on Global Trends in Science, Technology, Humanities, Commerce & Management 2022 (ICGTSTHCM 2022)
Vol. 8, No. 2, January 2022,ISSN (Print) 2277-7261

Review of Covid 19 Image Analysis

Dr. V. M .Deshmukh
Department of Electronics and Telecommunication, COET, Bambhori, India
vmdeshmukh947@gmail.com
M.S.Sadavarte
Department of Electronics and Telecommunication, GCOE, Jalgaon, India
maheshsada@yahoo.co.in

Abstract—COVID-19 is a worldwide epidemic, as announced by the World Health Organization (WHO) in March 2020. Image Processing methods can play vital roles in identifying COVID-19 patients by visually analyzing their chest x-ray images.As the cost and required time of conventional RT-PCR tests to detect COVID-19, researchers are trying to use medical images like X-Ray and Computed Tomography (CT) images to detect it with the help of Artificial Intelligence (AI) based systems. In this paper, we reviewed some of these newly emerging AI-based models that can detect COVID-19 from medical images using X-Ray or CT of lung images. We explored and analyzed datasets, preprocessing techniques, segmentation, feature extraction, classification and experimental results which can be helpful for finding future research directions in the domain of automatic diagnosis of Covid-19 disease using Artificial Intelligence (AI) based frameworks.

I. Keywords—COVID-19; Deep Learning; Medical Image

INTRODUCTION

Over the past two years, the Coronavirus has rapidly spread to all parts of the world. Research is continuing to find a cure for this disease while there is no exact reason for this outbreak. As the number of cases to test for Coronavirus is increasing rapidly day by day, it is impossible to test due to the time and cost factors. Five times more deadly than the flu, COVID-19 causes significant morbidity and mortality. Like other pneumonias, pulmonary infection with COVID-19 results in inflammation and fluid in the lungs. COVID-19 looks very similar to other viral and bacterial pneumonias on chest radiographs, which makes it difficult to diagnose. Over recent years, image processing and machine learning has turned very reliable in the medical field. Using machine learning to predict COVID-19 in patients will reduce the time delay for the results of the medical tests and modulate health workers to give proper medical treatment to them. Here we propose a computer vision model to detect and localize COVID-19 which would help doctors provide a quick and confident diagnosis. This study focuses on leveraging deep learning techniques to automatically detect COVID-19 pneumonia in chest X-ray images. As a result, patients could get the right treatment before the most severe effects of the virus take hold.

Currently, COVID-19 can be diagnosed via polymerase chain reaction to detect genetic material from the virus or chest radiograph. However, it can take a few hours and sometimes days before the molecular test results are back. By contrast, chest radiographs can be obtained in minutes. While guidelines exist to help radiologists differentiate COVID-19 from other types of infection, their assessments vary. In addition, non-radiologists could be supported with better localization of the disease, such as with a visual bounding box.

RELATED WORK

1. The latest threat to global health is the COVID-19 outbreak. Although there exist large datasets of chest X-rays (CXR) and computed tomography (CT) scans, few COVID-19 image collections are currently available due to patient privacy. At the same time, there is a rapid growth of COVID-19-relevant articles in the biomedical literature, including those that report findings on radiographs. Here, in [1] authors present COVID-19-CT-CXR, a public database of COVID-19 CXR and CT images, which are automatically extracted from COVID-19-relevant articles from the PubMed Central Open Access (PMC-OA) Subset. Authors extracted figures, associated captions, and relevant figure descriptions in the article and separated compound figures into subfigures. Because a large portion of figures in COVID-19 articles are not CXR or CT, authors designed a deep-learning model to distinguish them from other figure types and to classify them accordingly.

   Results: The final database includes 1,327 CT and 263 CXR images (as of May 9, 2020) with their relevant text.
2. In the preceding several months, the outbreak of COVID-19 has become one of the global severe public health issues. It is critical to screen for COVID-infected or suspected patients in time. Given that the method of nucleic acid test strip detection is laborious and time-consuming, the Chest Xray images screening method has become the object of [2] because of its robust availability and easy accessibility. Authors in [2] introduces a new neural network model, COVID-GATNet, to assist radiologists in automatically diagnosing CXR images, thus improving the detection speed of suspected infected

people. The study integrates three CXR data sets published on the internet and Kaggle competition, including CXR images of healthy, other types of pneumonia, and COVID-19 positive patients. Because there is less open-source data for COVID-19 positive CXR images than the other two types of data, this research dilated CODIV-19 positive CXR images by scaling, rotating, adjusting brightness and other increase methods of image data. Then, the expanded COVID-19 positive CXR data set is divided into a training set and test set at a ratio of 8:2 to complete the experiment and evaluation of COVID-GATNet. Research by combining Densenet Convolutional Neural Network (DenseNet) and Graph Attention Network (GAT), COVID-GATNet has a direct connection between any two network layers in each dense block and uses the attention mechanism, which significantly reduces the parameters of the model and improves the classification performance.

Results: Experimental results show that the accuracy of COVID-GATNet is best to achieve 94.1%, and the F-1 score also with 95.2%. Compared with COVID-Net, COVID-Net accuracy is 93.3%, and the F-1score is 94.8%. The experimental results and diagrams show that the proposed model performs well and can effectively assist clinicians in screening and detecting patients' state, helping to classify pulmonary diseases and observe the pulmonary status of patients.

3. Recently, deep-learning-based computer vision methods have demonstrated great promise for use in medical imaging applications, including X-rays, magnetic resonance imaging, and CT imaging. However, training a deep-learning model requires large volumes of data, and mediccal staff faces a high risk when collecting COVID-19 CT data due to the high infectivity of the disease. Another issue is the lack of experts available for data labeling. In order to meet the data requirements for COVID-19 CT imaging, we propose a CT image synthesis approach based on a conditional generative adversarial network that can effectively generate high-quality and realistic COVID-19 CT images for use in deep-learning-based medical imaging tasks. Experimental results show that the proposed method [3] outperforms other state-of-the-art image synthesis methods with the generated COVID-19 CT images and indicates promising for various machine learning applications including semantic segmentation and classification.
4. Authors in [4] develop a dual-sampling attention network to automatically diagnose COVID-19 from the community acquired pneumonia (CAP) in chest computed tomography (CT). In particular, authors [4] propose a novel online attention module with a 3D convolutional network (CNN) to focus on the infection regions in lungs when making decisions of diagnoses. Note that there exists imbalanced distribution of the sizes of the infection regions between COVID-19 and CAP, partially due to fast progress of COVID-19 after symptom onset. Therefore, authors [4] develop a dual-sampling strategy to mitigate the imbalanced learning. The method is evaluated (to best knowledge) upon the largest multi-center CT data for COVID-19 from 8 hospitals. In the training-validation stage, authors collect 2186 CT scans from 1588 patients for a 5-fold cross-validation. In the testing stage, authors employ another independent large-scale testing dataset including 2796 CT scans from 2057 patients.
Results: Results show that The algorithm can identify the COVID-19 images with the area under the receiver operating characteristic curve (AUC) value of 0.944, accuracy of 87.5%, sensitivity of 86.9%, specificity of 90.1%, and F1-score of 82.0%. With this performance, the proposed algorithm could potentially aid radiologists with COVID-19 diagnosis from CAP, especially in the early stage of the COVID-19 outbreak.
5. Currently, Coronavirus disease (COVID-19), one of the most infectious diseases in the 21st century, is diagnosed using RT-PCR testing, CT scans and/or Chest X-Ray (CXR) images. CT (Computed Tomography) scanners and RT-PCR testing are not available in most medical centers and hence in many cases CXR images become the most time/cost effective tool for assisting clinicians in making decisions. Deep learning neural networks have a great potential for building COVID-19 triage systems and detecting COVID-19 patients, especially patients with low severity. Unfortunately, current databases do not allow building such systems as they are highly heterogeneous and biased towards severe cases. Authors in [5] propose COVID Smart Data based Network (COVID-SDNet) methodology for improving the generalization capacity of COVID-classification models.
Results: The approach reaches good and stable results with an accuracy of 97.72% ± 0.95%, 86.90% ± 3.20%, 61.80% ± 5.49% in severe, moderate and mild COVID-19 severity levels. The approach could help in the early detection of COVID-19.
6. Authors in [6] review the rapid responses in the community of medical imaging (empowered by AI) toward COVID-19. For example, AI-empowered image acquisition can significantly help automate the

scanning procedure and also reshape the workflow with minimal contact to patients, providing the best protection to the imaging technicians. Also, AI can improve work efficiency by accurate delineation of infections in X-ray and CT images, facilitating subsequent quantification. Moreover, the computer-aided platforms help radiologists make clinical decisions, i.e., for disease diagnosis, tracking, and prognosis. In this review paper [6], authors thus cover the entire pipeline of medical imaging and analysis techniques involved with COVID-19, including image acquisition, segmentation, diagnosis, and follow-up. Authors in [6] particularly focus on the integration of AI with X-ray and CT, both of which are widely used in the frontline hospitals, in order to depict the latest progress of medical imaging and radiology fighting against COVID-19.

7. As a complement to RT-PCR, Computed tomography (CT) can be used for diagnosing COVID-19. Authors in [7] have described a Mask R-CNN (region-based convolution neural network) approach for the detection of the ground glass opacities (GGOs) in chest CT images of COVID-19 infected persons.
   Results: The proposed approach provides an accuracy of 98.25% during instance segmentation. Therefore, the authors in [7] believe this proposed method will aid health professionals to fasten the screening and validation of the initial assessment towards COVID-19 patients.
8. Global health has been seriously threatened due to the rapid spread of the Coronavirus disease. In some cases, patients with high risk require early detection. Considering the less RT-PCR sensitivity as a screening tool, medical imaging techniques like computed tomography (CT) provide great advantages when compared. To reduce the fatality CT or X-ray image diagnosis plays an important role. To lessen the burden of radiologists in this global health crisis use of computer-aided diagnosis is crucial. As a reason, automated image segmentation is also of great benefit for clinical resolution assistance in quantitative research and health monitoring.
   Results: Authors in [8] have presented an approach of CT (Computed Tomography) Segmentation of lung images using the U-Net architecture.
9. Covid-19 virus, which has emerged in the Republic of China in an undetermined cause, has affected the whole world quickly. It is important to detect positive cases early to prevent further spread of the outbreak. In the diagnostic phase, radiological images of the chest are determinative as well as the RT-PCR (Reverse Transcription-Polymerase Chain Reaction) test. It was classified with the ResNet50 model, which is a convolutional neural network architecture in Covid-19 detection using chest x-ray images. Chest X-Ray image analysis can be done and infected individuals can be identified thanks to artificial intelligence quickly.
   Results: The experimental results are encouraging in terms of the use of computer-aided in the field of pathology. It can also be used in situations where the possibilities and RT-PCR tests are insufficient.
10. Authors in [10] have developed a novel Joint Classification and Segmentation (JCS) system to perform real-time and explainable COVID- 19 chest CT diagnosis. To train The JCS system, authors construct a large scale COVID- 19 Classification and Segmentation (COVID-CS) dataset, with 144,167 chest CT images of 400 COVID- 19 patients and 350 uninfected cases. 3,855 chest CT images of 200 patients are annotated with fine-grained pixel-level labels of opacifications, which are increased attenuation of the lung parenchyma. Authors [10] also have annotated lesion counts, opacification areas, and locations and thus benefit various diagnosis aspects.
    Results: Extensive experiments demonstrate that the proposed JCS diagnosis system is very efficient for COVID-19 classification and segmentation. It obtains an average sensitivity of 95.0% and a specificity of 93.0% on the classification test set, and 78.5% Dice score on the segmentation test set of the COVID-CS dataset.
11. Authors in [11] propose a conceptually simple framework for fast COVID-19 screening in 3D chest CT images. The framework can efficiently predict whether or not a CT scan contains pneumonia while simultaneously identifying pneumonia types between COVID-19 and Interstitial Lung Disease (ILD) caused by other viruses. In the proposed method, two 3D-ResNets are coupled together into a single model for the two above-mentioned tasks via a novel prior-attention strategy. Authors extend residual learning with the proposed prior-attention mechanism and design a new so-called prior-attention residual learning (PARL) block. The model can be easily built by stacking the PARL blocks and trained end-to-end using multi-task losses. More specifically, one 3D-ResNet branch is trained as a binary classifier using lung images with and without pneumonia so that it can highlight the lesion areas within the lungs. Simultaneously, inside the PARL blocks, prior-attention maps are generated from this branch and used to guide another branch to learn more

discriminative representations for the pneumonia-type classification.

Results: Experimental results demonstrate that the proposed framework can significantly improve the performance of COVID-19 screening. Compared to other methods, it achieves a state-of-the-art result. Moreover, the proposed method can be easily extended to other similar clinical applications such as computer-aided detection and diagnosis of pulmonary nodules in CT images, glaucoma lesions in Retina fundus images, etc.

12. Authors in [12] tried to classify chest CT image of Covid-19 patient. CNN produce spatial characteristic from images so it very expeditious way for image classification problem. Three techniques are evaluated through experiments. The results of the experiments show the test set has 1119 Covid-19 chest CT images and 446 normal chest CT images.

    Results: The experiment results represent that the offer model delivered the highest accuracy score of 97.57% among the other models, Inception ResNet-V2 and Inception-V3.
13. Authors in [13] have proposed to use concatenation of two different transfer learning models using an open-source dataset of 2500 CT-Scan images and 2500 X-ray images for classifying CT-Scan images and X-ray images into two classes: normal and COVID-19 Pneumonia. Authors have used DenseNet121, MobileNet, Xception, InceptionV3, ResNet50, and VGG16 models for image recognition in our work.

    Results: As a result, authors achieve the best classification accuracy of 99.87% of the concatenation of ResNet50 and VGG16 networks. Authors also achieved the best classification accuracy of 98.00% when using a single modality of CT-Scan ResNet50 networks and classification accuracy of 98.93% for X-Ray VGG16 networks. The multimodal fusion method shows a better classification accuracy compared to the method of using a single modality of biomarkers.
14. Authors in [14] present COVID-19Net, a deep neural network-based algorithm to assist doctors in diagnosing COVID-19 through the radiographic images.

    Results: In the experimental parts, the algorithm could diagnose COVID-19 and other related diseases like SARS, Streptococcus, ARDS, and Pneumocystis with average accuracy and area under the ROC curve (AUC) of respectively.
15. Authors in [15] propose anamorphic depth embedding-based lightweight CNN, called Anam-Net, to segment anomalies in COVID-19 chest CT images. The proposed Anam-Net has 7.8 times fewer parameters compared to the state-of-the-art UNet (or its variants), making it lightweight capable of providing inferences in mobile or resource constraint (point-of-care) platforms. The results from chest CT images (test cases) across different experiments showed that the proposed method could provide good Dice similarity scores for abnormal and normal regions in the lung. Authors in [15] have benchmarked Anam-Net with other state-of-the-art architectures, such as ENet, LEDNet, UNet++, SegNet, Attention UNet, and DeepLabV3+. The proposed Anam-Net was also deployed on embedded systems, such as Raspberry Pi 4, NVIDIA Jetson Xavier, and mobile-based Android application (CovSeg) embedded with Anam-Net to demonstrate its suitability for point-of-care platforms.
16. Deep learning is a data-greedy algorithm to achieve high performance when adequately trained. A common challenge for machine learning in the medical domain is the accessibility to properly annotated data. Authors in [16] apply a conditional adversarial network (cGAN) to perform image to image (Pix2Pix) translation from the non-COVID-19 chest X-Ray domain to the COVID-19 chest X-Ray domain. The objective is to learn a mapping from the normal chest X-Ray visual patterns to the COVID-19 pneumonia chest X-ray patterns. The original dataset has a typical imbalanced issue because it contains only 219 COVID-19 positive images but has 1,341 images for normal chest X-Ray and 1,345 images for viral pneumonia. A U-Net based architecture is applied for the image-to-image translation to generate synthesized COVID-19 X-Ray chest images from the normal chest X-ray images. A 50-convolutional-layer residual net (ResNet) architecture is applied for the final classification task. After training the GAN model for 100 epochs, authors use the GAN generator to translate 1,100 COVID-19 images from the normal X-Ray to form a balanced training dataset (3,762 images) for the classification task.

    Results: TheResNet based classifier trained by the enhanced dataset achieves the classification accuracy of 97.8% compared to 96.1% in the transfer learning mode. When trained with the original imbalanced dataset, the model achieves an accuracy of 96.1% compared to 95.6% in the training from trainby-scratch model. In addition, the classifier trained by the enhanced dataset has more stable measures in precision, recall, and F1 scores across different image classes. Authors [16] conclude that the GAN-based

data enhancement strategy is applicable to most medical image pattern recognition tasks, and it provides an effective way to solve the common expertise dependence issue in the medical domain.

17. In [17], an automated method for the diagnosis of COVID-19 from the chest X-Ray images is proposed. The method presents an improved depthwise convolution neural network for analysing the chest X-Ray images. Wavelet decomposition is applied to integrate multiresolution analysis in the network. The frequency sub-bands obtained from the input images are fed in the network for identifying the disease. The network is designed to predict the class of the input image as normal, viral pneumonia, and COVID-19. The predicted output from the model is combined with Grad-CAM visualization for diagnosis. A comparative study with the existing methods is also performed. The metrics like accuracy, sensitivity, and F1-measure are calculated for performance evaluation.
Results: The performance of the proposed method is better than the existing methodologies and thus can be used for the effective diagnosis of the disease.
18. COVID-19 typically known as Coronavirus disease is an infectious disease caused by a newly discovered coronavirus. Currently detection of coronovirus depends on factors like the patients' signs and symptoms, location where the person lives, travelling history and close contact with any COVID-19 patient. In order to test a COVID-19 patient, a healthcare provider uses a long swab to take a nasal sample. The sample is then tested in a laboratory setting. If person is coughing up then the saliva (sputum), is emitted for testing. The diagnosis becomes even more critical when there is a lack of reagents or testing capacity, tracking the virus and its severity and coming in contact with COVID-19 positive patients by a healthcare practitioner. In this scenario of COVID-19 pendamic, there is a need of streaming diagnosis based on retrospective study of laboratory data in form of chest X-rays using deep learning. Authors in [18] proposed a demystify technique to detect COVID-19 using assembling medical images with the help of deep nets.
Results: The study shows promising results with accuracy of 91.67% for diagnosis of COVID-19 and I00% accuracy in proving the survival ratio.
19. In [19], a dataset of CT images of confirmed and negative COVID-19 was used for the screening of COVID-19. Some preprocessing operations were applied to enhance the COVID-19 CT images which aim at including only the Area of Interest (AOI). This was accomplished in three stages. First, a conversion of the CT images to the binary scale was performed by applying a global threshold algorithm. Then, the median filter algorithm was applied to remove random noise. Then, authors in [19] include only the ROI (the lung) and exclude other parts of the images. Finally, authors applied VGGNet 19 to extract features from the preprocessed CT images, which is a popular CNN architecture, trained previously on ImageNet.
Results: The proposed pipeline showed high performance by achieving 98.31%, 100%, 98.19% and 98.64% of accuracy, recall, precision and f1-score, respectively. To the best of the knowledge, these results are the best published on this dataset when compared to a set of recently published works. Also, the proposed model overcomes several popular CNNs architectures.
20. The present work allows efficient detection of COVID-19 from chest X-Rays at a level exceeding practicing radiologists. The algorithm in [20] uses the architecture EfficientNet extended and named K-EfficientNet. The K-EfficientNet is associated with progressive resizing, which resizes the images from 112×112 to 224×224 during the training process. By combining six publicly available and independent datasets, authors get a large dataset named K-COVID containing 14,124 X-Rays images of patients affected by Pneumonia or COVID-19 and patient with Normal X-Ray images. **Results:** The application of transfer learning on the ImageNet dataset and data augmentation achieve 97.3% accuracy and 100% sensitivity, and 100% Positive Predictive Value on COVID-19 detection.
21. Authors in [21] review the imaging characteristics and computing models that have been applied for the management of COVID-19. CT, positron emission tomography - CT (PET/CT), lung ultrasound, and magnetic resonance imaging (MRI) have been used for detection, treatment, and follow-up. The quantitative analysis of imaging data using artificial intelligence (AI) is also explored.
Results: The findings indicate that typical imaging characteristics and their changes can play crucial roles in the detection and management of COVID-19. In addition, AI or other quantitative image analysis methods are urgently needed to maximize the value of imaging in the management of COVID-19.
22. A real time PCR (polymerise chain reaction) [22] is a standard tool for diagnosis for pathological testing. There are failure cases for this tool as it gives more false test results which make path to look for alternate

tool. Chest x-rays is a better alternative for PCR for COVID-19 screening. But here accuracy of results matters a lot. Here in [22] a diagnosis recommender system for examining lung images is proposed which can assist the doctors and reduce the burden over them.

Results: Deep neural network technique CNN (convolution neural network)is used for achieving best accuracy results.

23. In [23], authors try to establish a new deep convolutional neural network tailored for segmenting the chest CT images with COVID-19 infections. Authors[23] first maintain a large and new chest CT image dataset consisting of 165,667 annotated chest CT images from 861 patients with confirmed COVID-19. Inspired by the observation that the boundary of the infected lung can be enhanced by adjusting the global intensity, in the proposed deep CNN, authors introduce a feature variation block which adaptively adjusts the global properties of the features for segmenting COVID-19 infection. The proposed FV block can enhance the capability of feature representation effectively and adaptively for diverse cases. Authors fuse features at different scales by proposing Progressive Atrous Spatial Pyramid Pooling to handle the sophisticated infection areas with diverse appearance and shapes. The proposed method in [23] achieves state-of-the-art performance.
Results: Dice similarity coefficients are 0.987 and 0.726 for lung and COVID-19 segmentation, respectively. Authors conducted experiments on the data collected in China and Germany and show that the proposed deep CNN can produce impressive performance effectively. The proposed network enhances the segmentation ability of the COVID-19 infection, makes the connection with other techniques and contributes to the development of remedying COVID-19 infection.
24. Traditionally, convolutional neural networks need large amounts of data labelled by humans to train. Self supervision has been proposed as a method of dealing with small amounts of labelled data. The aim of study in [24] is to determine whether self supervision can increase classification performance on a small COVID-19 CT scan dataset. Authors in [24] also aims to determine whether the proposed self supervision strategy, targeted self supervision, is a viable option for a COVID-19 imaging dataset. A total of 10 experiments are run comparing the classification performance of the proposed method of self supervision with different amounts of data. The experiments run with the proposed self supervision strategy perform significantly better than their non-self supervised counterparts.
Results: Authors get almost 6% increase on average with self supervision compared to no self supervision, and more than 8% increase in accuracy in the best run with self supervision when compared to no self supervision. The results suggest that self supervision can improve classification performance on a small COVID-19 CT scan dataset.
25. Authors in [25] aim to integrate an image preprocessing technology for anomaly detection with supervised deep learning for chest CT imaging-based COVID-19 diagnosis. In [25], a matrix profile technique was introduced to CT image anomaly detection in two levels. At one-dimensional level, CT images were simply flatted and transformed to a one-dimensional vector so that the matrix profile algorithm could be implemented for them directly. At two-dimensional level,a matrix profile was calculated in a sliding window way for every segment in the image. An anomaly severity score (CT-SS) was calculated, and the difference of the CT-SS between the COVID-19 CT images and Non-COVID-19 CT images was tested. A sparse anomaly mask was calculated and applied to penalize the pixel values of each image. The anomaly weighted images were then used to train standard DenseNet deep learning models to distinguish the COVID-19 CT from Non-COVID-19 CT images.
Results: The metric Area Under the Curve(AUC) on one dataset were 0.7799(weighted)vs. 0.7391(unweighted), 0.7812(weighted) vs. 0.7410(unweighted), 0.7780(weighted) vs. 0.7399(unweighted), 0.7045(weighted) vs. 0.6910(unweighted) for DenseNet121, DenseNet169, DenseNet201, and the baseline model VGG19, respectively. The same trend was observed using another independent dataset. The significant results revealed the critical value of using this existing state-of-the-art algorithm for image anomaly detection. Furthermore, the end-to-end model structure has the potential to work as a rapid tool for clinical imaging-based diagnosis.
26. The application of Contrast Limited Adaptive Histogram Equalization (CLAHE) and Convolutional Neural Networks (CNN) methods are implemented in [26] to analyze the dataset with two scenarios in obtaining the detection results.
Results: The results of this research reveal that the application of CLAHE is likely to affect Covid-19 detection accuracy using CNN. Also, the application of the CNN basic model shows significant results

compared to the application of VGG16 transfer learning.

27. Authors in [27] measure whether the traditional deep learning algorithm can rely solely on lung CT images as a basis for the presence of new coronary pneumonia. Using the classic deep learning algorithms of AlexNet, VGG, ResNet, SqueezeNet and DenseNet as the basis, using the lung CT data of patients with new coronary pneumonia published on Kaggle as training and testing, and testing whether the pre-training migration learning method will Make the algorithm get a higher accuracy rate.
Results: According to the results, the accuracy rate of all algorithms without the pre-training model is more than 70%, and the accuracy rate of some algorithms reaches 82%. It shows that the deep learning algorithm, driven by a small amount of data, can not be completely used as a means of identification, but the algorithm using deep learning can help doctors identify. Moreover, with the increase of data, a more optimized learning algorithm can also obtain higher accuracy.
28. Deep learning (DL) has proved successful in medical imaging and, in the wake of the recent COVID-19 pandemic, some works have started to investigate DL-based solutions for the assisted diagnosis of lung diseases. While existing works focus on CT scans, authors in [28] studies the application of DL techniques for the analysis of lung ultrasonography (LUS) images. Specifically, authors present a novel fully-annotated dataset of LUS images collected from several Italian hospitals, with labels indicating the degree of disease severity at a frame-level, video-level, and pixel-level (segmentation masks). Finally, authors benchmark state of the art deep models for estimating pixel-level segmentations of COVID-19 imaging biomarkers.
Results: Experiments on the proposed dataset demonstrate satisfactory results on all the considered tasks, paving the way to future research on DL for the assisted diagnosis of COVID-19 from LUS data.

METHODOLOGY

As illustrated in Figure 1, the workflow of thisstudy begins with collection of primary dataset containing two image classes: one class belonged to chest X-rays of COVID-19-confirmed cases and the other class of images belonged to the normal people without the disease. In the next phase of the study, the concerned medical professionals will analyse the dataset and remove some of the X-ray images which are not clear in terms of quality and diagnostic parameters. Hence, the resulted dataset will be very clean, as each X-ray image was of good quality as well as clear in terms of significant diagnostic parameters according to their expertise. In the third phase, the dataset will be augmented using standard augmentation techniques to increase its size. The resulted dataset will be used to train the model in the next phase. After training, the model will be tested for its performance in the disease detection. The testing of proposed model will be done using test dataset held from the primary dataset as well as using the independent validation dataset.

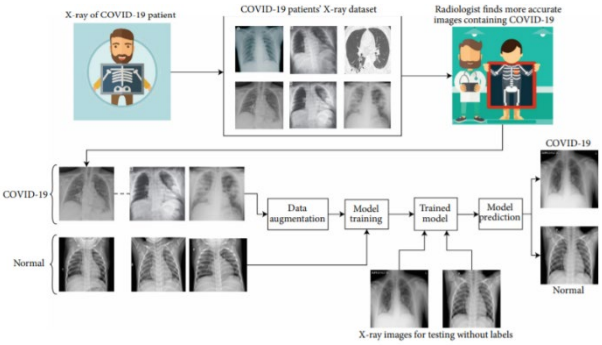

Figure 1: System development workflow

• CONCUSION

Numerous works using machine learning algorithms in healthcare domain were identified in the Systematic Literature Review (SLR). The main goal of this study is to develop a deep learning model that could predict whether a patient is suffering from COVID-19. Motivated by the need for fast and accurate analysis of radiography images, a number of COVID-19 pneumonia detection models based on state-of-the-art CNN models have been proposed and results have shown to be promising. However, those studies are reporting the results on small datasets under binary classification (COVID-19 pneumonia and non-COVID-19 cases) or three-class classification (COVID-19 pneumonia, other pneumonias and normal cases) problem. In the proposed research, we will prepare a comparatively large dataset consisting chest X-rays images of COVID-19 pneumonia, viral pneumonia, bacterial pneumonia, and normal cases. To develop such a model, a literature study is set to identify a suitable algorithm.

REFERENCES

[1] Y. Peng, Y. Tang, S. Lee, Y. Zhu, R. M. Summers and Z. Lu, "COVID-19-CT-CXR: A Freely Accessible and Weakly Labeled Chest X-Ray and CT Image Collection on COVID-19 From Biomedical Literature," in *IEEE Transactions on Big Data*, vol. 7, no. 1, pp. 3-12, 1 March 2021.

[2] J. Li, D. Zhang, Q. Liu, R. Bu and Q. Wei, "COVID-GATNet: A Deep Learning Framework for Screening of COVID-19 from Chest X-Ray

Images," *2020 IEEE 6th International Conference on Computer and Communications (ICCC)*, Chengdu, China, 2020, pp. 1897-1902.

[3] Y. Jiang, H. Chen, M. Loew and H. Ko, "COVID-19 CT Image Synthesis With a Conditional Generative Adversarial Network," in *IEEE Journal of Biomedical and Health Informatics*, vol. 25, no. 2, pp. 441-452, Feb. 2021.

[4] Ouyang *et al*., "Dual-Sampling Attention Network for Diagnosis of COVID-19 From Community Acquired Pneumonia," in *IEEE Transactions on Medical Imaging*, vol. 39, no. 8, pp. 2595-2605, Aug. 2020.

[5] S. Tabik *et al*., "COVIDGR Dataset and COVID-SDNet Methodology for Predicting COVID-19 Based on Chest X-Ray Images," in *IEEE Journal of Biomedical and Health Informatics*, vol. 24, no. 12, pp. 3595-3605, Dec. 2020.

[6] F. Shi *et al*., "Review of Artificial Intelligence Techniques in Imaging Data Acquisition, Segmentation, and Diagnosis for COVID-19," in *IEEE Reviews in Biomedical Engineering*, vol. 14, pp. 4-15, 2021

[7] A. Kundu, C. Mishra and S. Bilgaiyan, "COVID-SEGNET: Diagnosis of Covid-19 Cases on Radiological Images using Mask R-CNN," *2021 Seventh International conference on Bio Signals, Images, and Instrumentation (ICBSII)*, Chennai, India, 2021, pp. 1-5.

[8] S. Walvekar and S. Shinde, "Efficient Medical Image Segmentation Of COVID-19 Chest CT Images Based on Deep Learning Techniques," *2021 International Conference on Emerging Smart Computing and Informatics (ESCI)*, Pune, India, 2021, pp. 203-206.

[9] Z. KARHAN and F. AKAL, "Covid-19 Classification Using Deep Learning in Chest X-Ray Images," *2020 Medical Technologies Congress (TIPTEKNO)*, Antalya, Turkey, 2020, pp. 1-4.

[10] Y. -H. Wu *et al*., "JCS: An Explainable COVID-19 Diagnosis System by Joint Classification and Segmentation," in *IEEE Transactions on Image Processing*, vol. 30, pp. 3113-3126, 2021.

[11] J. Wang *et al*., "Prior-Attention Residual Learning for More Discriminative COVID-19 Screening in CT Images," in *IEEE Transactions on Medical Imaging*, vol. 39, no. 8, pp. 2572-2583, Aug. 2020.

[12] I. P. Sari, Widodo, M. Nugraheni and P. Wanda, "A Basic Concept of Image Classification for Covid-19 Patients Using Chest CT Scan and Convolutional Neural Network," *2020 1st International Conference on Information Technology, Advanced Mechanical and Electrical Engineering (ICITAMEE)*, Yogyakarta, Indonesia, 2020, pp. 175-178.

[13] N. Hilmizen, A. Bustamam and D. Sarwinda, "The Multimodal Deep Learning for Diagnosing COVID-19 Pneumonia from Chest CT-Scan and X-Ray Images," *2020 3rd International Seminar on Research of Information Technology and Intelligent Systems (ISRITI)*, Yogyakarta, Indonesia, 2020, pp. 26-31.

[14] D. A. Dharmawan and L. Listyalina, "COVID-19Net: A Deep Neural Network for COVID-19 Diagnosis via Chest Radiographic Images," *2020 1st International Conference on Information Technology, Advanced Mechanical and Electrical Engineering (ICITAMEE)*, Yogyakarta, Indonesia, 2020, pp. 232-237.

[15] N. Paluru *et al*., "Anam-Net: Anamorphic Depth Embedding-Based Lightweight CNN for Segmentation of Anomalies in COVID-19 Chest CT Images," in *IEEE Transactions on Neural Networks and Learning Systems*, vol. 32, no. 3, pp. 932-946, March 2021.

[16] Z. Liang, J. X. Huang, J. Li and S. Chan, "Enhancing Automated COVID-19 Chest X-ray Diagnosis by Image-to-Image GAN Translation," *2020 IEEE International Conference on Bioinformatics and Biomedicine (BIBM)*, Seoul, Korea (South), 2020, pp. 1068-1071.

[17] K. K. Singh and A. Singh, "Diagnosis of COVID-19 from chest X-ray images using wavelets-based depthwise convolution network," in *Big Data Mining and Analytics*, vol. 4, no. 2, pp. 84-93, June 2021.

[18] A. Channa, N. Popescu and N. u. R. Malik, "Robust Technique to Detect COVID-19 using Chest X-ray Images," *2020 International Conference on e-Health and Bioengineering (EHB)*, Iasi, Romania, 2020, pp. 1-6.

[19] M. A. Kamel, M. Abdelshafy, M. AbdulRazek, O. Abouelkhir, A. Fawzy and A. T. Sahlol, "Efficient Classification Approach Based on COVID-19 CT Images Analysis with Deep Features," *2021 International Conference on Computing, Communication, and Intelligent Systems (ICCCIS)*, Greater Noida, India, 2021, pp. 459-464.

[20] P. A. K. K. Diallo and Y. Ju, "Accurate Detection of COVID-19 Using K-EfficientNet Deep Learning Image Classifier and K-COVID Chest X-Ray Images Dataset," *2020 IEEE 6th International Conference on Computer and Communications (ICCC)*, Chengdu, China, 2020, pp. 1527-1531.

[21] D. Dong *et al*., "The Role of Imaging in the Detection and Management of COVID-19: A Review," in *IEEE Reviews in Biomedical Engineering*, vol. 14, pp. 16-29, 2021.

[22] B. Jabber, J. Lingampalli, C. Z. Basha and A. Krishna, "Detection of Covid-19 Patients using Chest X-ray images with Convolution Neural Network and Mobile Net," *2020 3rd International Conference on Intelligent Sustainable Systems (ICISS)*, Thoothukudi, India, 2020, pp. 1032-1035.

[23] Q. Yan *et al*., "COVID-19 Chest CT Image Segmentation Network by Multi-Scale Fusion and Enhancement Operations," in *IEEE Transactions on Big Data*, vol. 7, no. 1, pp. 13-24, 1 March 2021.

[24] N. Ewen and N. Khan, "Targeted Self Supervision For Classification On A Small Covid-19 Ct Scan Dataset," *2021 IEEE 18th International Symposium on Biomedical Imaging (ISBI)*, Nice, France, 2021, pp. 1481-1485.

[25] Q. Liu, C. K. Leung and P. Hu, "A Two-Dimensional Sparse Matrix Profile DenseNet for COVID-19 Diagnosis Using Chest CT Images," in *IEEE Access*, vol. 8, pp. 213718-213728, 2020.

[26] B. K. Umri, M. Wafa Akhyari and K. Kusrini, "Detection of Covid-19 in Chest X-ray Image using CLAHE and Convolutional Neural Network," *2020 2nd International Conference on Cybernetics and Intelligent System (ICORIS)*, Manado, Indonesia, 2020, pp. 1-5.

[27] X. Wu, Z. Wang and S. Hu, "Recognizing COVID-19 positive: through CT images," *2020 Chinese Automation Congress (CAC)*, Shanghai, China, 2020, pp. 4572-4577.

[28] S. Roy *et al*., "Deep Learning for Classification and Localization of COVID-19 Markers in Point-of-Care Lung Ultrasound," in *IEEE Transactions on Medical Imaging*, vol. 39, no. 8, pp. 2676-2687, Aug. 2020.

PRATIBHA: INTERNATIONAL JOURNAL OF SCIENCE, SPIRITUALITY, BUSINESS AND TECHNOLOGY (IJSSBT)
Special Issue: International Conference on Global Trends in Science, Technology, Humanities, Commerce & Management 2022 (ICGTSTHCM 2022)
Vol. 8, No. 2, January 2022,ISSN (Print) 2277-7261

Solar Absorption Refrigeration Systems Use Productive Thermal Storage PCMs: Review

Bhushan Youraj Patil[*], *Dr. Nilesh P. Salunke*[2] *and Dr. Vijay R. Diware*[3]

[1] Asst. Professor, SES's R C Patel Institute of Technology, Shirpur, Maharashtra, India

[2] Principal, SVKM's Institute of Technology, Dhule, Maharashtra, India

[3] Associate Professor, SSBT's College of Engineering & Technology, Bambhori, Jalgaon, Maharashtra, India
[1] bhushanpatilsai15@gmail.com, [2] nilesh.salunke@svkm.ac.in, [3] vrdiware65@rediffmail.com

Abstract

Composite phase change materials (PCMs) for thermal energy storage are gaining popularity due to their high latent heat storage capacity, improved thermal transfer performance, minimal volume variation, and lack of seepage. The goal of this review is to present techniques for engineering the thermal properties of composite PCMs (e.g., latent heat, thermal conductivity, durability, and thermal stability) for a variety of advanced large-scale applications and for achieving desired thermos-physical, chemical, and mechanical properties. Additionally, the methods and materials used in composite synthesis are discussed. The challenges and elements that influence composite PCMs' thermal energy storage capability are also discussed. Furthermore, the potential for generating energy storage and conversion materials, as well as current improved uses of composite PCMs (including medical, building, electronics, solar, and energy storage and conversion), are mentioned. This research will most likely serve as a starting point for the development of multifunctional organic composite PCMs.

Keywords: Solar Energy, Engineering thermal parameters, Composite PCMs, Thermal energy storage

I. Introduction

The design of composite phase change materials (PCMs) for thermal energy storage has gotten a lot of attention lately because of their high latent heat storage capability, improved thermal transfer performance, minimal volume variation, and seepage-free properties. The goal of this review is to present techniques for engineering the thermal properties of composite PCMs (e.g., latent heat, thermal conductivity, durability, and thermal stability) for a variety of advanced large-scale applications and for achieving desired thermo-physical, chemical, and mechanical properties. In addition, the methods and materials used to create composites are discussed. The challenges and elements that influence composite PCMs' thermal energy storage capability are also examined.

Furthermore, the possibility for generating energy storage and conversion materials is mentioned, as well as current improved uses of composite PCMs (including medical, building, electronics, solar, and energy storage and conversion). This research will almost certainly serve as a starting point for the development of multifunctional organic composite PCMs [1]. Due to its high energy density and capacity to store and release heat at a consistent temperature during phase shift, PCMs have gotten a lot of interest in recent years. Solid-solid PCMs, solid-liquid PCMs, and liquid-gas PCMs are the three types of solid-solid PCMs. Solid-liquid phase transitions usually result in a minor change in volume and a lot of latent heat, therefore they're well-known and commonly used.

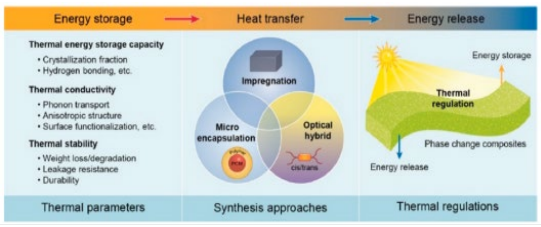

Fig. No. 1 Thermal energy management scheme for phase transition composites' thermal parameter.

PCMs that are solid-liquid can be divided into three categories: inorganic, organic, and eutectic PCMs. Salt hydrates, salt composites, and metallics are examples of inorganic PCMs. Organic PCMs include fatty acids, esters, and alcohols, as well as paraffins and non-paraffins. Organic-organic, inorganic-inorganic, and inorganic-organic pairings can all be used to make eutectic PCMs. Organic PCMs and salt hydrates exhibit phase segregation and sub-cooling; inorganic PCMs have limited thermal conductivity and segregation; and eutectic PCMs and molten salts are corrosive. Various techniques of solving these difficulties, notably for organic materials and inorganic hydrates, have been presented.

Encapsulation of PCMs to prevent sub-cooling and leakage, as well as the use of highly thermally conductive materials like metal foams and carbon materials to improve their thermal conductivity, are examples. However, due to low heat conductivity and chemical incompatibility, these approaches are ineffective for molten salt-based PCMs. According to recent study, the usage of PCMs could be an efficient way to overcome these challenges. For shape stabilisation, PCMs typically include a PCM, a TCEM (thermal conductivity enhancement material), and a CSM (ceramic skeleton material). An outstanding combination of energy density, power density, and mechanical qualities has been demonstrated using such a combination. A hierarchical structure capable of encapsulating the PCM and providing a significant increase in thermal conductivity might be created by combining these three chemically and physically suitable materials. Understanding the structure-property correlations for composites is thus critical for material formulation, design, and production. [1]

II. Literature Overview

Technologies for storing mechanical, electrical, chemical, and thermal energy have been introduced for large-scale applications [2]. Among these, thermal energy storage materials employing phase change materials (PCMs), have broad application prospects because of their large phase-change enthalpy and capability to store enthalpy of heating at constant temperatures [3]. PCMs can be re-examined and applied in various areas, such as dressings to treat burnt wounds [4], electronics [5,6], solar water heating system in different climate zones [7], building energy storage engineering [7,8], temperature-regulating textiles [9], battery thermal management [10], reaction inhibition for exothermic runaway of batch reactors [11], and condensing heat recovery system for air-conditioning [12]. For example, the integration of PCM-impregnated gypsum boards with night ventilation saves energy by 73% [13].

Organic PCMs (e.g., paraffin waxes, glycols, and fatty alcohols) have gotten more attention than inorganic PCMs (e.g., metal alloys, eutectic mixtures, and salt hydrates), owing to the former's lower super cooling, lack of phase separation, broad ranges of phase-transition temperatures for practical use, corrosion resistance, favourable reversibility, chemical stability properties, and commercial availability [14–16]. As a result, organic PCMs have been widely studied in order to improve energy use efficiency. However, various obstacles prevent organic PCMs from being used directly in practical applications, including their low heat transfer rate, leakage above their melting temperature, and difficulty regulating the materials throughout the phase-transition process. Several ways have been developed to generate more shape-stable PCMs in order to address these issues (also termed as phase change composites). The type, size, and composition of additives and/or virgin PCMs determine most of the thermal parameters of PCMs (e.g., heat enthalpy, reliability, energy conversion capacity, and thermal conductivity).

GNPs' effective photon capture, electrical conductivity, and nano heating capabilities allow for these improvements. Although some micro porous supporting materials (for example, porous carbonised woods/lauric acid) aided PCMs in heterogeneously nucleating [20], most of the phase change composites exhibited a fixed crystallization temperature. When PCMs move from liquid to solid, they usually show delayed solidification and a lower freezing point, and they start crystallising before the transition reaches the melting temperature. As a result, it exhibits negligible super cooling suppression and discharges latent heat across a broader temperature range. These high-temperature ranges aren't conducive to efficient energy storage. Similarly, various thermal capabilities, such as energy-storage capacity, crystallinity, and dependability of PCMs, are caused by varied interfacial interactions among composite components and uneven thermal recycle. Researchers are striving to create novel thermal control technologies for composite PCMs to overcome these issues. Organic light-responsive compounds with reversible photo isomerization have recently been introduced into PCMs. During the charging/discharging process, these chemicals regulate spontaneous heat loss. A new sort of knob controls the melting, freezing, and super chilling qualities, which can be used to cook or heat after dark. For diverse applications ranging from microelectronic to energy storage and conversion devices, it is critical to engineer the thermal properties of composite PCMs (e.g., heat enthalpy, thermal conductivity, and thermal stability). Most existing reviews, to our knowledge, are focused on PCMs' energy conversion and storage performance, their properties and commercialization, carbon based composite PCMs, composite PCM fabrication, PCMs for construction applications, macroscopically three-dimensional (3D), and PCMs for medical applications [16], Nano and/or porous confined PCMs, as well as their heat conductivity. As a result, we give a comprehensive overview of the difficulties and solutions related to the numerous potential for improving performance and controlling the essential thermal properties of composite PCMs. The study also contains the primary synthesis methodologies, recent advanced applications, and future research prospects.

III. Synthesis techniques of phase change composites

Because of their superior physical, thermal, chemical, and energy storage and conversion capabilities, shape-stable composite PCMs have sparked a lot of interest in current thermal energy storage applications (such as light, magnetic, and electrical thermal),. In the large-scale manufacture of the target materials, the engineering chemistry involved in composite PCM design played a significant role. As a result, strategies like developing required composite PCMs are used.
A) Impregnation,
B) Micro encapsulations,
C) Nano encapsulation,
D) Other confinement technologies

A. Impregnation method

Encapsulation or impregnation are applied in the design of shape-stable PCMs by incorporating pristine PCMs into supporting materials. Table 1 presents the thermal properties of shape-stable PCMs designed using the impregnation method.

The thermal parameters including R, Fc, and ς were calculated using
ΔT = Tm - Tf, where Tm and Tf are the melting and freezing temperatures, respectively, of the composite PCMs

$$R = \left(\frac{\Delta H_{m,composite}}{\Delta H_{m,PCM}}\right) \times 100$$

$$Fc = \left(\frac{\Delta H_{m,composite}}{\beta \Delta H_{m,PCM}}\right) \times 100$$

$$\varsigma = \left(\frac{\Delta T_{composite} - \Delta T_{PCM}}{\Delta T_{PCM}}\right) \times 100$$

where ΔHm, composite, ΔHm, PCM, ΔT composite, and ΔTPCM are the phase change enthalpy of the composite PCMs, phase-change enthalpy of the pristine PCMs, weight ratio of PCMs in the composites, variation in the temperature of the composites, and variation in the temperature of the pristine PCMs, respectively. Fc reveals the influence of the interaction on the latent heat, and it is determined from the confinement of PCM molecules in the supporting materials [21]. As tabulated, the Fc values of a few of the PCMs in the composite materials were larger (> 1.0), and those of the other composites were less than one. These can be described using two main factors:
1) The internal interface that decreases the crystallinity of the PCMs
2) The weak hydrogen bonds that occurs between the composite constituents.

Table No. 1 Thermal properties of phase change composites determined by impregnation approach

PCMs	Supporting materials	R (%)	ΔH kJ/kg	Tm (°C)	Tf (°C)	ΔT* (°C)	ς (%)	Fc (%)
Polyethylene glycol	SiO2	92.3	164.9	60.4	37.9	22.5	–	95.2
Polyethylene glycol	3D Ti3C2Tx	90.2	167.7	–	–	–	–	94.9
Polyethylene glycol	Carbon fiber/SiO2	67.3	142.6	57.5	34.8	22.7	3.8	79.1
Polyethylene glycol	(3,6),-connected Zn-MOF	92.2	159.8	50.4	23.8	26.6	–	108.4
Polyethylene glycol	Melamine foam/rGO/BN	90.8	160.7	63.5	34.7	28.8	15.2	100
Polyethylene glycol	GO/carbon nanotubes (CNTs),	66.3	120.7	33.8	10.1	23.7	–	78
Polyethylene glycol	3D cellulose/BN nanosheet	67	136.8	60.2	41.6	18.6	–	95.7
Dodecanoic acid	Graphene	81.1	157.6	45.1	36.7	8.4	–	101.4
Stearic acid	Ultrathin graphite sheets	59.3	113.7	53.1	53.5	–	–	94
Stearic acid	3D graphitic porous carbon	83.5	171.5	71.2	65.3	5.9	–	98.5
Stearic acid	Porous hollow Co3O4/expanded graphite	85.7	192.5	69.4	68.2	1.2	50	95.2
Paraffin	Expanded graphite/CNTs	57.1	157.4	36.4	35.5	0.9	–	95.1
Paraffin	Honeycomb carbon fiber	88.3	192.2	60	50	10	37	101.2
Paraffin	MMC-14	56.5	95	25.5	22	3.5	13.5	94.2
Paraffin	Melamine foam	88.3	139.8	56.8	45.1	11.7	4.5	91.2
Lauric-stearic acid	Diatomite/expanded graphite	70.2	117.3	31.2	30	1.2	–	97.3
1-tetradecanol	Delignified wood/modified SiO2	59.9	125.4	35.7	36.5	–	–	100
1-tetradecanol	Graphene oxide aerogel	99.9	230.3	46.7	25.6	21.1	6.8	105.2
Tetradecylamine	Graphene sponge	101	293.1	39	32	7	–	>100.0
1-hexadecanol	Porous carbon	98.5	219.4	50.8	40.4	10.4	5.5	109.4
n-dodecane	Biochar	60.2	90.5	−4.1	–	–	–	> 71.6
n-octadecane	3D-graphene aerogel	95.3	195.7	35	13.8	21.2	–	100.3
n-octadecane	Porous TiO2	44.8	119.8	29.2	27.3	1.9	–	74.7
Octadecane	Expanded graphite	91.7	235.2	30.9	28	2.9	–	> 90

n-eicosane	nano–SiO2/expanded graphite	55.8	135.8	37.7	34.3	3.4	–	79.7
n-eicosane	Ti2O3/polydopamine@carbon foam	84.5	200.1	36.4	33.7	2.7	35	100.6
PCMs	**Supporting materials**	**R (%)**	**ΔH (kJ/kg)**	**Tm (°C)**	**Tf (°C)**	**ΔT* (°C)**	**ς (%)**	**Fc (%)**

B. Microencapsulation

Microencapsulation is a technique used to introduce a PCM as a core (energy-storage), and inorganic and/or organic polymers as a shell (supporting materials),. It prevents leakage of PCMs, improves the thermo-mechanical performances, and provides enhanced protection from the external environment. Microencapsulated PCMs (micro PCMs), can be utilized for specific applications such as textile, building, medical treatment including thermal therapy, and flame-retardant via shell engineering. Most of the composite PCMs show a considerable decline in γ as calculated using Eq.

$$\gamma = \left(\frac{\Delta H_{m,PCM} - \Delta H_{m,microPCM}}{\Delta H_{m,PCM}} \right) \times 100$$

The efficiency of thermal energy storage decreases as the percentage of latent heat loss increases.

Table No. 2 Thermal properties and synthesis techniques of micro PCMs

PCM core	**Shell materials**	**Synthesis approaches**	**ΔH_m (kJ/kg)**	**γ (%)**	**PCM core**
n-eicosane	TiO2	Emulsion-templated polycondensation	187	24.1	n-eicosane
n-eicosane	SiO2/CdS	Interfacial polycondensation	~70	71.4	n-eicosane
n-eicosane	Sporopollenin exine capsules	Hydrothermal	158	37.3	n-eicosane
n-eicosane	Fe3O4/SiO2	Sol-gel	170.9	7.6	n-eicosane
n-octadecane	Poly(methyl methacrylate),/TiO2	Photocurable pickering emulsion	179.9	32.7	n-octadecane
n-octadecane	Melamine–formaldehyde (MF),	In situ polycondensation	141.3	41.4	n-octadecane
n-octadecane	TiO2- polyurea	Interfacial polymerization	181.1	23	n-octadecane
n-octadecane	SiO2/graphene	Polycondensation and miniemulsion	108.2	46.4	n-octadecane
1-Tetradecanol/ pigment	Poly methylated melamine–formaldehyde	In situ polymerization	165.9	27.4	1-Tetradecanol/ pigment
Stearic acid	2D-montmorillonite/AgNPs	Hydrothermal	188.3	9.5	Stearic acid
Paraffin	Cu–Cu2O	Hydrothermal	126.8	36.5	Paraffin
Paraffin	Chitosan/Fe3O4	Multi-emulsification polymerization and cross-linking	80	62.1	Paraffin
Paraffin	SiO2/Ti4O7	Sol-gel method	122.4	27.8	Paraffin
Paraffin	SiO2-TiO2	Sol-gel method	93.7	60.2	Paraffin
Paraffin	GO platelet-patched shell structure	Emulsion polymerization	158.4	10.8	Paraffin
Paraffin	Mixed cellulose/GO	Self-assembly approach	152.2	13.2	Paraffin
Paraffin	TiO2/GO	In situ hydrolysis and poly condensation	75	61.9	Paraffin
Paraffin	Graphene/MF	In situ polymerization	204	19.7	Paraffin
Paraffin	Hydrated salt	Emulsification	227.3	13	Paraffin
Paraffin	Polystyrene/cellulose nanocrystal	Pickering emulsion polymerization	160.3	17.2	Paraffin
Palmitic acid	CuCO3	Self-assembly method	48.8	56.1	Palmitic acid
PCM core	**Shell materials**	**Synthesis approaches**	**ΔH_m (kJ/kg)**	**γ (%)**	**PCM core**
n-eicosane	TiO2	Emulsion-templated polycondensation	187	24.1	n-eicosane
n-eicosane	SiO2/CdS	Interfacial polycondensation	~70	71.4	n-eicosane
n-eicosane	Sporopollenin exine capsules	Hydrothermal	158	37.3	n-eicosane
n-eicosane	Fe3O4/SiO2	Sol-gel	170.9	7.6	n-eicosane
n-octadecane	Poly(methyl methacrylate),/TiO2	Photocurable pickering emulsion	179.9	32.7	n-octadecane

C. Nano encapsulation

Nano encapsulation of PCMs is attracting tremendous attention because of the convenient synthesis process and improvement in thermal properties.

D. Other synthesis approaches

In addition to the frequently used techniques stated above, numerous other strategies have been formulated for developing phase change composites, including macro encapsulation. Optically hybrid PCMs/PCM-light-responsive matrixes, which are termed as optically hybrid PCMs, is a recently developed strategy applied to enhance the energy-storage and -release property of PCMs.

IV. Challenges and opportunities

Composite PCMs are a new type of material for thermal energy storage. It is critical to recognise the possibility for engineering thermal characteristic controlling methods. The next sections address the governing processes and challenges related with the use of phase change composites for thermal energy storage, heat transport, and stability, as well as the sub cooling phenomenon of organic composite PCMs. Following that, the possibility for unique composite PCM applications is highlighted.

A. Thermal energy storage

- Thermal energy storage capacity is an imperative parameter of composite PCMs. It can be realized by employing latent heat involved in the phase transitions of PCMs, such as solid–liquid transition.
- The energy-storage/release performance of a phase change composite depends on the loading of the composite components and the intermolecular interactions.
- The latent heat of the HPC–paraffin wax composite increased with an increase in the paraffin content. The latent heat of the composite PCM increased to 152.2 kJ/kg when the wt% of paraffin wax was increased to 77% (the maximum loading ratio).

B. Textural properties

PRATIBHA: INTERNATIONAL JOURNAL OF SCIENCE, SPIRITUALITY, BUSINESS AND TECHNOLOGY (IJSSBT)
Special Issue: International Conference on Global Trends in Science, Technology, Humanities, Commerce & Management 2022 (ICGTSTHCM 2022)
Vol. 8, No. 2, January 2022,ISSN (Print) 2277-7261

The influence of textural properties (such as pore size, specific surface area, and porosity characteristics), of the host and guest materials played a significant role in high heat production and low convective cooling states. The pore size of the supporting materials, chain length, and functional groups of the PCMs are the complementary factors that affect a composite's thermal properties.

- specific surface area of a porous carbon increased from 487.9 m2/g to 876.6 m2/g,
- latent heat of 1-hexadecanol in the composite increased from 204.4 to 215.5 kJ/kg
- As the pore dimension increased from 11.6 to 50 nm,
- Fc improved from 51.6% to 83.6%,
- Enthalpy increased from 98.5 to 101 kJ/g.

Fig. 2 generally describes the influence of pore size on the crystallinity and energy storage capacity of PCMs in the supporting framework. Hence, compared with the pristine PCMs, the phase transition temperature/melting point and energy-storage efficiency were mostly reduced owing to the thermodynamic and geometrical influences of the non-melting interface layer of an organic molecule. It should be noted that the description may have a few exceptions in terms of crystallinity and energy storage capacity when the molecular length and loading content of the PCMs are considered.

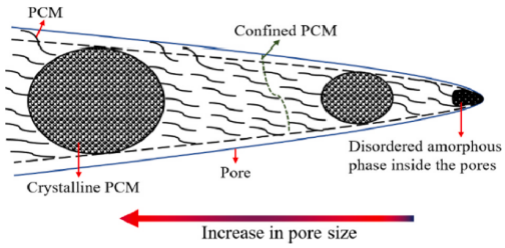

Fig. no 2. Schematic description of PCM and pore interaction and enhancement of the crystallinity and energy storage capacity of phase change composites. The crystallinity increased from the right (amorphous PCM), to the left (crystallized PCMs)

C. Surface engineering of composite components

The surface functionality of composite components plays an imperative role in the regulation and description of the thermal characteristics of designed composites. Organic PCMs such as paraffin waxes, carboxylic acids (fatty acids),, PEG, and sugar alcohols normally show high heating enthalpy and solid–liquid transition with a broad range of freezing and melting points.

D. Synthesis conditions and dynamic properties of materials

The immersion time and temperature play an imperative role in PCM adsorption and consequently, influence the latent heat storage of composite materials. An increase in the encapsulation temperature and time mostly results in an increase in the PCM loading up to the optimum loading ratio.

E. Heat transfer/thermal transport

Presently, different strategies and approaches are being adopted to advance and regulate the heat flow in composite materials (Fig. 3),. The most common approaches to enhancing the heat transfer performance are to incorporate additives with high thermal conductivity into PCMs and to enclose PCMs with a conductive medium. Notably, composite PCMs with low thermal conductivity may also be required depending on the application sector (e.g., building envelope),. In a similar application area, the introduction of PCMs into materials with low thermal conductivity is viable. Table 3 presents the thermal conductivity performance of various composite PCMs. Other influencing features (e.g., atomic size/mass, temperature, and binding energy), can also contribute to the improvement mechanisms.

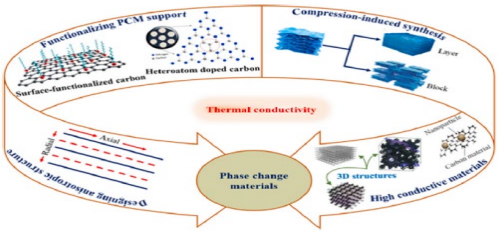

Fig. no.3. Mechanism of thermal conductivity improvement of phase change composites.

1. Functionalizing/modifying supporting materials

In most cases, the modification of supporting materials through a chemical method (chemical functionalization through doping and/or grafting functional groups), can affect their intrinsic structures and, in turn, influence the heat transfer performance of the PCM matrix. It is suitable for continuous heat transfer and reduces the thermal resistance between the PCM and support. The organic functional group improved the adsorption of PCM via capillary force and intermolecular forces. This, in turn, improved the shape-stability of hybrid composite PCMs.

2. Introducing matrices with high thermal conductivity

Materials with high thermal conductivity, It is noteworthy that microencapsulated PCMs with various varieties of organic shells have stable shapes, large thermal transport areas, and a low risk of leakage in phase transition processes.

4.3. Thermal stability of composite PCMs

The thermal stability parameters durability, leakage resistance, and thermal degradation are the most important ones for practical thermal energy-storage applications of composite PCMs.

3. Subcooling phenomenon

The supercooling of PCMs is a practical challenge in phase-change energy storage technology. It hinders the recovery of stored enthalpy. Supercooling is a metastable property where the material is observed to be liquid below the fusion temperature. Although supercooling is high for inorganic

PCMs, a few organic PCMs (e.g., sugar alcohols), also exhibit certain subcooling characteristics. However, nucleating agents are introduced to reduce the subcooling by increasing the nucleation rate of the composites and to trigger the crystallization process. Heterogeneous nucleating materials have relatively high fusion temperatures and maintain the solid-state during the phase change process

Table No.3 Thermal conductivity properties of recently reported phase change composites

Organic PCMs	Supportive materials	Synthesis methods	k (W/(m·K),*	Improvement (%),
Polyethylene glycol	Expanded graphite	Vacuum impregnation	0.2315	43.2
Polyethylene glycol	Anisotropic cellulose/BN nanosheet	Vacuum impregnation	4.764	1400
Polyethylene glycol	Melamine foam /rGO/BN	Impregnation	0.79	146.7
Polyethylene glycol	CNTS (axial),	One-step polymerization and solution assisted infiltration	2.4	~900
Stearic acid	Ultrathin graphite sheets	Impregnation	2.691	907.9
Stearic acid	Co3O4/EG	Solution impregnation	2.53	666.67
n-octaadecane	3D-GA	Solution and vacuum impregnation	1.636	987
n-octadecane	Porous TiO2	Vacuum impregnation	0.45	138
Octadecanol	Expanded perlite/EG	Vacuum impregnation	6.623	–
Paraffin	SiO2/Ti4O7	Sol-gel method	1.322	334.9
Paraffin	3D-EG block	Self-assembly and casting way	15.66	7730
Paraffin	Expanded natural graphite	Compression and impregnation	20.2	6633.3
Paraffin	Melamine foam/cellulose nanofiber/GNPs	Vacuum-assisted encapsulation	1.42	407
HDA	CNTs	Diels-Alder reaction	0.877	338.5

V. Future Scope

With their strong seepage resistance and huge latent heat storage capacity, shape-stable PCMs have unique application possibilities. The primary breakthroughs in the large-scale use of composite PCMs include structural–thermal functions, encapsulation and form stability, and innovative and adaptive materials. Shape-stable PCMs are comparable to structural batteries in that they can store heat while also having chemical and physical/mechanical properties.

Recent advanced applications of phase change composites

With the development of versatile designing strategies of smart materials (materials that enable response to user's requirement beyond the individual constituent of the composite by activating its function, e.g., biochar), composite PCMs are being applied in various "high technology" areas (e.g., National Aeronautics and Space Administration (NASA),),, and other areas such as smart drug delivery, flame retardants and electronics. In addition to the energy storage applications, phase change composites also contribute with medical, building, electronic, solar, and energy conversion applications.

- Medical applications
- Building applications
- Electronics applications
- Solar

Energy storage and conversion

The design of multifunctional PCMs have also attracted substantial attention for effective energy exploitation. PCMs can capture energy from diverse sources (e.g., magnetic, light, and electric), and transform it into enthalpy of heating (Fig. 4),. Therefore, it has a number of applications such as photothermal, magnetothermal, and electric–thermal.

- Photothermal conversion Light-harvesting additives including nanomaterials and organic dyes on the surface of phase-change composites have received notable consideration because of their large energy-storage and –conversion performances.
- Magnetothermal conversion A magnetically initiated approach for energy conversion (e.g., solar thermoelectric), and thermal charging has remarkable applications (e.g., thermoelectric generators),. The magnetically movable optical charging strategy is demonstrated to accelerate the energy conversion capacity (mostly solar–thermal conversion), with a uniform temperature distribution within the charged matrixes. The high content of supporting materials in the composite PCMs inhibits their large-scale application owing to the large size of the supporting materials, difficulty of processing the composites, and unstable distribution of the composites during the phase-transition route.
- In solar-to-thermal energy transformation (via conventional thermal diffusion-based thermal charging), light-harvesting materials absorb and convert solar to thermal energy before transporting the resultant thermal energy within the PCMs by thermal diffusion.
- Electrothermal conversion fabricating electrically conductive supporting materials for PCMs has undergone momentous progress in terms of the conversion of electrical energy to heating enthalpy/thermal energy because of the insulating characteristics of PCMs. The obtained composite provided a significant electrothermal energy conversion efficiency of 67.4% and motion-sensing properties, under an applied voltage bias of 4.0 V and when coated with a layer of thermoplastic polyurethane.

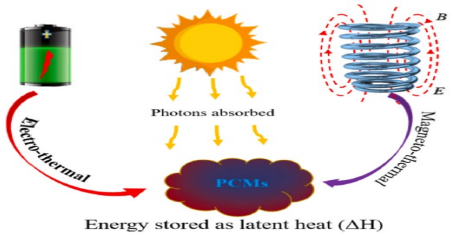

Fig. no 4. Illustration of different energy conversion approaches of PCMs.

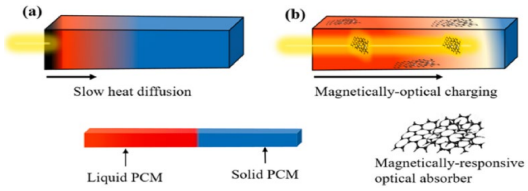

Fig. no 5. Schematic description of solar–thermal energy storage driven by (a), conventional slow heat diffusion and (b), magnetically optical charging system. Under slow heat diffusion, the incident light irradiation is received by non-optical supporting materials, which gradually transfer the energy to liquid PCMs. In a magnetically optical charging system, the incident light is transformed to thermal energy. Subsequently, it is infiltrated by liquid PCMs, which enhances the phase transition charging interface further

VI Conclusions and perspectives

To sum up, a systematic approach was used to investigate the thermal properties of recently investigated composite PCMs (with a focus on engineering the thermal parameters and applications in various areas),. Various studies are currently being carried out in order to create shape-stabilized organic phase-change composites. As a result of the positive results, the synthesis techniques, design of supporting materials for PCMs, microstructure and phonon transmission mechanisms, shape stability and reliability tests, and various thermal energy storage systems with improved performance have all been investigated in order to achieve a variety of practical applications (e.g., building energy conservation, solar, electronics, thermal therapy, and energy storage and conversion process),.

The following are some key results and recommendations:

1. Surface engineering of supporting materials plays a critical role in the crystallinity and energy storage capacity of composite PCMs. Meanwhile, the employment of shape-stable PCMs as encapsulating media is recommended to lower the influence of supporting scaffolds on the total energy storage capacity.
2. The development of facile synthesis strategies is essential for certain target applications such as coolant in electronic devices for cooling applications.
3. Notwithstanding the advancements, nano-confined composite PCMs exhibited an inflexible and fixed crystallization temperature, which resulted in an inadequate response of their phases to varying ambient temperatures. Therefore, extensive research is proposed to achieve high enthalpy of heating and reduced sub/supercooling phenomenon of organic PCMs.
4. The assembly of PCMs with materials displaying high thermal conductivity is the most frequently used approach for enhancing the charging/discharging rates of the composites. However, the interface between the PCMs and thermally conductive additives is random, which hinders the accurate prediction of the heat transfer performance of phase change composites. Thus, it is necessary to further investigate the combination forms of dual- or multi-phase phase-change composites.
5. The stability of composite PCMs is an important parameter for practical usage (e.g., building, solar),. The development of flexible phase-change composites and fabrication of dynamic cross-linked composite PCMs have been recommended for prolonged energy storage and thermal regulating engineering.
6. The integration of photo-switching dopants such as azobenzene and magnetically movable optical charging with nontransparent PCMs yielded thermal energy storage management systems with improved performance parameters such as waste heat recovery and energy storage and conversion process (e.g., photothermal, magnetothermal, and electrothermal),. However, this technology is still in its infancy.
7.

Acknowledgements

The authors claim that they have no known personal and financial interests that could have influenced the findings of this study.

References

[1] D.G. Atinafu, Y.S. Ok, H.W. Kua, and S. Kim "Thermal properties of composite organic phase change materials (PCMs),: A critical review on their engineering chemistry", Applied Thermal Engineering, Elsevier., Vol. 20, (2020),, pp. 1359-4311.

[2] D. Feng, Y. Feng, L. Qiu, P. Li, Y. Zang, H. Zou, Z. Yu, and X. Zhang, "Review on nanoporous composite phase change materials: Fabrication, characterization, enhancement and molecular simulation, Renew. Sustain". Energy Rev. Vol. 109, (2019),, pp. 578–605.

[3] K. Pielichowska, K. Pielichowski, "Phase change materials for thermal energy storage", Prog. Mater. Sci. Vol. 65, (2014), pp. 67–123.

[4] S. Becherini, M. and Mitmoen, C.D. Tran, "Natural sporopollenin microcapsules facilitated encapsulation of phase change material into

cellulose composites for smart and biocompatible materials", ACS Appl. Mater. Interfaces (2019).

[5] Y.-J. Lan, S.-J. Chang, C.-C. Li, "Synthesis of conductive microcapsules for fabricating restorable circuits", J. Mater. Chem. A Vol. 5 (2017),, pp. 25583–25593.

[6] F. Xue, X. Jin, X. Xie, X. Qi, J. Yang, Y. Wang, "Constructing reduced grapheme oxide/boron nitride frameworks in melamine foam towards synthesizing phase change materials applied in thermal management of microelectronic devices", Nanoscale Vol. 11, (2019), pp. 18691–18701.

[7] Z. Ding, W. Wu, Y. Chen, Y. Li, "Dynamic simulation and parametric study of solar water heating system with phase change materials in different climate zones", Sol. Energy Vol. 205, (2020), pp. 399–408.

[8] B.Y. Yun, S. Yang, H.M. Cho, S.J. Chang, S. Kim, "Design and analysis of phase change material based floor heating system for thermal energy storage", Environ. Res. Vol. 173, (2019), pp.480–488.

[9] Y. Lu, X. Xiao, J. Fu, C. Huan, S. Qi, Y. Zhan, Y. Zhu, G. Xu, "Novel smart textile with phase change materials encapsulated core-sheath structure fabricated by coaxial electrospinning", Chem. Eng. J. Vol. 355, (2019), pp.532–539.

[10] W. Wu, J. Liu, M. Liu, Z. Rao, H. Deng, Q. Wang, X. Qi, S. Wang, "An innovative battery thermal management with thermally induced flexible phase change material", Energy Convers. Manag. Vol. 221, (2020), 113145.

[11] Q. Chen, L. Ni, J. Jiang, T. Parker, Z. Chen, Z. Cheng, W. Jiang, Q. Wang, "Inhibition of exothermic runaway of batch reactors for the homogeneous esterification using nano-encapsulated phase change materials", Appl. Therm. Eng. Vol. 178, (2020), 115531.

[12] S. Zhang, W. Wu, S. Wang, "Integration highly concentrated photovoltaic module exhaust heat recovery system with adsorption air-conditioning module via phase change materials", Energy Vol. 118, (2017), pp.1187–1197.

[13] D.G. Atinafu, W. Dong, X. Huang, H. Gao, G. Wang, "Introduction of organic-organic eutectic PCM in mesoporous N-doped carbons for enhanced thermal conductivity and energy storage capacity", Appl. Energy Vol. 211, (2018),.

[14] L. Chen, R. Zou, W. Xia, Z. Liu, Y. Shang, J. Zhu, Y. Wang, J. Lin, D. Xia, A. Cao, "Electro- and photodriven phase change composites based on wax-infiltrated carbon nanotube sponges", ACS Nano Vol. 6, (2012), pp.10884–10892.

[15] J. Yang, L.-S. Tang, L. Bai, R.-Y. Bao, Z.-Y. Liu, B.-H. Xie, M.-B. Yang, W. Yang, "High-performance composite phase change materials for energy conversion based on macroscopically three-dimensional structural materials", Mater. Horizons Vol. 6, (2019), pp.250–273.

[16] X. Wang, X. Cheng, Y. Li, G. Li, J. Xu, "Self-assembly of three-dimensional 1-octadecanol/ graphene thermal storage materials", Sol. Energy Vol. 179, (2019), pp.128–134.

[17] B. Mu, M. Li, "Synthesis of novel form-stable composite phase change materials with modified graphene aerogel for solar energy conversion and storage", Sol. Energy Mater. Sol. Cells Vol. 191, (2019), 466–475.

[18] H. Wu, S. Deng, Y. Shao, J. Yang, X. Qi, Y. Wang, "Multiresponsive shape-adaptable phase change materials with cellulose nanofiber/graphene nanoplatelet hybridcoated melamine foam for light/electro-to-thermal energy storage and utilization", ACS Appl. Mater. Interfaces Vol. 11, (2019), pp. 46851–46863

[19] D.G. Atinafu, W. Dong, C. Wang, G. Wang, "Synthesis of porous carbon from cotton using an Mg(OH),2 template for form-stabilized phase change materials with high encapsulation capacity, transition enthalpy and reliability", J. Mater. Chem. A Vol. 6, (2018).

[20] Z. Yang, Y. Deng, J. Li, "Preparation of porous carbonized woods impregnated with lauric acid as shape-stable composite phase change materials", Appl. Therm. Eng. Vol. 150, (2019), pp. 967–976,

[21] H. Zhang, Y. Yuan, Q. Sun, X. Cao, "Enhanced thermal energy storage performance of polyethylene glycol by using interfacial interaction of copper-based metal oxide", Adv. Eng. Mater. Vol. 19, (2017), pp.1600-601.

PRATIBHA : INTERNATIONAL JOURNAL OF SCIENCE, SPIRITUALITY, BUSINESS & TECHNOLOGY (IJSSBT)

Vol. 8, No. 2, January 2022

ISSN (Print) : 2277-7261

ISSN (on-line) : 2278-3857

http : www.ijssbt.org

SHRAM SADHANA BOMBAY TRUST'S

COLLEGE OF ENGINEERING & TECHNOLOGY,

BAMBHORI, JALGAON (INDIA)

ISSN 2277-7261